NOAA OAR Special Report

PMEL Tsunami Forecast Series: Vol. 73

A Tsunami Forecast Model for Kailua-Kona, Hawaii

(Draft)

Liujuan Tang, Chris Moore and Nannan Wang

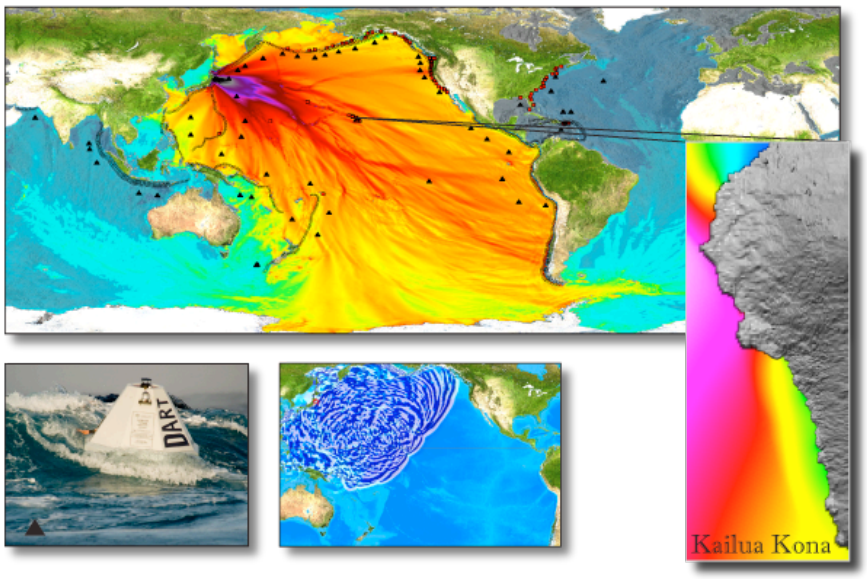

February 2014

NOAA Center for Tsunami Research (NCTR)
Pacific Marine Environmental Laboratory

Contents

List of Tables

Rachel Tang 2/20/14 1:51 PM
Deleted: 39

PMEL Tsunami Forecast Series: Vol. 73

A Tsunami Forecast Model for Kailua-Kona, Hawaii

Liujuan Tang, Christopher Moore and Nannan Wang

Abstract

This report describes the development, verifications, and testing of a tsunami forecast model (2 arc sec) for Kailua-Kona, Hawaii. A reference inundation model with higher resolution of 2/3 arc sec was also developed in parallel to provide modeling references. Both models were tested for 34 scenarios, which include 16 past tsunamis and a set of 18 simulated M_w 9.3 tsunamis. A point at 2.3 m water depth near Kona Pier was chosen as a warning point for forecast purposes.

The wave analyses of the amplitude time series at the warning point shows a wide range of resonant periods from 6–126 min. 68% of the tested scenarios show peak resonant period (T_P) near 8 (±2) min. For some cases, waves of long resonant periods can have similar magnitude as those of short periods.

The numerical consistency between the forecast and reference models is good in general, including the amplitude time series at the warning point, and maximum amplitude and current in the forecast area. When T_P > 10 min, the uncertainty in the forecast η_{max} at the warning point is within 20%. When $T_P \leqslant 10$ min and $\eta_{max} > 1$m, the uncertainty is within 31%. When $\eta_{max} < 1$ m, the uncertainty in η_{max} is within 25 cm. Scenarios from portions of the Central Aleutian subduction zones near the Unimak

Islands may have additional uncertainty (about 0–41%), depending on whether or not a strong resonance of extremely short period (6 min) is excited on the site.

The simulated M_w 9.3 tsunamis show an impressive local variability of tsunami amplitudes at Kailua-Kona, indicating the complexity of forecasting tsunami amplitudes at a coastal location. It is essential to use high-resolution models in order to provide accurate simulations that are useful for coastal tsunami forecasts. Tsunamis propagating from the east, particularly from Japan, Kamchatka, and Izu subduction zones, have shown the late arrival of the maximum wave η_{max} in high frequency ($T_P \approx 8$ min). The η_{max} could be the 10^{th} –12^{th} wave, arriving about 1–4 hr after the first wave. Both incident waves from far-fields and local resonances contribute to the late η_{max}.

The study highlights tsunamis originating from Japan, Kamchatka, Izu, Northern Tonga (Samoa), the Aleutian Islands, Southern Chile, East Philippines, and Canada subduction zones, all of which can potentially generate large waves and cause flooding in Kailua-Kona. It also shows the waterfront near Kona Pier and the end of Kailua bay are under high flooding risk once inundation occurs in the forecast area.

Due to the unique tsunami-resonant characteristics of the site, a coastal water-level station is highly recommended for Kailua-Kona area, in order to provide tsunami data for model calibration and to improve forecast accuracy.

1 Introduction

The National Oceanic and Atmospheric Administration (NOAA) Center for Tsunami Research at NOAA's Pacific Marine Environmental Laboratory (PMEL) has developed a tsunami forecasting system for operational use by NOAA's two Tsunami Warning

Centers located in Hawaii and Alaska (Titov et al., 2005; Titov, 2009). The forecast system combines real-time deep-ocean tsunami measurements from tsunameters (Deep-ocean Assessment and Reporting of Tsunami (DART)) (González et al., 2005; Meinig et al., 2005; Bernard et al., 2006; Bernard and Titov, 2007) with the Method of Splitting Tsunami (MOST) model, a suite of finite difference numerical codes based on the nonlinear shallow water wave equations (Titov and Synolakis, 1998; Titov and González, 1997; Synolakis, et al., 2008; Titov et al., 2011) to produce real-time forecasts of tsunami arrival time, heights, periods and inundation. To achieve accurate and detailed forecasts of tsunami impact for specific sites, high-resolution tsunami forecast models are under development for United States coastal communities at risk (Tang et al., 2008a; 2009; 2010; Arcas and Uslu, 2010; Wei and Arcas, 2010). The resolution of these models has to be high enough to resolve the dynamics of a tsunami inside a particular harbor, including influences of major harbor structures such as breakwaters. These models have been integrated as crucial components into the forecast system.

Presently, as shown in Figure 1, a system of 55 tsunameter stations, are deployed in the Pacific, Atlantic, Indian Oceans, Caribbean Sea, Gulf of Mexico and South China Sea (40 U.S.-, 8 Australian-, 1 Chilean-, 1 China-, 2 Indian-, 1 Indonesian-, 1 Thailand- and 1 Russian-owned) (Spillane et al., 2008). The pre-computed propagation models currently have 1,725 scenarios covering the major tsunami-genetic subduction zones in the oceans (Table 1), and high-resolution forecast inundation models are now set up for 57 U.S. coastal communities. As of 2013, the fully implemented system uses real-time data from the tsunameter network to provide high-resolution tsunami forecasts for 75 communities in the U.S., with additional models envisioned later for other communities. Since its first

testing in the 17 November 2003 Rat Island tsunami, the forecast system has produced experimental real-time forecasts for more than 20 tsunamis in the Pacific and Indian oceans (Titov et al., 2005; Wei et al., 2008; Titov, 2009; Titov and Tang, 2011; Tang et al., 2012; http://nctr.pmel.noaa.gov/database_devel.html). The forecast method has also been tested with nine additional events that produced deep-ocean tsunamis and near-field tsunamis (http://nctr.pmel.noaa.gov/database_devel.html; Wei et al., 2012).

The recent 2011 Japan tsunami caused severe flooding and damage in the Kailua-Kona area (Figure 2), highlighting the need for a forecast flooding model. This report describes the development, testing and applications of the Kailua-Kona forecast model. The objective is to provide NOAA's Tsunami Warning Centers with the ability to assess the danger of a tsunami generated in the Pacific Ocean on Kailua-Kona, and to enable the community to respond appropriately by providing accurate and timely forecasts. A secondary objective is to explore the potential tsunami impact to the site from earthquakes at major subduction zones in the Pacific.

The report is organized as follows: Section 2 briefly introduces NOAA's tsunami forecast method. Section 3 describes the model development. Section 4 presents the results and discussion, which includes sensitivity of the forecast model to model setup, verification, and testing for past and simulated tsunamis. Summary and conclusions are provided in section 5.

2 Forecast Method

NOAA's real-time tsunami forecasting scheme is a process that comprises two steps: (1) construct a propagation scenario via inversion of deep-ocean tsunameter

measurements with pre-computed tsunami source functions; and (2) run high-resolution forecast models in real time to provide coastal predictions (Titov et al., 1999; 2005; Titov 2009; Tang et al., 2009; 2012). The DART-constrained tsunami source, the corresponding offshore scenario from the tsunami source function database, and high-resolution forecast models cover the entire evolution of earthquake-generated tsunamis, generation, propagation and coastal inundation, providing a complete tsunami forecast capability.

2.1 Constructing a Propagation Scenario Based on Tsunameter Measurements and Tsunami Source Functions

Several real-time data sources, including seismic data, coastal tide gage and deep-ocean data have been used for tsunami warning and forecasting (Satake et al., 2008; Whitmore, 2003; Titov, 2009). NOAA's strategy for the real-time forecasting is to use deep-ocean measurements at tsunameter stations as the primary data source due to several key features. (1) Tsunameters provide a direct measure of tsunami waves, unlike seismic data, which are an indirect measure of tsunamis. (2) The deep-ocean tsunami measurements are in general the earliest tsunami information available, since tsunamis propagate much faster in deep ocean than in shallow coastal areas where coastal tide gages are located. (3) Compared to coastal tide gages, tsunameter data with a high signal to noise ratio can be obtained without interference from harbor and local shelf effects. (4) Wave dynamics of tsunami propagation in deep ocean is assumed to be linear (Kânoğlu and Synolakis, 2006; Liu, 2009). This linear process allows application of efficient inversion schemes.

Time series of tsunami observations in deep-ocean can be decomposed into a linear combination of a set of tsunami source functions in the time domain using a linear Least Squares method (Percival et al., 2011). We call coefficients obtained through this inversion process *tsunami source coefficients*. During real-time tsunami forecasting, seismic waves propagate much faster than tsunami waves. Therefore, the initial seismic magnitude can be estimated before the tsunameter data are available. Since time is of the essence, the initial tsunami forecast is based on the seismic magnitude only. The tsunameter inverted source will update the forecast when it is available.

Titov et al. (1999; 2001) conducted sensitivity studies for far-field tsunamis on different parameters in the elastic deformation model described by Gusiakov (1978) and Okada (1985). The results showed that source magnitude and location essentially define far-field tsunami signals for a wide range of subduction zone earthquakes. Other parameters have secondary influence and can be pre-defined during a forecast. Based on these results, tsunami source function databases for the Pacific, Atlantic, and Indian Oceans have been built using pre-defined source parameters: length = 100 km, width = 50 km, slip = 1 m, rake = 90 and rigidity = 4.5 x 10^{10} N/m^2. Other parameters are location-specific; details of the databases are described in Gica et al. (2008). Each tsunami source function is equivalent to a tsunami from a typical M_w = 7.5 earthquake with defined source parameters. Figure 1a shows the locations of tsunami source functions.

The tsunami source functions in the database are computed with a time step of 10 sec and a spatial resolution of 4 arc min (approximately 7.4 km along the N–S direction). The outputs, offshore wave height and depth-average velocities of the entire domain, are then

compressed and saved every 1 min in time and 16 arc min in space (Tolkova, 2007). The current propagation scenarios do not include inundation and a vertical wall is placed at a 20-m water depth (Gica et al., 2008). The friction term is set to zero. When tsunami waves propagate into shallow water, under the steady-state assumption, where there are not any energy losses or inputs, the decrease in transport speed must be compensated for by an increase in energy density in order to maintain a constant energy flux. The low spatial resolution and simplified boundary conditions of the propagation model result in inaccurate near-shore dynamics. As a consequence, the numerical dissipation (due to the low spatial resolution) will cause energy decay in the propagation modeling (Tang et al., 2012). Based on the consideration of energy conservation, we have developed high-resolution, site-specific inundation forecast models built on the MOST model to simulate the near shore wave dynamics.

Energy released from an earthquake, followed by portions of the earthquake energy transferring into the water column, are complex dynamic processes at this stage of tsunami generation. However, the goal of tsunameter inversion is not to quantify energy at the initial stage of tsunami generation. Instead, we try to quantify the wave energy that propagates outside the source area in the form of surface long gravity waves, which can be well measured by the tsunameter stations. It is also the propagated energy that results in the coastal impacts. Our estimates of the tsunami source (the propagation scenario) focus on the characteristics of tsunami propagation. They are directly constrained by the deep ocean tsunami data. Regardless of the details of earthquake processes for tsunami generation at the initial stage, the inversion can ensure that the propagation scenario gives the best approximation to the tsunami measurements, and therefore, the best estimation of

the total energy transferred by the tsunami waves. The database can immediately provide offshore forecasts of tsunami amplitudes and all other wave parameters once the inversion is complete. The tsunami source, which combines real-time tsunami measurements with tsunami source functions, provides an accurate offshore tsunami scenario without additional time-consuming model runs.

2.2 Coastal Predictions by Using High-Resolution Forecast Models in Real-Time

High-resolution forecast models are designed for the final stage of the evolution of tsunami waves: coastal runup and inundation. Once the tsunameter-constrained tsunami source is obtained (as a linear combination of tsunami source functions), the pre-computed time series of offshore wave height and depth-averaged velocity from the model propagation scenario is applied as the dynamic boundary conditions for the forecast models. This saves the simulation time of basin-wide tsunami propagation. Tsunami inundation and nearshore currents are highly nonlinear processes, therefore a linear combination would not provide accurate solutions. A high-resolution model is also required to resolve shorter tsunami wavelengths nearshore with accurate bathymetric/topographic data. The forecast models are constructed with the Method of Splitting Tsunami (MOST) model, a finite difference tsunami inundation model based on nonlinear shallow-water wave equations (Titov and González*,* 1997). Each forecast model contains three telescoping computational grids with increasing resolution, covering regional, intermediate and nearshore areas. Runup and inundation are computed at the coastline. For example, Figure 3 shows forecast model setup for several tsunami forecast models in Hawaii, detailing the telescoping grids used:

(a) One regional grid of 2-arc-min (~3600m) resolution covers the main Hawaiian Islands (Fig. 3a).

(b) Then the Hawaiian Islands are divided into four intermediate grids of 12- to 18-arc-second (~ 360–540m) for four natural geographic areas (Figs. 3b 1–4):

(b1) Ni'ihau, Ka'ula Rock, and Kauai (Kauai complex),

(b2) Oahu,

(b3) Molokai, Maui, Lanai, and Kaho'olawe (the Maui Complex),

(b4) Hawaii.

(c) Each intermediate grid contains 2-arc-sec (~60 m) nearshore grids (Figs. 3c 1–4). The highest resolution grid includes the population center and coastal water level stations for forecast verification. The grids are derived from the best available bathymetric/topographic data at the time of development, and will be updated as new survey data become available. Forecast models have been developed for 13 coastal communities in Hawaii (Figure 3).

The forecast models are optimized for speed and accuracy. By reducing the computational areas and grid resolutions, each model is optimized to provide 4-hour event forecasting results in 10 min of computational time using one single processor, while still providing good accuracy for forecasting. To ensure forecast accuracy at every step of the process, the model outputs are validated with historical tsunami records and compared to numerical results from a reference inundation model with higher resolutions and larger computational domains. In order to provide warning guidance for long duration during a tsunami event, each forecast model has been tested to output a 24-hour simulation since tsunami generation.

3 Model Development

3.1 Forecast area

The main Hawaiian Islands are the younger and southernmost portion of the Hawaii Archipelago. From northwest to southeast, the islands form four natural geographic groups via shared channels and an inter-island shelf, including (1) Ni'ihau, Ka'ula Rock, and Kauai, (Kauai complex) (2) Oahu, (3) Molokai, Maui, Lanai, and Kaho'olawe, (the Maui Complex), and (4) Hawaii. Kailua-Kona is the chief western city on Hawaii Island. The Port of Kailua-Kona is located in a popular resort area on the western shores of the Big Island. The whole western coastline of Hawaii island is called Kona, and the largest town in the area is Kailua. The 2010 US Census reported a population of almost 12 thousand residents in the Port of Kailua-Kona. Figure 4 presents an aerial photo of this area and a chart is shown in Figure 5. The population density data is in Figure 6.

The Island of Hawaii (Big Island) is located at the southeast end of the Hawaii Archipelago (Fig. 3). To its northwest, there is the Maui complex, with the deep Alenuihaha Channel in between (water depth > 200m). The coast of Kailua-Kona is characterized by sudden steep offshore slopes from 100 m down to 4000 m depth. From 0 to 100 m depth, the slope is quite gentle, only 0.013. From 100 m to 1000 m water depth, it has the steepest offshore slope of 0.3822, and then 0.15 slope from 1000 m to 4000 m depth (Fig. 5).

No coastal water level station exists in the forecast area. The Port of Kailua-Kona is about 47km (29 miles) south-southwest of Kawaihae Harbor and about 97 km (60 miles) west of Hilo Harbor, on the same Hawaii island. At Kawaihae tide station, the mean

range of tide is 0.461 m, and the mean high water is 0.222 m above mean sea level.

3.2 Tsunami History

The Hawaiian Islands have a long history of distant and local destructive tsunamis (Pararas-Carayannis, 1969; Soloviev and Go, 1984; Lander and Lockridge, 1989; Soloviev et al., 1992; Table 2; NGDC, 2009). The descriptions for Kailua-Kona were extracted from the references as follows. The height in Pararas-Carayannis (1969) refers to maximum runup height or amplitude. Walker (2004) summarized the runups on the Island of Hawaii for the 1946, 1952, 1957, 1960 and 1964 tsunamis (Fig. 7).

On 15 June 1896, a tsunami originating from Sanriku, Japan produced a 2.4-m height at Kailua (Pararas-Carayannis, 1969).

On 9 August 1901, a tsunami originating from Rikuchu, Japan, covered the wharf to a depth of 1 m. No damage was reported. (Pararas-Carayannis, 1969). The tsunami reached a 1.2-m height.

On 16 August 1906, a tsunami originating from an earthquake near Talcahuano, Chile caused some damage in Kailua (Pararas-Carayannis, 1969).

On 3 March 1933, a series of ten large waves generated by an earthquake near Sanriku, Japan caused considerable damage at Kailui-Kona. The last wave was the highest (Pararas-Carayannis, 1969).

On 1 April 1946, a 3.3-m height was observed at Kailua for the Unimak tsunami (Pararas-Carayannis, 1969).

On 4 March 1952, a tsunami originating from Hokkaido, Japan, produced a 0.6-m height at Kailua (Pararas-Carayannis, 1969). The 4 November 1952 Kamchatka also produced a 0.6-m height.

On 9 March 1957, a 1.5-m height was reported at Kailua for the Andreanof tsunami.

On 22 May 1960, a 2.4-m height was reported at Kailua for the Chile tsunami (Pararas-Carayannis, 1969).

At 17:07:48 UTC (7:07 AM HST in Hawaii) on 15 October 2006, An Mw 6.5 earthquake occurred 29 km NNE of Kailua-Kona, Hawaii (http://earthquake.usgs.gov/). Numerous people suffered minor injuries, at least 1,173 buildings and numerous roads were damaged, and landslides blocked roads on Hawaii. Power outages occurred throughout the Hawaiian Islands. Damage was estimated at $73 million. A tsunami with a wave height of 10 cm was recorded at Kawaihae Harbor. Earthquakes on the volcanic Island of Hawaii are not rare. The largest on record was the 1868 Mw 7.9 earthquake near the south coast which triggered a tsunami that drowned 46 people and spawned numerous landslides that resulted in 31 deaths (http://earthquake.usgs.gov/). A Mw 6.9 tremor on 21 August 1951 damaged scores of homes on the Kona coast and triggered numerous damaging landslides (http://earthquake.usgs.gov/earthquakes/eqinthenews/2006/ustwbh/#summary).

On 11 March 2011, the Japan tsunami hit hard (Hawaii County, 2011). The following damage was reported by the County of Hawaii:

“King Kamehameha’s Kona Beach Hotel on Ali‘i Drive suffered extensive water damage to its ground floor, and observers reported possible damage to the Ahu‘ena Heiau on the hotel grounds. Shops across Ali‘i Drive from King Kamehameha’s Kona Beach

Hotel also suffered extensive damage. Large amounts of debris were also deposited on Kailua Pier, and two vehicles left parked on the pier were damaged when the tsunami pushed them across the pier. A hall at Pu‘uhonua Road suffered severe damage, while the Puu O Honaunau National Historic Park (City of Refuge) also reported flooding. Extensive damage was reported to businesses on both sides of Ali‘i Drive, including the Bubba Gump Shrimp Company, the ground floor of the Kona Reef Hotel, and the Kona Inn Restaurant. In Kailua-Kona, crews reported one single-family home was destroyed, and one suffered major damage. Six Kailua apartments or condominiums suffered major damage, and 19 had minor damage. The Kona Village Resort had 20 guest units damaged when they were lifted off their foundations. Two restaurants at the resort were flooded. The Four Seasons Resort Hualalai reported water damage to utility buildings, pools and damage to a restaurant at the resort” (Hawaii County, 2011).

Figure 2 shows four photos taken from the 2011 Japan tsunami. As a city that has repeatedly been damaged and flooded by tsunamis, Kaikua-Kona needs a forecast model to aid site-specific evacuation decisions.

3.3 Bathymetry and Topography

Tsunami inundation modeling requires accurate bathymetry in coastal areas as well as high-resolution topography and bathymetry in the nearshore area. Two gridded digital elevation models (DEMs), one at medium resolution (6 arc sec) for the Hawaiian Islands and a high resolution (1/3 arc sec) DEM for Kailua-Kona, were developed by NCTR and NGDC respectively.

3.3.1 Hawaiian DEM in 6-arc-sec resolution

The 6-arc-sec Hawaiian DEM was developed at the NOAA Center for Tsunami Research (NCTR) in 2007. The same source grid has been used for forecast model developments for Hilo, Kahului, Honolulu, Pearl Harbor and Lahaina (Tang et al, 2009; 2010). The grid was compiled from several data sources; Figure 8a is an overview of the spatial extents of each data source used. In areas where multiple datasets overlap, higher-resolution and newer datasets were generally preferred, and superseded datasets were used for comparison and verification. An overview of the data sources used is as follows. In general, the data sources listed first superseded data sources listed later when they overlapped.

Source details for the datasets incorporated into the model grids:

- Joint Airborne Lidar Bathymetry Technical Center of Expertise (JALBTCX), US Army Corps of Engineers, Mobile District. Online reference: http://shoals.sam.usace.army.mil/hawaii/pages/Hawaii_Data.htm.
- Monterey Bay Aquarium Research Institute (MBARI) Hawaii Multibeam Survey, Version 1. Online reference: http://www.mbari.org/data/mapping/hawaii/.
- USGS Pacific Seafloor Mapping Project. Online reference: http://walrus.wr.usgs.gov/pacmaps/data.html.
- Japan Agency for Marine-Earth Science and Technology (JAMSTEC) 1998–1999 multibeam bathymetric surveys. Published in: Takahashi, E., et al., eds. (2002): *Hawaiian Volcanoes: Deep Underwater Perspectives*. American Geophysical Union Monograph 128.

JAMSTEC trackline data was recorded by the R/V *Mirai* during transits near in 1999 and 2002. Online reference: http://www.jamstec.go.jp/mirai/index_eng.html.

- United States Army Corps of Engineers (USACE), Honolulu District. Online reference: http://www.poh.usace.army.mil/.
- NOAA National Geophysical Data Center (NGDC). Online reference: http://www.ngdc.noaa.gov/mgg/gdas/gd_sys.html.
- NOAA National Ocean Service (NOS). Sounding points were digitized from NOS nautical charts 19347, 19358, 19359, 19364, 19366, 19342, 19381, and 19324. Sounding data from electronic chart (ENC) 19357 was used. These data were included in relatively shallow regions where other data sources were sparse or unavailable, or for quality control of other sources.
- Smith, W. H. F., and D. T. Sandwell, Global seafloor topography from satellite altimetry and ship depth soundings, *Science*, v. 277, p. 1957-1962, 26 Sept., 1997. Online reference: http://topex.ucsd.edu/WWW_html/mar_topo.html.
- USGS Geological Long-Range Inclined Asdic (GLORIA) surveys. Online data reference: http://walrus.wr.usgs.gov/infobank/
- NOAA Coastal Services Center (CSC). http://www.csc.noaa.gov/. The Interferometric Synthetic Aperture Radar (IfSAR) topographic data were collected and processed for CSC by Intermap Technologies Inc. The data are subject to a restrictive license agreement and are not publicly available.
- USGS National Elevation Dataset. Online reference: http://seamless.usgs.gov/

The Scanning Hydrographic Operational Airborne Lidar Survey (SHOALS) project, which provides high-resolution unified topographic and bathymetric data around for nearshore areas of several Hawaiian Islands, was essential to accurate modeling of reef and intertidal regions where conventional bathymetric survey data is usually coarse or unavailable. Quality data in this region is especially essential because bathymetric inaccuracies significantly impact tsunami wave dynamics in shallow water. The 2005 NOAA CSC IfSAR survey provided similarly valuable high-resolution topography for the entire island, enabling greater confidence in predicting inundation extents. The USGS National Elevation Dataset (NED) was used on other islands outside of the primary study area.

High-resolution gridded datasets derived from multibeam surveys are available for many parts of the archipelago, and were used wherever available. In deep water where high-resolution multibeam data were not available, the grid was developed by the interpolation of a combination of USGS GLORIA surveys and the Smith and Sandwell (1997) two-minute global seafloor dataset.

All selected input datasets were converted to the mean high water (MHW) vertical datum, as necessary. Bathymetry datasets were converted from the survey tidal datum (usually mean lower low water or mean sea level) using offset surfaces interpolated from NOS tide gauges at Kahului, Kawaihae (Hawaii), and Kaunakakai (Molokai). The CSC IfSAR topographic data were vertically referenced to the GRS80 ellipsoid. It was converted to MHW using an offset surface interpolated from seven National Geodetic Survey (NGS) benchmark stations on Maui that had ellipsoid and tidal heights recorded.

Raw data sources were imported to ESRI ArcGIS-compatible file formats. Horizontal positions were reprojected, where necessary, to the WGS84 horizontal geodetic datum using ArcGIS. In the point datasets, single sounding points that differed substantially from neighboring data were removed. Gridded datasets were checked for extreme values by examination of contour lines, and, where available, by comparison between multiple data sources.

To compile the multiple data sources into a single grid, subsets of the source data were created in the priority order described above. A triangulated irregular network (TIN) was created from the detided vector point data (geodas, usace, csc_lidar). Also added to the TIN were points taken from the edges of the gridded data regions to ensure a smooth interpolated transition between areas with different data sources. This TIN was linearly interpolated using ArcGIS 3D Analyst to produce an intermediate 1-arc-sec and 6-arc-sec raster grid. The gridded datasets were then bilinearly resampled to these resolutions and overlaid on top of the intermediate grids.

3.3.2 Kailua-Kona DEM in 1/3-arc-sec resolution

A high-resolution DEM in 1/3-arc-sec (~10 m) was developed for the Kailua-Kona and Keauhou area by the National Geophysical Data Center (Carignan et al., 2011). The DEM was generated from diverse digital datasets in the region (grid boundary and sources shown in Fig. 8b). The topographical Lidar data from the State of Hawaii Civil Defense/Federal Emergency Management Agency and the Hawaii Department of Business, Economic Development & Tourism have approximately 1-m spatial resolution.

The detail of the data sources and methodology used in developing the DEM can be found in (Carignan et al., 2011).

The bathymetry and topography used in the development of this forecast model was based on the digital elevation model provided by the National Geophysical Data Center and the author considers it to be a good representation of the local topography/bathymetry. As new digital elevation models become available, forecast models will be updated and report updates will be posted at http://nctr.pmel.noaa.gov/forecast_reports/.

3.4 Model Setup

By sub-sampling from the DEMs as described in section 3.3, two sets of computational grids were derived for Kailua-Kona, a reference inundation model (Fig. 9) and the optimized forecast model (Fig. 10). The reference grids consist of four levels of telescoped grids with increasing resolution. The A-grid covers the entire Hawaiian Ridge, Mid-Pacific Mountains, Mellish Seamount, and southern end of the Emperor Seamount Chain including Koko Guyot in 1-arc-min resolution (Fig. 9a). The B-grid covers the Island of Oahu, the Maui Complex and the Island of Hawaii in 6-arc-sec resolution (Fig. 9b). The C-grid covers the southwest coast of Hawaii in 2-arc-sec resolution. D-grid includes Kailua-Kona and Keauhou in 20-m resolution. Runup and inundation simulations are computed on the coastline in C and D grids (Fig. 9c, d). The optimized forecast model has three levels of telescoped grids (Fig. 10). Grid details at each level and input parameters are summarized in Table 3. Since no coastal water level station is in the area, a point (204.0046 °E, 19.6397° N) at 2.3 m water depth near the end of Kailua

Bay was chosen as the warning point (Fig. 9d).

For a 4-hr event simulation, it takes approximately 30 minutes to compute a forecast model using the current operational MOST version 2 (Table 3). With MOST version 4, which has parallel computing capability, the computational time can be reduced to 16 min. MOST 2 requires all grids to start computation simultaneously, while the B- and C-grids of MOST 4 can start computation after the first wave reaches the inner grids. Therefore, MOST 4 can significantly save computational time for tsunamis coming from the east. Table 4 summarizes the computational time for different numbers of processors used for the Kailua-Kona forecast model of the 2011 Japan tsunami. Since it takes a few hours for the first wave to reach the B-grid, the simulation time was set to 8 hours to ensure there is at least a 4-hr tsunami simulation within C-grid.

The Hawaiian A-grid in Fig. 3 (210 × 150 nodes) usually takes 2–10% of the total computational time. However, the large Kailua-Kona A-grid costs 79% of the total computational time, due to its large grid size (1351 x 889 nodes). The efficiency of parallel computing depends on the total node number (grid size). Higher efficiency can be achieved for grids with a greater number of nodes. When the total number of nodes is small, such as the 114 × 334 of the forecast C-grid, multiple processors can actually cost more computational time than a single processor (Table 4).

We also developed a transitional forecast model for Kailua-Kona, which has the regular A-grid as many other forecast sites in Hawaii (Fig. 3a). We refer to it as set 1. It is capable of simulating four hours of tsunami wave dynamics in minutes of computational time. We refer to the forecast model with the larger A grid (same 2-arc-min resolution but with larger coverage) in Figure 10 as set 2. Set 1 serves as a transition for set 2. During

an event, results from set 1 will first become available. Results from set 2 will replace those of set 1 within minutes. The B- and C-grids are identical for both sets. In the next section, we will show and discuss results from set 2.

4 Results and discussion

4.1 Verification and Testing of the Forecast Model

Since no water level station was available at Kailua-Kona, we evaluated the forecast model performance through comparisons of tsunami amplitude time series, peak period, maximum amplitude, and current in the area with results from the reference model.

Both the reference and the forecast models were tested with the sixteen past tsunamis summarized in Table 2. Figure 11 shows the amplitude time series at the warning point computed by both models. Figure 12 shows how the model setup could affect the model results, which will be discussed in section 4.2. The computed maximum water elevation above MHW and maximum current are plotted in Figure 13 for all grids. The 2011 Japan tsunami generated the largest amplitude of 1.38 m at the warning point (Fig. 11(16)). It is also the largest tsunami at Kailui-Kona nearshore among the 16 past events (Fig. 13(16)). The 1960 Chile tsunami produced the largest offshore amplitude around the Hawaiian Islands (Fig. 13(4)). Table 5 summarizes the maximum amplitude (η_{max}) at the warning point for the 16 tsunamis for both reference and forecast models. The two models produce a large discrepancy in η_{max} for the 1946 Unimak and 2011 Japan tsunamis. As will be discussed in section 4.2, the resonant waves of high frequency, which are sensitive to the model setup, contribute to this discrepancy.

Recorded historical tsunamis provide only a limited number of events, from limited locations. More comprehensive test cases of destructive tsunamis with different directionalities are needed to check the stability and robustness of the forecast model. A similar set of eighteen simulated magnitude 9.3 tsunamis as in Tang et al. (2008a; 2008b) was selected here for further testing (Table 6). Results computed by the forecast model are compared with those from the high-resolution reference model in Table 6, and Figures 14 and 15. Both models were numerically stable for all of the scenarios and computed similar maximum water elevation and inundation in the study area (Figs. 14 and 15). Waveforms computed by the forecast model agree well with those of the reference model except tsunamis from the Japan and Izu subduction zones (Fig. 14(1, 8)).

The amplitude time series at the warning point for 34 scenarios shows that tsunami waves with amplitudes that are 2–6 times greater than the first wave can arrive 1–4 hr later (Figs. 11 and 14). Both incident waves from the far-field and local resonances can contribute to the amplified waves. Therefore, a substantially large A-grid, covering the entire Hawaiian Island Chain, Mid-Pacific Mountains, Mellish Seamount and southern end of the Emperor Seamount Chain including Koko Guyot can better capture the amplified late waves, especially when the waves are coming from the northwest. The large A-grid provides a more accurate simulation of the waves interacting with the major wave scatterers that are important to the forecast site, with the cost of longer computational time.

As shown in Figures 13 and 15, the forecast model produced similar patterns of maximum amplitudes and currents as those of the reference model. The Japan, Izu, Kamchatka, Aleutian, Northern Tonga (Samoa), Canada, Southern Chile, and East

Philippines subduction zones can potentially generate large amplitude waves and cause inundation in Kailua-Kona. The computed maximum wave amplitude reaches 5 m at the warning point in the Japan M_w 9.3 scenario. The waterfront near Kona Pier and at end of Kailua Bay is under high flooding risk once inundation occurs in the forecast area.

Tsunami waves in the study area vary significantly for the eighteen Mw 9.3 scenarios (Fig. 15). These results show the complexity and high nonlinearity of tsunami waves and currents nearshore, demonstrating again the value of the forecast model for providing accurate site-specific forecast details.

Wavelet analyses were performed for the 34 scenarios to explore peak resonant periods for the site. Figures 16 and 17 show the amplitude spectrograms for the past and simulated tsunamis, respectively. The spectrograms show a wide range of resonant periods (T_p) from 6 to 126 min. The most common T_p is 8 (±2) min, (for 23 scenarios, or 68% of the testing cases) (Fig. 18). In addition, long resonant periods, such as 67–126 min, can have similar amplitudes as short period waves (Fig. 16(11, 14)). Although the spectrograms of the forecast model show longer T_p of 26 and 38 min for the Mw 9.3 Chile and Central America scenarios, respectively, the short 8-min period, which is the T_p of the reference model, still exists in both spectrograms as the second peak period. The rest of the scenarios show excellent agreement in T_p between the two models.

4.2 Uncertainty of the Forecast Maximum Amplitudes

Tables 5 and 6 and Figure 18 summarize the difference of the computed $\eta_{\max}$ at the warning point between the forecast and reference models for the 34 scenarios (16 past tsunamis and 18 simulated M_w 9.3 scenarios). For the M_w 9.3 scenarios, the forecast

model results show similar η_{max} as those of the reference model except for tsunamis coming from west to north, particularly from the Japan, Izu, Kamchatka and Central Aleutian subduction zones. Among the 16 past tsunamis, the 1946 Unimak tsunami produces the largest discrepancy with a difference of 41% (0.42 m) (reference η_{max} = 1.01 m). The 2011 Japan tsunami shows the second largest discrepancy of 31% (0.43 m) with the reference η_{max} =1.38 m.

Next, we chose the 1946 Unimak tsunami for further testing. Test results reveal η_{max} is very sensitive to the offshore water depth (d_w), a model parameter used for the A- and B-grids at which a vertical wall is placed, of the reference grids for this tsunami. For the same set of reference grids, 20 m and 1 m for d_w produces η_{max} of 1.01 m and 0.47 m, respectively (Fig. 12). That is to say, this difference in d_w increases η_{max} by a factor of two. The forecast model shows η_{max} = 0.7 m and 0.59 m for d_w = 20 m and 1 m, respectively. . Differing d_w may represent varying shoreline shapes, resulting in differing numerical dissipation. Without observations, it is difficult to fine-tune this parameter. As shown in Fig. 16(1), the 1946 Unimak tsunami is the only tsunami showing a strong resonant period of 6 min, lower than the most commonly seen 8 min. This extremely short resonant period may also account for the large discrepancy. The forecast model can underestimate the short period waves due to its low spatial resolution.

Among the 18 M_w = 9.3 scenarios, the No. 1 Japan scenario (T_P = 8 min) produces the largest difference of 1.48 m or 30% (η_{max} =4.95 m for the reference model). The No. 2 Kamchatka and No. 18 Izu scenarios (with (T_P = 8 and 9 min) also show relatively large difference of 0.8 m or 25% (η_{max} =3.36 and 3.49 m for the reference model). One common characteristic of the three scenarios is the late arrival of η_{max}, which is the 10th,

12^{th}, and 12^{th} wave respectively, arriving about 1–2 hr after the first wave (Fig. 14(1, 2 and 18)). For the Japan scenario, even the 24^{th} wave exceeds 3 m elevation (Fig. 14(1)). The multiple scattering of the first wave chain with the major wave scatterers in the northwest Pacific can amplify these later waves (Tang et al., 2012). Therefore late wave chains are sensitively to model setup, such as the grid resolutions and offshore water depth. The coarse forecast A-grid may have more numerical dissipation in shallow water, especially for large amplitude waves of high frequency.

The forecast model was tested with both d_w = 20 m and d_w = 1 m for the 34 scenarios. The results are summarized in Tables 7 and 8. Since d_w = 1 m produces larger later waves for tsunamis from the east, it was chosen for the forecast model.

Figure 18 quantifies the uncertainty in the forecast $\eta_{\max}$. When T_P >10 min, the uncertainty in the forecast $\eta_{\max}$ is within 20%. When $T_P \leqslant$10 min and $\eta_{\max}$ > 1 m, the uncertainty is within 31%. When $\eta_{\max}$ < 1 m, uncertainty is within 25 cm. Scenarios from a portion of the Central Aleutian subduction zones near the Unimak Island may have additional uncertainty (about 0–41%), depending on whether or not a strong resonance of extremely short period (6 min) is excited on the site.

5 Summary and Conclusions

This report documents the development and testing of a tsunami forecast model for the coastal community of Kailua-Kona, Hawaii. The computational grids for the forecast model were derived from the best available bathymetric and topographic data sources at the time of development. The forecast model is optimally constructed at a resolution of 2

arc sec (~60 m). A reference inundation model of higher resolution, 2/3 arc sec (~20 m), was also developed in parallel in order to provide modeling references for the forecast model. Both models were tested for 34 scenarios, including 16 past tsunamis and a set of 18 simulated magnitude 9.3 tsunamis. Since no coastal water level station exists at the forecast site, a point at 2.3-m water depth at the end of Kailua bay, east of Kona Pier, was chosen as the warning point.

The wave analyses of the amplitude time series show a wide range of resonant periods in the site, from 6–126 min. 68% of the tested scenarios have peak resonant period (T_P) near 8 (±2) min. For many cases, waves with very long resonant periods (67–126 min) can have similar influence as those of short periods (6–10 min).

Tsunamis propagating from the west, particularly from Japan, Kamchatka and Izu subduction zones, have shown the late arrival of the maximum wave $\eta_{\max}$ of short period (~8 min). The $\eta_{\max}$ could be the 10^{th} – 12^{th} wave, arriving about 1–4 hr after the first wave. Both incident waves from the far-field and local resonances contribute to the late $\eta_{\max}$.

The numerical consistency between the model outputs on the amplitude time series at warning point, maximum amplitude, and current in the forecast area are good in general. When $T_P > 10$ min, the uncertainty in the forecast $\eta_{\max}$ at the warning point is within 20%. When $T_P \leqslant 10$ min and $\eta_{\max} > 1$ m, the uncertainty is within 30%. When $\eta_{\max} < 1$ m, the uncertainty in $\eta_{\max}$ is within 25 cm. Scenarios from a portion of Central Aleutian subduction zones near Unimak Islands may have additional uncertainty (about 0–41%), depending on whether or not a strong resonance of extremely low period (6 min) is excited at the site.

The developed forecast model involves a substantially large A-grid (2 arc min), covering the entire Hawaiian Island Chain, Middle Pacific Mountains, Mellish Seamount and Koko Guyot. It can provide a more accurate simulation of the waves interacting with the major wave scatterers that are important to the forecast site, with the cost of longer computational time. It should be noted that the forecast system would adapt MOST version 4, which will have parallel computation capability in the near future and reduce computation time to minutes. We also developed a transitional forecast model for Kailua-Kona, which has the smaller, regular A-grid as many other forecast sites in Hawaii. We refer to it as set 1. It is capable of simulating four hours of tsunami wave dynamics in minutes of computational time. We refer to the forecast model with the larger A grid as set 2. Set 1 serves as a transition for set 2. During an event, results from set 1 will first become available. Results from set 2 will replace those of set 1 within minutes. The B- and C-grids are identical for both sets.

In order to achieve a timely and effective forecast, and as a transition before MOST version 4 becomes operational, we developed a transitional forecast model for Kailua-Kona, which has the smaller, regular Hawaiian A-grid as other forecast sites on the Big Island, e.g. Kawaihae and Hilo forecast models. We refer to it as set 1. It is capable of simulating four hours of tsunami wave dynamics in minutes of computational time. We refer to the forecast model with the larger A grid here as set 2. Set 2 will replace results from set 1 during real time, when it is available.

The Japan, Kamchatka, Izu, Northern Tonga (Samoa), Aleutian, Southern Chile, East Philippines, and Canada subduction zones can potentially generate large amplitude waves and cause inundation in Kailua-Kona. The computed maximum wave amplitude reaches

1.38 m and 5 m at the warning point for the 2011 Japan tsunami and the M_w 9.3 Japan scenario, respectively, among the past events and simulated scenarios. For the M_w 9.3 Japan scenario, even the 24th wave exceeds 3-m elevation. The waterfront near Kona Pier and the end of Kailua Bay are under high flooding risk once inundation occurs in the forecast area.

Due to the unique tsunami-resonant characteristics of the site, a coastal water level station is highly recommended for Kailua-Kona area, in order to provide tsunami data for model calibration and to improve forecast accuracy.

Acknowledgements

The author thanks Elena Tolkova for MOST version 4 development; Jean Newman for preparing the cover page; Michael Dunlap and Sandra Bigley for comments and editing; Burak Uslu for providing tables and graphics for the propagation database. Collaborative contributions of the National Weather Service, the National Geophysical Data Center, and the National Data Buoy Center were invaluable.

Funding for this publication and all work leading to development of a tsunami forecast model for Kailua-Kona, Hawaii was provided by the National Oceanic and Atmospheric Administration. This publication is partially funded by the Joint Institute for the Study of the Atmosphere and Ocean (JISAO) under NOAA Cooperative Agreement NA10OAR4320148, Contribution No. 2122. This is PMEL Contribution No. 3412.

References

Arcas, D., and B. Uslu (2010): A Tsunami Forecast Model for Crescent City, California. NOAA OAR Special Report, *PMEL Tsunami Forecast Series*: Vol. 2, 112 pp, Gov. Print. Off., Seattle, Wash.

Bernard, E.N., H.O. Mofjeld, V.V. Titov, C.E. Synolakis, and F.I. González (2006): Tsunami: Scientific frontiers, mitigation, forecasting, and policy implications. *Proc. Roy.* Soc. Lon. A, 364(1845), 1989–2007, doi: 10.1098/rsta.2006.1809.

Bernard, E.N., and V.V. Titov (2007): Improving tsunami forecast skill using deep ocean observations. *Mar. Technol. Soc. J., 40*(3), 23–26.

Carignan, K.S., L.A. Taylor, B.W. Eakins, D.Z. Friday, P.R. Grothe, E. Lim and M. Love (2011): Digital Elevation Models of Keauhou and Kawaihae, Hawaii: Procedures, Data Sources and Analysis. NOAA National Geophysical Data Center (NGDC).

Gica, E., M.C. Spillane, V.V. Titov, C.D. Chamberlin, and J.C. Newman (2008): Development of the forecast propagation database for NOAA's Short-Term Inundation Forecast for Tsunamis (SIFT). *NOAA Tech. Memo. OAR PMEL-139*, 89pp., Gov. Print. Off., Seattle, Wash.

Gusiakov, V.K. (1978): Static displacement on the surface of an elastic space. Ill-posed problems of mathematical physics and interpretation of geophysical data. Novosibirsk, VC SOAN SSSR, 23–51 (in Russian).

González, F.I., E.N. Bernard, C. Meinig, M. Eble, H.O. Mofjeld, and S. Stalin (2005): The NTHMP tsunameter network. *Nat. Hazards, 35*(1), Special Issue, U.S. National Tsunami Hazard Mitigation Program, 25-39.

Hawaii County (2011): Hawaii County Surveys Tsunami Damage, Kona hit hard. http://www.bigislandvideonews.com/2011/03/11/hawaii-county-surveys-tsunami-damage-kona-hit-hard/.

Kânoğlu, U., and C.E. Synolakis (2006): Initial value problem solution of nonlinear shallow water wave equations, *Phys. Rev. Lett*., 97(14), 148501, doi:10.1103/PhysRevLett.97.148501.

Lander, J.F., and P.A. Lockridge (1989): United States Tsunamis 1690-1988. NOAA National Environmental Satellite, Data and Information Service, National Geophysical Data Center, Boulder, Colorado, August 1989, 265pp.

Liu, P.L.-F. (2009): Tsunami modeling—Propagation, in *The Sea*, Vol. 15, edited by E. Bernard and A. Robinson, chap. 9, pp. 295– 319, Harvard Univ. Press, Cambridge, Mass.

López, A.M., and E.A. Okal (2006): A seismological reassessment of the source of the 1946 Aleutian 'tsunami' earthquake. *Geophysical Journal International, 165*(3), Page 835-849, Jun 2006, doi: 10.1111/j.1365-246X.2006.02899.x.

Meinig, C., S.E. Stalin, A.I. Nakamura, F. González, and H.G. Milburn (2005): Technology Developments in Real-Time Tsunami Measuring, Monitoring and Forecasting. In Oceans 2005 MTS/IEEE, 19–23 September 2005, Washington, D.C.

NGDC (2009): Global Tsunami Database (2000 BC to present). National Geophysical Data Center, http://www.ngdc.noaa.gov/seg/hazard/tsu_db.shtml.

Okada, Y. (1985): Surface deformation due to shear and tensile faults in a half-space. *Bull. Seismol. Soc. Am., 75*, 1135-1154.

Pararas-Carayannis, G. (1969): *Catalog of Tsunamis in The Hawaii Islands*. World Data Center A Tsunami, ESSA – Coast and Geodetic Survey, 94 pp.

Percival, D.B., D.W. Denbo, M.C. Eble, E. Gica, H.O. Mofjeld, M.C. Spillane, L. Tang, and V.V. Titov (2011): Extraction of tsunami source coefficients via inversion of DART® buoy data. *Nat. Hazards, 58*(1), doi: 10.1007/s11069-010-9688-1, 567–590.

Satake, K., Y. Hasegawa, Y. Nishimae, and Y. Igarashi (2008): Recent Tsunamis That Affected the Japanese Coasts and Evaluation of JMA's Tsunami Warnings. OS42B-03, AGU Fall Meeting, San Francisco.

Smith, W.H.F., and D.T. Sandwell (1997): Global seafloor topography from satellite altimetry and ship depth soundings. *Science, 277*, 1957–1962.

Soloviev, S.L., and Ch.N Go (1984): *Catalog of Tsunamis on the Eastern Shore of Pacific Ocean*. Canadian Translation of Fisheries and Aquatic Sciences, No. 5078, 293 pp.

Soloviev, S.L., Ch.N Go, and Kh.S Kim (1992): *Catalog of Tsunamis in The Pacific* 1969-1982. Results of Researches on The International Geophysical Projects,

Academy of Sciences of the USSR Soviet Geophysical Committee, Moscow, 1992, 208 pp.

Spillane, M.C., E. Gica, V.V. Titov, and H.O. Mofjeld (2008): Tsunameter network design for the U.S. DART® arrays in the Pacific and Atlantic Oceans, *Tech. Memo, OAR PMEL-143*, 165pp., Gov. Print. Off., Seattle, Wash.

Synolakis, C.E., E.N. Bernard, V.V. Titov, U. Kânoğlu, and F.I. González (2008): Validation and verification of tsunami numerical models. *Pure Appl. Geophys165.,* (11–12), 2197–2228.

Tang, L., C.D. Chamberlin, E. Tolkova, M. Spillane, V.V. Titov, E.N. Bernard, and H.O. Mofjeld (2006): Assessment of potential tsunami impact for Pearl Harbor, Hawaii. *NOAA Tech. Memo. OAR PMEL-131*, 36 pp., Gov. Print. Off., Seattle, Wash.

Tang, L., C. Chamberlin and V.V. Titov, (2008a): Developing tsunami forecast inundation models for Hawaii: procedures and testing, *NOAA Tech. Memo., OAR PMEL -141*, 46 pp., Gov. Print. Off., Seattle, Wash.

Tang, L., V.V. Titov, Y. Wei, H.O. Mofjeld, M. Spillane, D. Arcas, E.N. Bernard, C. Chamberlin, E. Gica, and J. Newman (2008b): Tsunami forecast analysis for the May 2006 Tonga tsunami. *J. Geophys. Res., 113*, C12015, doi: 10.1029/2008JC004922.

Tang, L., V.V. Titov, and C.D. Chamberlin (2009): Development, Testing, and Applications of Site-specific Tsunami Inundation Models for Real-time Forecasting. *J. Geophys. Res., 114*, C12025, doi:10.1029/2009JC005476.

Tang, L., V.V. Titov, and C.D. Chamberlin (2010): A Tsunami Forecast Model for Hilo, Hawaii. *NOAA OAR Special Report, PMEL Tsunami Forecast Series*, Vol. 1, 44 pp., Gov. Print. Off., Seattle, Wash.

Tang, L., V.V. Titov, E.N. Bernard, Y. Wei, C. Chamberlin, J.C. Newman, H. Mofjeld, D. Arcas, M. Eble, C. Moore, B. Uslu, C. Pells, M.C. Spillane, L.M. Wright, and E. Gica (2012): Direct energy estimation of the 2011 Japan tsunami using deep-ocean pressure measurements. *J. Geophys. Res., 117*, C08008, doi:10.1029/2011JC007635.

Titov, V.V., C.W. Moore, D.J.M. Greenslade, C. Pattiaratchi, R. Badal, C.E. Synolakis, and U. Kânoğlu (2011): A new tool for inundation modeling: Community Modeling Interface for Tsunamis (ComMIT). *Pure Appl. Geophys., 168*, 2121–2131, doi:10.1007/s00024-011-0292-4.

Titov, V.V., and L. Tang (2011): Estimating tsunami magnitude in real time using tsunameter data, paper presented at XXV IUGG General Assembly, Melbourne, Victoria, Australia, 28 Jun to 7 Jul.

Titov, V.V. (2009): Tsunami forecasting. Chapter 12 in *The Sea*, Vol. 15: Tsunamis, Harvard University Press, Cambridge, MA and London, England, 371–400.

Titov, V.V., F.I. González, E.N. Bernard, M.C. Eble, H.O. Mofjeld, J.C. Newman, and A.J. Venturato (2005): Real-time tsunami forecasting: Challenges and solutions. *Natural Hazards, 35*(1), Special Issue, U.S. National Tsunami Hazard Mitigation Program, 41–58.

Titov, V.V., H.O. Mofjeld, F.I. González, and J.C. Newman (2001): Offshore forecasting of Alaskan tsunamis in Hawaii. In *Tsunami Research at the End of a Critical Decade*, edited by G.T. Hebenstreit, pp. 75-90 Kluwer Acad., Dordrecht, Netherlands.

Titov, V.V., H.O. Mofjeld, F.I. González, and J.C. Newman (1999): Offshore forecasting of Alaska-Aleutian subduction zone tsunamis in Hawaii. *NOAA Tech. Memo. ERL PMEL-114*, January 1999, 22 pp., Gov. Print. Off., Seattle, Wash.

Titov, V.V., and C.S. Synolakis (1998): Numerical modeling of tidal wave runup. *Journal of Waterway, Port, Coastal and Ocean Engineering, ASCE, 124*(4), 157-171.

Titov, V.V., and F.I. González (1997): Implementation and testing of the Method of Splitting Tsunami (MOST) model. *NOAA Tech. Memo. ERL PMEL-112*, 11 pp., Gov. Print. Off., Seattle, Wash.

Tolkova, E. (2007): Compression of MOST Propagation Database. *NOAA Tech. Memo. OAR PMEL-134*, 9 pp., Gov. Print. Off., Seattle, Wash.

Pararas-Carayannis, G.(1969): Catalog of Tsunamis in The Hawaii Islands, World Data Center A Tsunami, ESSA – Coast and Geodetic Survey, 94 pp.

Walker, D.A. (2004): Regional Tsunami evacuations for the state of Hawaii: a feasibility study on historical runup data. *Science of Tsunami Hazards, 22*(1), 3-22.

Wei, Y., E. Bernard, L. Tang, R. Weiss, V. Titov, C. Moore, M. Spillane, M. Hopkins, and U. Kânoğlu (2008): Real-time experimental forecast of the Peruvian tsunami of August 2007 for U.S. coastlines. *Geophys. Res. Lett., 35*, L04609, doi: 10.1029/2007GL032250.

Wei, Y., and D. Arcas (2010): A tsunami forecast model for Kodiak, Alaska. *NOAA OAR Spec. Rep./PMEL Tsunami Forecast Ser. 4*, 96 pp., Gov. Print. Off., Seattle, Wash.

Wei, Y., C. Chamberlin, V.V. Titov, L. Tang, and E.N. Bernard (2012): Modeling of 2011 Japan Tsunami - lessons for near-field forecast. *Pure Appl. Geophys*., doi: 10.1007/s00024-012-0519-z.

Whitmore, P.M. (2003): Tsunami amplitude prediction during events: A test based on previous tsunamis. In *Science of Tsunami Hazards, 21*, 135–143.

Table 1. Tsunami source functions in the Pacific, Atlantic and Indian Oceans.

Source Zone			Tsunami source functions	
No.	**Abbr.**	**Name**	**Line/zone**	**Numbers**
1	ACSZ	Aleutian-Alaska-Canada-Cascadia	BAZYXW	184
2	CSSZ	Central-South American	BAZYX	382
3	EPSZ	East Philippines	BA	44
4	KISZ	Kamchatka-Kuril-Japan Trench-Izu Bonin-Marianas-Yap	BAZYXW	229
5	MOSZ	Manus Ocean Convergence Boundary	BA	34
6	NVSZ	New Britain-Solomons-Vanuatu	BA	74
7	NGSZ	North New Guinea	BA	30
8	NTSZ	New Zealand-Kermadec-Tonga	BA	81
9	NZSZ	South New Zealand	BA	14
10	RNSZ	New Ryukus-Kyushu-Nankai	BA	44
11	KISZ	Kamchatskii-Bering Source Zone	BAZ	13
			Subtotal:	**1129**
12	ATSZ	Atlantic	BA	214
13	SSSZ	South Sandwich	BAZ	33
			Subtotal:	**247**
14	IOSZ	Adaman-Nicobar-Sumatra-Java	BAZY	307
15	MKSZ	Makran	BA	20
16	WPSZ	West Philippines	BA	22
			Subtotal:	**349**
			Total:	

Table 2 Tsunami sources for past events.

Earthquake / Seismic				Model		
Event	**USGS Date Time (UTC) Epicenter**	**CMT Date Time (UTC) Centroid**	**Magnitude Mw (CMT)**	**Tsunami Magnitude[1]**	**Subduction Zone**	**Tsunami Source**
1946 Unimak	01 Apr 12:28:56 52.75ºN 163.50ºW	n/a	[2]8.5	8.5	Aleutian-Alaska-Cascadia (ACSZ)	7.5 × b23 + 19.7 × b24 + 3.7 × b25
1952 Kamchatka	04 Nov 16:58:26.0 [3]52.76ºN 160.06ºE	n/a	[3]9.0	8.7	Kamchatka-Kuril-Japan-Izu-Mariana-Yap (KISZ)	Tang et al. (2006)
1957 Andreanov	09 Mar 14:22:31 51.56ºN 175.39ºW	n/a	[3]8.6	8.7	Aleutian-Alaska-Cascadia (ACSZ)	31.4 × a15 + 10.6 × a16 + 12.2 × a17
1960 Chile	22 May 19:11:14 [3]38.29ºS 73.05ºW	n/a	[4]9.5	n/a	Central-South America (CSSZ)	Kanamori & Ciper (1974)
1964 Alaska	28 Mar 03:36:00 [3]61.02ºN 147.65ºW	n/a	[3]9.2	8.9	Aleutian-Alaska-Cascadia (ACSZ)	15.4 × a34+19.4×a35+ 48.3 × z34+18.3×b34+15.1×b35
1994 East Kuril	04 Oct 13:22:58 43.73ºN 147.321ºE	04 Oct 13:23:28.5 43.60ºN 147.63ºE	8.3	8.2	Kamchatka-Kuril-Japan-Izu-Mariana-Yap (KISZ)	1.3 × a20 + 3.2 × z19 +5.9 × b20
1996 Andreanov	10 Jun 04:03:35 51.56ºN 175.39ºW	10 Jun 04:04:03.4 51.10ºN 177.410ºW	7.9	8.0	Aleutian-Alaska-Cascadia (ACSZ)	5.55 × b15
2003 Hokkaido	25 Sep 19:50:06 41.775ºN 143.904ºE	25 Sep 19:50:38.2 42.21ºN 143.84ºE	8.3	8.0	Kamchatka-Kuril-Japan-Izu-Mariana-Yap (KISZ)	3.6m × (100 × 100km) 109#rake, 20#dip, 230#strike, 25 m depth
2003 Rat Island	17 Nov 06:43:07 51.13ºN 178.74ºE	17 Nov 06:43:31.0 51.14ºN 177.86ºE	7.7	7.9	Aleutian-Alaska-Cascadia (ACSZ)	2.7 × b11 + 0.9 × a12
2006 Tonga	03 May 15:26:39 20.13ºS 174.161ºW	03 May 15:27:03.7 20.39ºS 173.47ºW	8.0	8.0	New Zealand-Kermadec-Tonga (NTSZ)	6.6 × b29 (Tang *et al*., 2008)
2006 Kuril	15 Nov 11:14:16 46.607ºN 153.230ºE	15 Nov 11:15:08 46.71ºN 154.33ºE	8.3	8.1	Kamchatka-Kuril-Japan-Izu-Mariana-Yap (KISZ)	3.2×a12+6.0×z12
2007 Kuril	13 Jan 04:23:20 46.272ºN 154.455ºE	13 Jan 04:23:48.1 46.17ºN 154.80ºE	8.1	7.8	Kamchatka-Kuril-Japan-Izu-Mariana-Yap (KISZ)	-3.2 × b13
2007 Solomon	01 Apr 20:39:56 8.481ºS 156.978ºE	01 Apr 20:40:38.9 7.76ºS 156.34ºE	8.1	8.2	New Britain-Solomons-Vanuatu (NVSZ)	12.0 × b10
2007 Peru	15 Aug 23:40:57 13.354ºS 76.509ºW	15 Aug 23:41:57.9 13.73ºS 77.04ºW	8.0	8.3	Central-South America (CSSZ)	3.6×a62+5.7×z63+5.3×b62
2009 Samoa	29 Sep 17:48:10 15.509ºS 172.034ºW	29 Sep 17:48:26.8 15.13ºS 171.97ºW	8.1	8.2	New Zealand-Kermadec-Tonga (NTSZ)	a34×6.4+3.2×c35
2010 Chile	27 Feb 06:34:14 35.909ºS 72.733ºW	27 Feb 06:35:15.4 35.95ºS 73.15ºW	8.8	8.8	Central-South America (CSSZ)	a87× 9.68+z88 ×24.5+a88×15.35+a91× 13.19+z92×24.82

[1] Preliminary source – derived from tsunami source functions and deep-ocean observations
[2] López and Okal (2006)
[3] United States Geological Survey (USGS)
[4] Kanamori and Ciper (1974)
[5] Tsunami source was obtained in real time and applied to the forecast

2011 Japan	11 March 05:46:23 38.322ºN 142.369 E	11 March 05:47:32.8 37.52ºS 143.05 E	9.1	8.8	Kamchatka-Kuril-Japan-Izu-Mariana-Yap (KISZ)	[5]4.66× b24 + 12.23 ×b25+26.31× a26+21.27×b26+22.75 ×a27+4.98× b27

Table 3. MOST setups of Kona reference and forecast models.

Grid	Region	Reference Model				Forecast model		
		Coverage Lon. (^{o}E) Lat. (^{o}N)	Cell Size (")	Time Step (sec)		Coverage Lon. (^{o}E) Lat. (^{o}N)	Cell Size (")	Time Step (sec)
A	Hawaii	165 - 210 10.4 - 40	60 (2701x 1777)	4	A	199 - 205.9667 18.0317 - 22.9983	120 (1351 x 889)	8.4
B	Big Island	201-206 17.5-22	6 (3001 x 2701)	0.7	B	202.84833 - 205.395 18.695 - 21.4283	24 (383 x 411)	2.8
C	Southeast Big Island	2203.87 – 204.1392 19.015 – 19.8483	2 (482 x 1501)	0.3	C	203.9248 - 204.0594 19.47065 - 19.8161	2-6 (144 x 334)	0.4
D	Kona	203.9388-204.0879	2/3 (806 x 1313)	0.12				

Minimum offshore depth (m)		20	1
Water depth for dry land (m)		0.1	0.1
Manning coefficient		0.025	0.04
Computational time for a 4-hr simulation	MOST V2		**30 minutes**
	MOST V4, 1 processor		**16 minutes**
	MOST V4, 2 processors		**10 minutes**

Table 4. Computational time vs. number of processors used for the Kona forecast model with MOST version 4. Results are based on an 8-hr event simulation of the 2011 Japan tsunami.

Number of Processors	1	2	4	8	16
A-grid (min)	26.0	18.1	11.4	6.9	4.9
B-grid (min)	3.2	2.2	1.6	1.3	1.3
C-grid (min)	4.0	3.2	2.9	4.0	4.5
Total time (min)	33.1	23.5	15.8	12.2	10.6

Table 5. Maximum wave crest at the Kona warning point computed by the reference and forecast models.

No.	Event ID	Ref. model η_{max} (m)	Ref. model tmax (hour)	Forecast Model η_{max} (m)	Forecast Model tmax (hour)	Error (m)	Error (%)
1	19460401	0.47	5.717	0.59	5.489	0.12	25
2	19521104	0.35	7.973	0.24	9.945	-0.11	-31
3	19570309	0.78	8.273	0.55	8.571	-0.24	-30
4	19600522	0.63	14.857	0.63	14.876	-0.01	0
5	19640328	0.21	6.612	0.15	5.558	-0.06	-27
6	19941004	0.34	9.918	0.28	9.933	-0.06	-17
7	19960610	0.25	8.217	0.17	10.493	-0.08	-32
8	20030925	0.04	9.218	0.03	9.222	-0.01	0
9	20031117	0.10	7.791	0.07	7.931	-0.04	-35
10	20060503	0.13	7.553	0.12	7.558	-0.01	0
11	20061115	0.10	8.184	0.10	8.210	-0.00	0
12	20070113	0.15	8.446	0.12	10.102	-0.03	-22
13	20070815	0.02	13.053	0.02	13.067	-0.00	0
14	20090929	0.17	6.217	0.16	6.213	-0.00	0
15	20100227	0.22	15.851	0.22	15.851	-0.00	0
16	20110311	1.38	8.718	0.95	8.748	-0.43	-31

Table 6. Sources of the 18 M_w 9.3 synthetic tsunamis and maximum wave crest at the Kona warning point computed by the reference and forecast models.

No.	Subd. Zone	Source alpha	Ref. model η_{max} (m)	Ref. model tmax (hour)	Forecast Model η_{max} (m)	Forecast Model tmax (hour)	Error (m)	Error (%)	Location
1	KISZ AB	22-31 29	4.95	8.866	3.47	8.884	-1.48	-30	Japan
2	KISZ AB	1-10 29	3.36	7.977	2.53	8.008	-0.83	-25	Kamchatka
3	ACSZ AB	16-25 29	2.49	7.519	1.91	5.512	-0.58	-23	Central Aleutian
4	ACSZ AB	22-31 29	1.54	7.212	1.58	6.038	0.03	2	Unimak
5	ACSZ AB	50-59 29	1.33	7.970	1.52	6.215	-1.21	14	Canada
6	ACSZ AB	56-65 29	0.80	6.767	0.61	7.040	-0.20	-25	Cascadia
7	CSSZ AB	1-10 29	0.26	7.170	0.26	7.164	-0.00	0	Central American
8	CSSZ AB	41-50 29	0.27	12.300	0.27	12.302	0.00	0	Columbia-Ecuador
9	CSSZ AB	86-95 29	0.97	16.433	0.80	16.429	-0.16	-17	Chile
10	CSSZ AB	100-109 29	2.39	16.534	2.31	16.384	-0.07	-3	Southern Chile
11	NTSZ AB	20-29 29	0.63	8.463	0.58	8.465	-0.05	-8	Tonga
12	NTSZ AB	30-39 29	2.81	6.166	2.68	6.171	-0.13	-5	Northern Tonga
13	NVSZ AB	28-37 29	1.02	8.034	1.18	8.029	0.16	16	Vanuatu
14	MOSZ AB	1-10 29	1.13	8.300	1.19	8.275	0.05	5	Manus
15	NGSZ AB	3-12 29	0.34	11.700	0.31	11.715	-0.03	-9	New Guinea
16	EPSZ AB	6-15 29	1.89	11.752	1.74	11.732	-0.15	-8	East Philippines
17	RNSZ AB	12-21 29	0.81	10.551	0.71	10.529	-0.10	-12	Nankai
18	KISZ AB	32-41 29	3.49	8.984	2.65	8.998	-0.84	-24	Izu

Table 7. Maximum sea surface elevation at the Kona warning point computed by the forecast model with 1- and 20-m offshore water depths for past tsunamis.

No.	Event ID	d_w =1m η_{max} (m)	tmax (hour)	d_w =20m η_{max} (m)	tmax (hour)	Error (m)	Error (%)
1	19460401	0.59	5.489	0.70	5.734	0.12	20
2	19521104	0.24	9.945	0.32	8.342	0.08	33
3	19570309	0.55	8.571	0.52	8.571	-0.02	-4
4	19600522	0.63	14.876	0.63	14.876	0.00	0
5	19640328	0.15	5.558	0.16	6.622	0.01	0
6	19941004	0.28	9.933	0.28	9.926	0.00	0
7	19960610	0.17	10.493	0.17	11.305	-0.01	0
8	20030925	0.03	9.222	0.03	9.222	0.00	0
9	20031117	0.07	7.931	0.07	7.931	-0.00	0
10	20060503	0.12	7.558	0.11	7.558	-0.00	0
11	20061115	0.10	8.210	0.10	8.210	-0.00	0
12	20070113	0.12	10.102	0.13	8.485	0.00	0
13	20070815	0.02	13.067	0.02	13.067	-0.00	0
14	20090929	0.16	6.213	0.16	6.213	-0.00	0
15	20100227	0.22	15.851	0.22	15.851	-0.00	0
16	20110311	0.95	8.748	0.87	8.867	-0.08	-8

Table 8. Maximum sea surface elevation at the Kona warning point computed by the forecast model with 1- and 20-m offshore water depth for simulated M_w 9.3 tsunamis.

No.	Subd. Zone	Source alpha	d_w =1 m η_{max} (m)	tmax (hour)	d_w =20 m η_{max} (m)	tmax (hour)	Error (m)	Error (%)	Location
1	KISZ AB	22-31 29	3.47	8.884	3.16	8.891	-0.31	-9	Japan
2	KISZ AB	1-10 29	2.53	8.008	2.50	8.344	-0.03	-1	Kamchatka
3	ACSZ AB	16-25 29	1.91	5.512	2.05	5.512	0.14	7	Central Aleutian
4	ACSZ AB	22-31 29	1.58	6.038	1.48	5.541	-0.09	-6	Unimak
5	ACSZ AB	50-59 29	1.52	6.215	1.82	6.215	0.30	20	Canada
6	ACSZ AB	56-65 29	0.61	7.040	0.53	6.081	-0.08	-13	Cascadia
7	CSSZ AB	1-10 29	0.26	7.164	0.28	9.866	0.03	12	Central American
8	CSSZ AB	41-50 29	0.27	12.302	0.27	12.295	-0.00	0	Columbia-Ecuador
9	CSSZ AB	86-95 29	0.80	16.429	0.76	16.429	-0.05	-6	Chile
10	CSSZ AB	100-109 29	2.31	16.384	2.26	16.384	-0.05	-2	Southern Chile
11	NTSZ AB	20-29 29	0.58	8.465	0.59	8.465	0.01	0	Tonga
12	NTSZ AB	30-39 29	2.68	6.171	2.71	6.171	0.03	1	Northern Tonga
13	NVSZ AB	28-37 29	1.18	8.029	1.18	8.029	0.00	0	Vanuatu
14	MOSZ AB	1-10 29	1.19	8.275	1.18	8.275	-0.01	0	Manus
15	NGSZ AB	3-12 29	0.31	11.715	0.29	11.715	-0.03	-8	New Guinea
16	EPSZ AB	6-15 29	1.74	11.732	1.83	11.725	0.09	5	East Philippines
17	RNSZ AB	12-21 29	0.71	10.529	0.70	10.529	-0.01	0	Nankai
18	KISZ AB	32-41 29	2.65	8.998	2.30	8.998	-0.35	-13	Izu

Appendix A. MOST Input Files

The following appendix lists the input files for Kona developed in 2012.

A1. Reference model *.in file for Kona , Hawaii for MOST version 4.0

```
# ----------   MOST Run 1  -------------
# 0. Preparations
echo '#-------------------------------------------------#'
echo '#                Preprocess MOST input         #'
echo '#-------------------------------------------------#'
set main_dir="/home/tg23/data/tang/sims/kona/"
set path_w="$main_dir/konav4_H12_20070113_rb3_12h/"
set path_e="/grid/tg23/data/tolkova/public_html/v4/v4code/RttdMost_mp"

if ( -d $path_w )  then
echo $path_w 'exist'
echo ' Removing files '
  cd $path_w
#   rm -r *
else
  echo Creating directory $path_w
  mkdir $path_w
  cd  $path_w
endif

ln -sf /home/tg23/data/tang/bathy/kona/kona_rb3r1/*.nc .

# ------------------------------------------------------------
# 1. Generate INPUT for MOST
# ~~~~~~~~~~~~~~~~~~~~~~~~
# ~~~~~~~~~~~A~~~~~~~~~~~~
cat > most3_facts_nc.inA<< EOF
0.001     Minimum amplitude of input offshore wave (m):
20        Input minimum depth for offshore (m)
0.1       Input "dry land" depth for inundation (m)
0.0009     Input friction coefficient (n**2)
2         Number of grids
2          Interpolation domain for outer boundary
2          inner boundary
RA_HI_1min_20120417.nc
RB_keauhou_6s_20111107.nc
1           Runup flag
4      Input time step (sec)
10800     Input amount of steps
0              COntunue after input stops
15     Input number of steps between snapshots
1      saving inner boundaries every n-th timestep
1        ...Saving grid every n-th node, n=
0        1=initial deformation
EOF
cp most3_facts_nc.inA most3_facts_nc.in
```

```
setenv OMP_NUM_THREADS 6
#$path_e A  $path_src most3_facts_nc.in
# ~~~~~~~~~~~~~~~~~~~~~~

# ~~~~~~~~~~~B~~~~~~~~~~~~
cat > most3_facts_nc.inB<<EOF
0.001     Minimum amplitude of input offshore wave (m):
20        Input minimum depth for offshore (m)
0.1       Input "dry land" depth for inundation (m)
0.0009    Input friction coefficient (n**2)
2         Number of grids
2         Interpolation domain for outer boundary
2         inner boundary
RB_keauhou_6s_20111107.nc
RC_BIgIs_SW2s_20120417.nc
1           Runup flag
0.7       Input time step (sec)
61714     Input amount of steps
0             COntunue after input stops
86    Input number of steps between snapshots
1     saving inner boundaries every n-th timestep
1       ...Saving grid every n-th node, n=
0       1=initial deformation
EOF
cp most3_facts_nc.inB most3_facts_nc.in
setenv OMP_NUM_THREADS 4
# $path_e B A most3_facts_nc.in

# ~~~~~~~~~~~C~~~~~~~~~~~~
cat > most3_facts_nc.inC<< EOF
0.001      Minimum amplitude of input offshore wave (m):
-300       Input minimum depth for offshore (m)
0.1        Input "dry land" depth for inundation (m)
0.0016     Input friction coefficient (n**2)
2          Number of grids
2
2
RC_BIgIs_SW2s_20120417.nc
RD_Keauhou_Kona_20m_20120424.nc
2          runup
0.3        Input time step (sec)
320000     Input amount of steps
0          countinue after input stop
100        Input number of steps between snapshots
1          ...Saving inner boundary
1          ...Saving grid every n-th node, n=
0
EOF
cp most3_facts_nc.inC most3_facts_nc.in
setenv OMP_NUM_THREADS 2
$path_e C B  most3_facts_nc.in
# ~~~~~~~~~~~~~~~~~~~~~~~~
# ~~~~~~~~~~~D~~~~~~~~~~~~
cat > most3_facts_nc.inD<< EOF
0.001      Minimum amplitude of input offshore wave (m):
-300       Input minimum depth for offshore (m)
0.1        Input "dry land" depth for inundation (m)
0.0009     Input friction coefficient (n**2)
1          Number of grids
2
2
```

```
RD_Keauhou_Kona_20m_20120424.nc
2         runup
0.12      Input time step (sec)
1440000   Input amount of steps
0         countinue after input stop
120       Input number of steps between snapshots
1         ...Saving inner boundary
1         ...Saving grid every n-th node, n=
0
EOF
cp most3_facts_nc.inD most3_facts_nc.in
setenv OMP_NUM_THREADS 2
$path_e D C  most3_facts_nc.in &
```

A2. Forecast model *.in file for Kona, Hawaii for MOST version 2.0

```
0.0001              Minimum amplitude of input offshore wave (m):
1                    Input minimum depth for offshore (m)
0.1                 Input "dry land" depth for inundation (m)
0.0016   Input friction coefficient (n**2)
1                   runup flag for grids A and B (1=yes,0=no)
300.0               blowup limit
0.4                 Input time step (sec)
180000              Input amount of steps
21                  Compute "A" arrays every n-th time step, n=
7                   Compute "B" arrays every n-th time step, n=
63                  Input number of steps between snapshots
1                   ...Starting from
1                    ...Saving grid every n-th node, n=
FA_HI_CP_2min_20120418.ssl
FB_keauhou_24s_20111107.ssl
Kona_2x2_6x6_20120420_subsR1.ssl
/home/tg23/data/tang/src_nc/src_sim_test/kona//
./
 1 1 1 1
1
1 66  112           Kona warning point 204.0046 °E, 19.6397 °N, water depth of 2.3 m
```

Figures

Figures

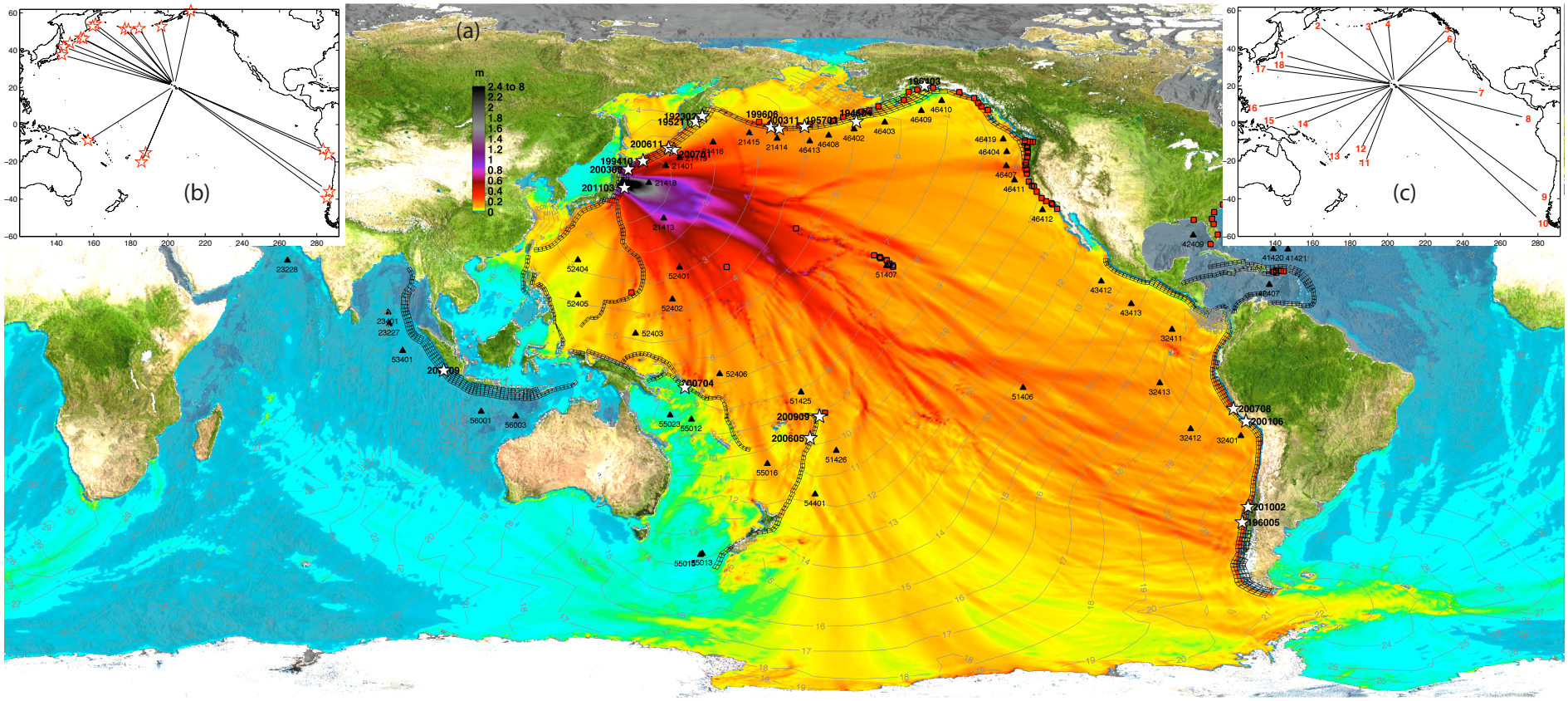

Figure 1: (a) Overview of the tsunami forecast system. System components include a tsunameter (DART) network (triangles), pre-computed tsunami source functions (unfilled black rectangles) and high-resolution forecast models (red squares). Filled color shows the computed maximum sea surface elevation in m offshore for the 2011 Japan tsunami. Contours indicate the travel time in hours. (b) Sixteen past tsunamis and (c) eighteen simulated magnitude 9.3 tsunamis were tested in this study.

(a) 

(b) 

(c)

(d)

Figure 2: Photos show (a-c) water levels and (d) aftermath at Kailua-Kona, Hawaii from the 2011 Japan tsunami. (a and b) Kailua Bay low and high water during the tsunami. (d) Damage at Alii Drive Kailua-Kona. (Photos a, b and d taken by Joel Noa; photo c from http://logisticsmonster.com/2011/03/10/8-9-magnitute-earthquake-hits-japan-major-tsunami-warnings/)

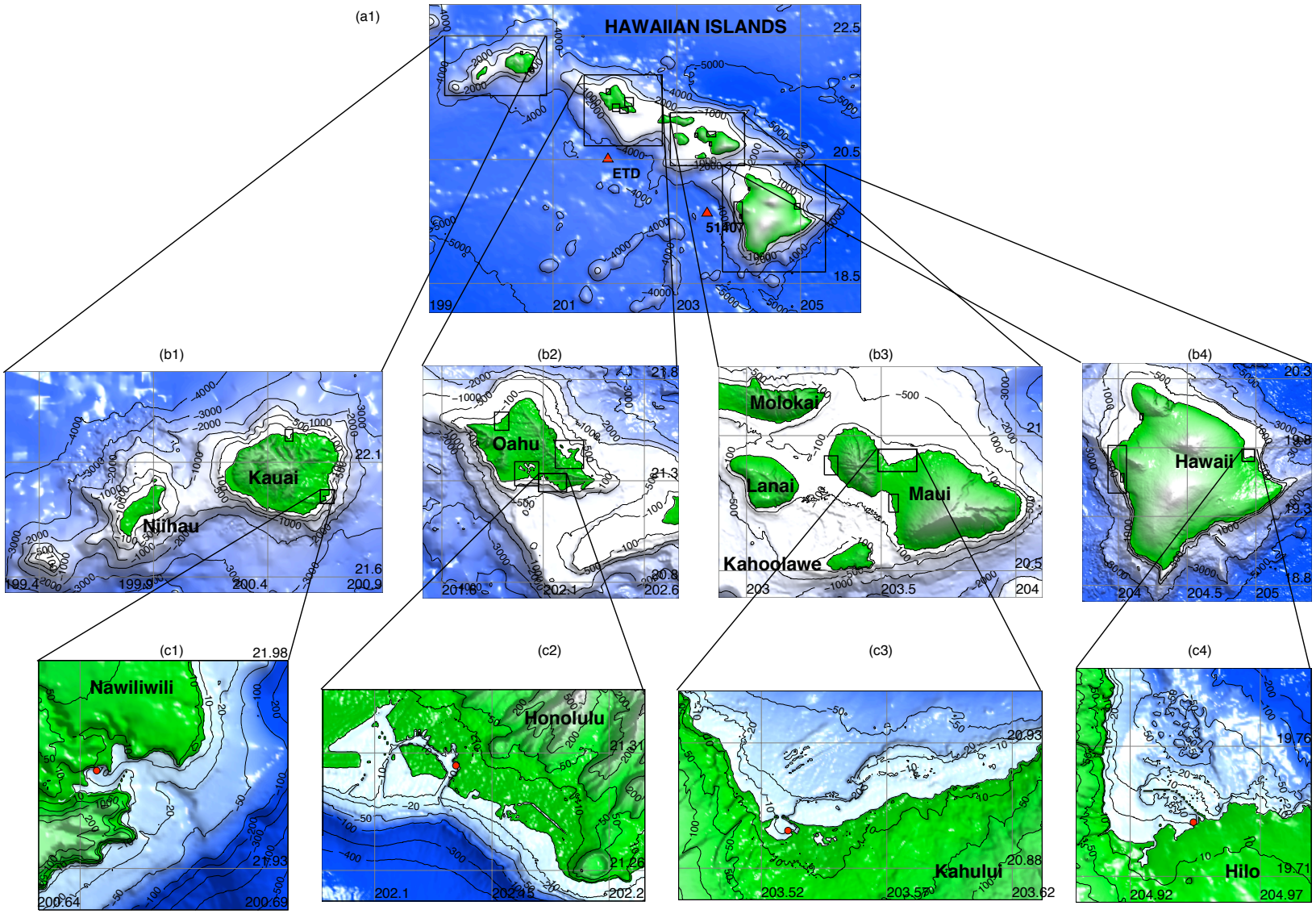

Figure 3: Forecast model setups for 13 forecast sites in Hawaii: (a) 2-arc-min (~3600m) regional, (b) 12-18-arc-sec (~360-540m) intermediate and (c) 2-arc-sec (~60m) nearshore grids for Nawiliwili, Honolulu, Kahului and Hilo. Red dots, coastal tide stations.

Figure 4: An aerial photo of Kona-Kailua (Image courtesy of Pacific Disaster Center 2000).

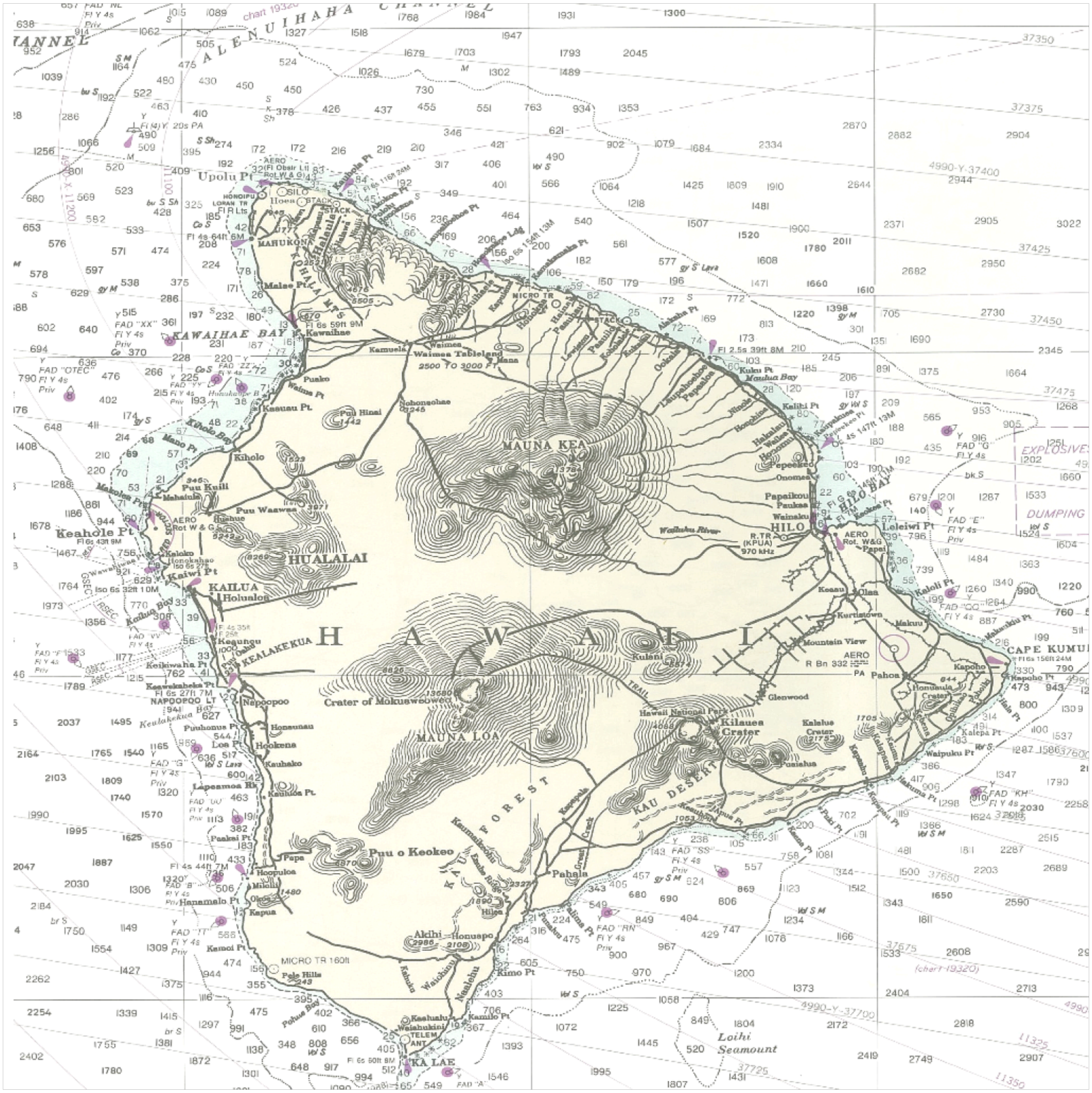

Figure 5: A chart of the Big Island, Hawaii (NOAA Chart 19010). Soundings in fathoms at Mean Lower Low Water. Contour and summit elevation values are in feet above Mean Sea Level.

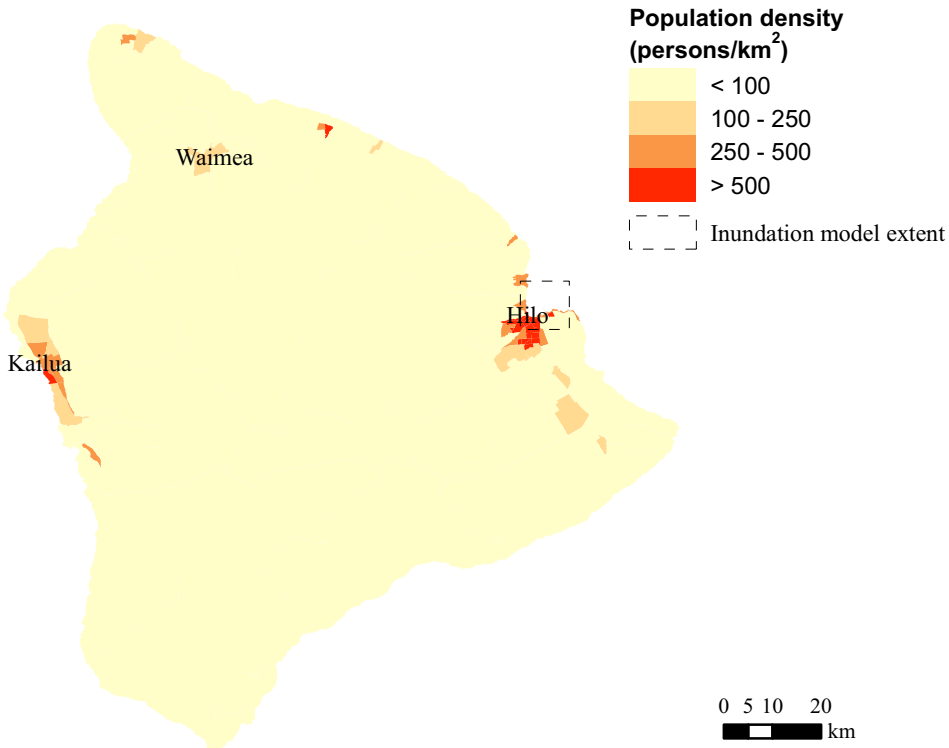

Figure 6: Population density, Hawaii. (Source: 2000Census)

Figure 7: Run-ups in feet for Kailua-Kona coast for the 1946, 1952,1957, 1960 and 1964 tsunamis (Image from Walker, 2004).

(a)

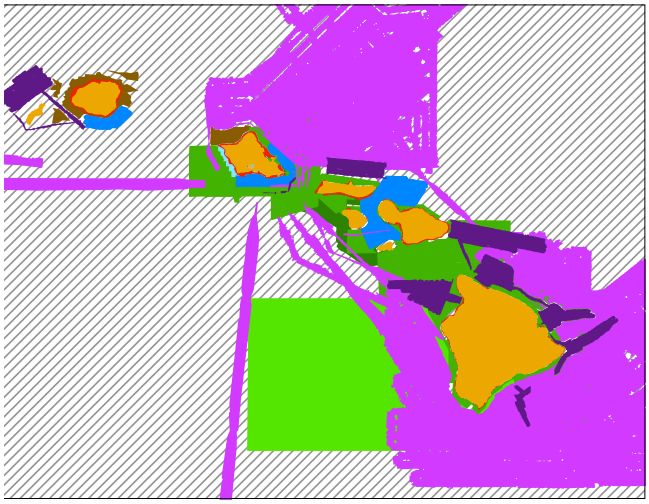

SHOALS LIDAR
JAMSTEC multibeam
MBARI multibeam
Navy multibeam
NOS digital echosounder
NOS multibeam
NOS lead-line surveys
USACE digital echosounder
USGS Seafloor Mapping Project multibeam
NOS nautical chart digitized contours
USGS GLORIA tracklines/Smith & Sandwell
NOAA CSC IfSAR topography
USGS National Elevation Dataset topography

(b)

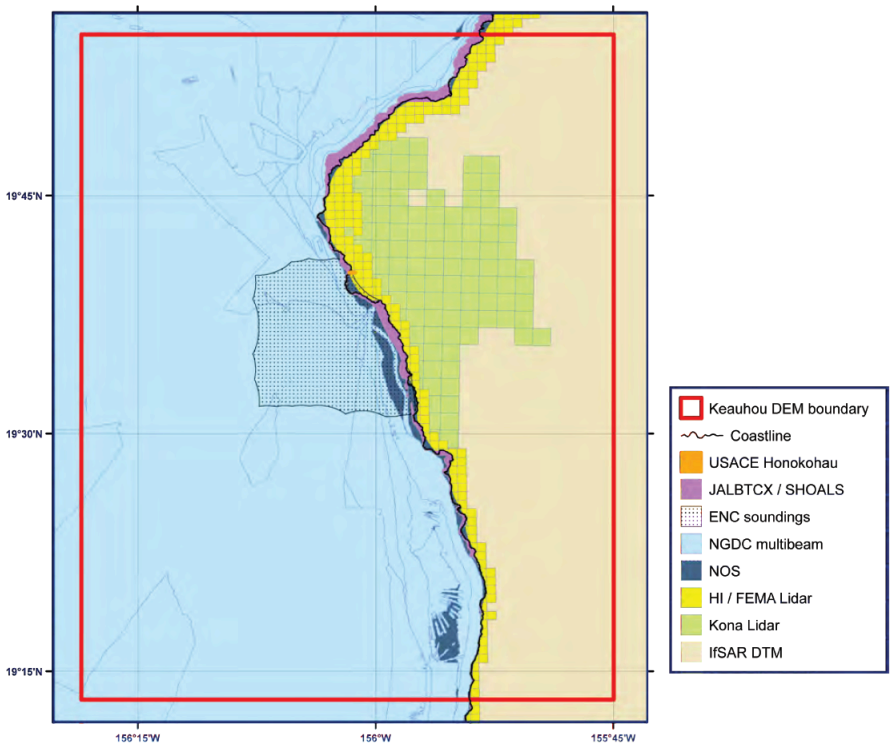

Figure 8: Bathymetric and topographic data source overview. (a) 6" sec (~180 m) Hawaii DEM developed at NCTR; (b) 1/3" (~10 m) Keauhou DEM developed by NGDC (Image from Carignan et al., 2011).

(a)

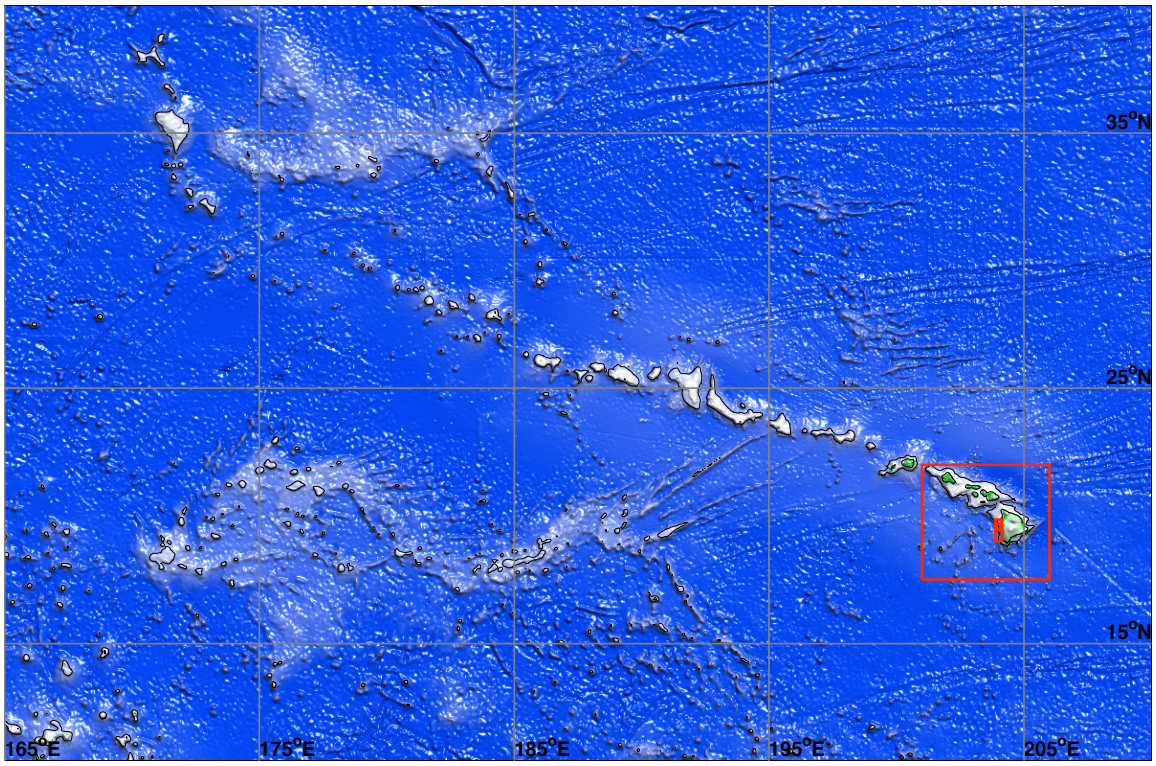
35°N
25°N
15°N
165°E
175°E
185°E
195°E
205°E

(b)

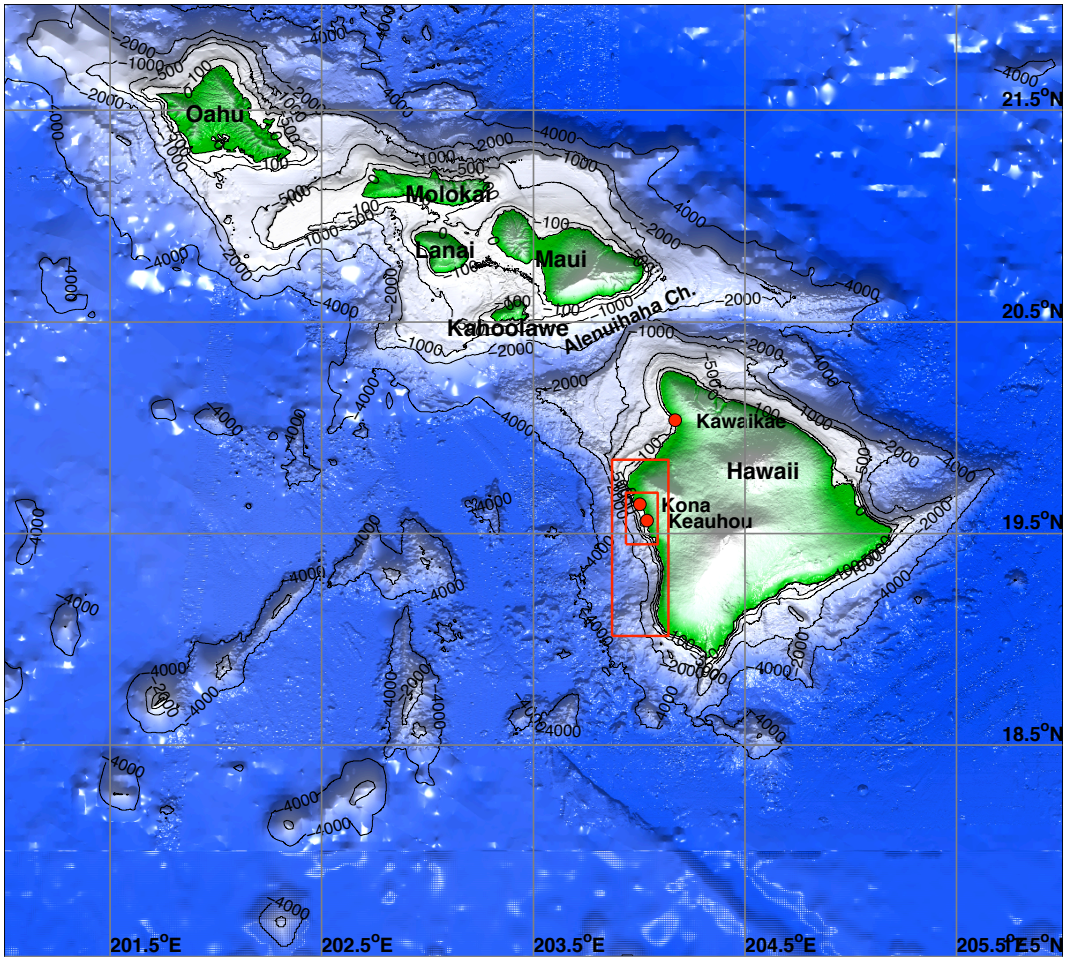
Oahu
Molokai
Lanai
Maui
Kahoolawe
Alenuihaha Ch.
Kawaikae
Hawaii
Kona
Keauhou
21.5°N
20.5°N
19.5°N
18.5°N
201.5°E
202.5°E
203.5°E
204.5°E
205.5°E

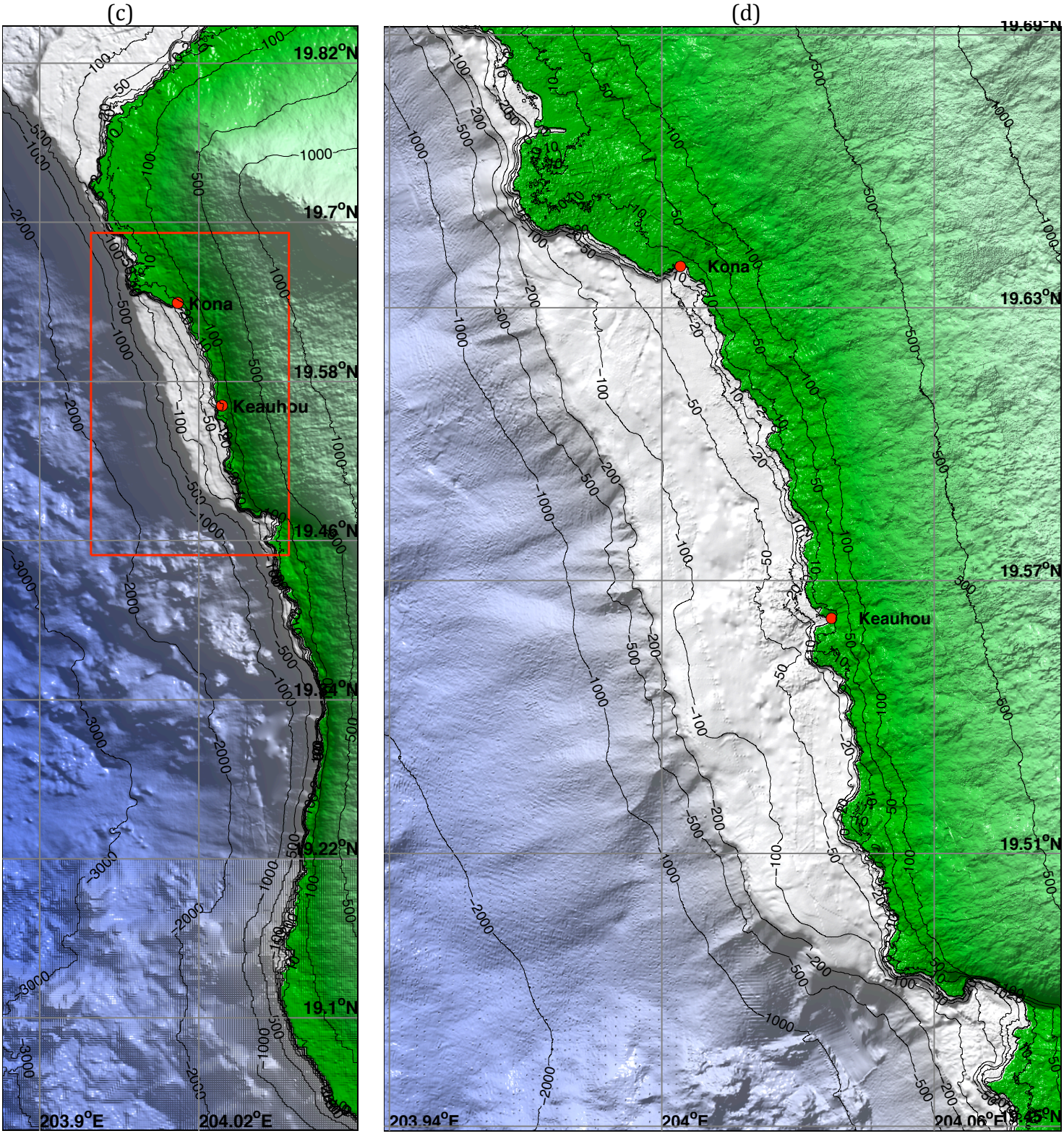

Figure 9: The Kailua-Kona reference model includes four layers of grids with increasing resolutions of (a) 60" (1800m), (b) 6" (180m), (c) 2" (60m) and (d) 2/3" (20m). □, nested grid boundary; ● warning points .

(a)

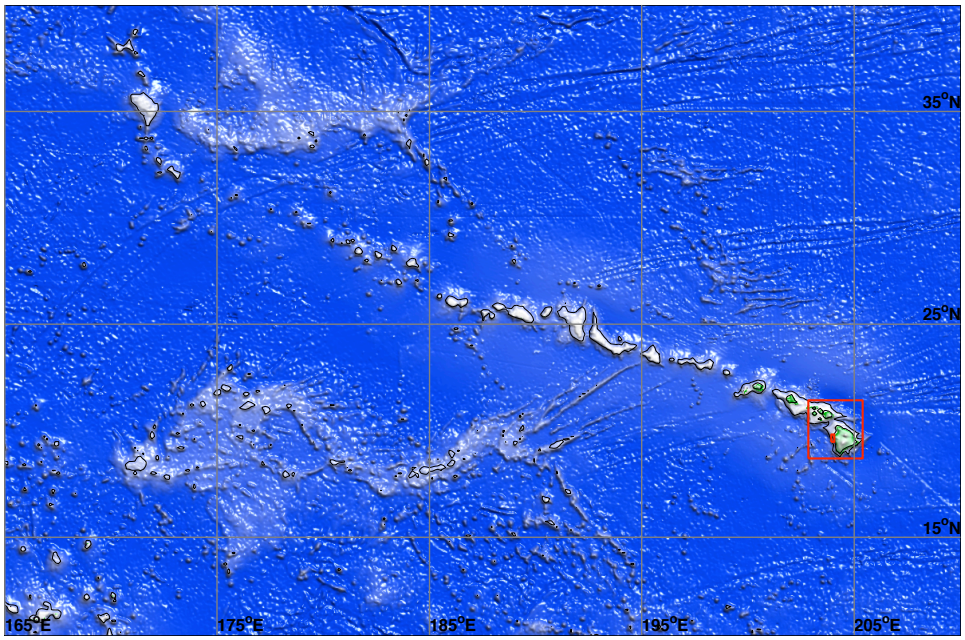
35°N
25°N
15°N
165°E
175°E
185°E
195°E
205°E

(b)

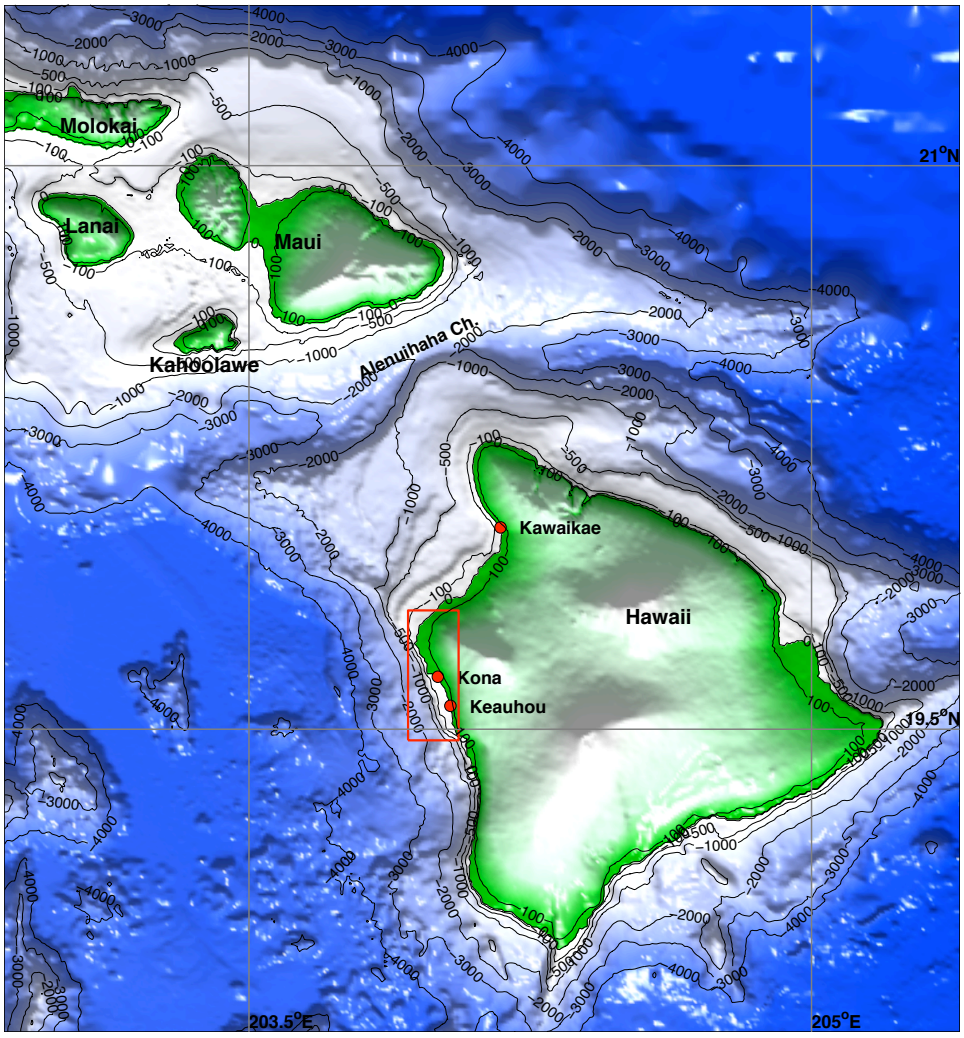
Molokai
Lanai
Maui
Kahoolawe
Alenuihaha Ch
Kawaikae
Hawaii
Kona
Keauhou
21°N
19.5°N
203.5°E
205°E

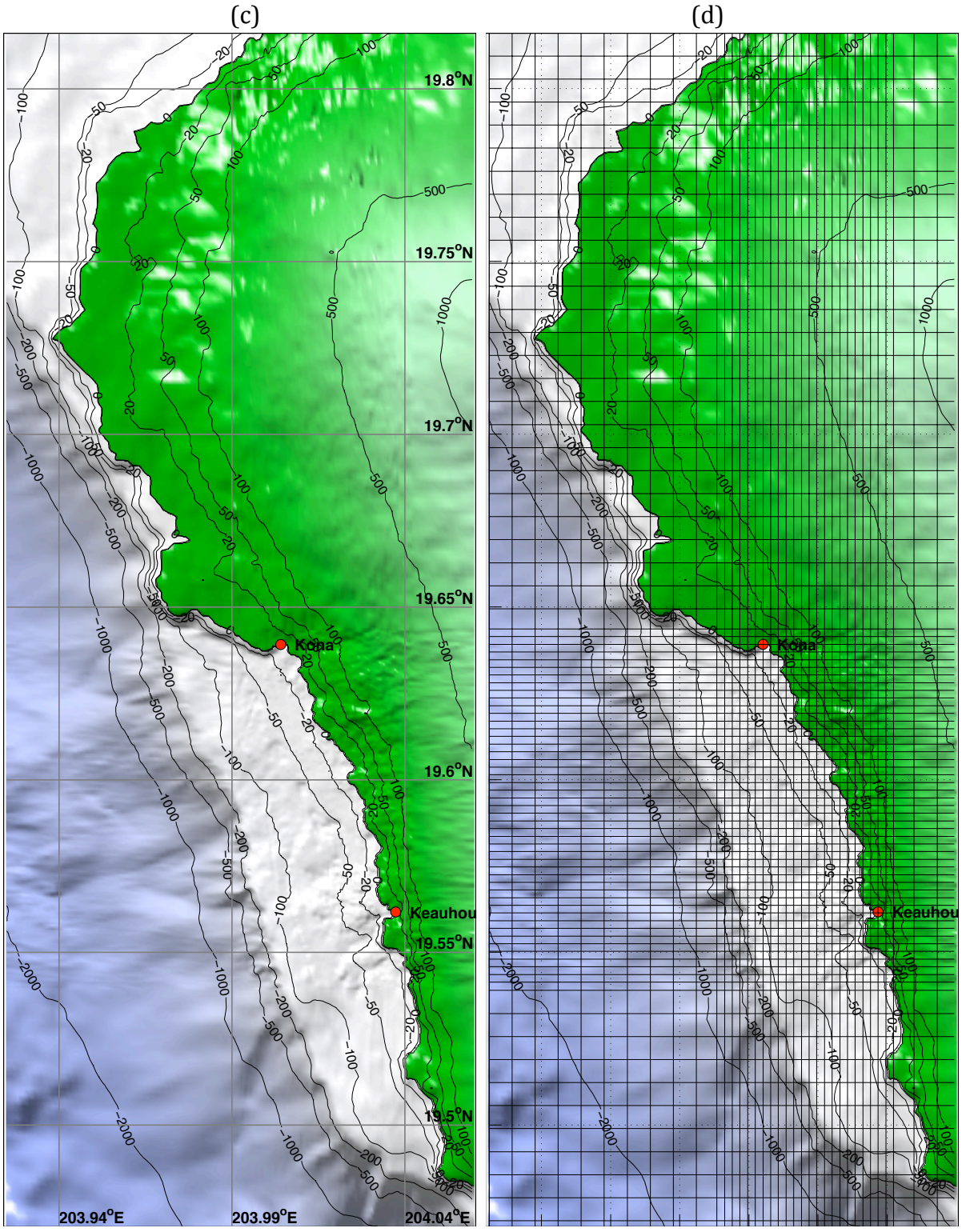

Figure 10: The Kailua-Kona forecast model includes three layers of grids with increasing resolutions of (a) 120" (3600 m), (b) 24" (720 m) and (c) 2- 6 "(60-180 m). (d) Each line represents every 4th node in C-grid. □, nested grid boundary; ●, Kailua-Kona warning point at 204.0046 °E, 19.6397 °N, water depth of 2.3 m.

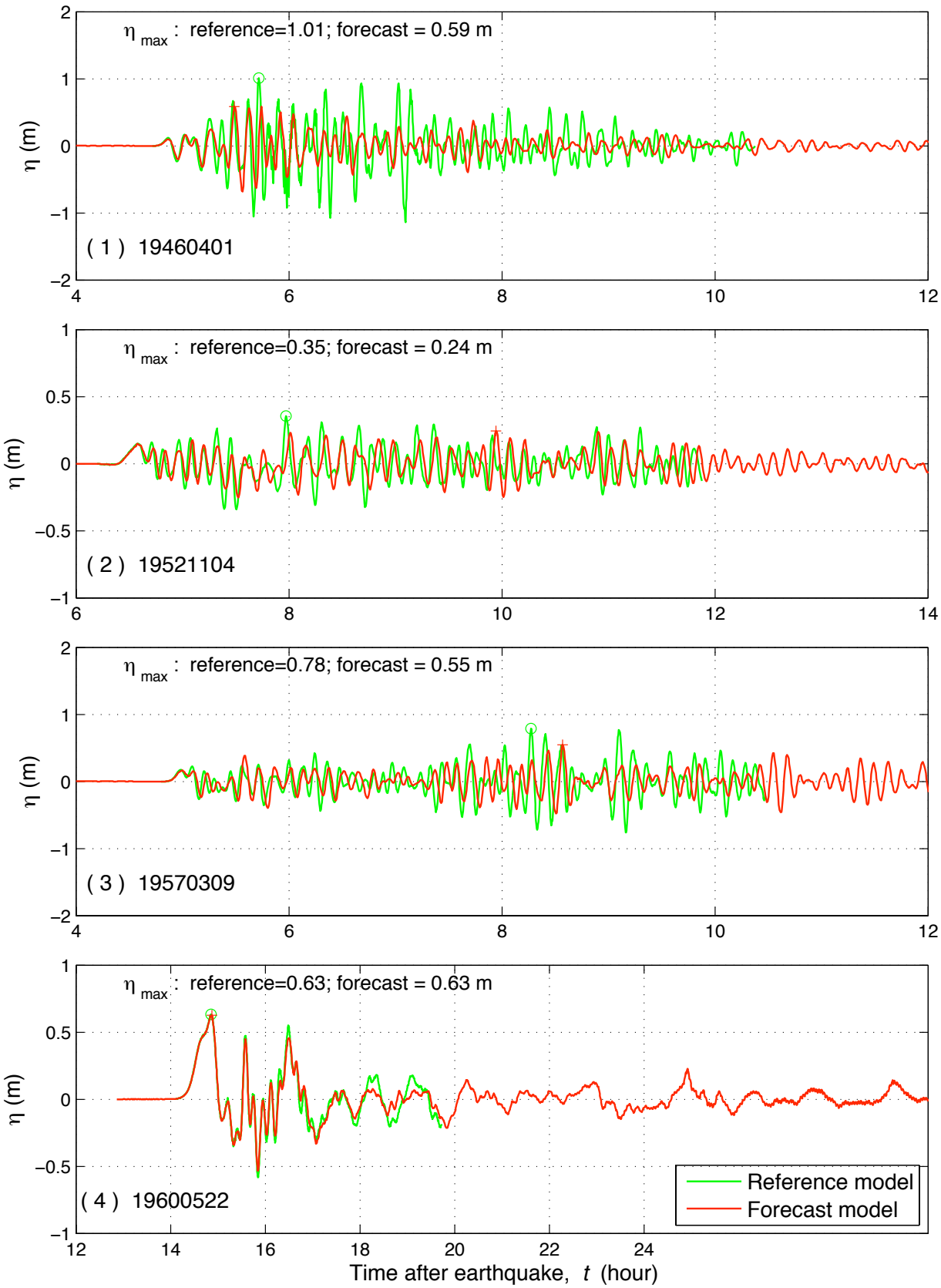

Figure 11: (1–4) Modeled time series of sea surface elevation η at Kailua-Kona warning point for the past tsunamis. o and + η_{max} , computed by the reference and forecast models respectively.

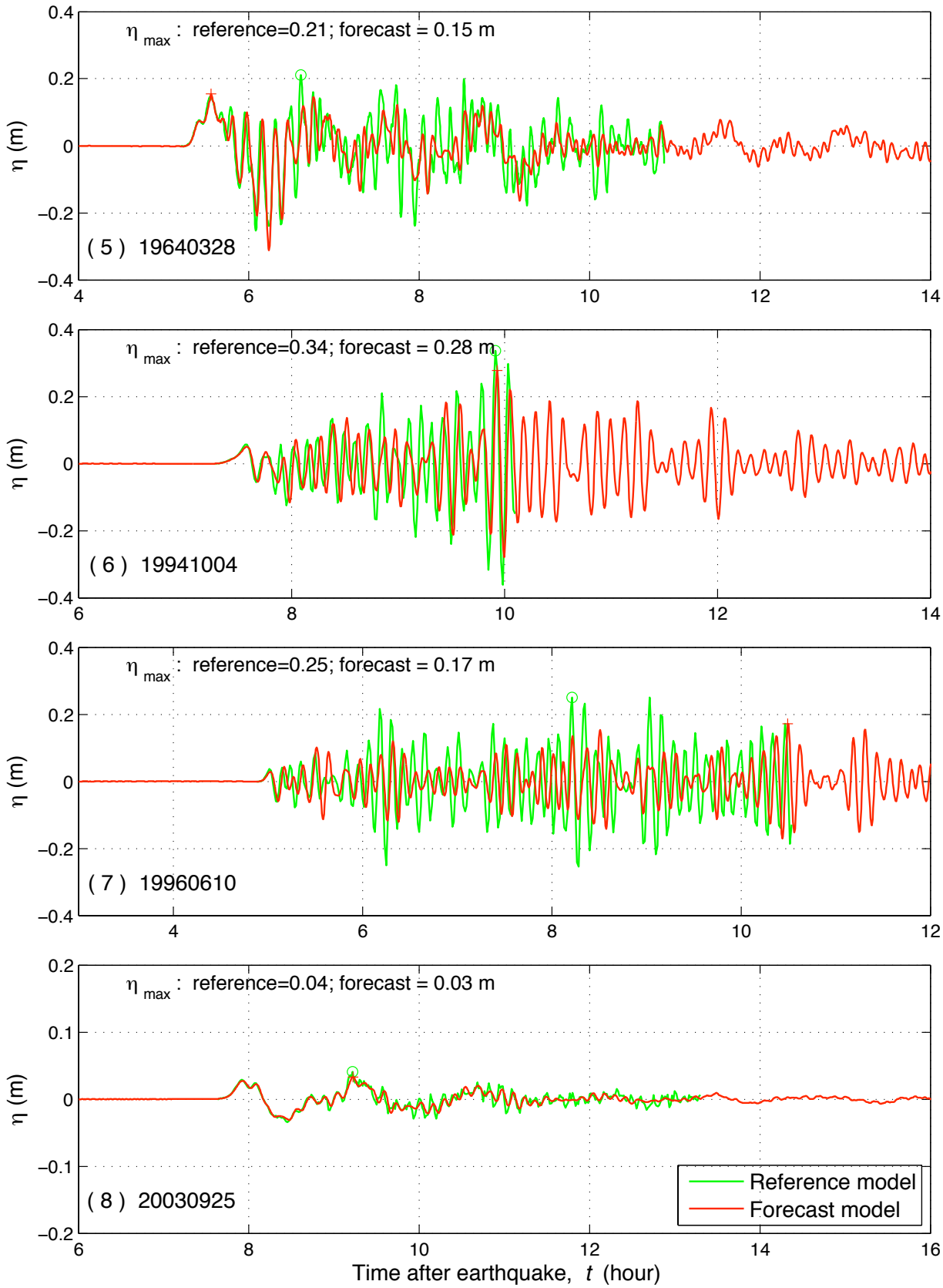

Figure 11 (5–8): Modeled time series of sea surface elevation η at Kailua-Kona warning point for the past tsunamis. o and + η_{max} , computed by the reference and forecast models respectively.

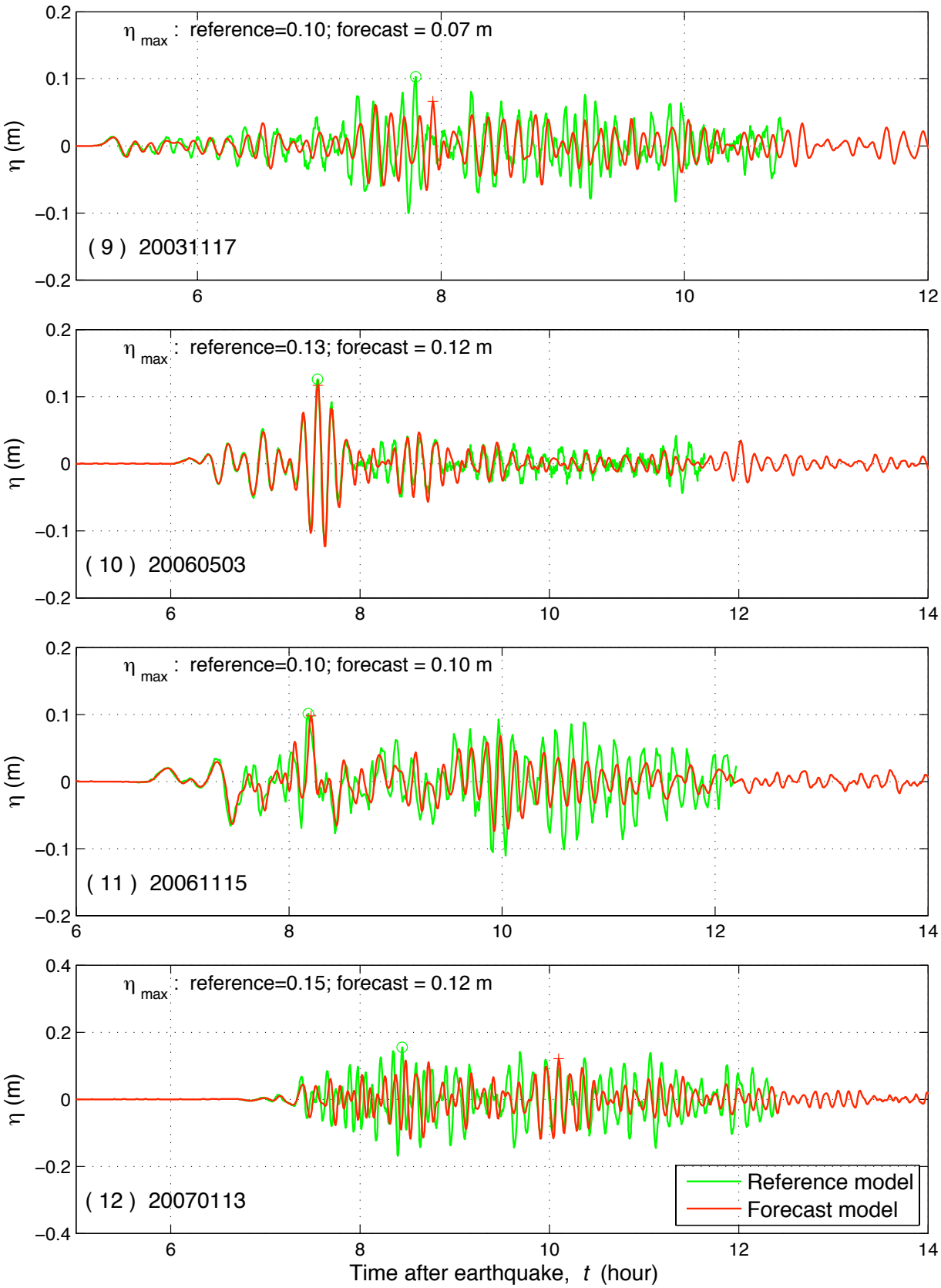

Figure 11 (9–12) Modeled time series of sea surface elevation η at Kailua-Kona warning point for the past tsunamis. o and + η_{max} , computed by the reference and forecast models respectively.

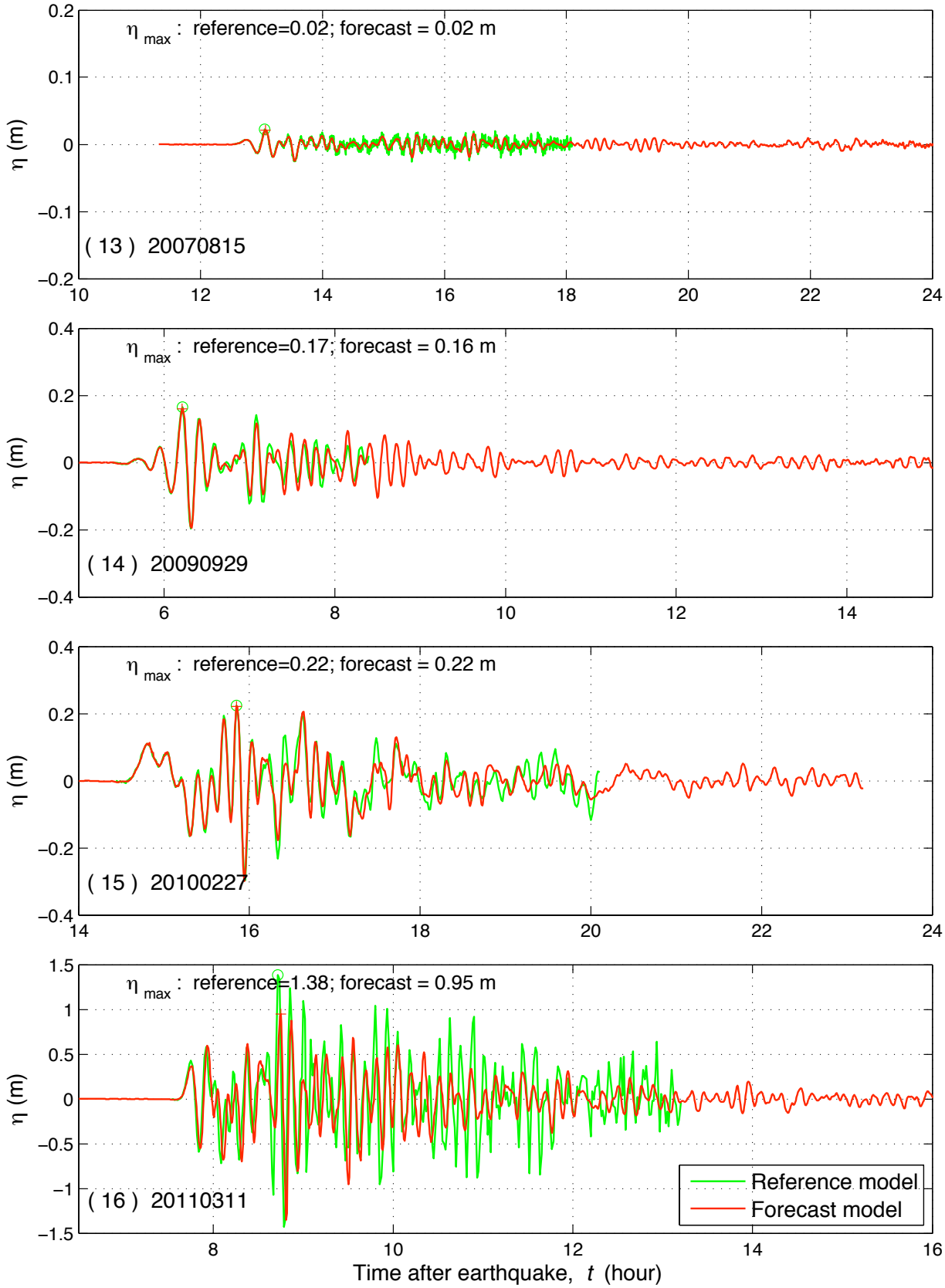

Figure 11 (13–16): Modeled time series of sea surface elevation η at Kailua-Kona warning point for the past tsunamis. o and + η_{max}, computed by the reference and forecast models respectively.

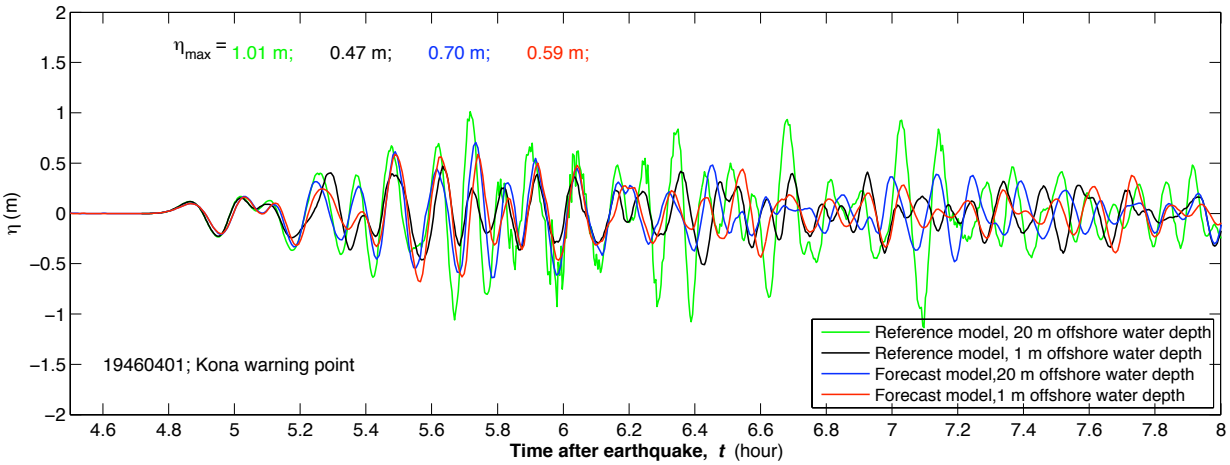

Figure 12: Computed η with different model setups for the 1946 Unimak tsunami.

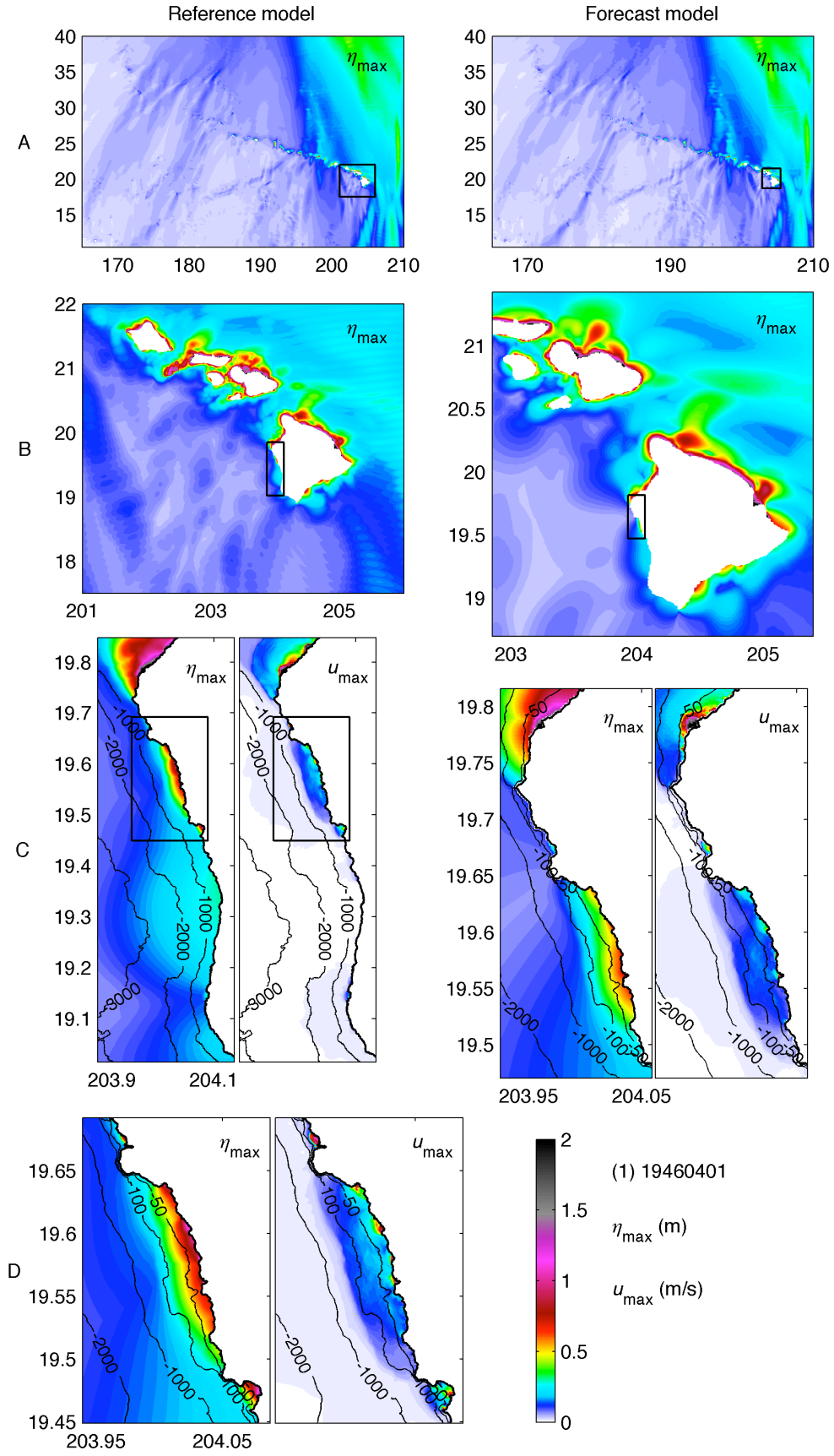

Figure 13 (1): Computed maximum sea surface elevation and current by the Kailua-Kona reference and forecast models for past tsunamis.

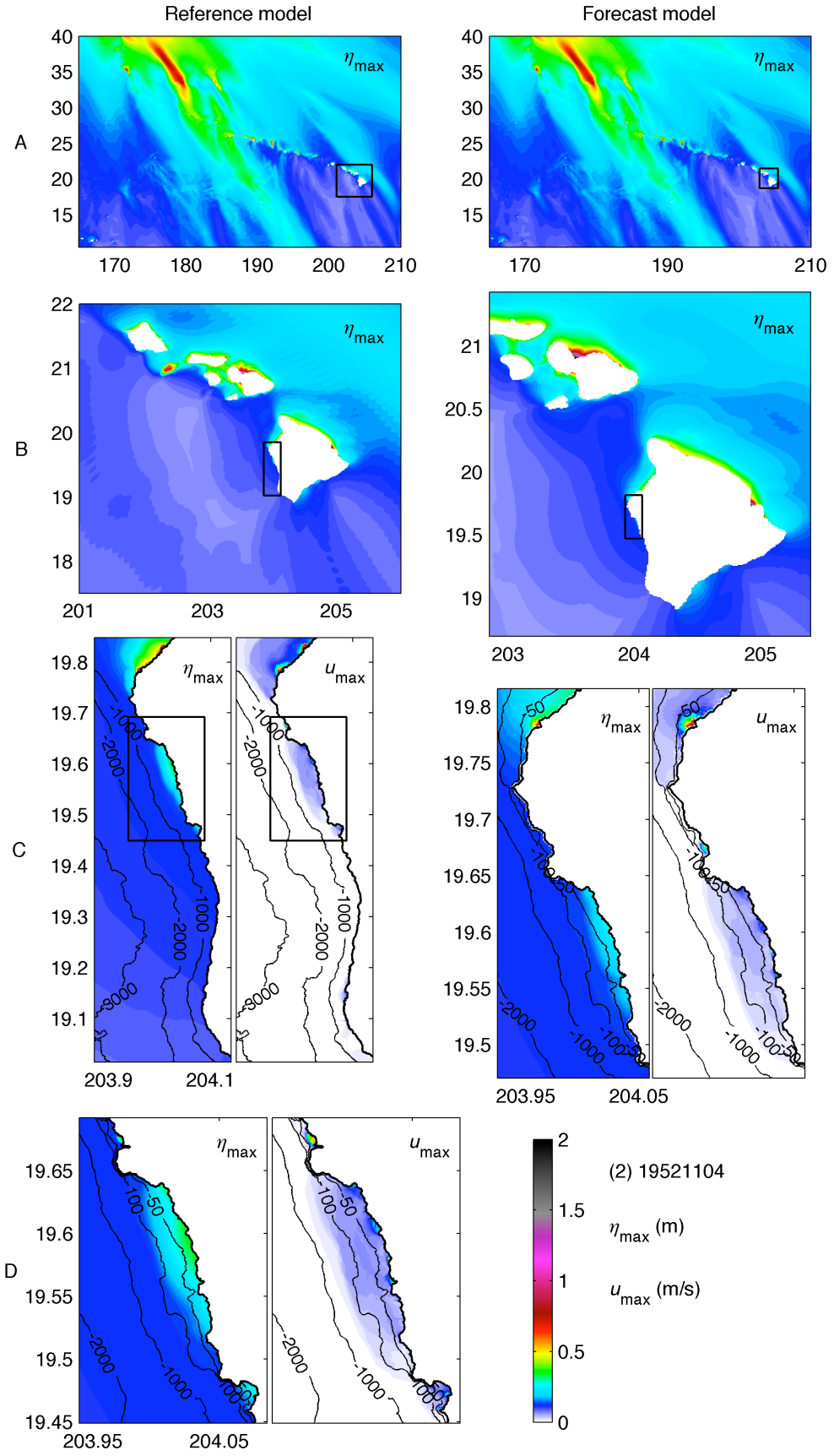

Figure 13 (2): Computed maximum sea surface elevation and current by the Kailua-Kona reference and forecast models for past tsunamis.

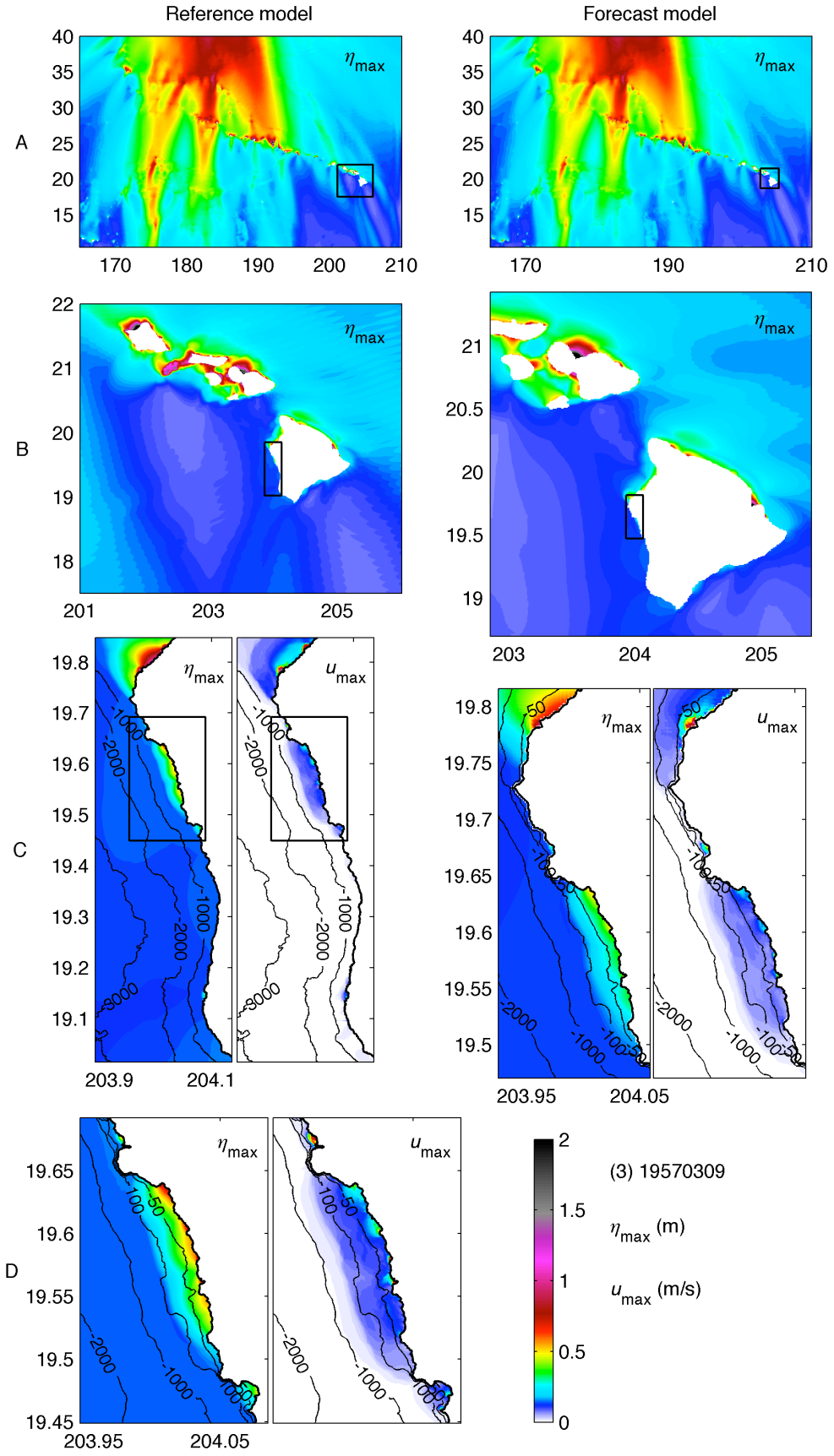

Figure 13 (3): Computed maximum sea surface elevation and current by the Kailua-Kona reference and forecast models for past tsunamis.

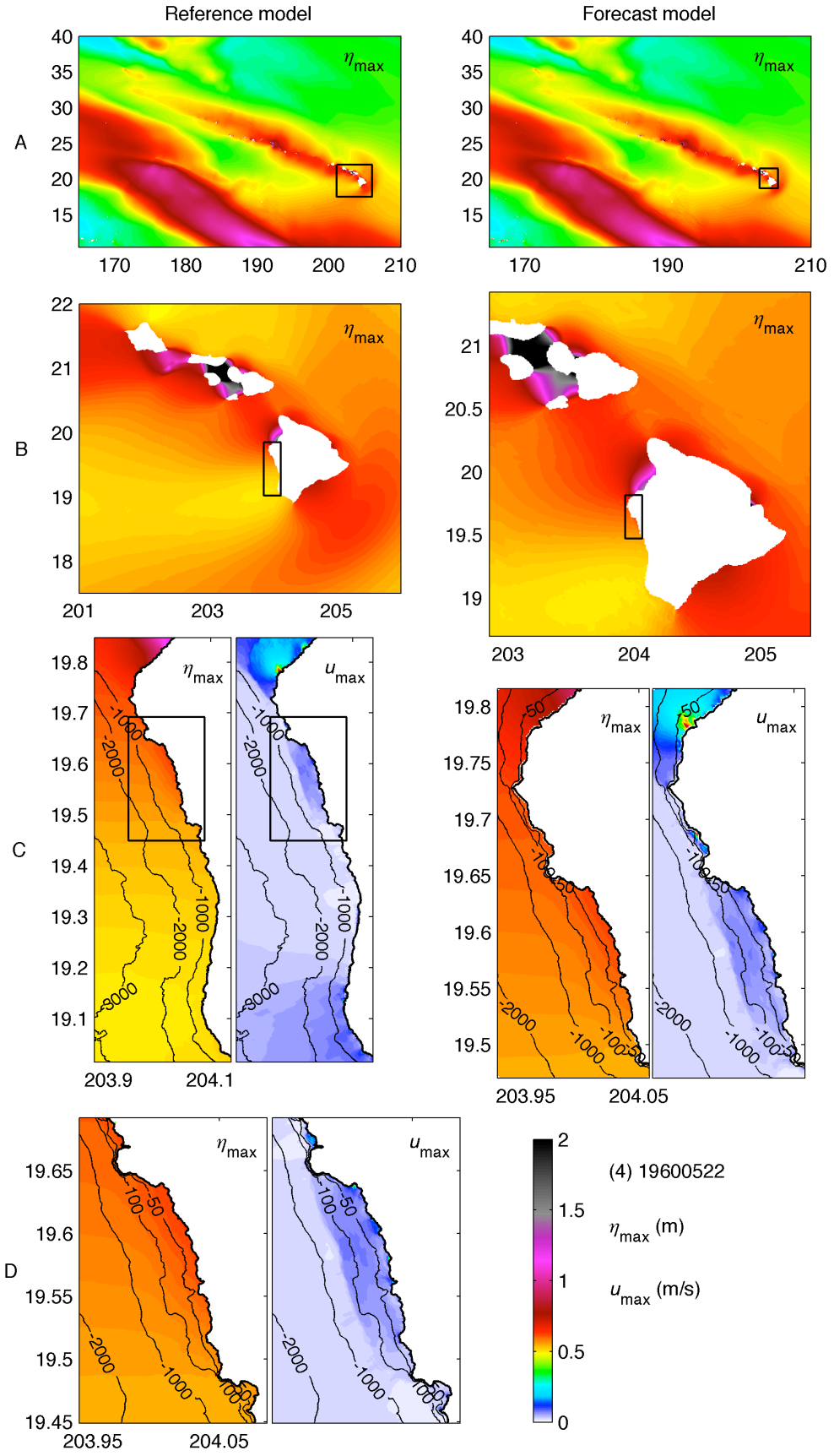

Figure 13 (4): Computed maximum sea surface elevation and current by the Kailua-Kona reference and forecast models for the 1960 Chile tsunami.

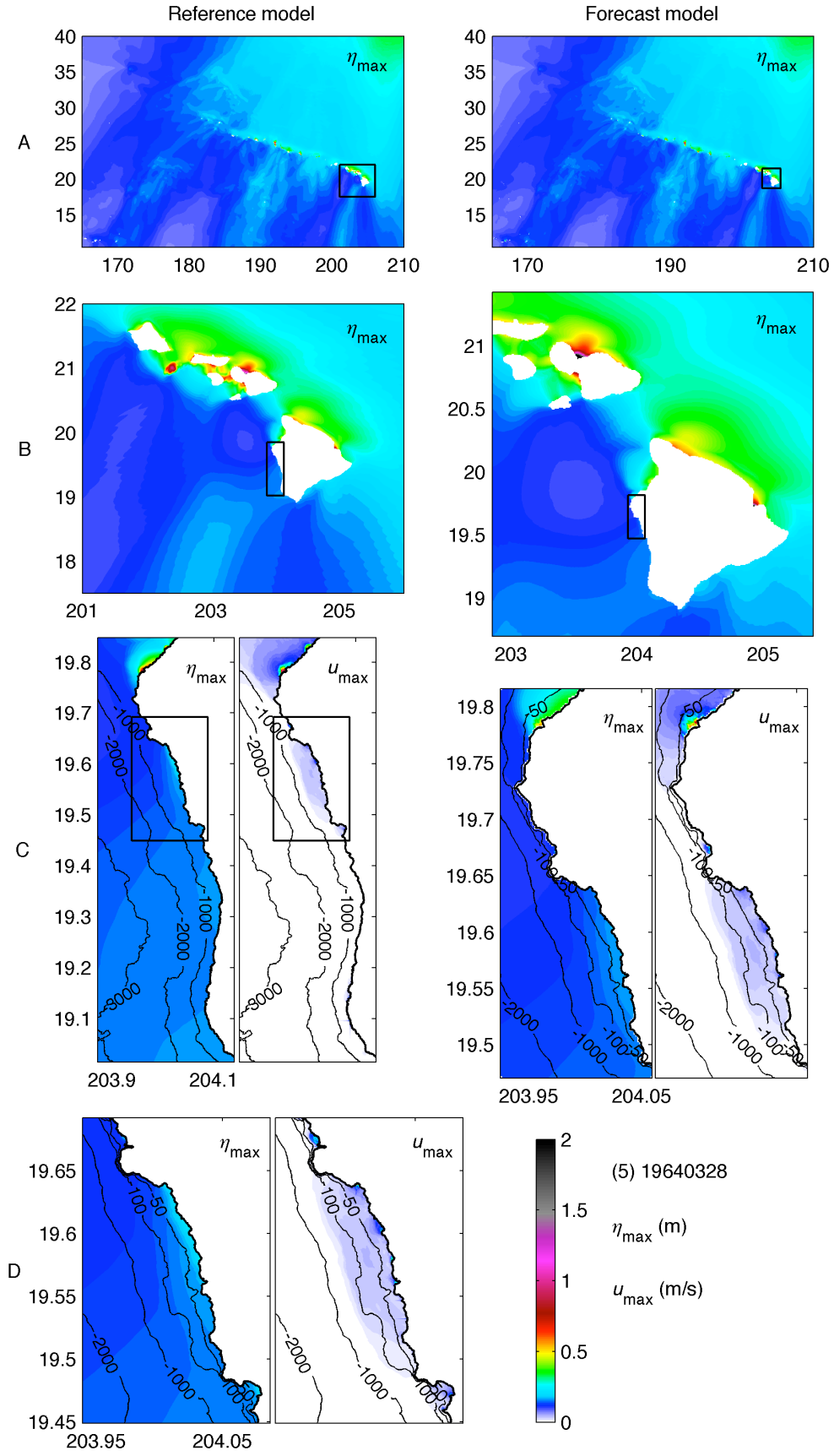

Figure 13 (5): Computed maximum sea surface elevation and current by the Kailua-Kona reference and forecast models for the 1964 Alaska tsinami.

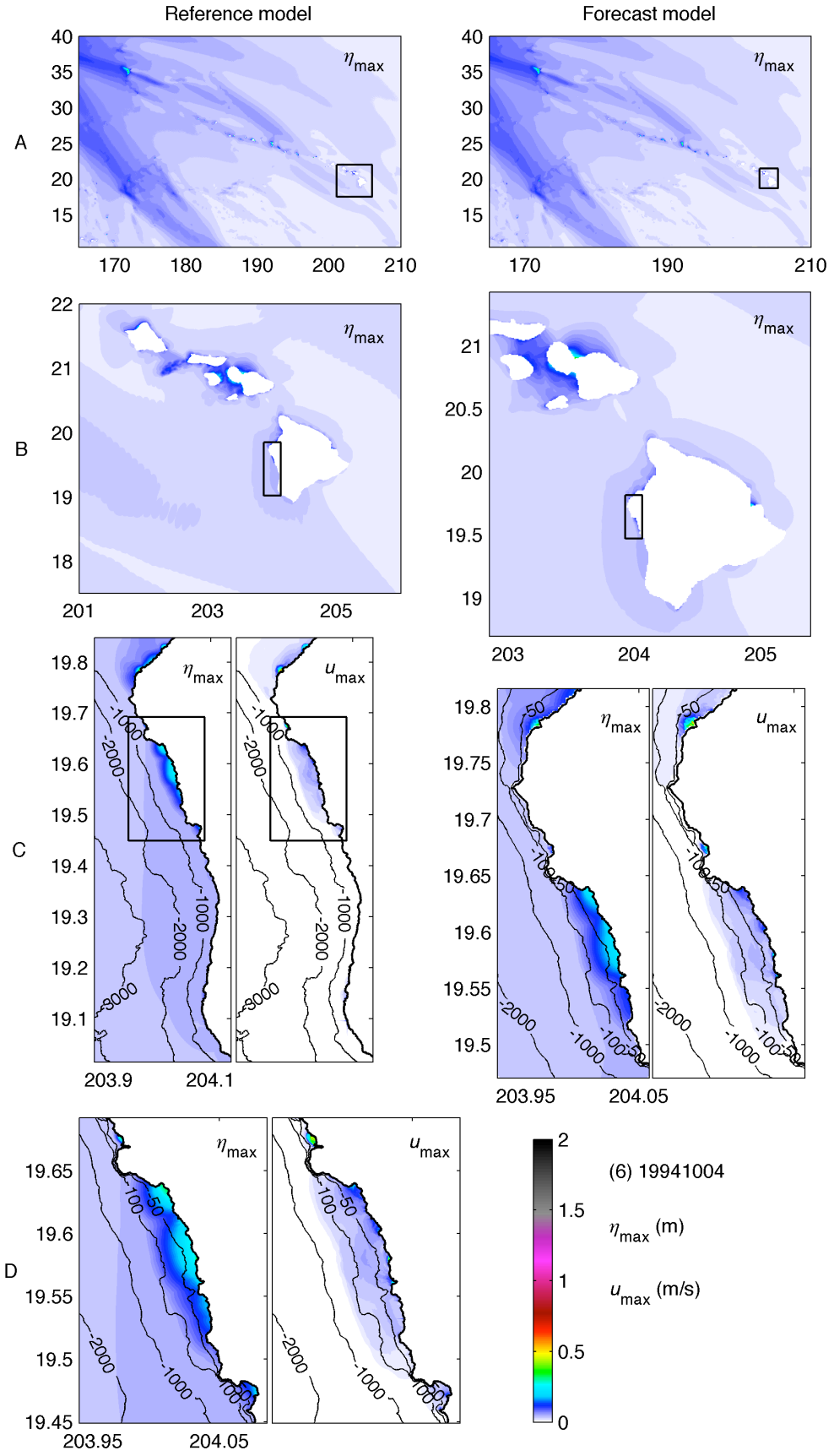

Figure 13 (6): Computed maximum sea surface elevation and current by the Kailua-Kona reference and forecast models for the 1994 Kuril Islands tsunami.

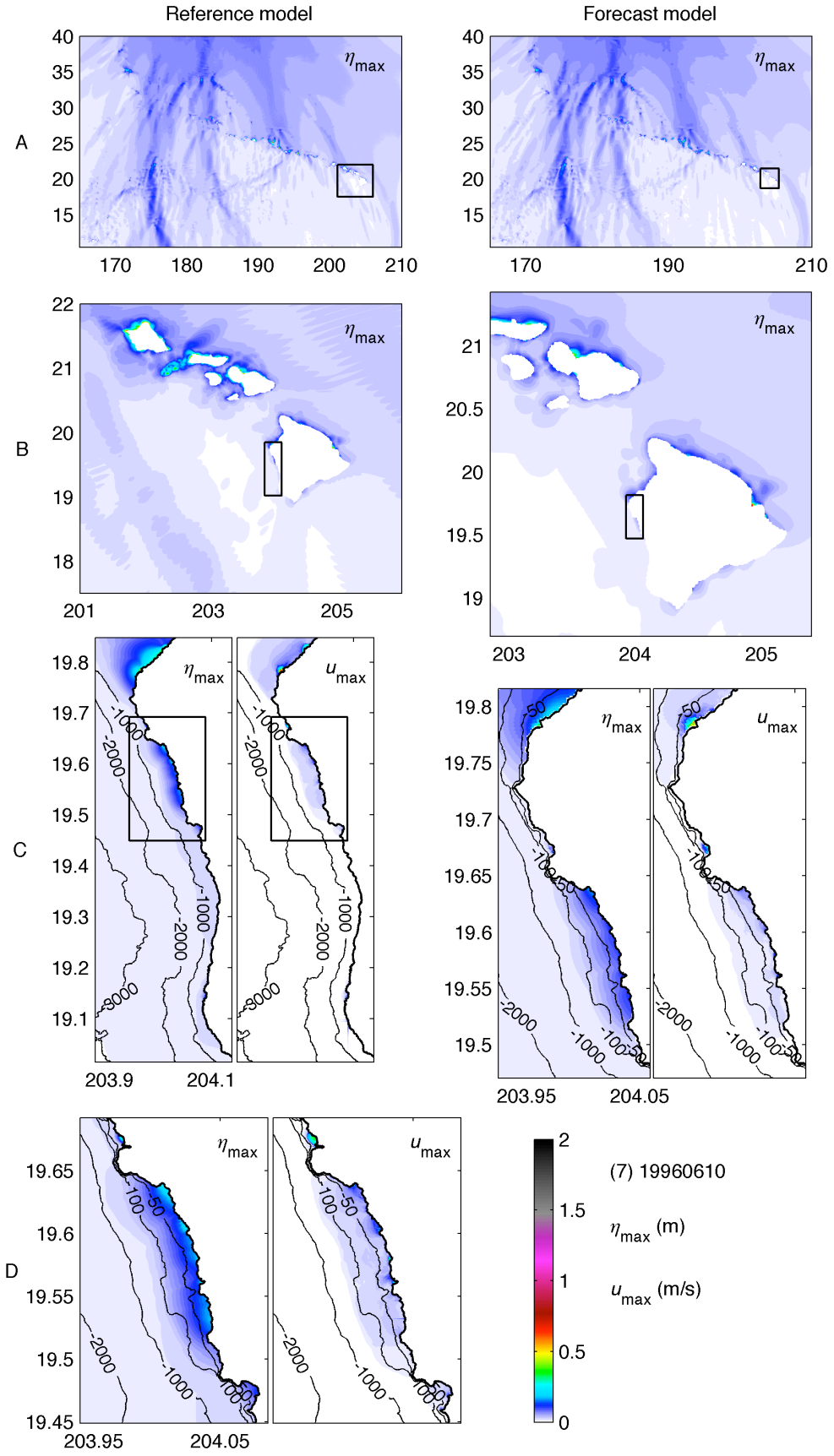

Figure 13 (7): Computed maximum sea surface elevation and current by the Kailua-Kona reference and forecast models for the 1996 Andreanov tsunami.

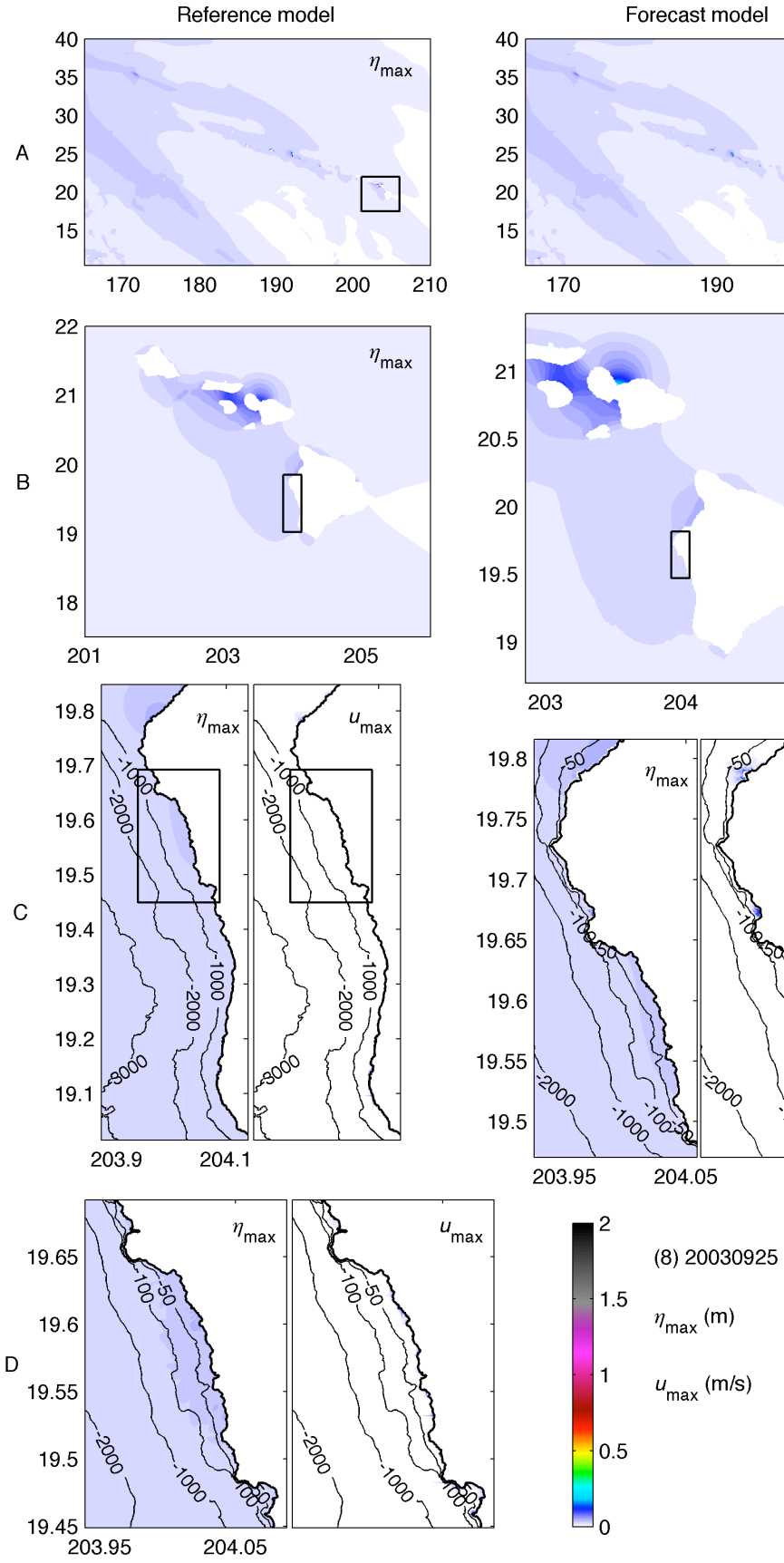

Figure 13 (8): Computed maximum sea surface elevation and current by the Kailua-Kona reference and forecast models for the 2003 Hokkaido tsunami.

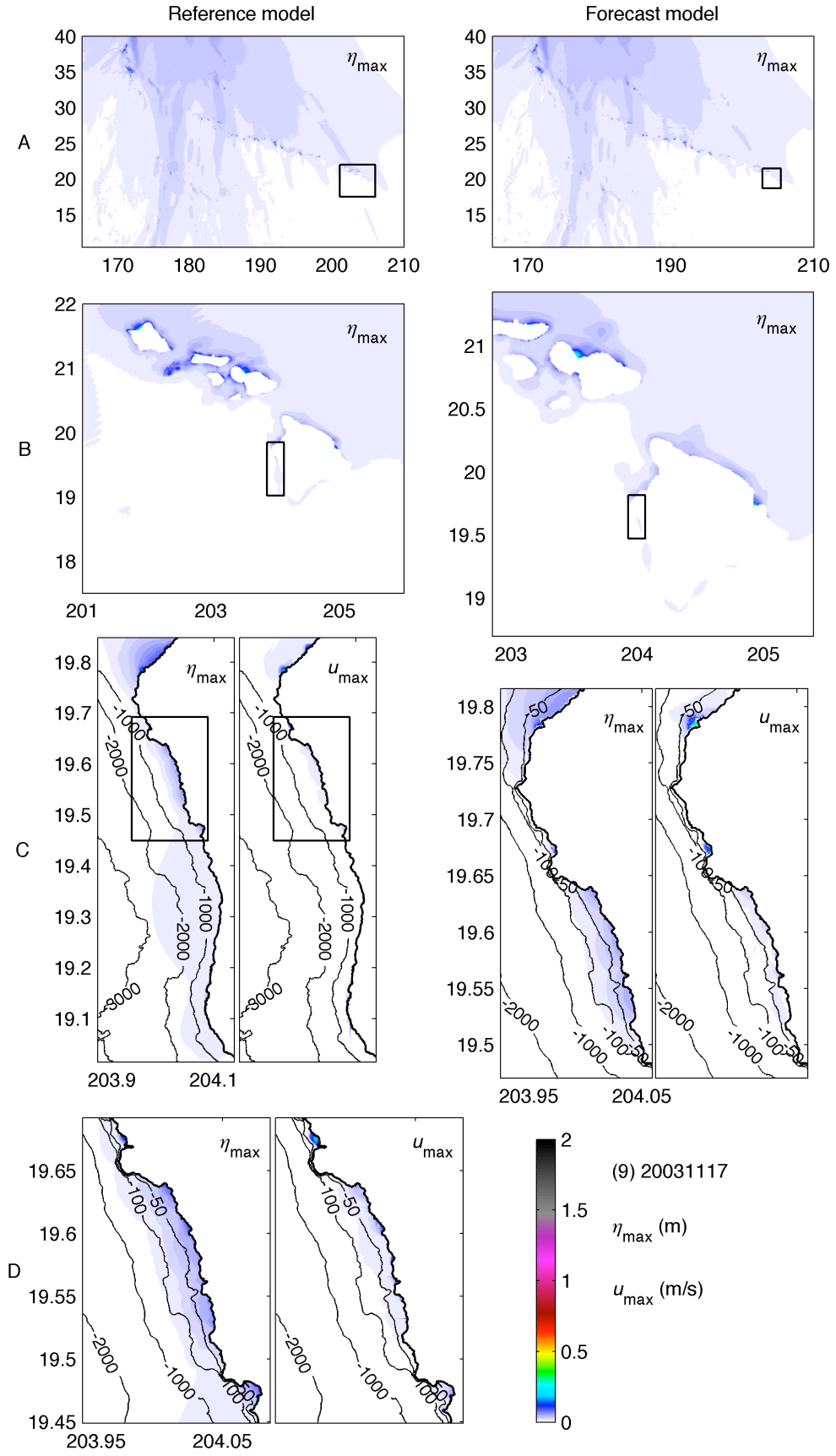

Figure 13 (9): Computed maximum sea surface elevation and current by the Kailua-Kona reference and forecast models for the 2003 Rat Islands tsunami.

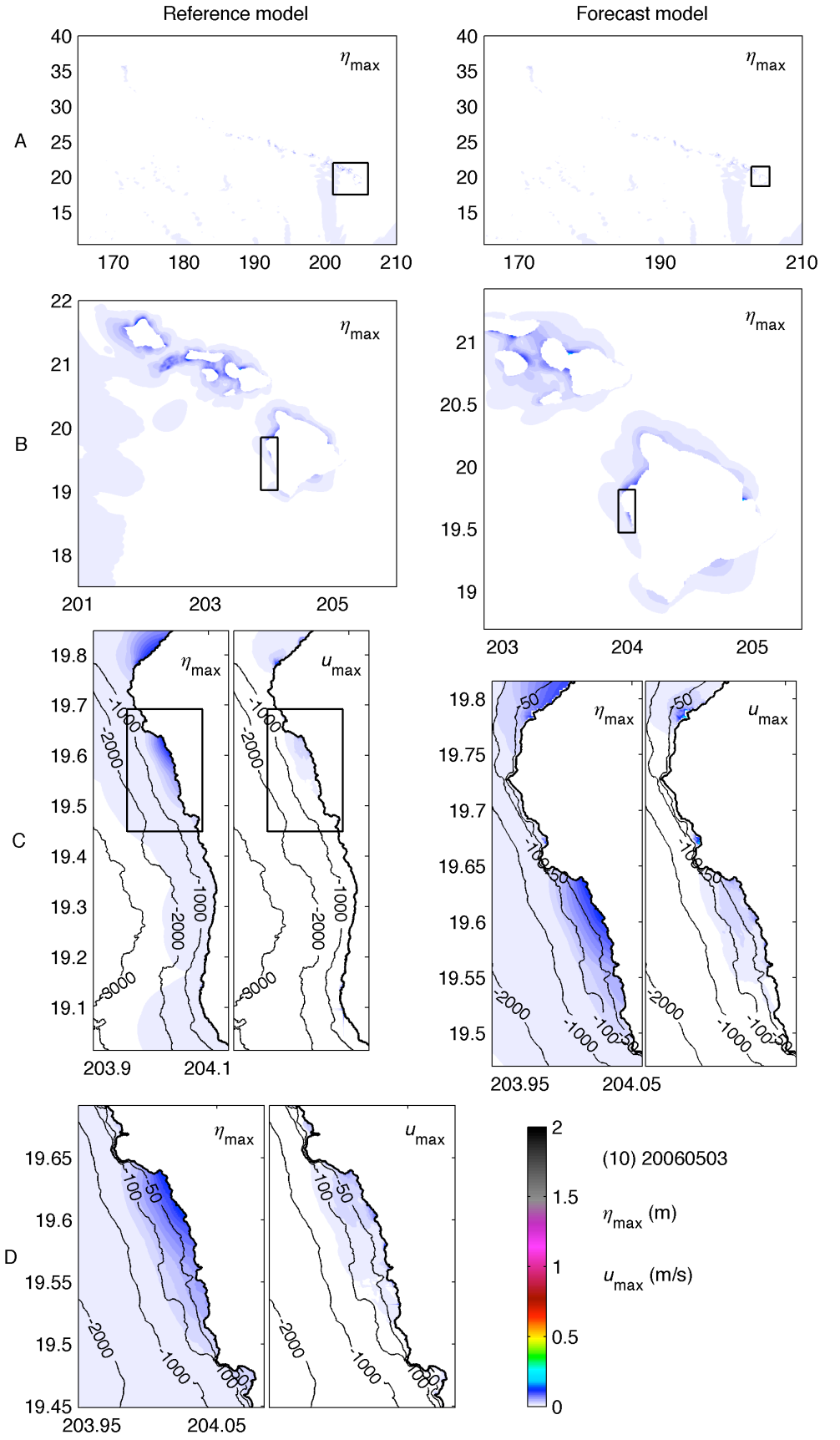

Figure 13 (10): Computed maximum sea surface elevation and current by the Kailua-Kona reference and forecast models for the 2006 Tonga tsunami.

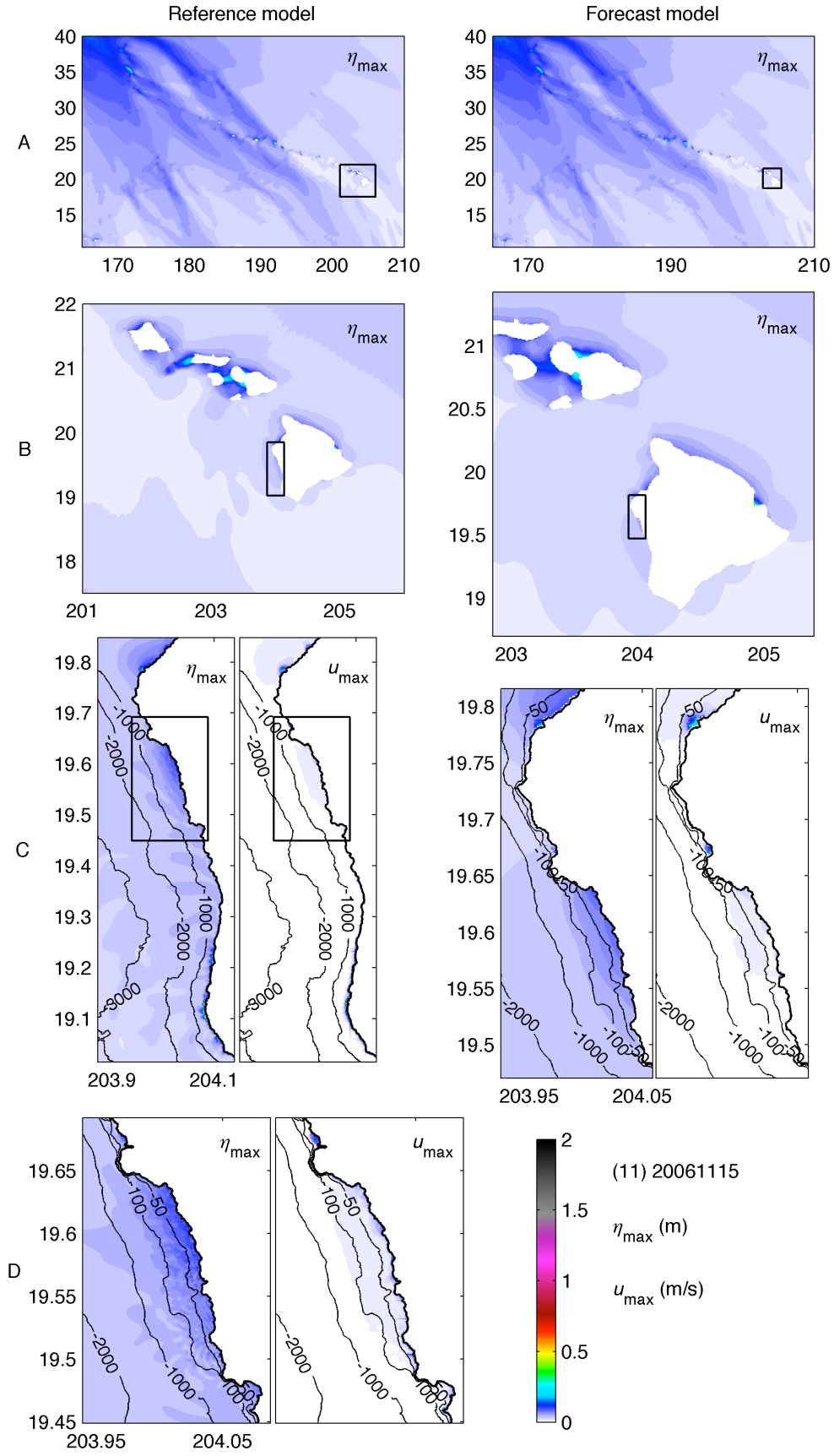

Figure 13 (11): Computed maximum sea surface elevation and current by the Kailua-Kona reference and forecast models for the 2006 Kuril Islands tsunami.

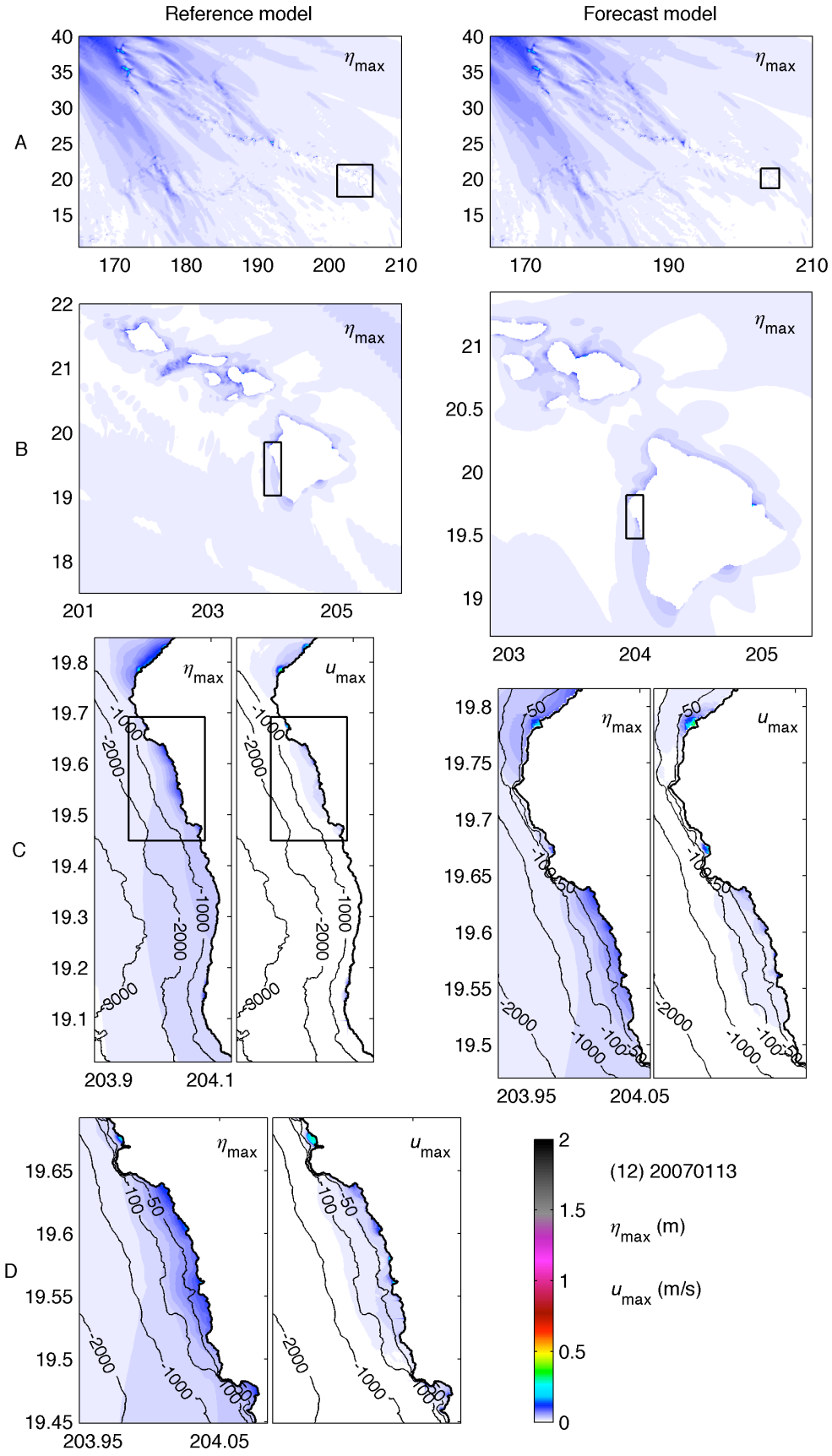

Figure 13 (12): Computed maximum sea surface elevation and current by the Kailua-Kona reference and forecast models for the 2007 Kuril Islands tsunami.

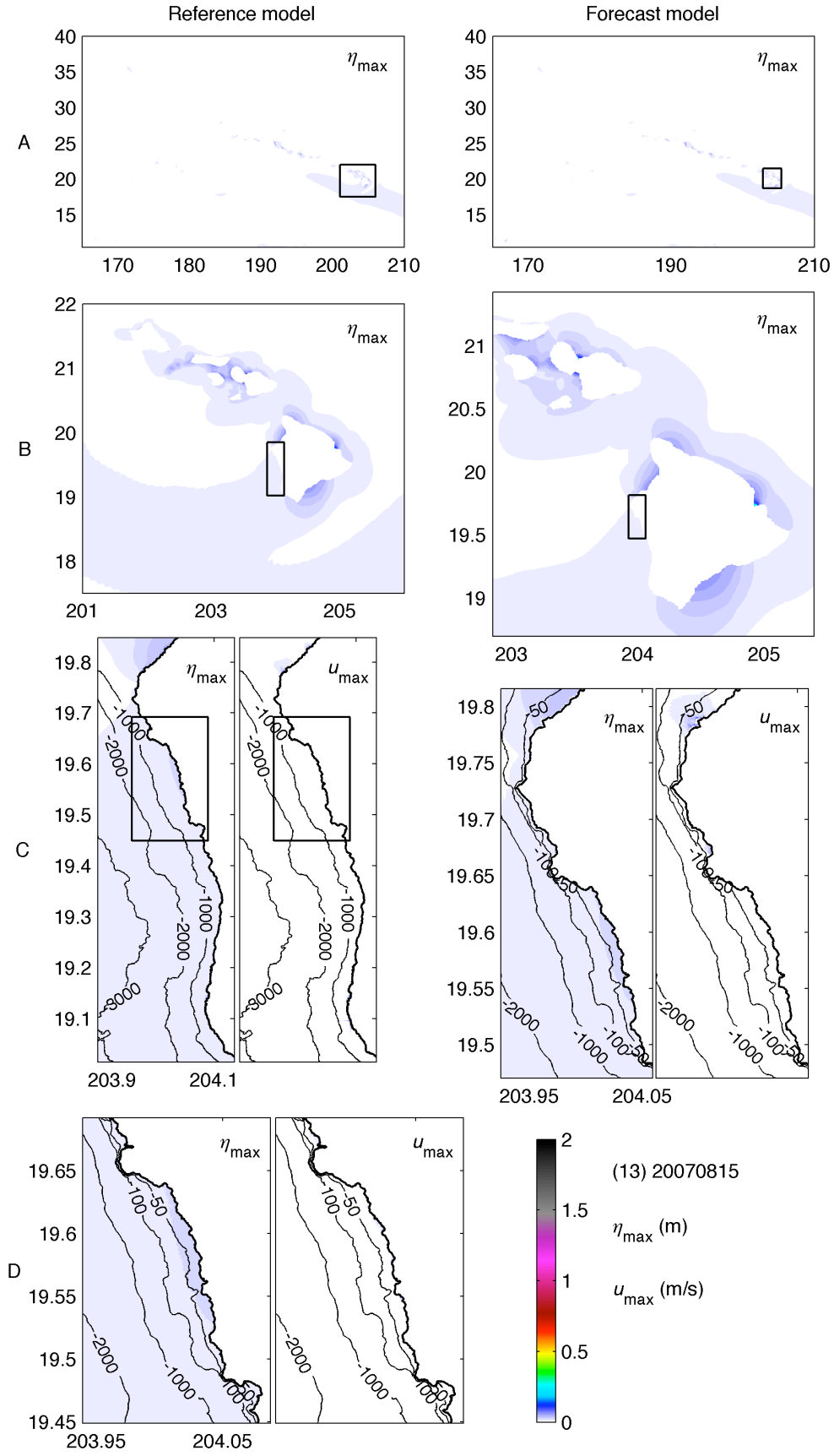

Figure 13 (13): Computed maximum sea surface elevation and current by the Kailua-Kona reference and forecast models for the 2007 Peru tsunami.

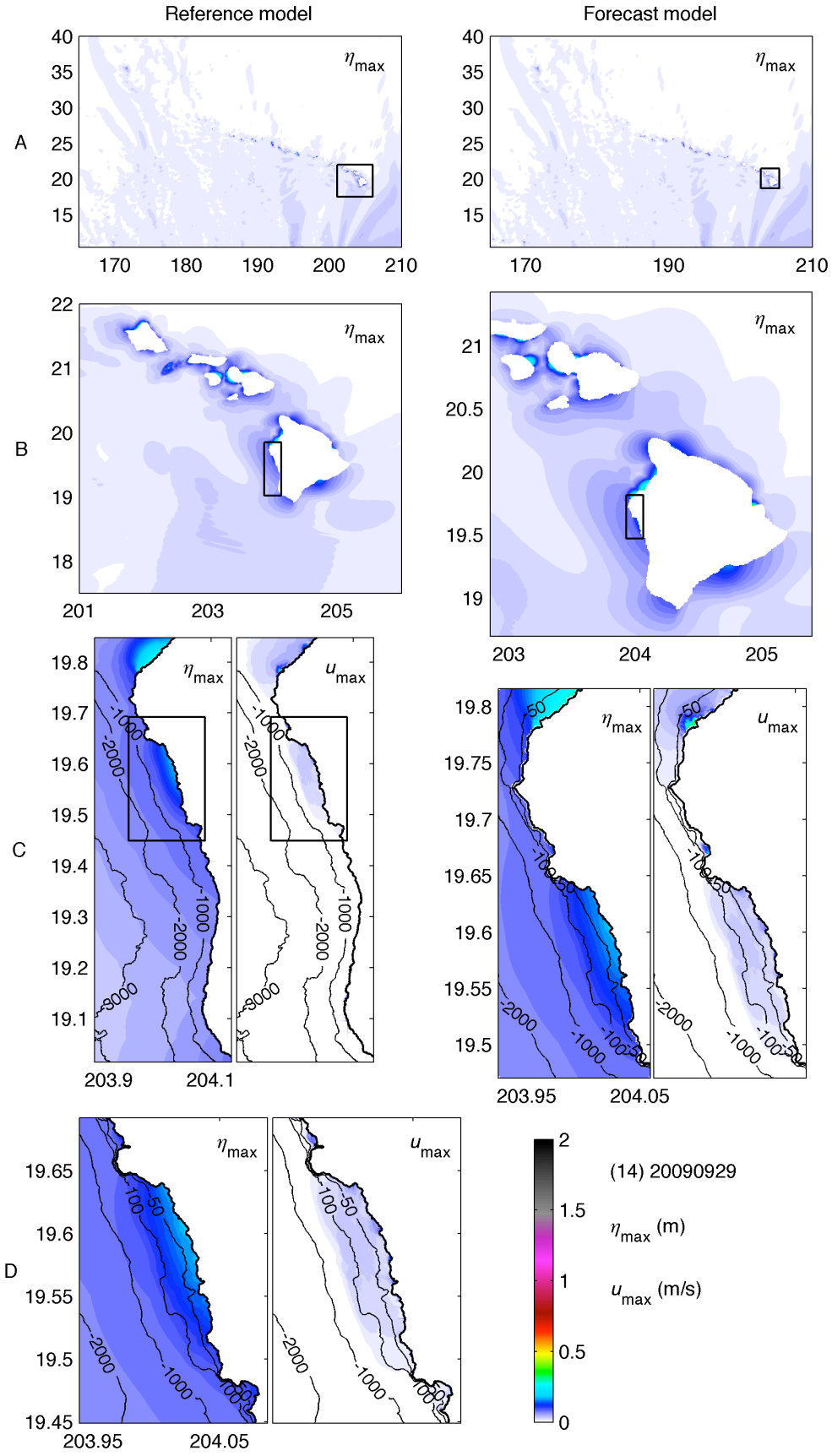

Figure 13 (14): Computed maximum sea surface elevation and current by the Kailua-Kona reference and forecast models for the 2009 Samoa tsunami.

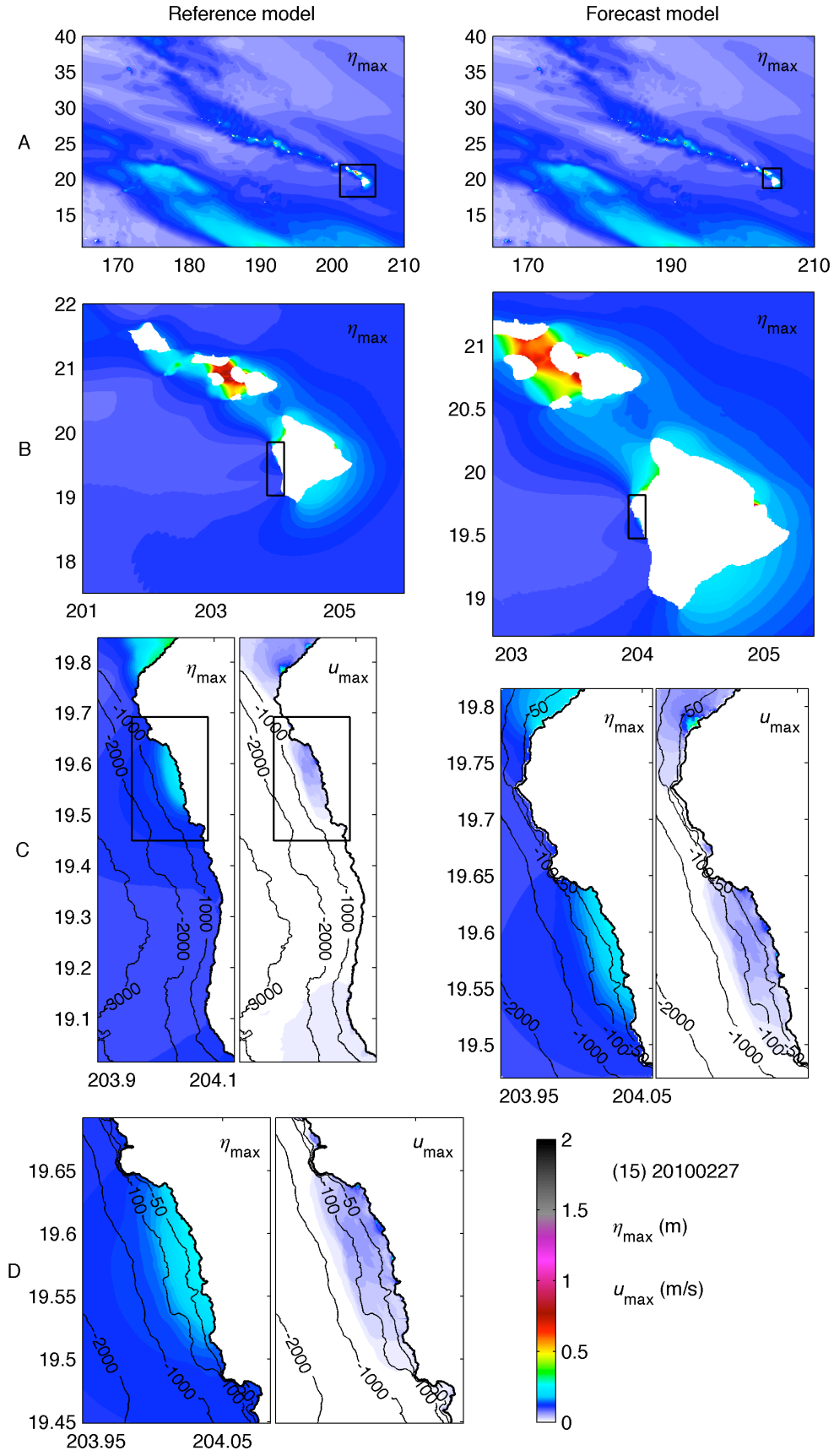

Figure 13 (15): Computed maximum sea surface elevation and current by the Kailua-Kona reference and forecast models for the 2010 Chile tsunami.

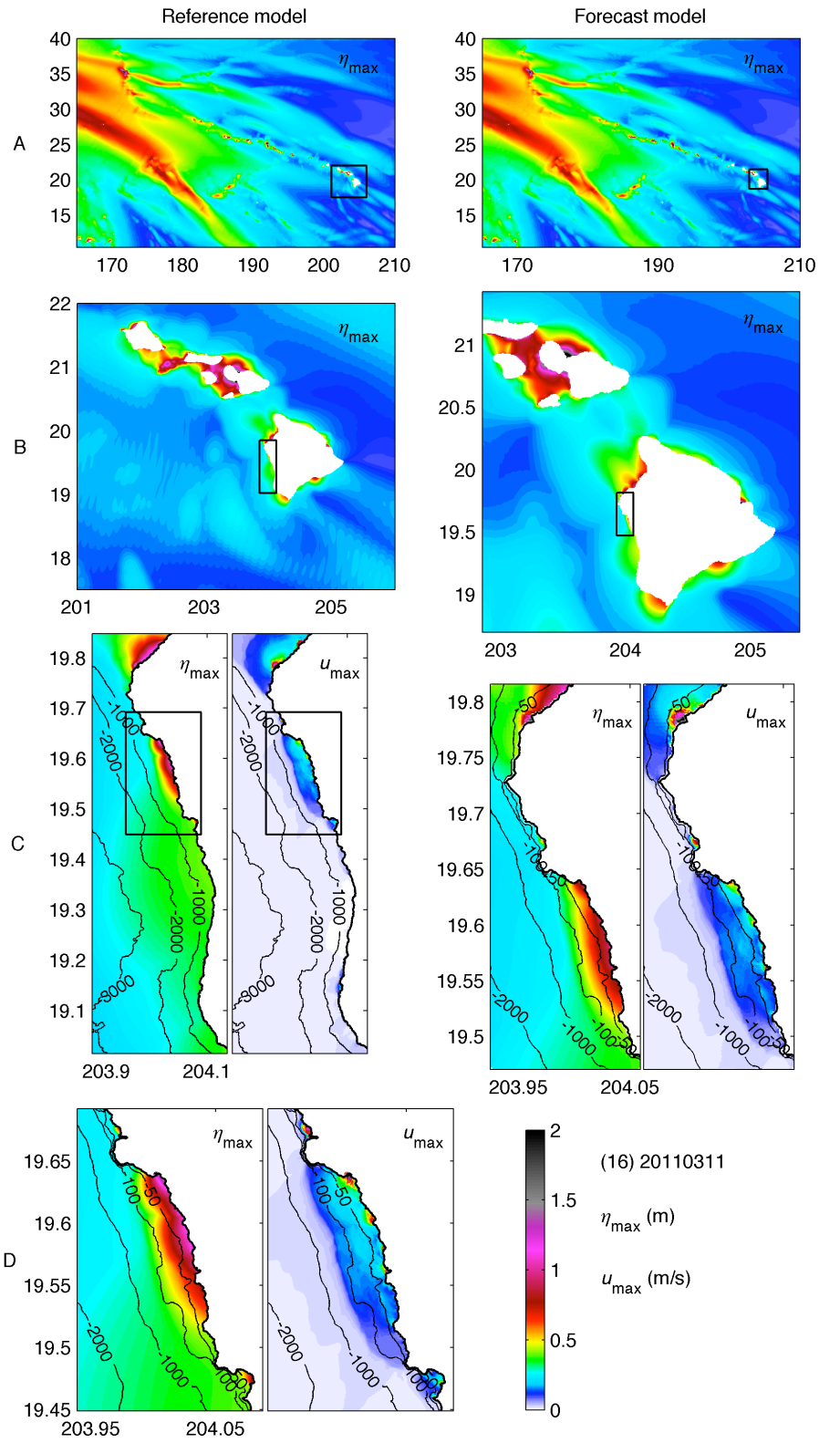

Figure 13 (16): Computed maximum sea surface elevation and current by the Kailua-Kona reference and forecast models for the 2011 Japan tsunami

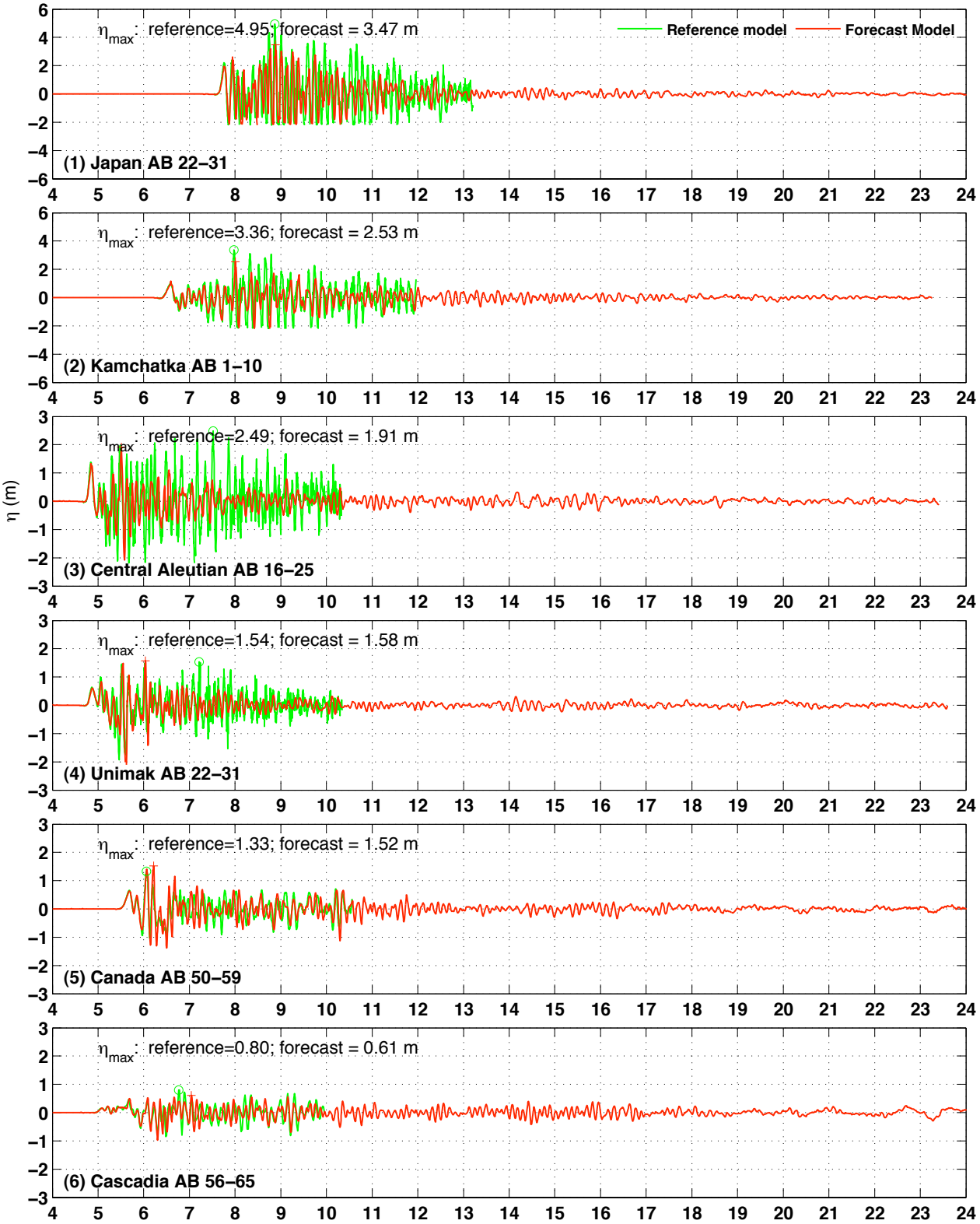
η (m)
Reference model
Forecast Model
ηmax: reference=4.95; forecast = 3.47 m
(1) Japan AB 22–31
ηmax: reference=3.36; forecast = 2.53 m
(2) Kamchatka AB 1–10
ηmax: reference=2.49; forecast = 1.91 m
(3) Central Aleutian AB 16–25
ηmax: reference=1.54; forecast = 1.58 m
(4) Unimak AB 22–31
ηmax: reference=1.33; forecast = 1.52 m
(5) Canada AB 50–59
ηmax: reference=0.80; forecast = 0.61 m
(6) Cascadia AB 56–65

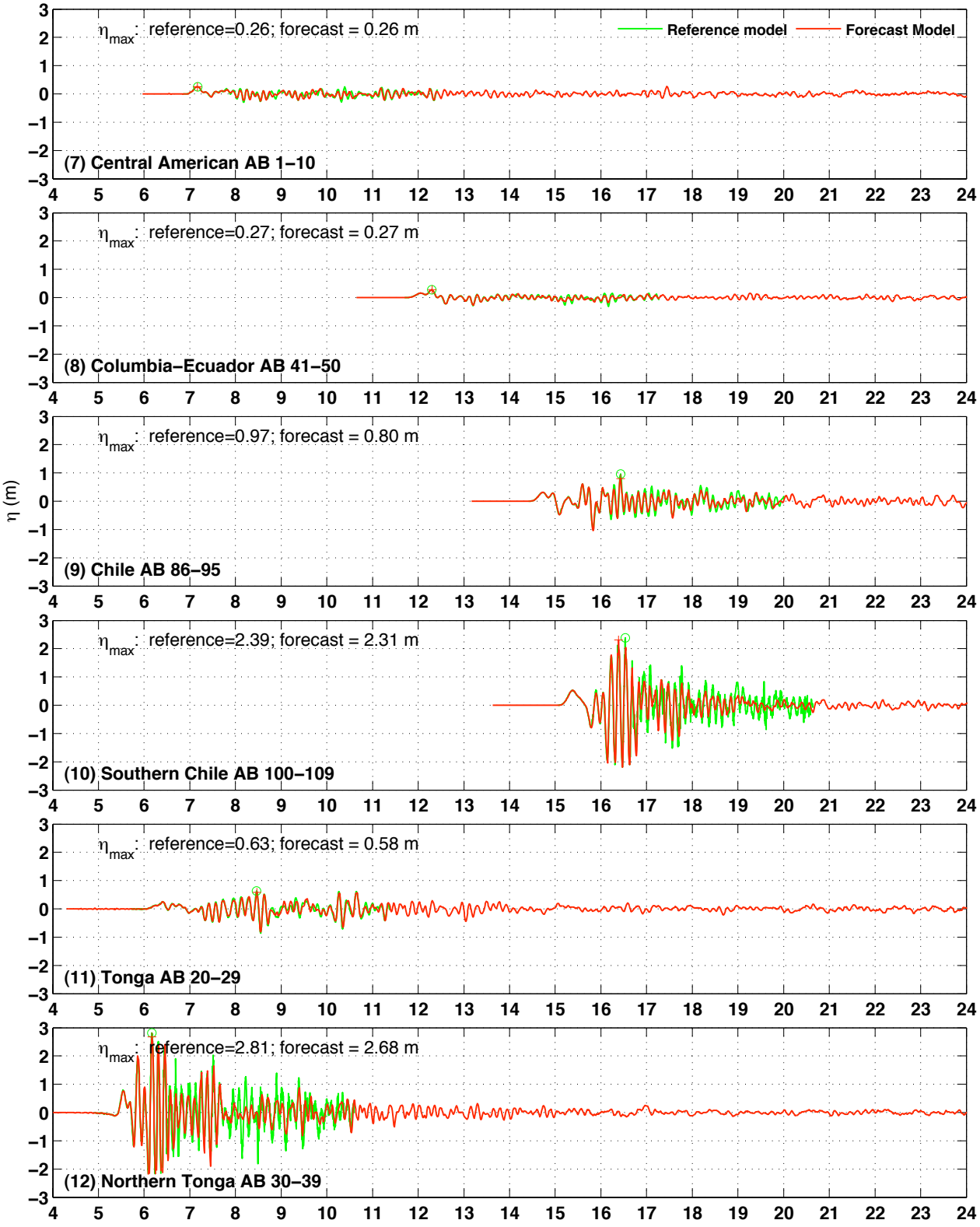
η (m)
ηmax: reference=0.26; forecast = 0.26 m
Reference model
Forecast Model
(7) Central American AB 1–10
ηmax: reference=0.27; forecast = 0.27 m
(8) Columbia–Ecuador AB 41–50
ηmax: reference=0.97; forecast = 0.80 m
(9) Chile AB 86–95
ηmax: reference=2.39; forecast = 2.31 m
(10) Southern Chile AB 100–109
ηmax: reference=0.63; forecast = 0.58 m
(11) Tonga AB 20–29
ηmax: reference=2.81; forecast = 2.68 m
(12) Northern Tonga AB 30–39

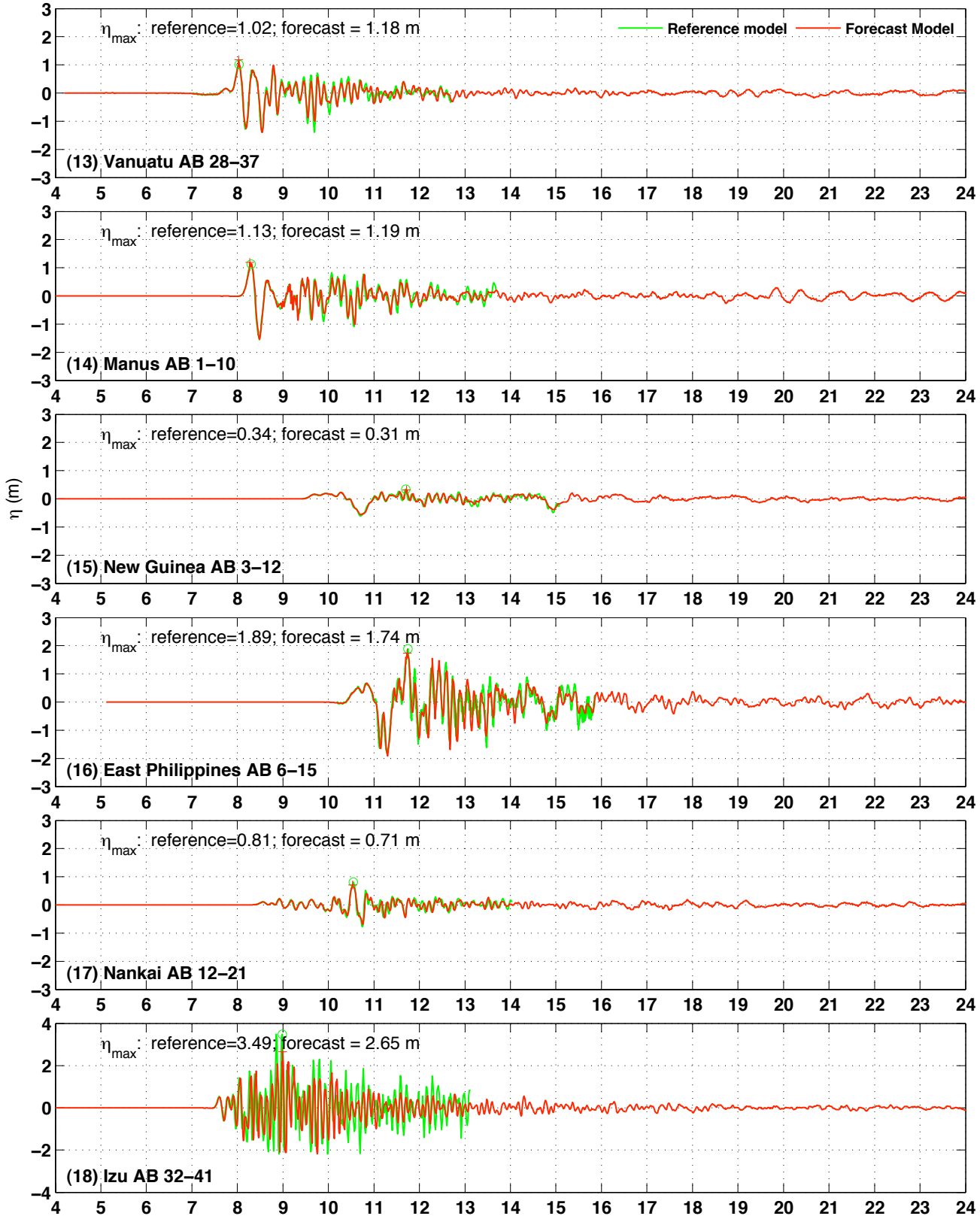

Figure 14: Modeled time series of sea surface elevation η at Kailua-Kona warning point for the eighteen simulated magnitude 9.3 tsunamis. o and + $\eta_{\max}$, computed by the reference and forecast models respectively.

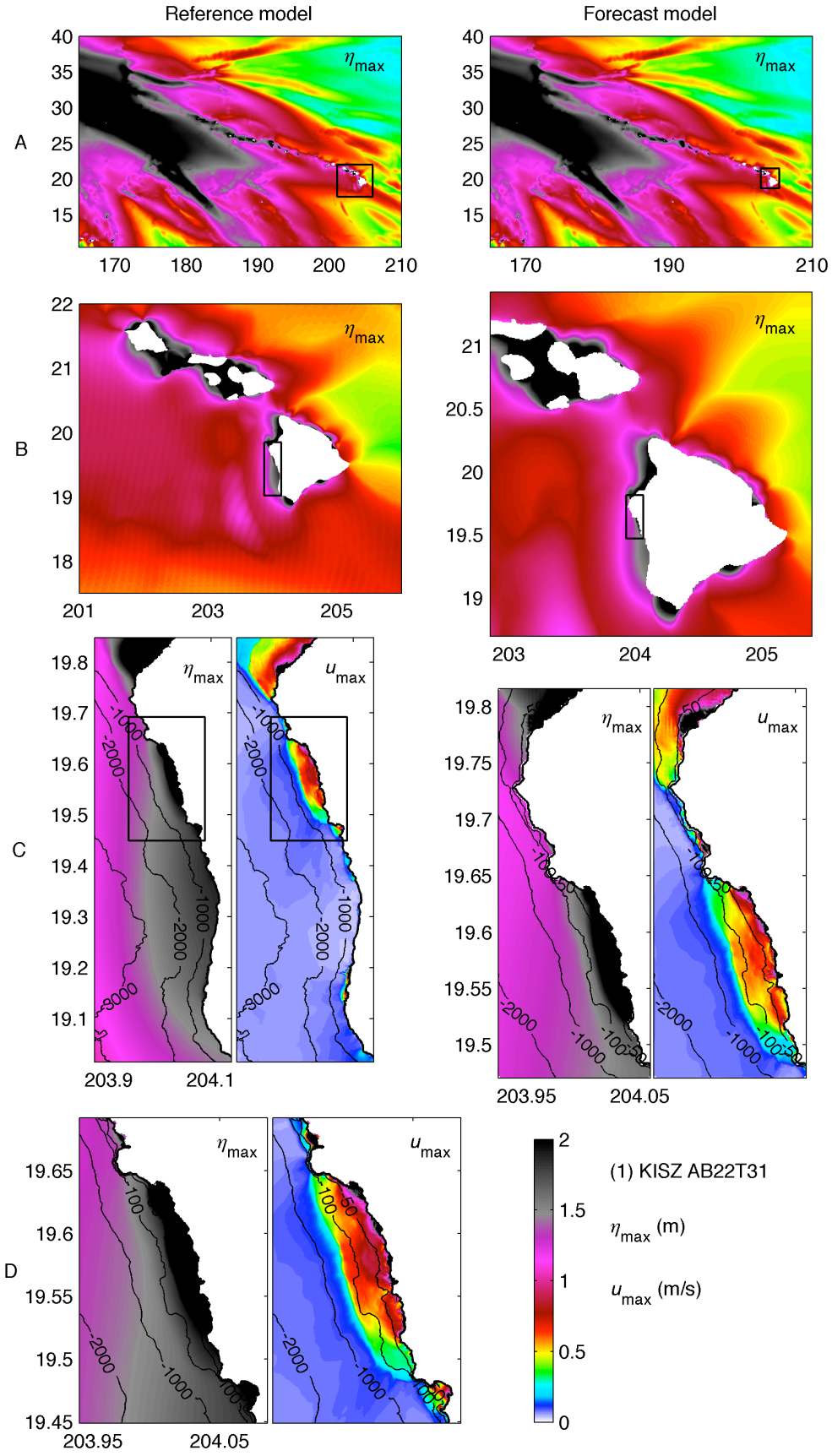

Figure 15 (1): Computed maximum sea surface elevation and flow speed by the Kona reference and forecast models from a M_w 9.3 Japan subduction zone tsunami.

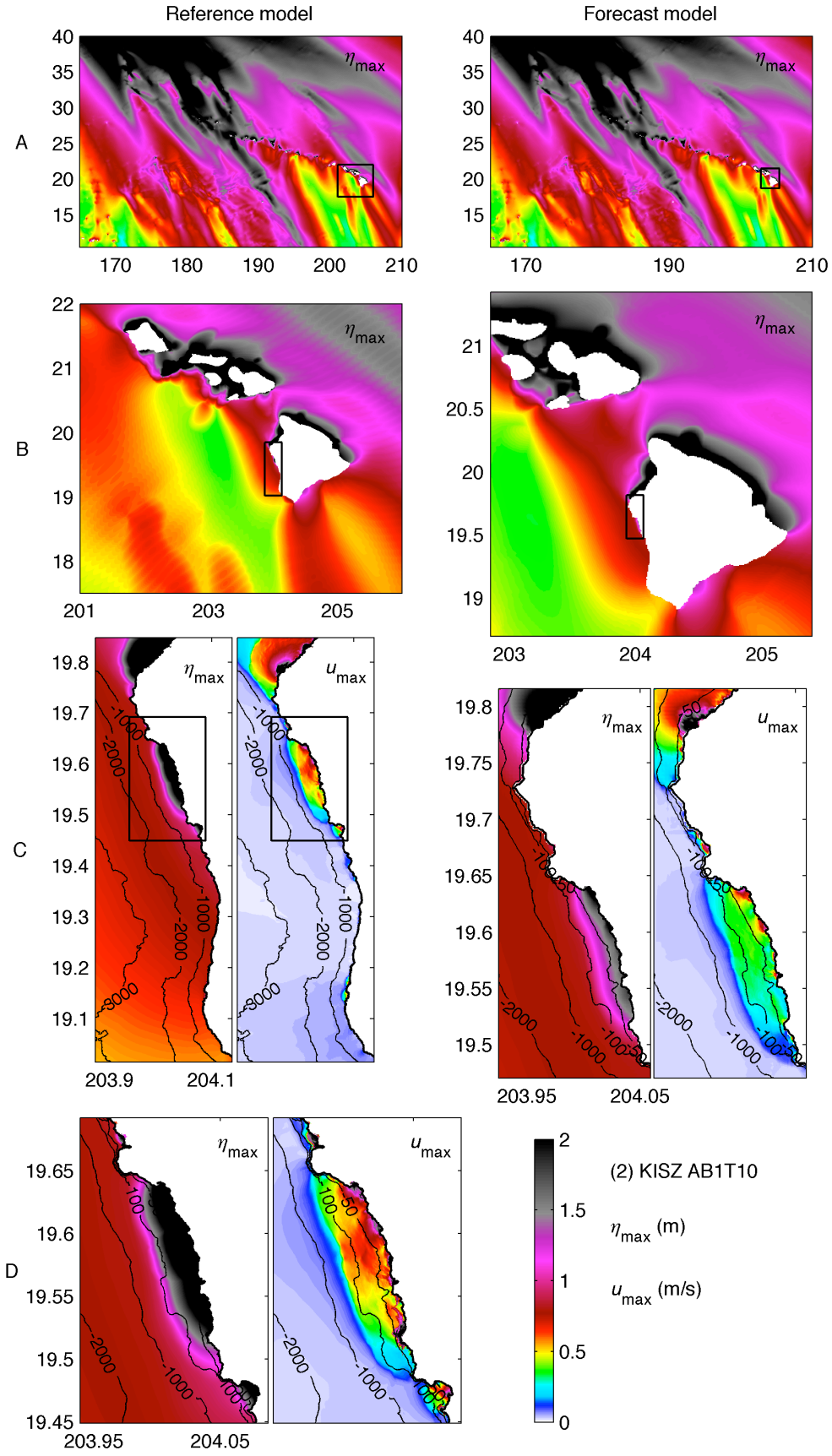

Figure 15 (1): Computed maximum sea surface elevation and flow speed by the Kona reference and forecast models from a M_w 9.3 Japan subduction zone tsunami.

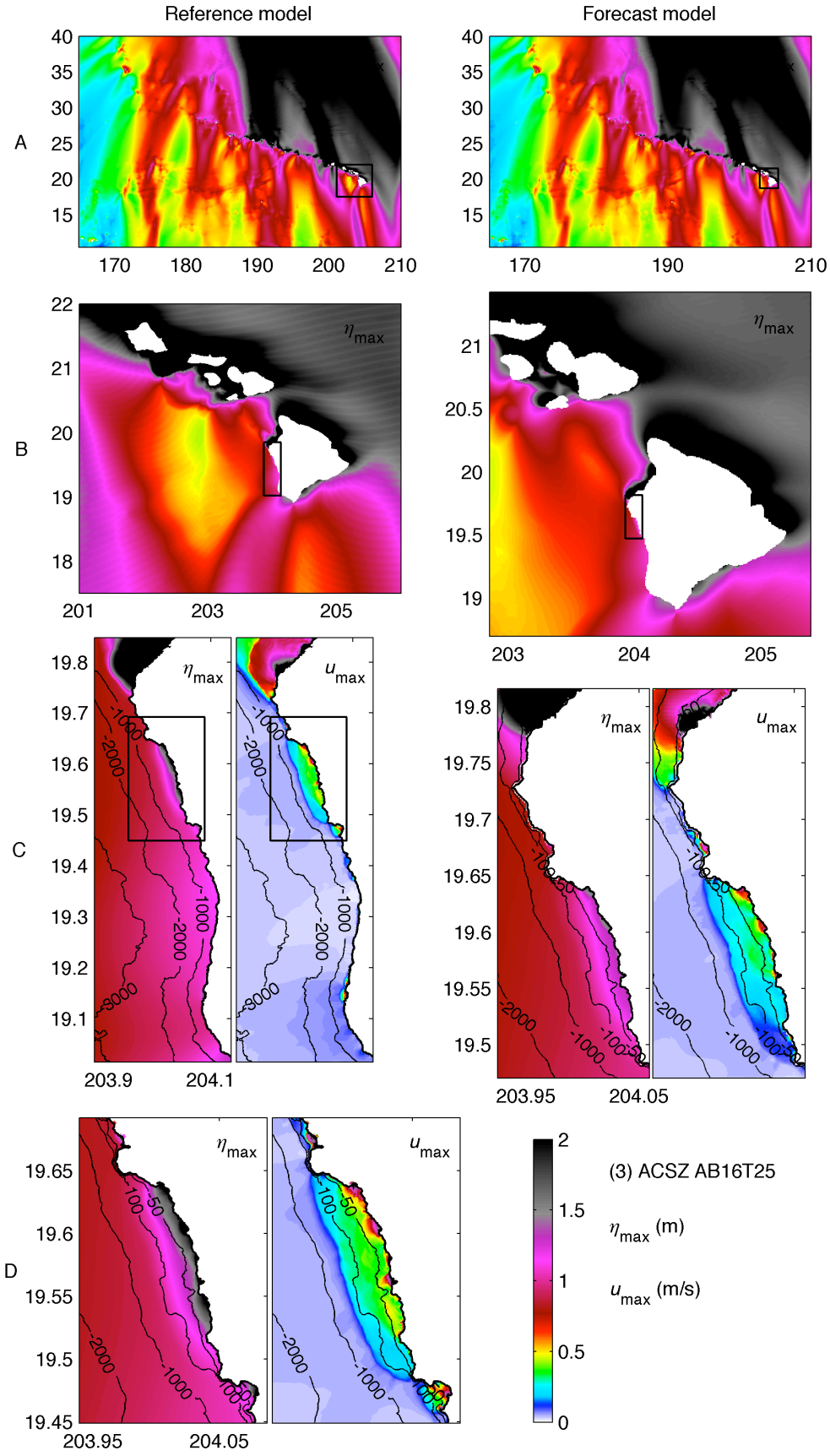

Figure 15 (2): Computed maximum sea surface elevation and flow speed by the Kona reference and forecast models from a M_w 9.3 Kamchatka subduction zone tsunami.

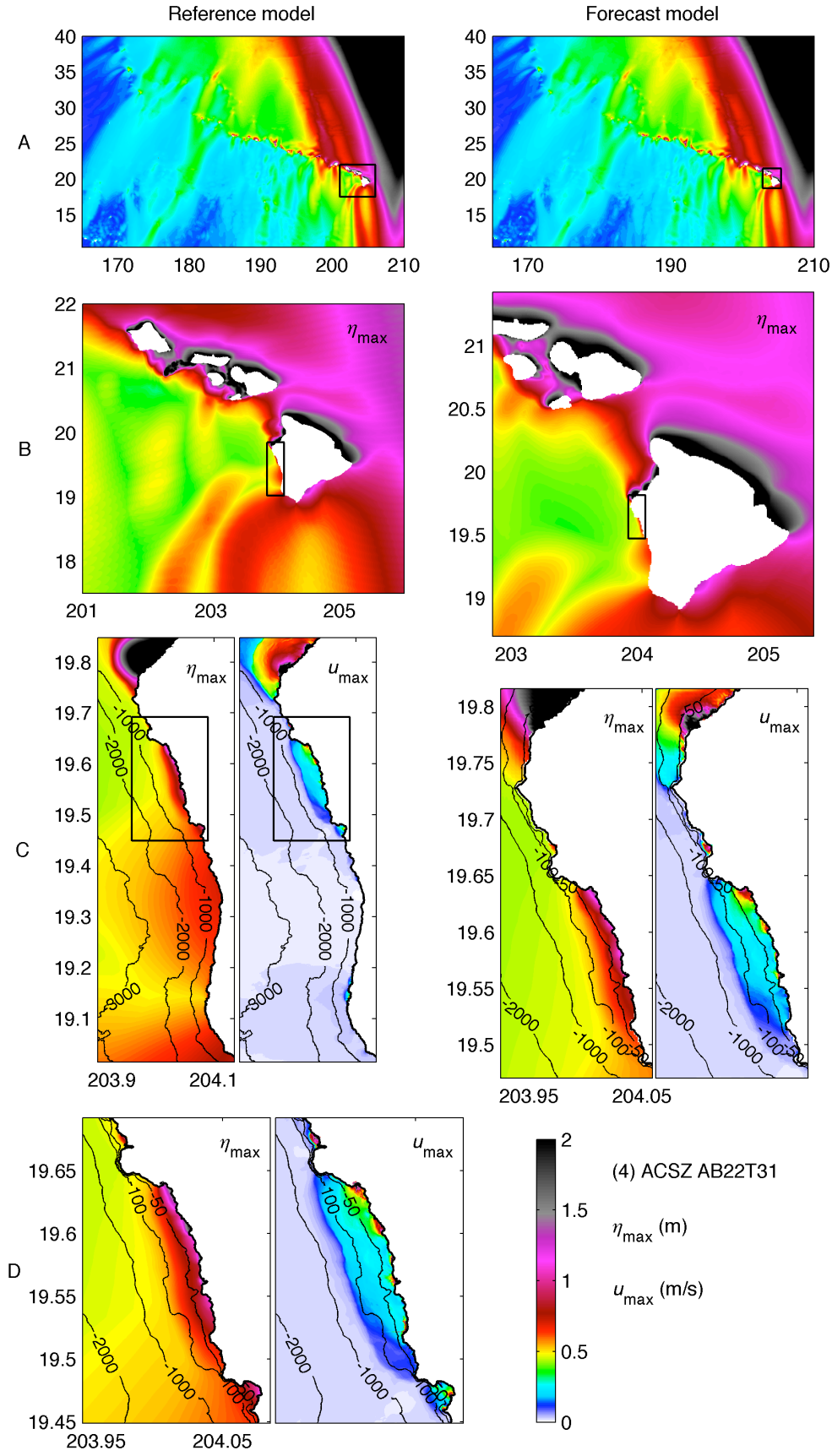

Figure 15 (4): Computed maximum sea surface elevation and flow speed by the Kailua-Kona reference and forecast models from a M_w 9.3 Unimak subduction zone tsunami.

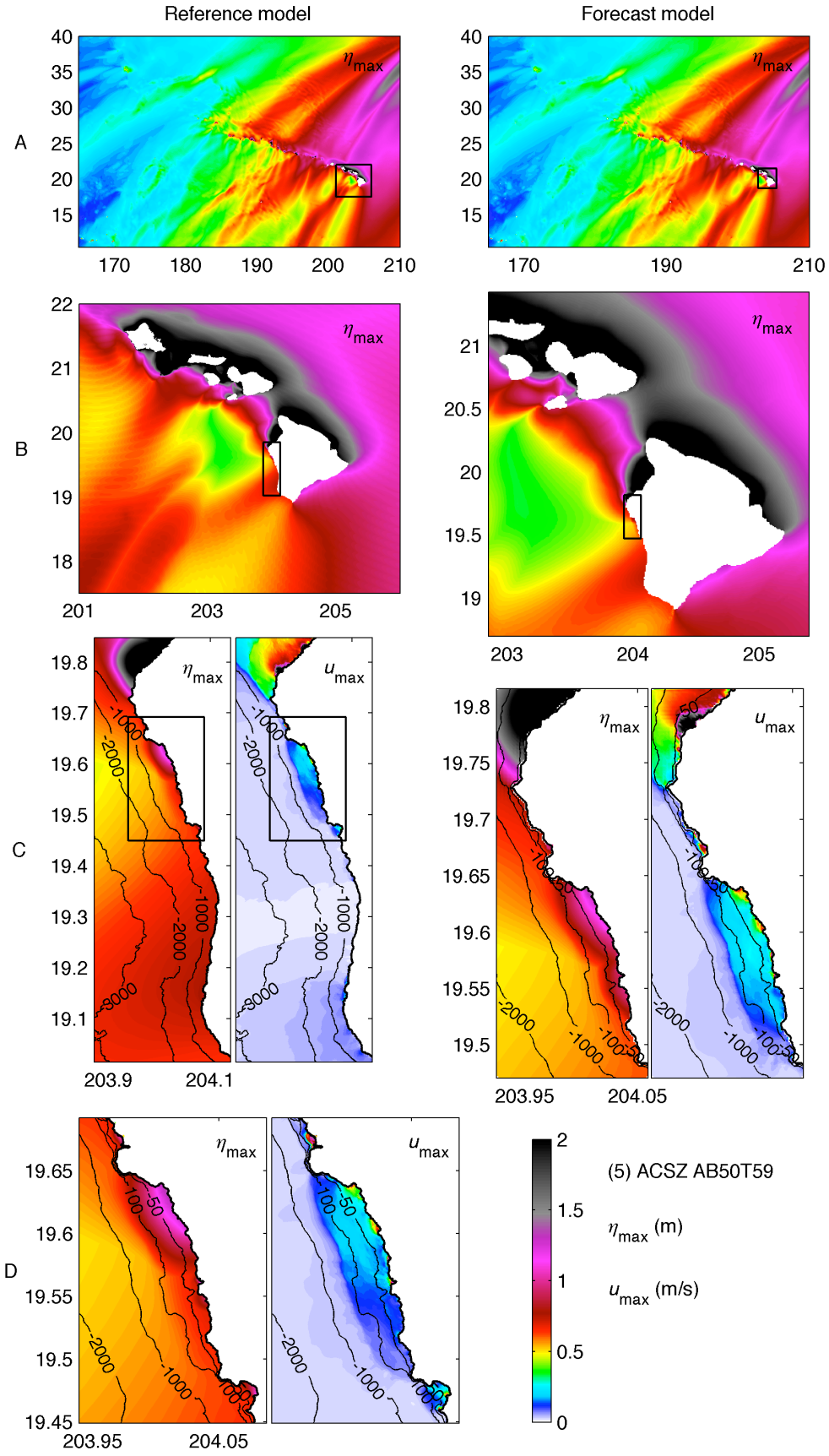

Figure 15 (5): Computed maximum sea surface elevation and flow speed by the Kailua-Kona reference and forecast models from a M_w 9.3 Canada subduction zone tsunami.

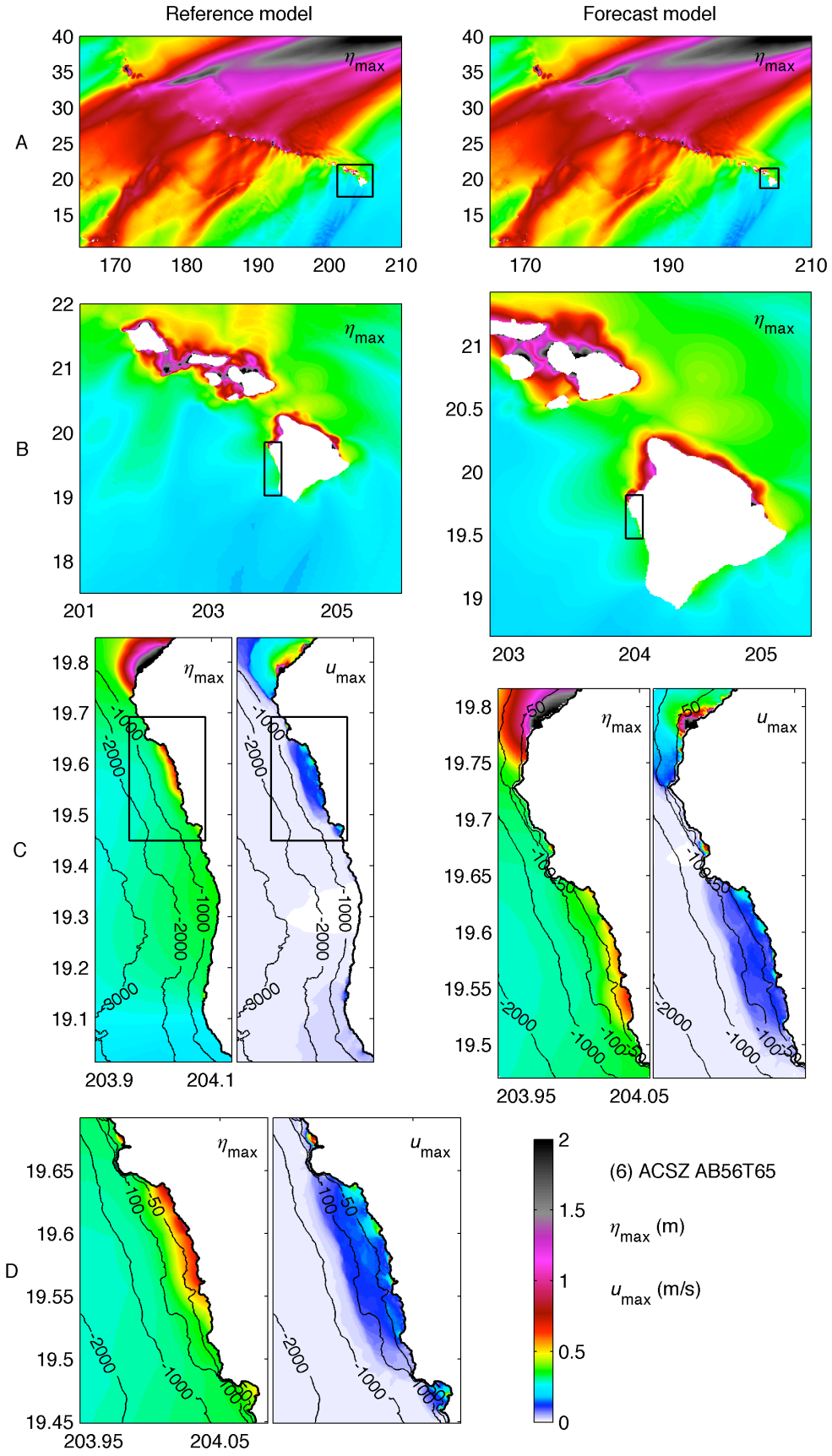

Figure 15 (6): Computed maximum sea surface elevation and flow speed by the Kona reference and forecast models from a M_w 9.3 Cascadia subduction zone tsunami.

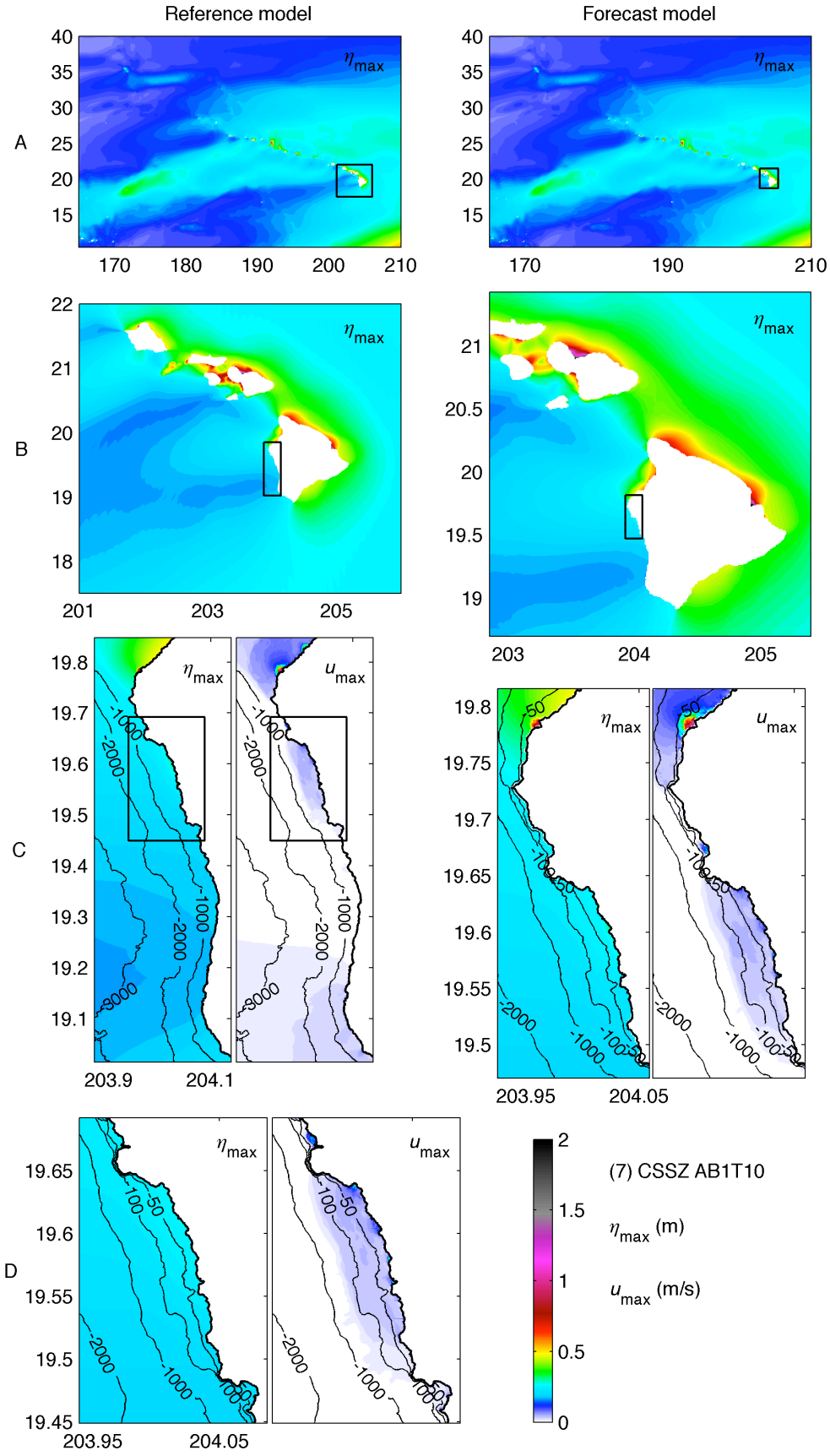

Figure 15 (7): Computed maximum sea surface elevation and flow speed by the Kona reference and forecast models from a M_w 9.3 Central American subduction zone tsunami.

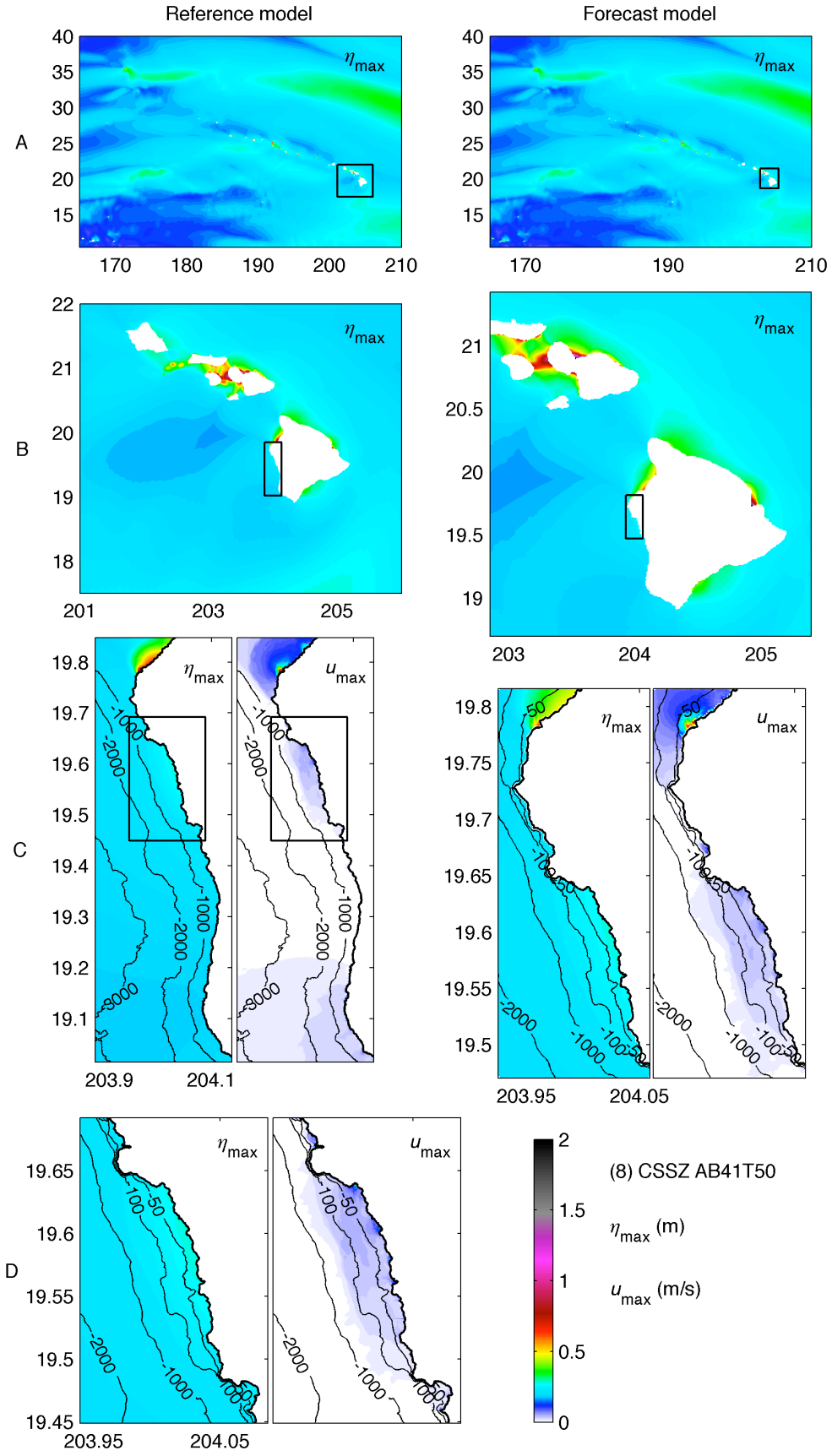

Figure 15 (8): Computed maximum sea surface elevation and flow speed by the Kona reference and forecast models from a M_w 9.3 Columbia-Ecuador subduction zone tsunami.

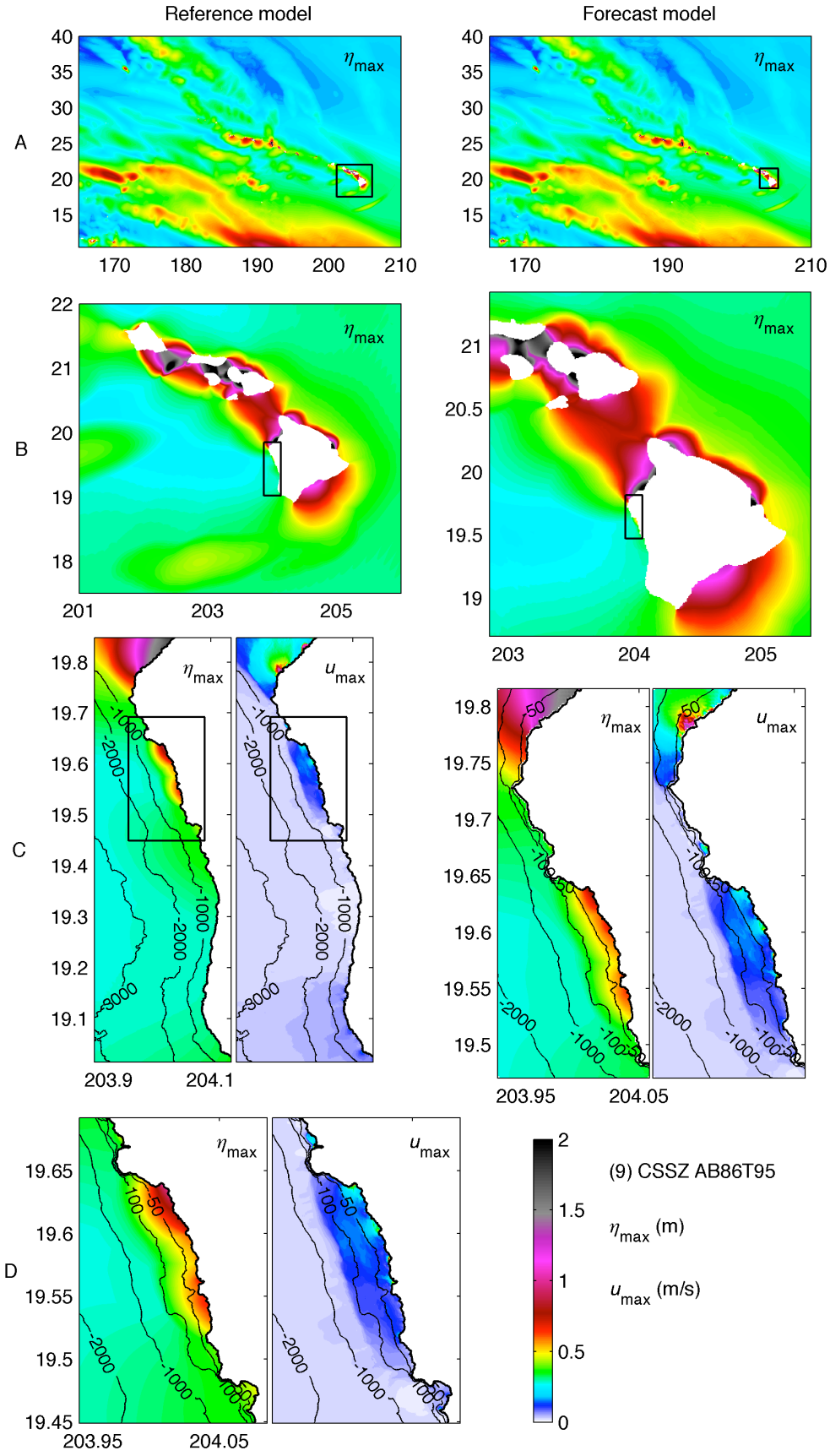

Figure 15 (9): Computed maximum sea surface elevation and flow speed by the Kailua-Kona reference and forecast models from a M_w 9.3 Chile subduction zone tsunami.

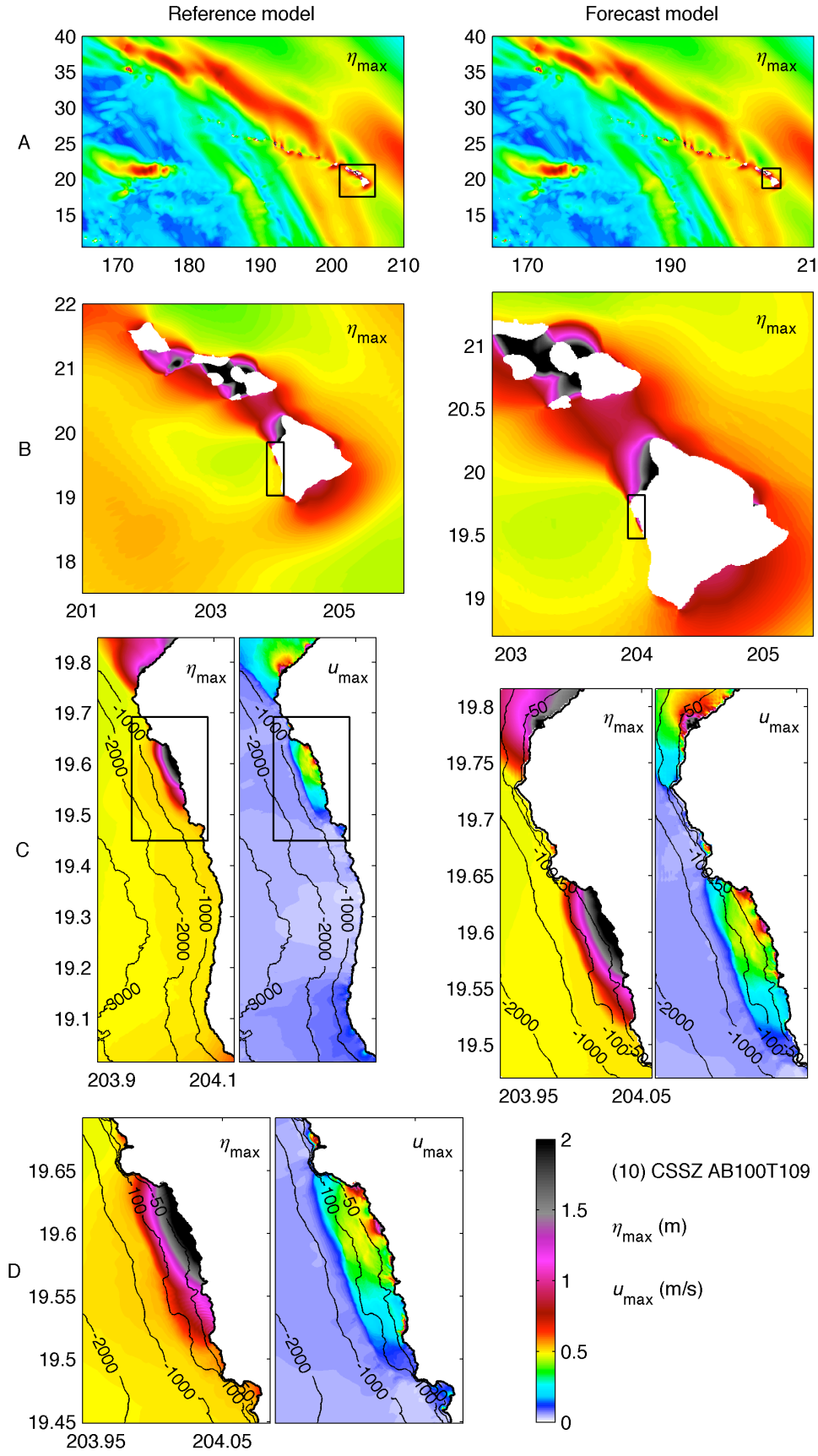

Figure 15 (10): Computed maximum sea surface elevation and flow speed by the Kailua-Kona reference and forecast models from a M_w 9.3 South Chile subduction zone tsunami.

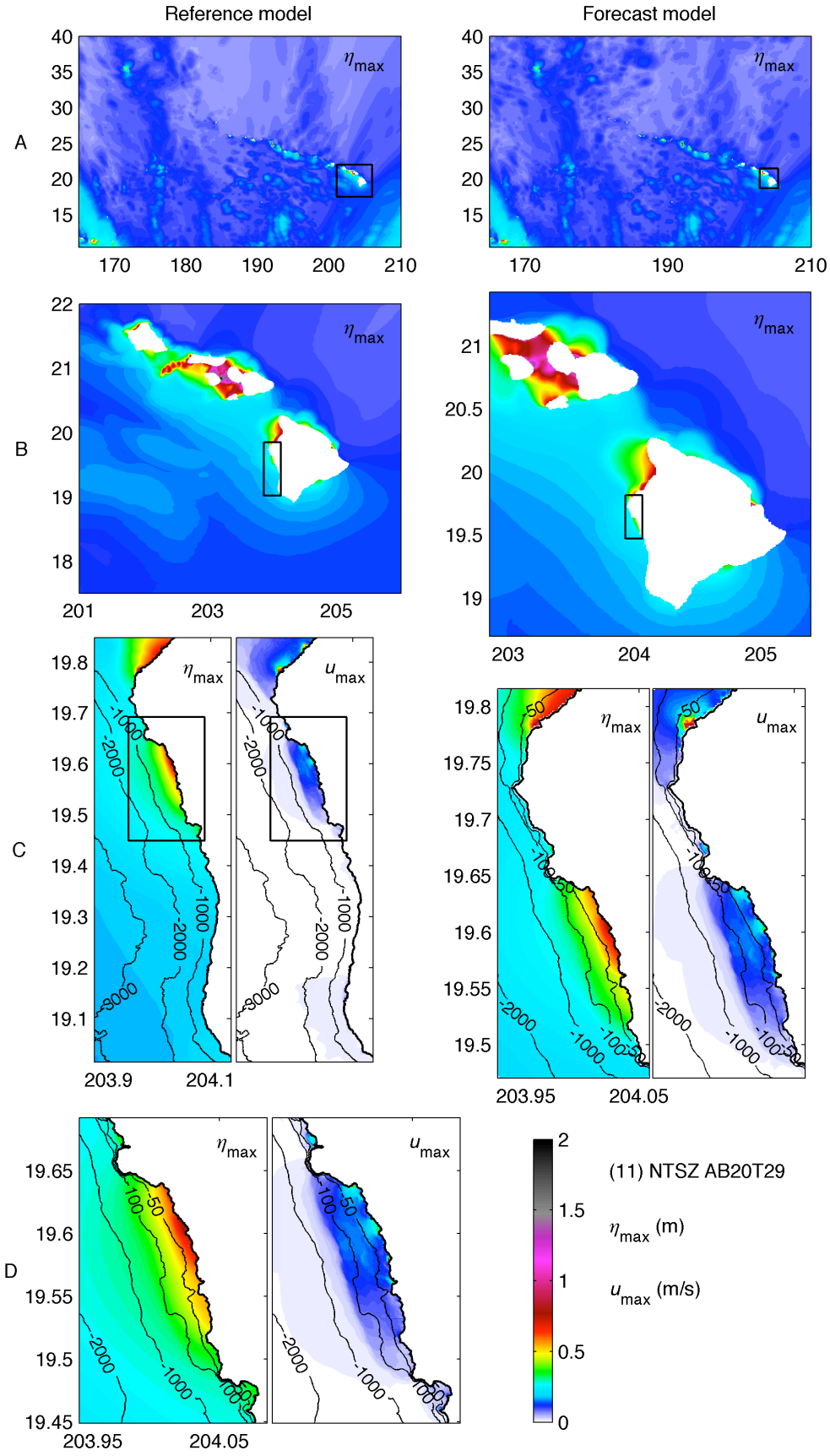

Figure 15 (11): Computed maximum sea surface elevation and flow speed by the Kailua-Kona reference and forecast models from a M_w 9.3 Tonga subduction zone tsunami.

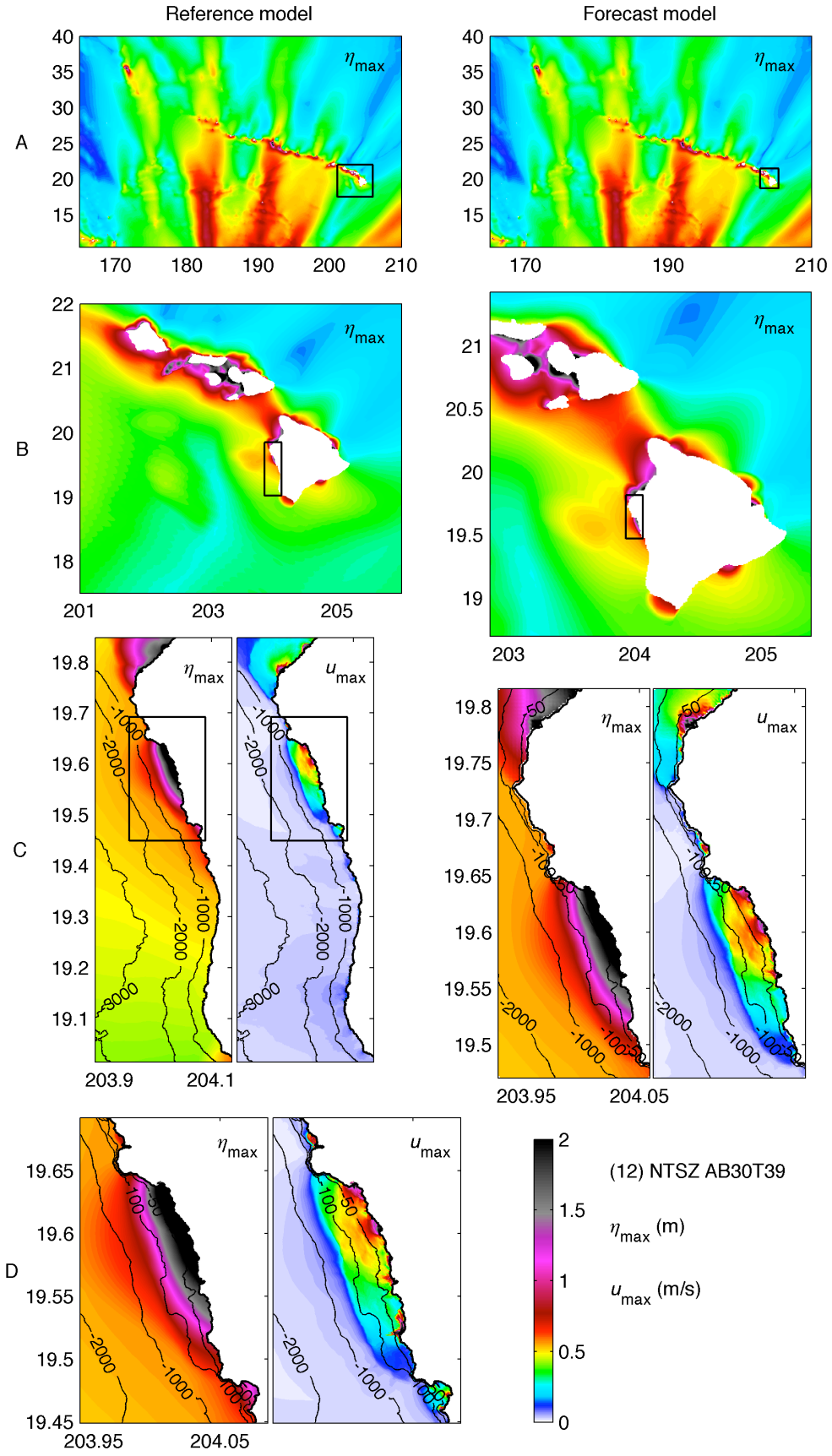

Figure 15 (12): Computed maximum sea surface elevation and flow speed by the Kailua-Kona reference and forecast models from a M_w 9.3 northern Tonga subduction zone tsunami.

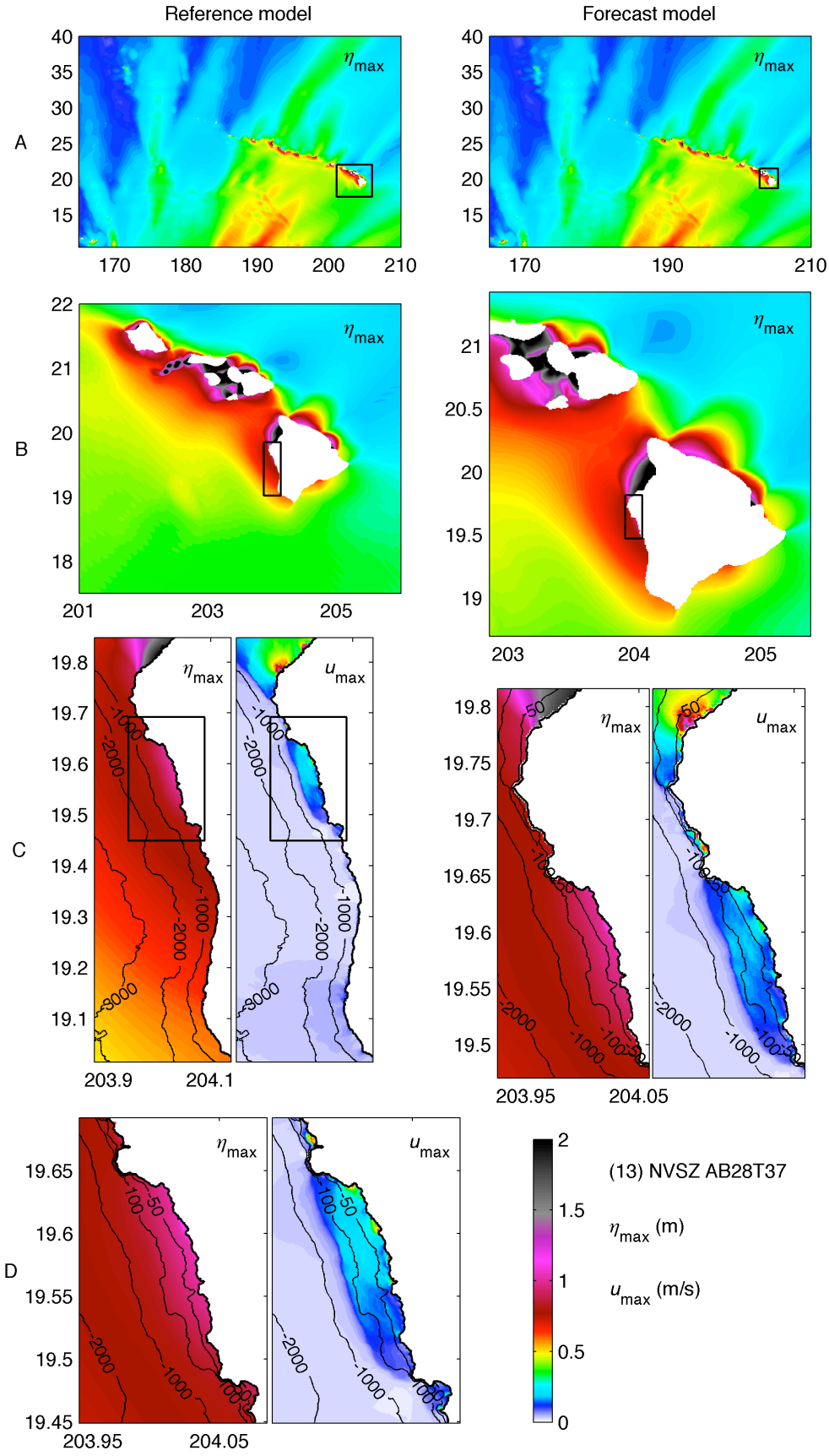

Figure 15 (13): Computed maximum sea surface elevation and flow speed by the Kailua-Kona reference and forecast models from a M_w 9.3 Vanuatu subduction zone tsunami.

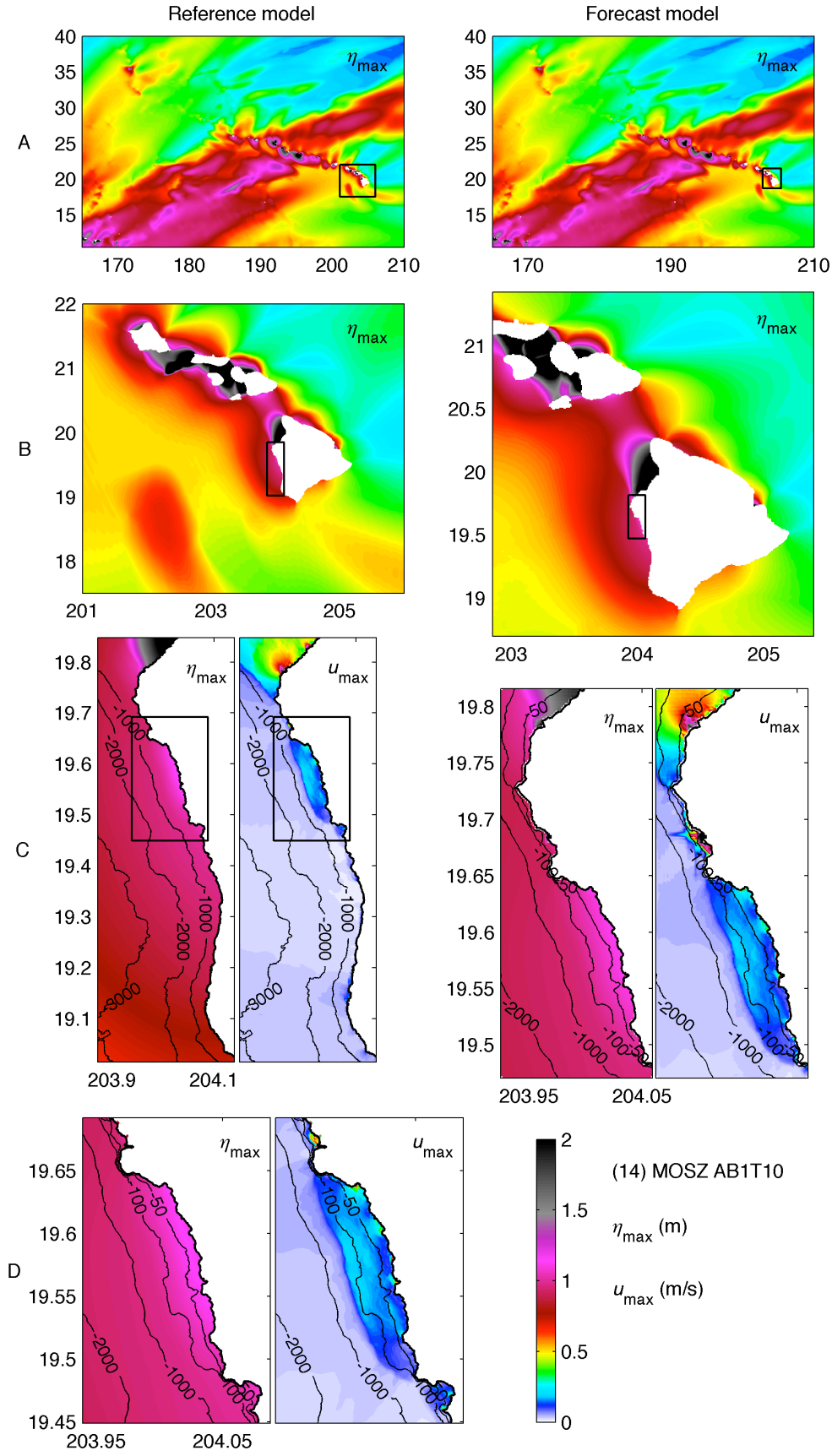

Figure 15 (14): Computed maximum sea surface elevation and flow speed by the Kailua-Kona reference and forecast models from a M_w 9.3 Manus subduction zone tsunami.

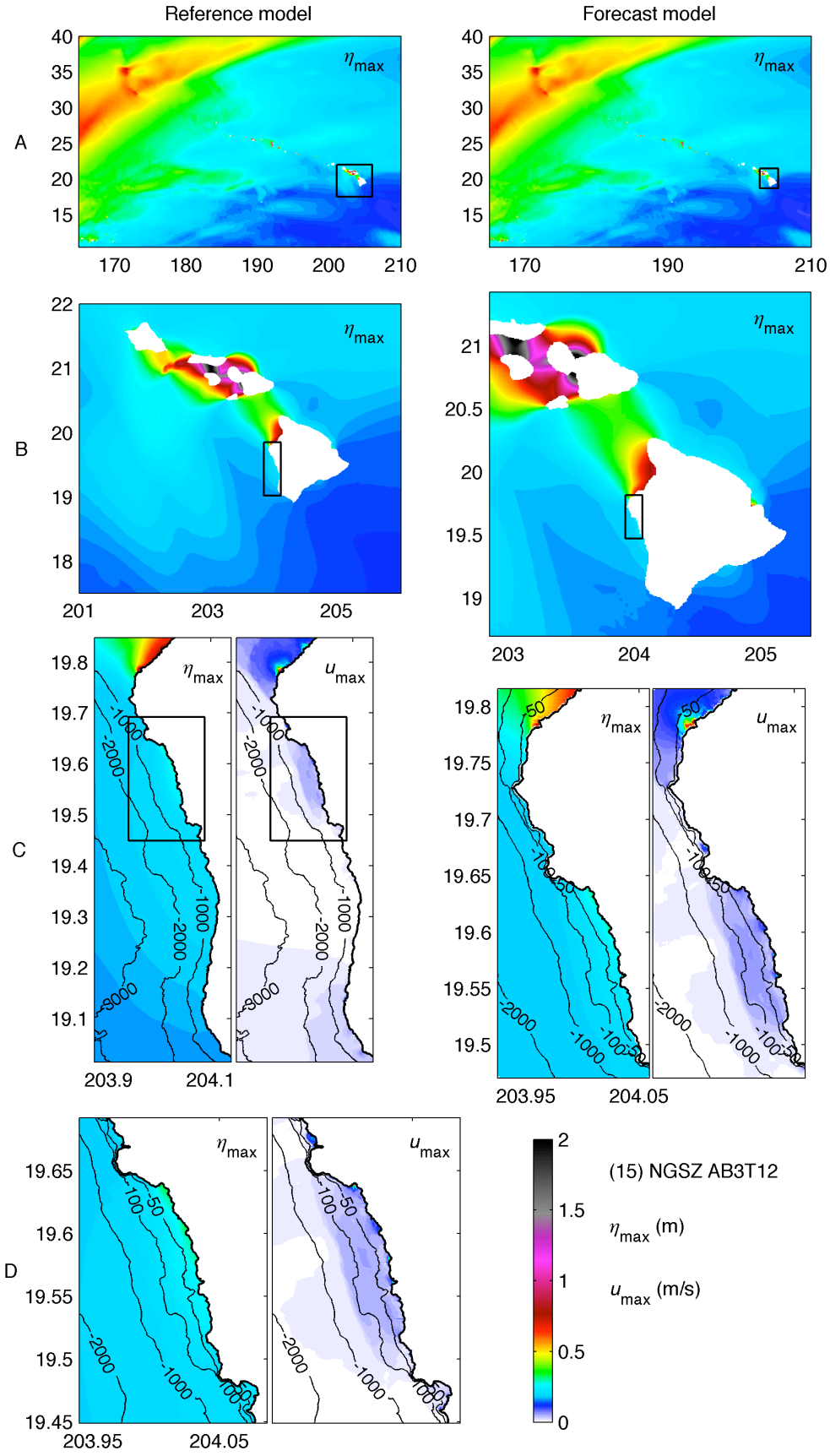

Figure 15 (15): Computed maximum sea surface elevation and flow speed by the Kailua-Kona reference and forecast models from a M_w 9.3 New Guinea subduction zone tsunami.

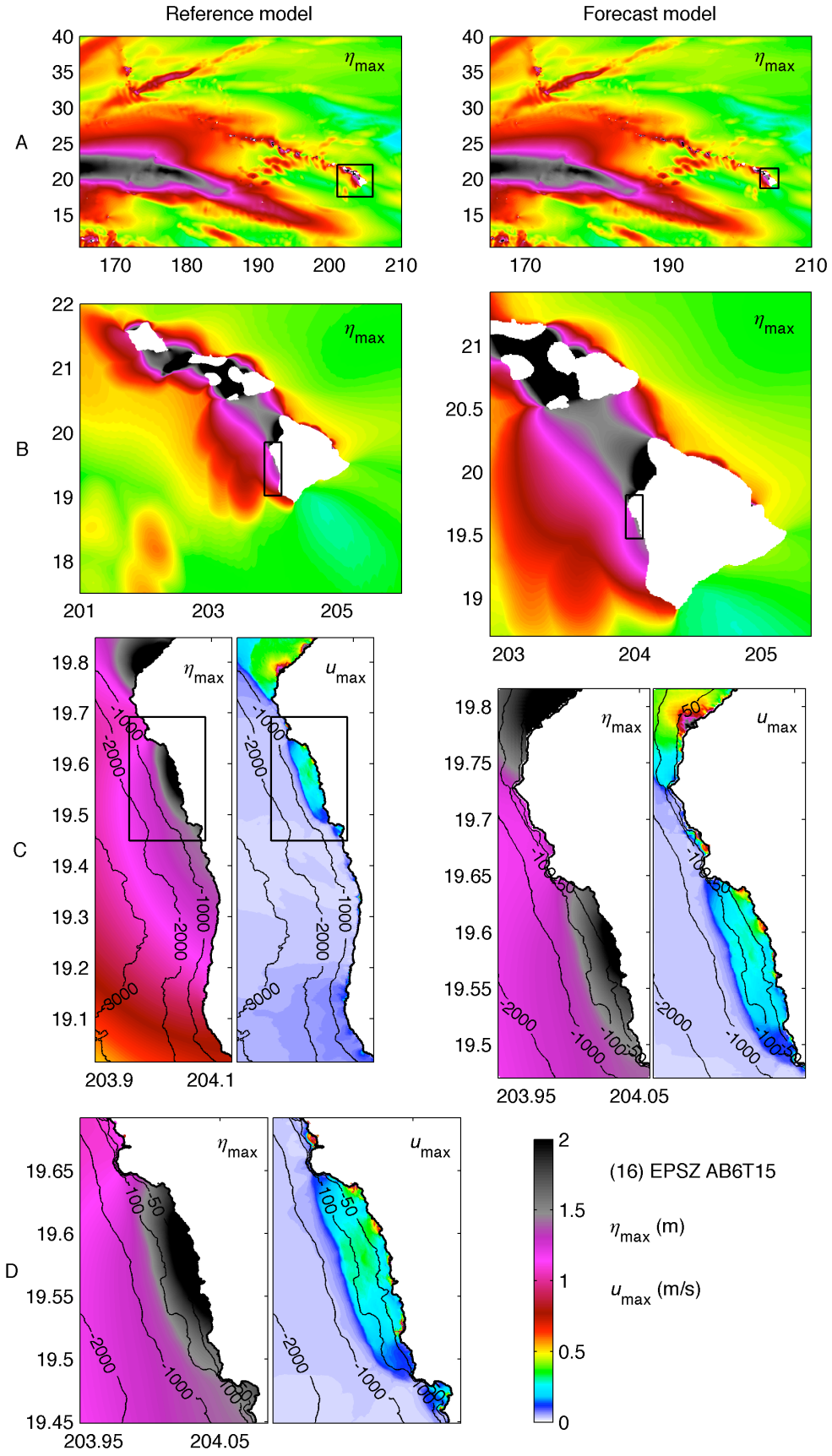

Figure 15 (16): Computed maximum sea surface elevation and flow speed by the Kailua-Kona reference and forecast models from a M_w 9.3 East Philippines subduction zone tsunami.

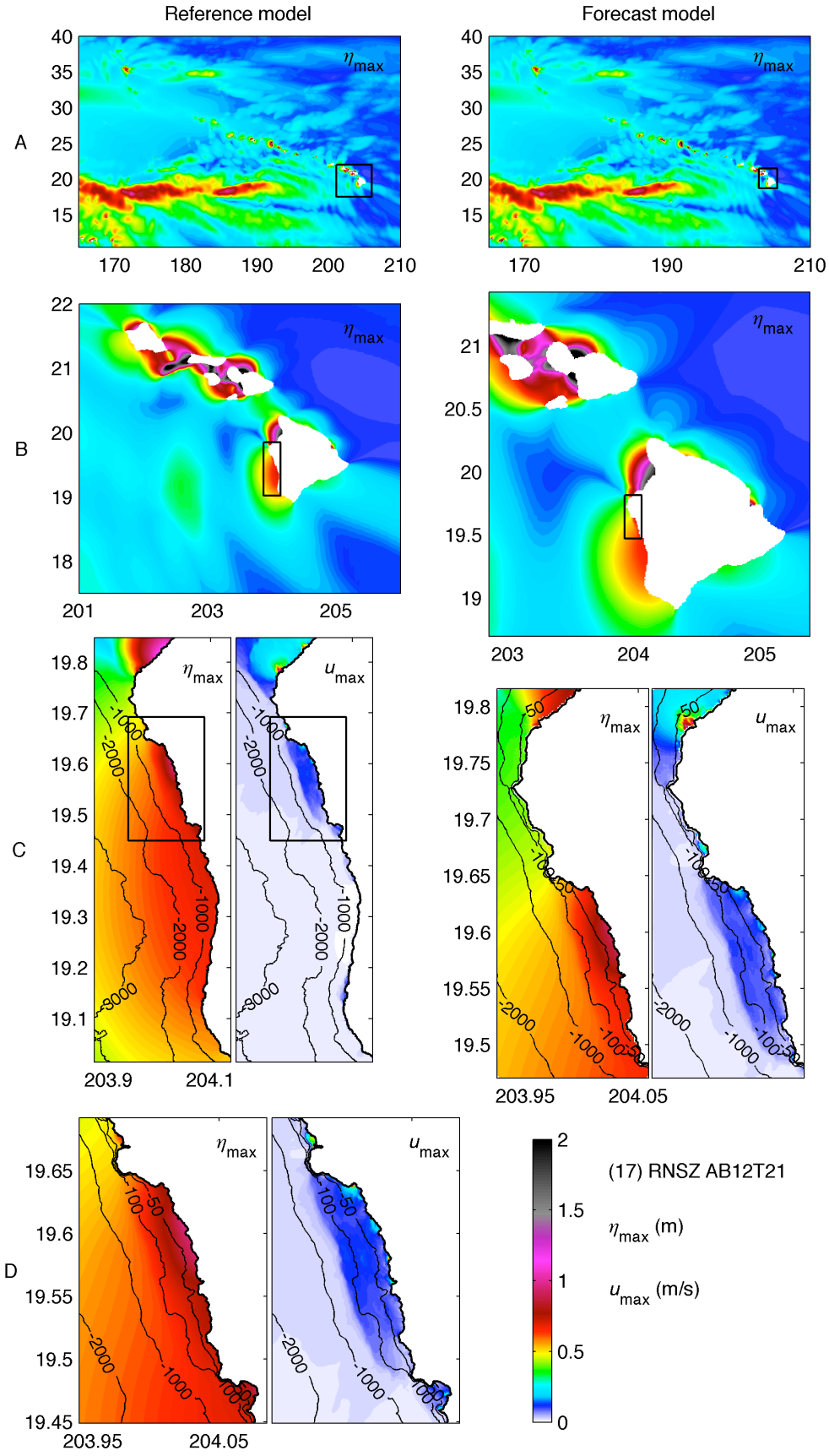

Figure 15 (17): Computed maximum sea surface elevation and flow speed by the Kailua-Kona reference and forecast models from a M_w 9.3 Nankai subduction zone tsunami.

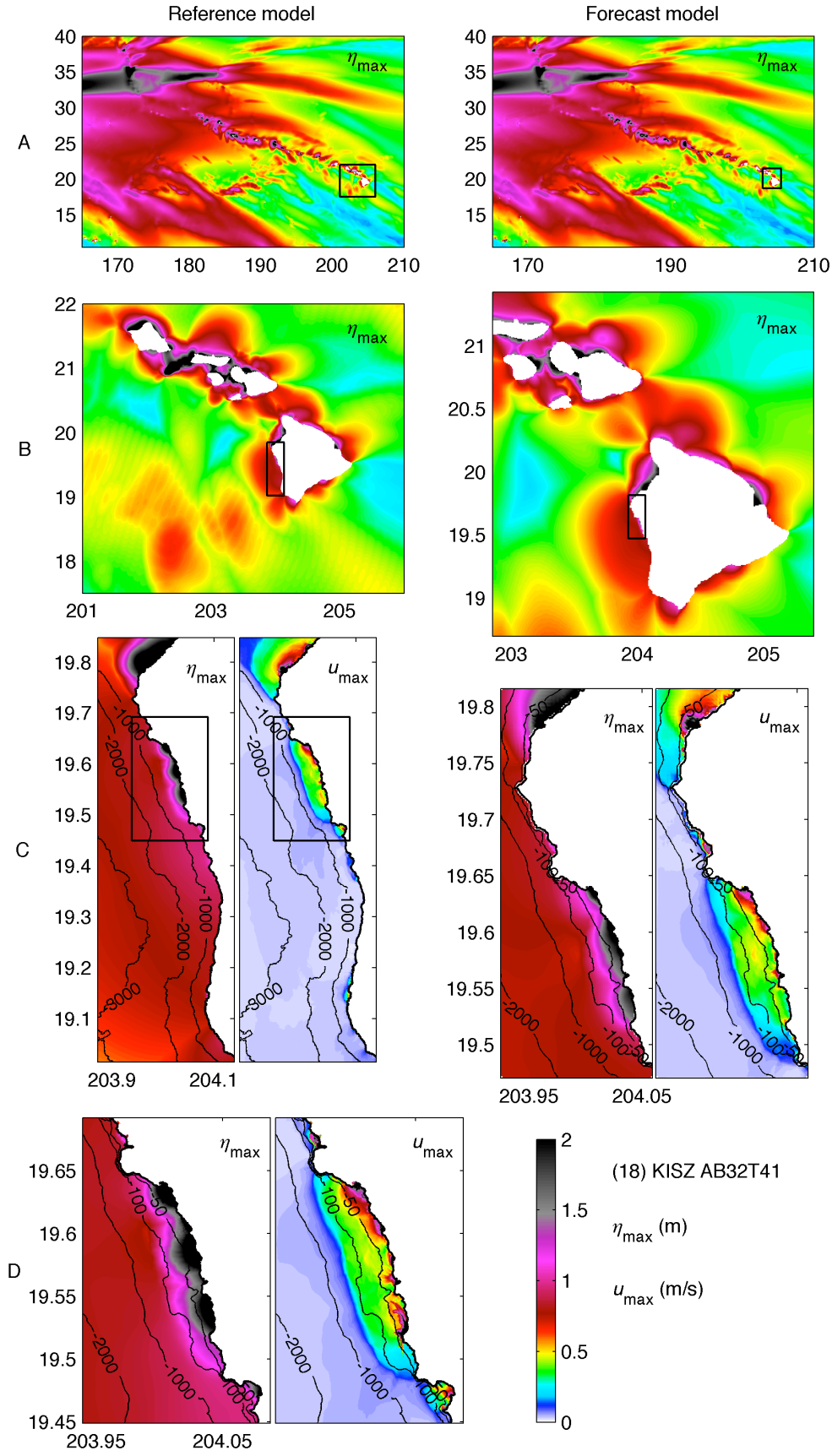

Figure 15 (18): Computed maximum sea surface elevation and current by the Kailua-Kona reference and forecast models from a M_w 9.3 Izu subduction zone tsunami.

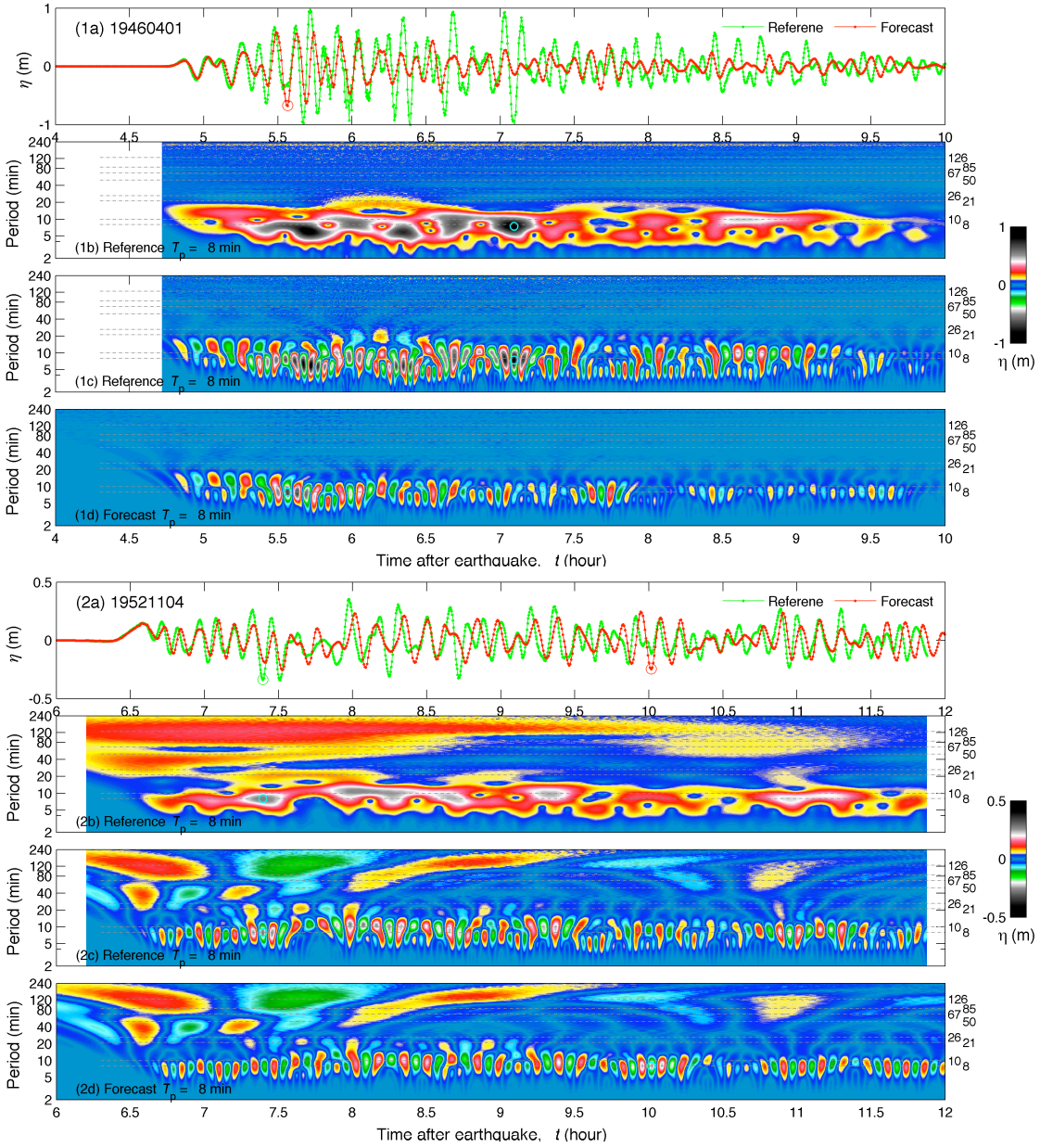
(1a) 19460401
Referene
Forecast
η (m)
(1b) Reference T_p = 8 min
(1c) Reference T_p = 8 min
(1d) Forecast T_p = 8 min
Period (min)
Time after earthquake, t (hour)
(2a) 19521104
(2b) Reference T_p = 8 min
(2c) Reference T_p = 8 min
(2d) Forecast T_p = 8 min

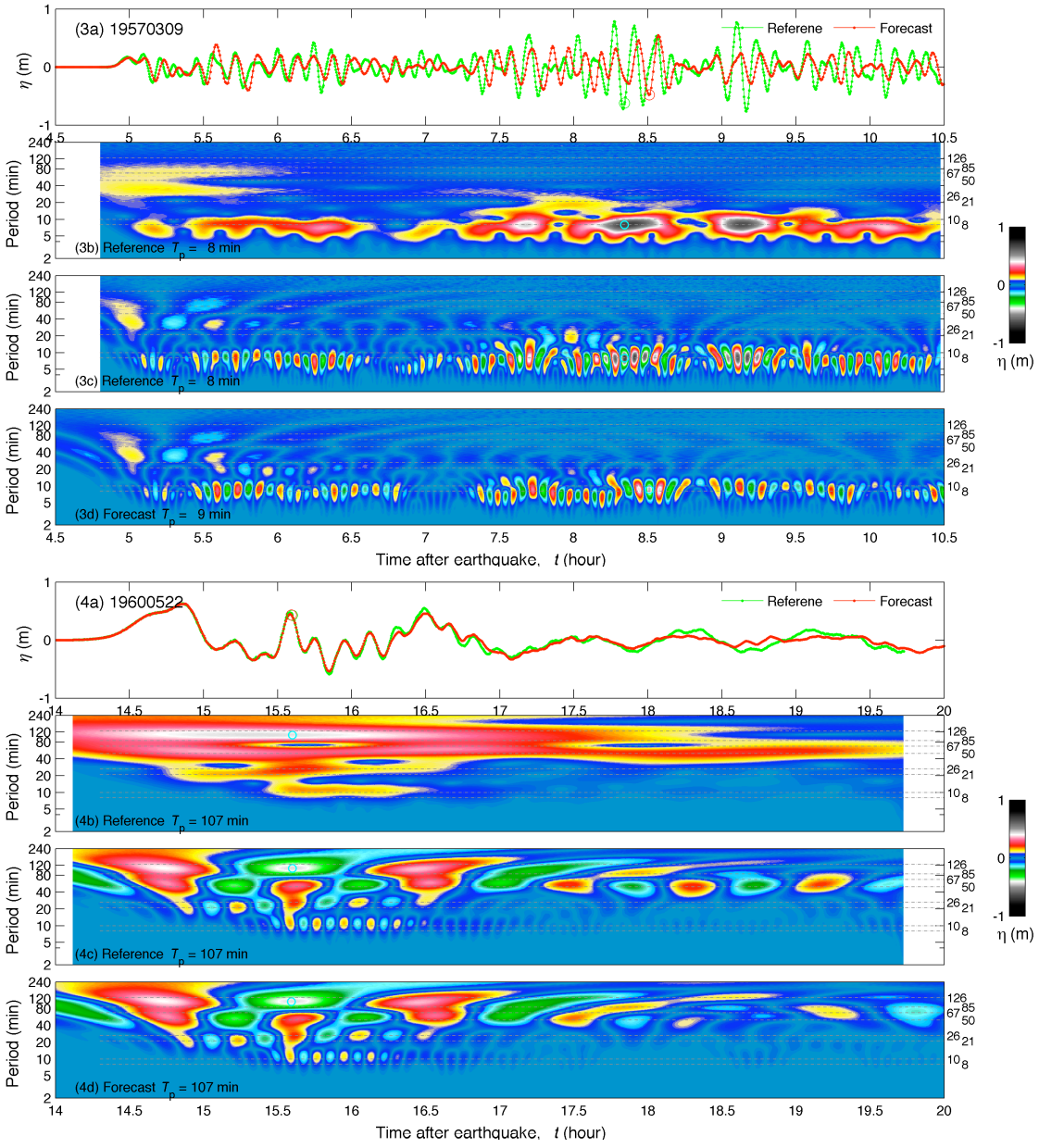
(3a) 19570309
Referene
Forecast
η (m)
Period (min)
(3b) Reference T_p = 8 min
(3c) Reference T_p = 8 min
(3d) Forecast T_p = 9 min
Time after earthquake, t (hour)
(4a) 19600522
(4b) Reference T_p = 107 min
(4c) Reference T_p = 107 min
(4d) Forecast T_p = 107 min

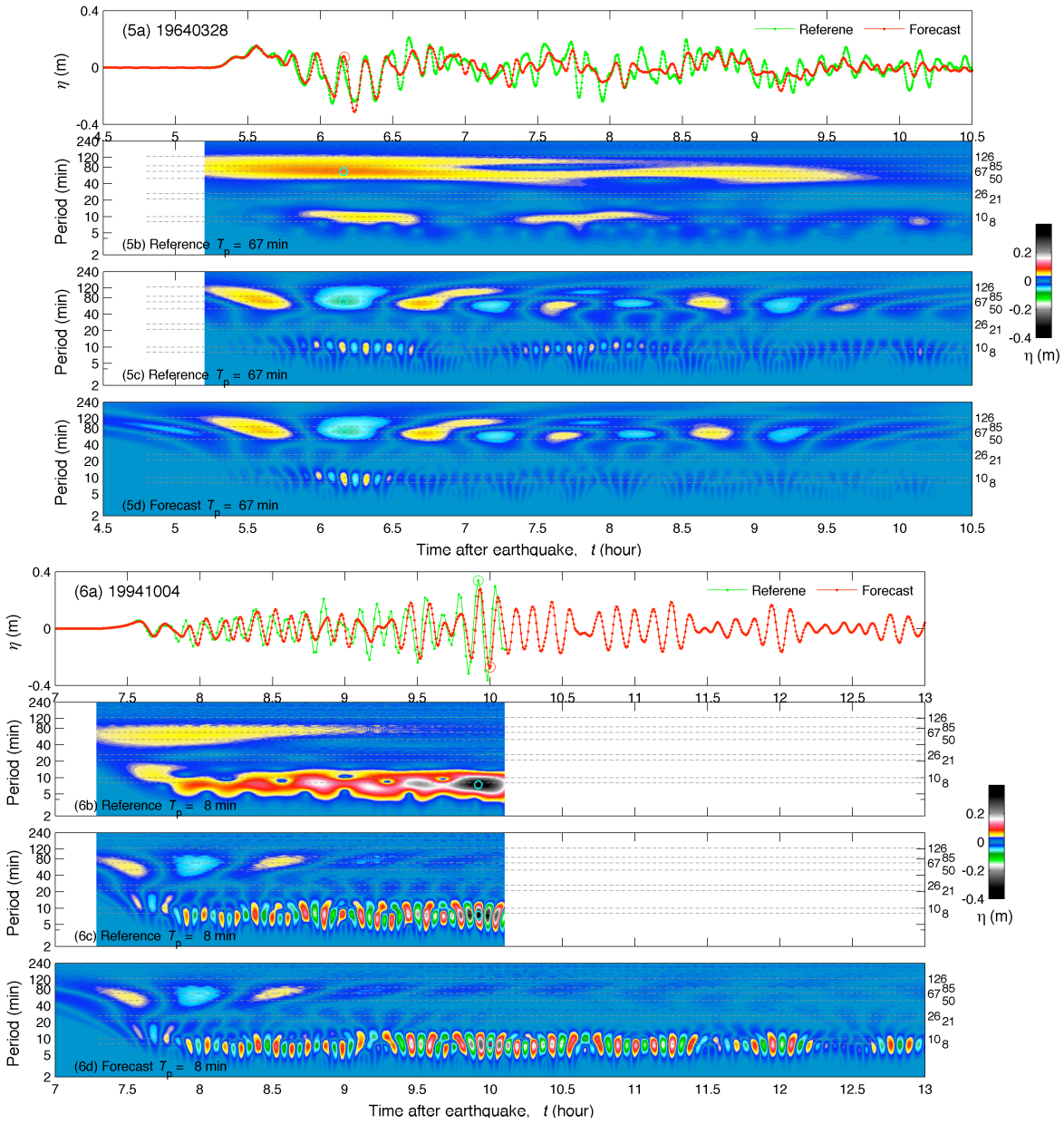
(5a) 19640328
Referene
Forecast
η (m)
Period (min)
(5b) Reference T_p = 67 min
(5c) Reference T_p = 67 min
(5d) Forecast T_p = 67 min
η (m)
Time after earthquake, t (hour)
(6a) 19941004
Referene
Forecast
η (m)
Period (min)
(6b) Reference T_p = 8 min
(6c) Reference T_p = 8 min
(6d) Forecast T_p = 8 min
η (m)
Time after earthquake, t (hour)

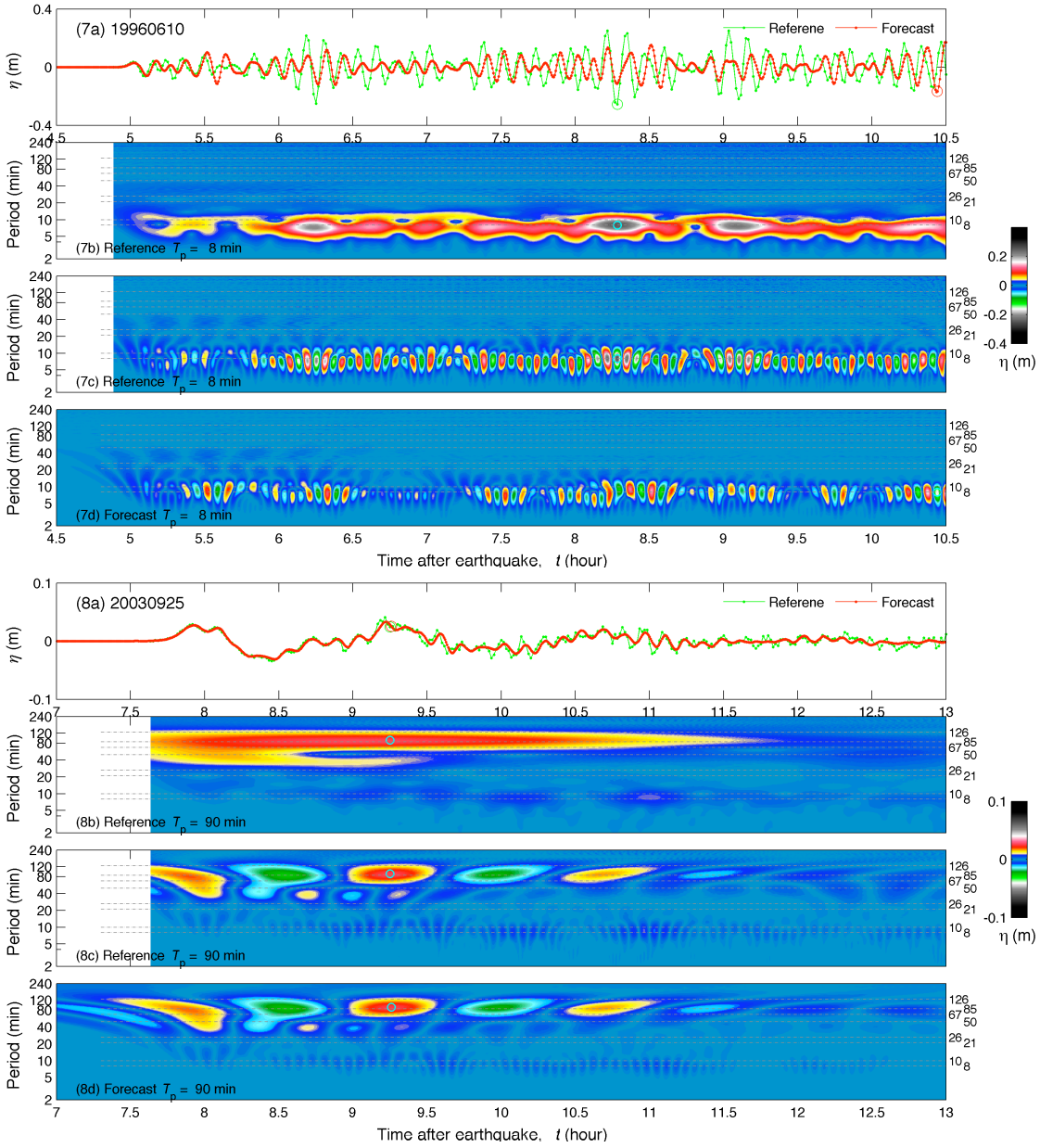
(7a) 19960610
Referene
Forecast
η (m)
Period (min)
(7b) Reference T_p = 8 min
(7c) Reference T_p = 8 min
(7d) Forecast T_p = 8 min
η (m)
Time after earthquake, t (hour)
(8a) 20030925
Referene
Forecast
η (m)
Period (min)
(8b) Reference T_p = 90 min
(8c) Reference T_p = 90 min
(8d) Forecast T_p = 90 min
η (m)
Time after earthquake, t (hour)

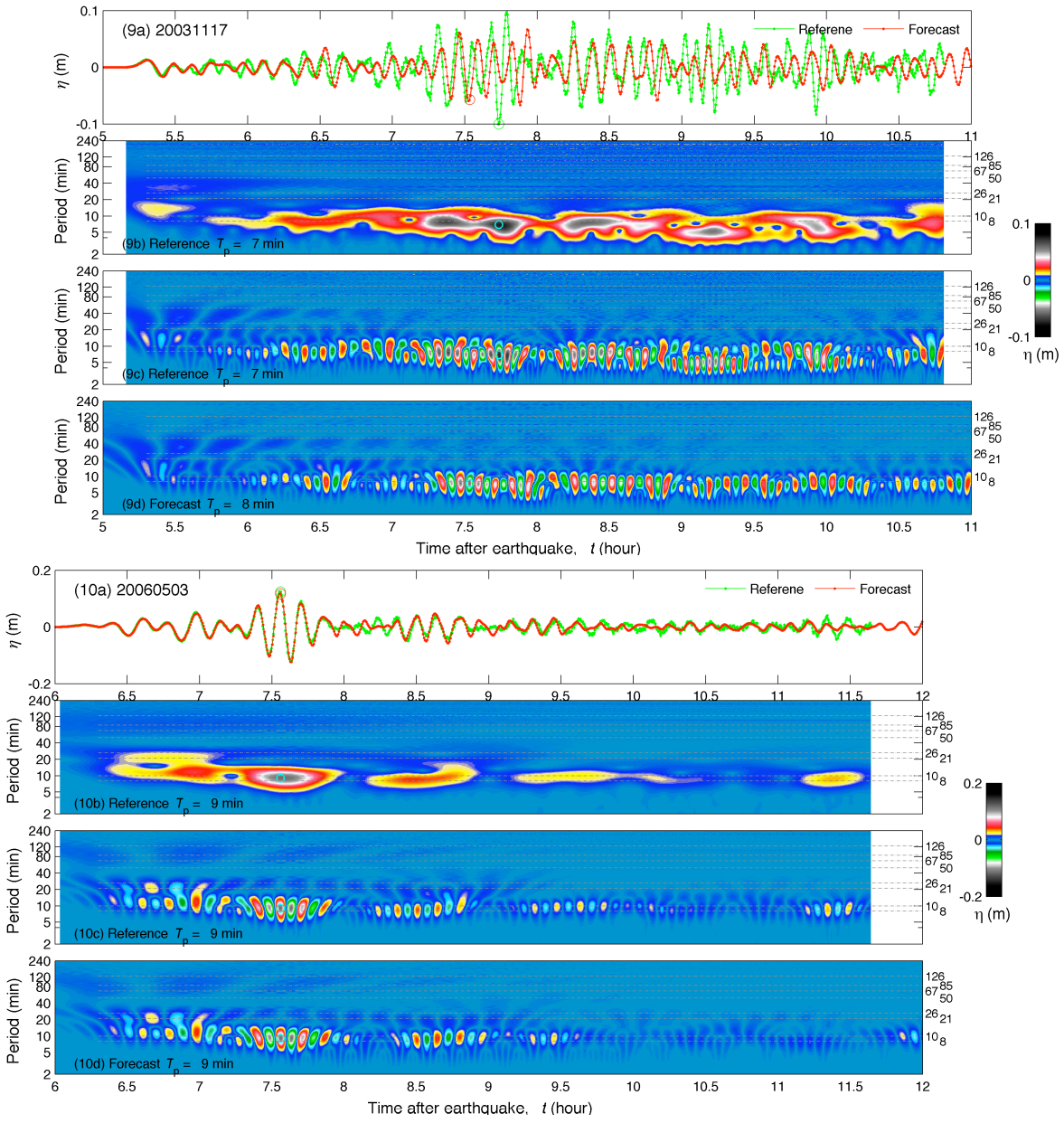
(9a) 20031117
Referene
Forecast
η (m)
Period (min)
(9b) Reference T_p = 7 min
(9c) Reference T_p = 7 min
(9d) Forecast T_p = 8 min
η (m)
Time after earthquake, t (hour)
(10a) 20060503
Referene
Forecast
η (m)
Period (min)
(10b) Reference T_p = 9 min
(10c) Reference T_p = 9 min
(10d) Forecast T_p = 9 min
η (m)
Time after earthquake, t (hour)

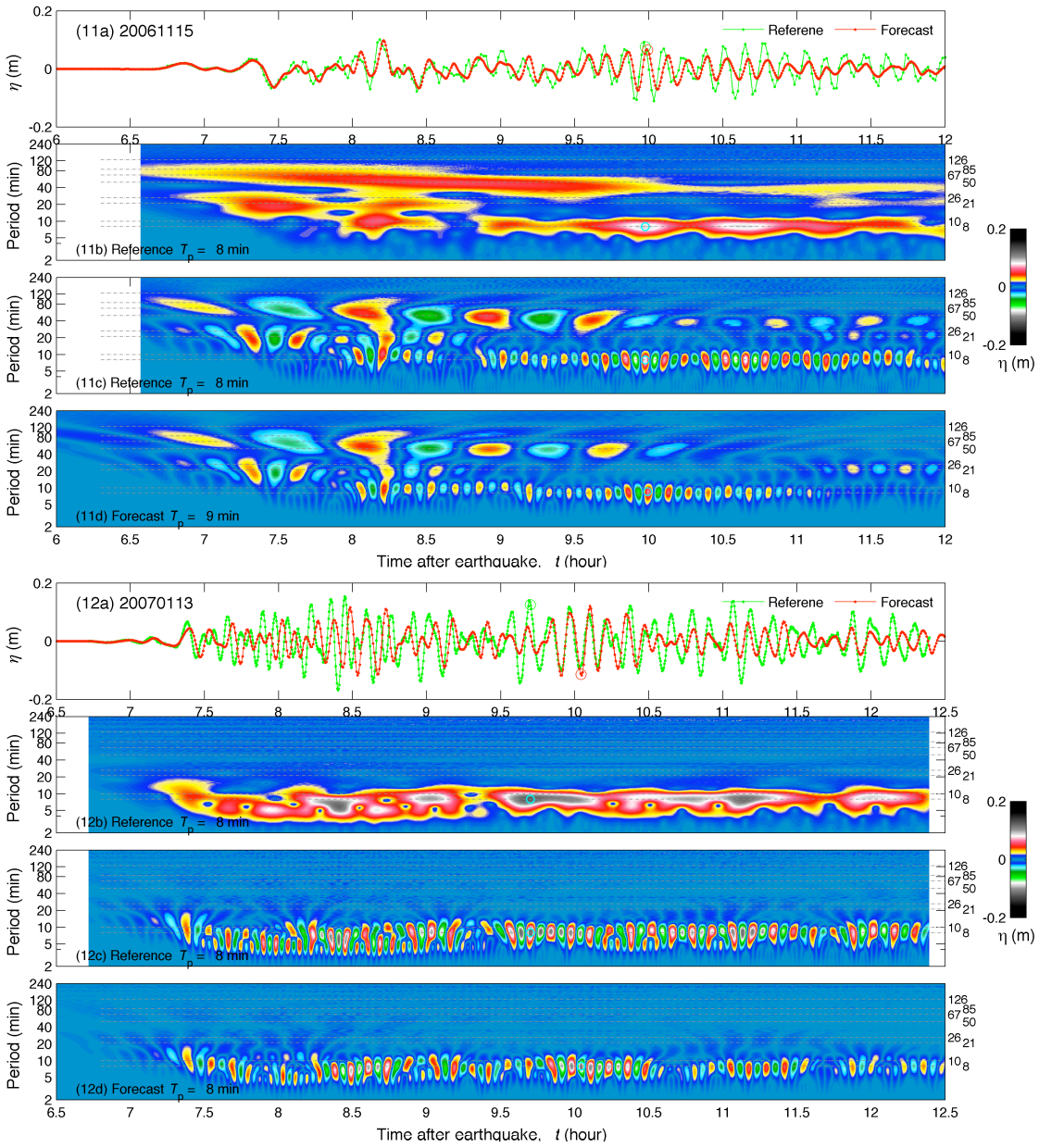
(11a) 20061115
Referene
Forecast
η (m)
(11b) Reference T_p = 8 min
(11c) Reference T_p = 8 min
(11d) Forecast T_p = 9 min
Period (min)
η (m)
Time after earthquake, t (hour)
(12a) 20070113
Referene
Forecast
η (m)
(12b) Reference T_p = 8 min
(12c) Reference T_p = 8 min
(12d) Forecast T_p = 8 min
Period (min)
η (m)
Time after earthquake, t (hour)

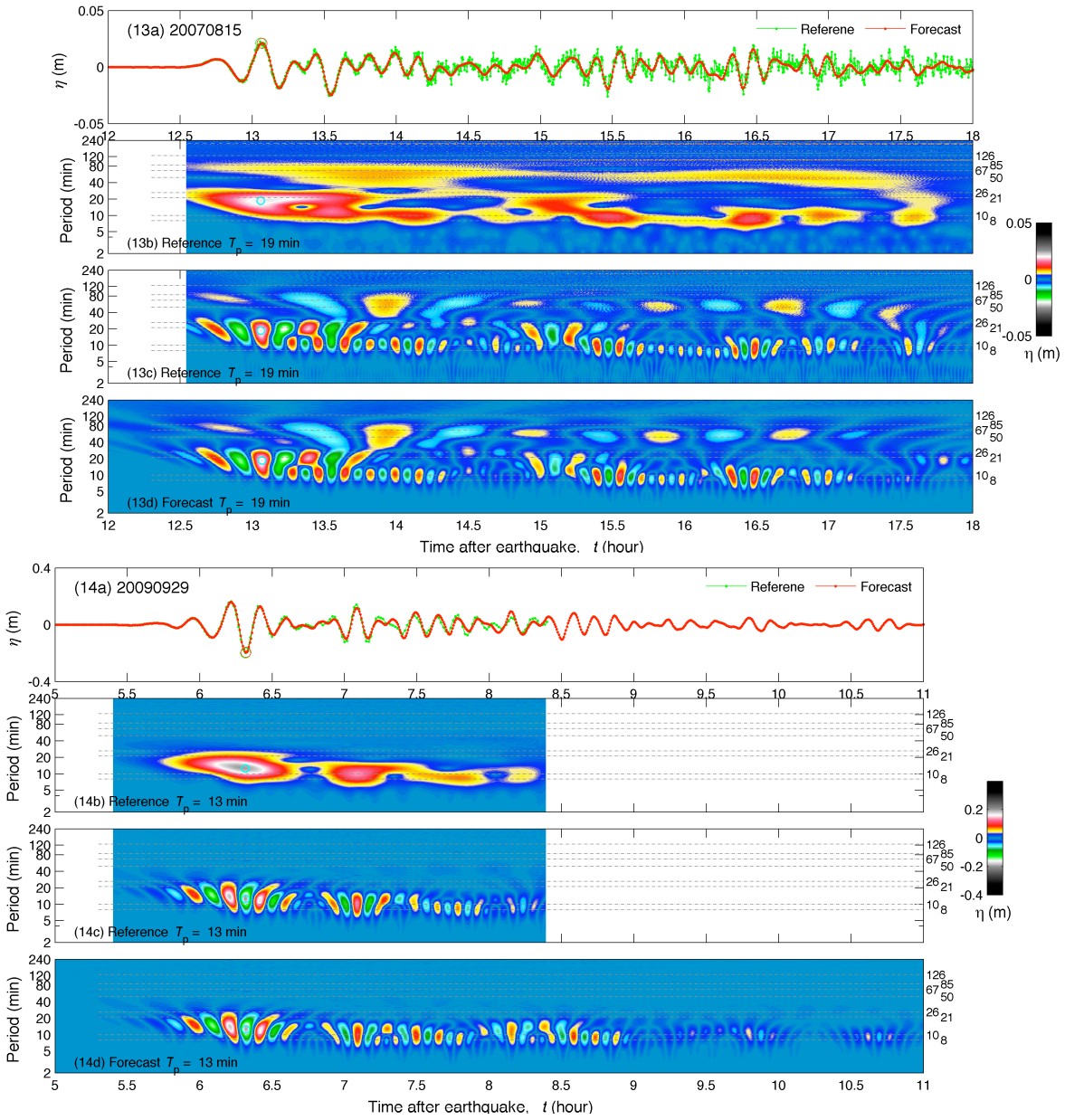
(13a) 20070815
Referene
Forecast
η (m)
(13b) Reference T_p = 19 min
(13c) Reference T_p = 19 min
(13d) Forecast T_p = 19 min
Period (min)
η (m)
Time after earthquake, t (hour)
(14a) 20090929
(14b) Reference T_p = 13 min
(14c) Reference T_p = 13 min
(14d) Forecast T_p = 13 min
Time after earthquake, t (hour)

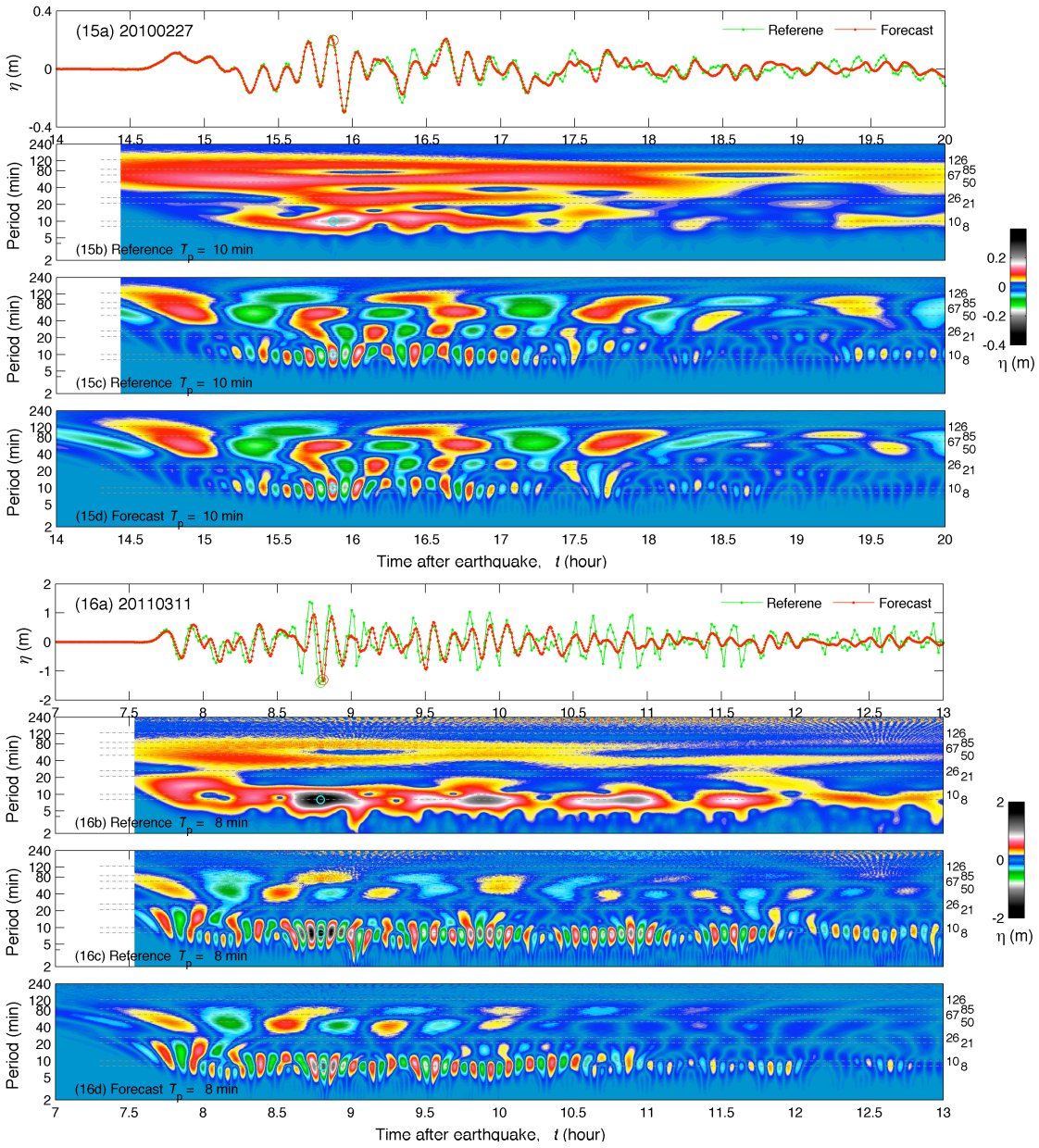

Figure 16 (1-16): (a) Modeled η time series at Kailua-Kona warning point for the 16 historical tsunamis. (b) Wavelet-derived amplitude spectra for the reference model. (c and d) Real part of the spectrograms computed by the reference and forecast models.

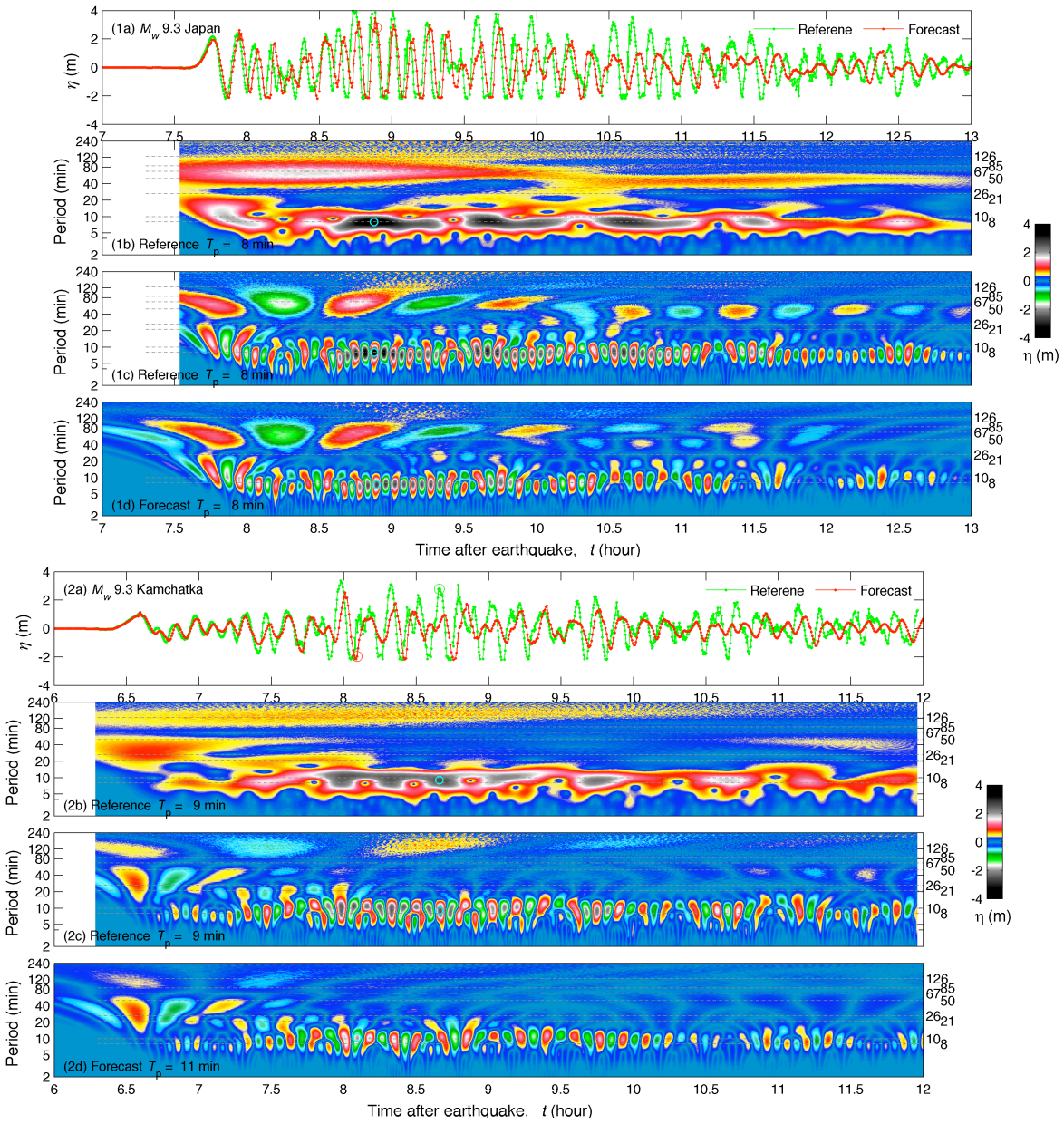
(1a) M_w 9.3 Japan
Referene
Forecast
η (m)
Period (min)
(1b) Reference T_p = 8 min
(1c) Reference T_p = 8 min
(1d) Forecast T_p = 8 min
η (m)
Time after earthquake, t (hour)
(2a) M_w 9.3 Kamchatka
Referene
Forecast
η (m)
Period (min)
(2b) Reference T_p = 9 min
(2c) Reference T_p = 9 min
(2d) Forecast T_p = 11 min
η (m)
Time after earthquake, t (hour)

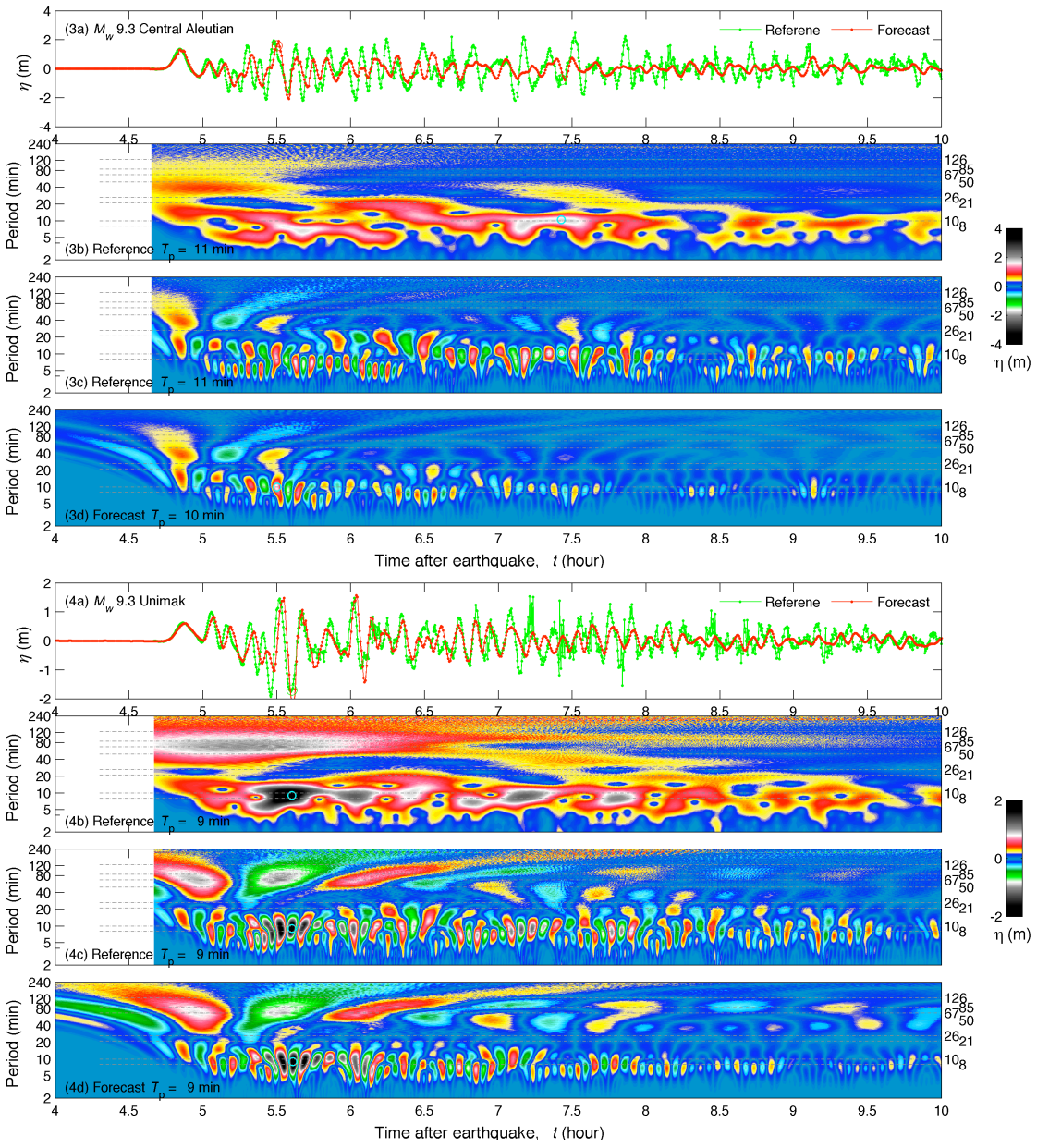
(3a) M_w 9.3 Central Aleutian
Referene
Forecast
η (m)
Period (min)
(3b) Reference T_p = 11 min
(3c) Reference T_p = 11 min
(3d) Forecast T_p = 10 min
η (m)
Time after earthquake, t (hour)
(4a) M_w 9.3 Unimak
Referene
Forecast
η (m)
Period (min)
(4b) Reference T_p = 9 min
(4c) Reference T_p = 9 min
(4d) Forecast T_p = 9 min
η (m)
Time after earthquake, t (hour)

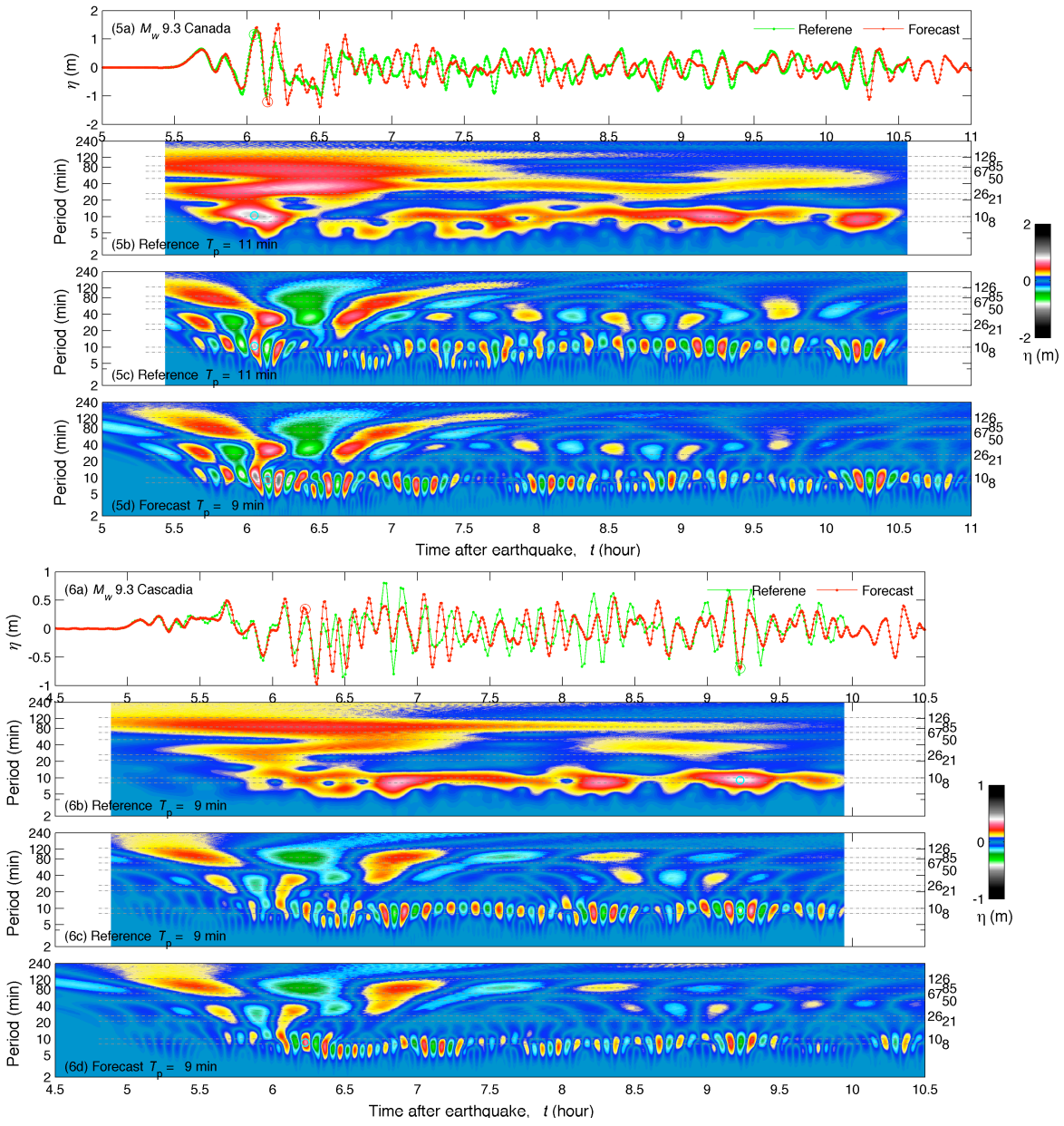
(5a) M_w 9.3 Canada
Referene
Forecast
η (m)
Period (min)
(5b) Reference T_p = 11 min
(5c) Reference T_p = 11 min
(5d) Forecast T_p = 9 min
η (m)
Time after earthquake, t (hour)
(6a) M_w 9.3 Cascadia
Referene
Forecast
η (m)
Period (min)
(6b) Reference T_p = 9 min
(6c) Reference T_p = 9 min
(6d) Forecast T_p = 9 min
η (m)
Time after earthquake, t (hour)

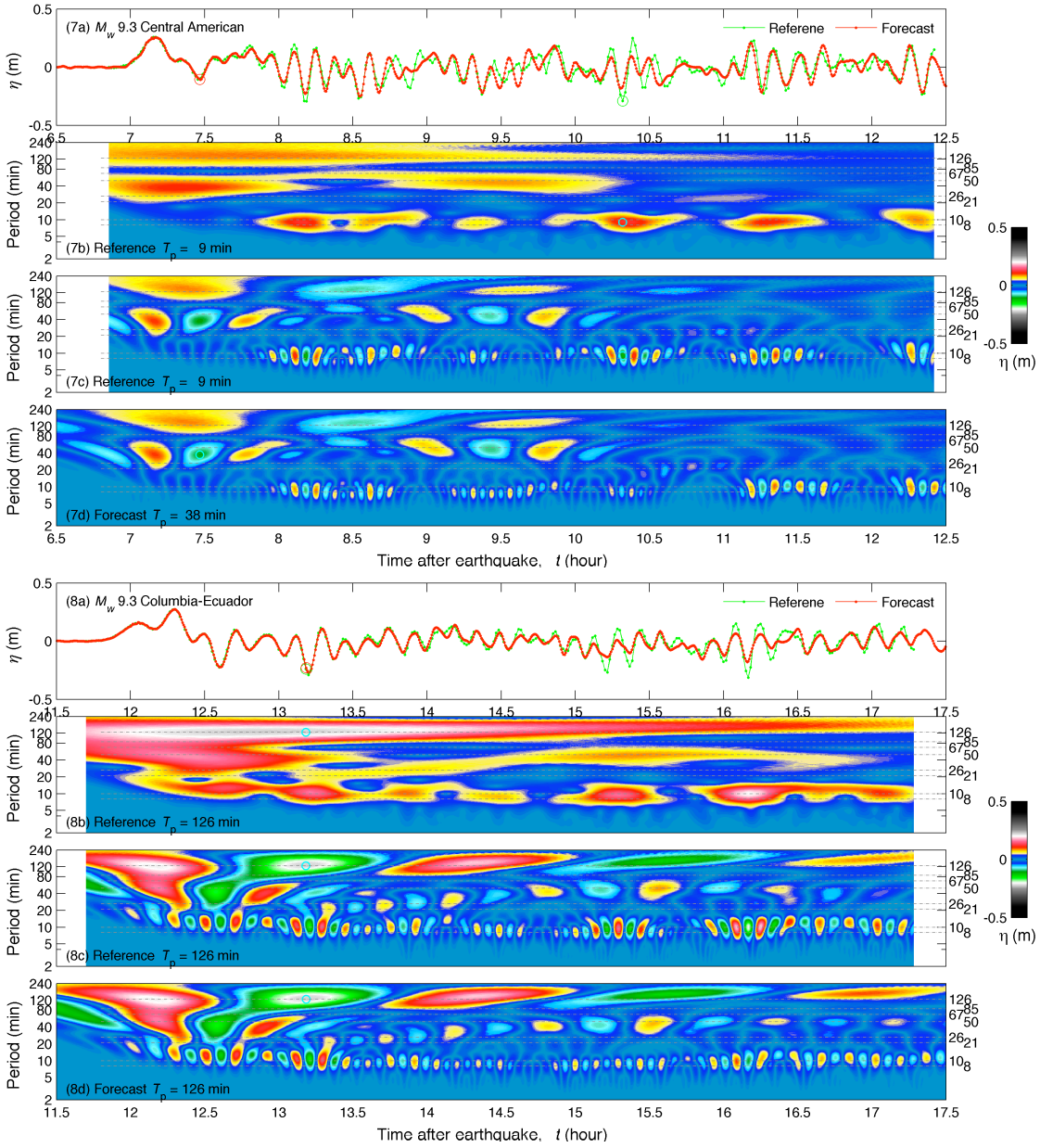
(7a) M_w 9.3 Central American
Referene
Forecast
η (m)
Period (min)
(7b) Reference T_p = 9 min
(7c) Reference T_p = 9 min
(7d) Forecast T_p = 38 min
η (m)
Time after earthquake, t (hour)
(8a) M_w 9.3 Columbia-Ecuador
Referene
Forecast
η (m)
Period (min)
(8b) Reference T_p = 126 min
(8c) Reference T_p = 126 min
(8d) Forecast T_p = 126 min
η (m)
Time after earthquake, t (hour)

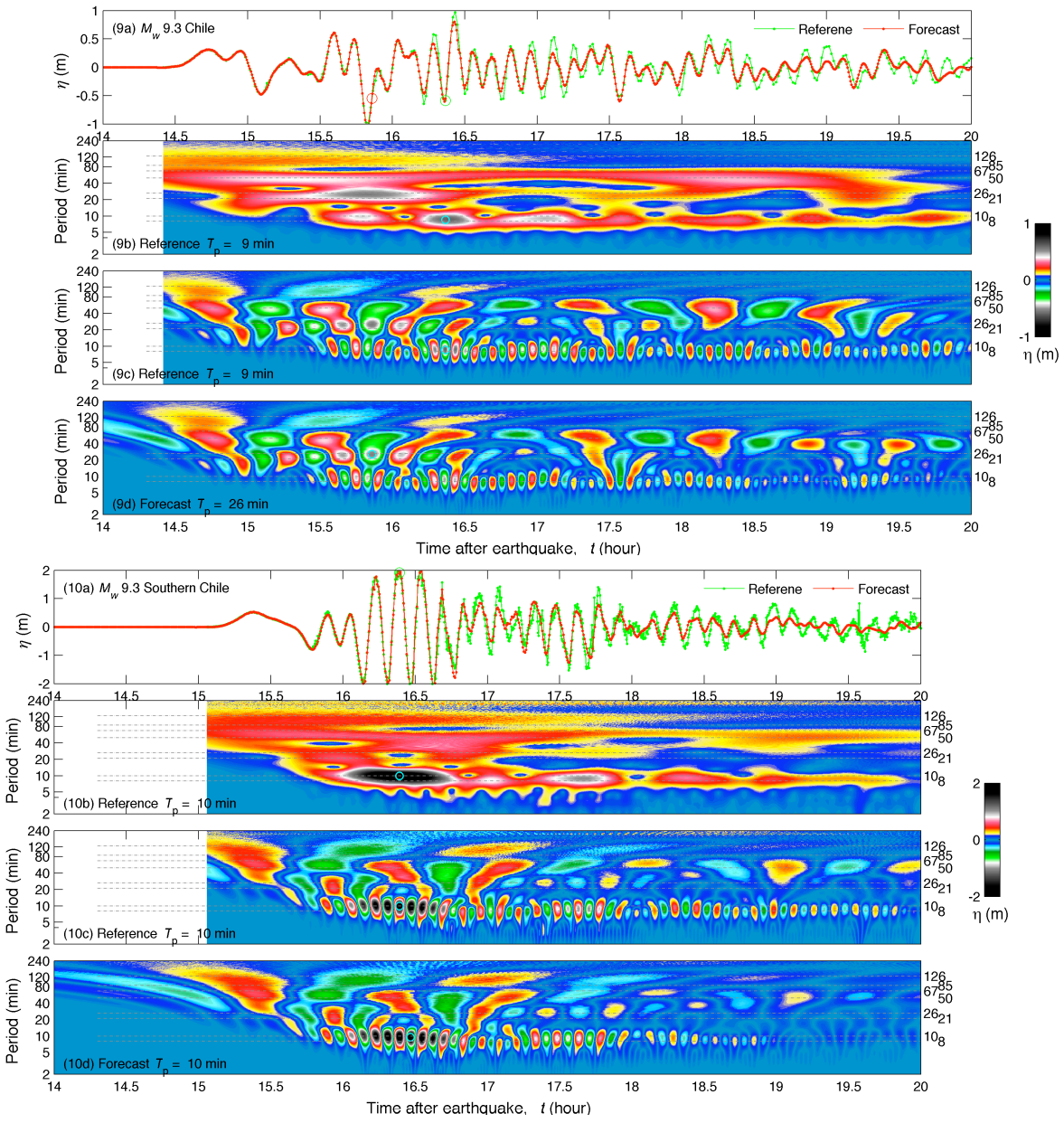
(9a) M_w 9.3 Chile
Referene
Forecast
η (m)
(9b) Reference T_p = 9 min
(9c) Reference T_p = 9 min
(9d) Forecast T_p = 26 min
Period (min)
η (m)
Time after earthquake, t (hour)
(10a) M_w 9.3 Southern Chile
Referene
Forecast
η (m)
(10b) Reference T_p = 10 min
(10c) Reference T_p = 10 min
(10d) Forecast T_p = 10 min
Period (min)
η (m)
Time after earthquake, t (hour)

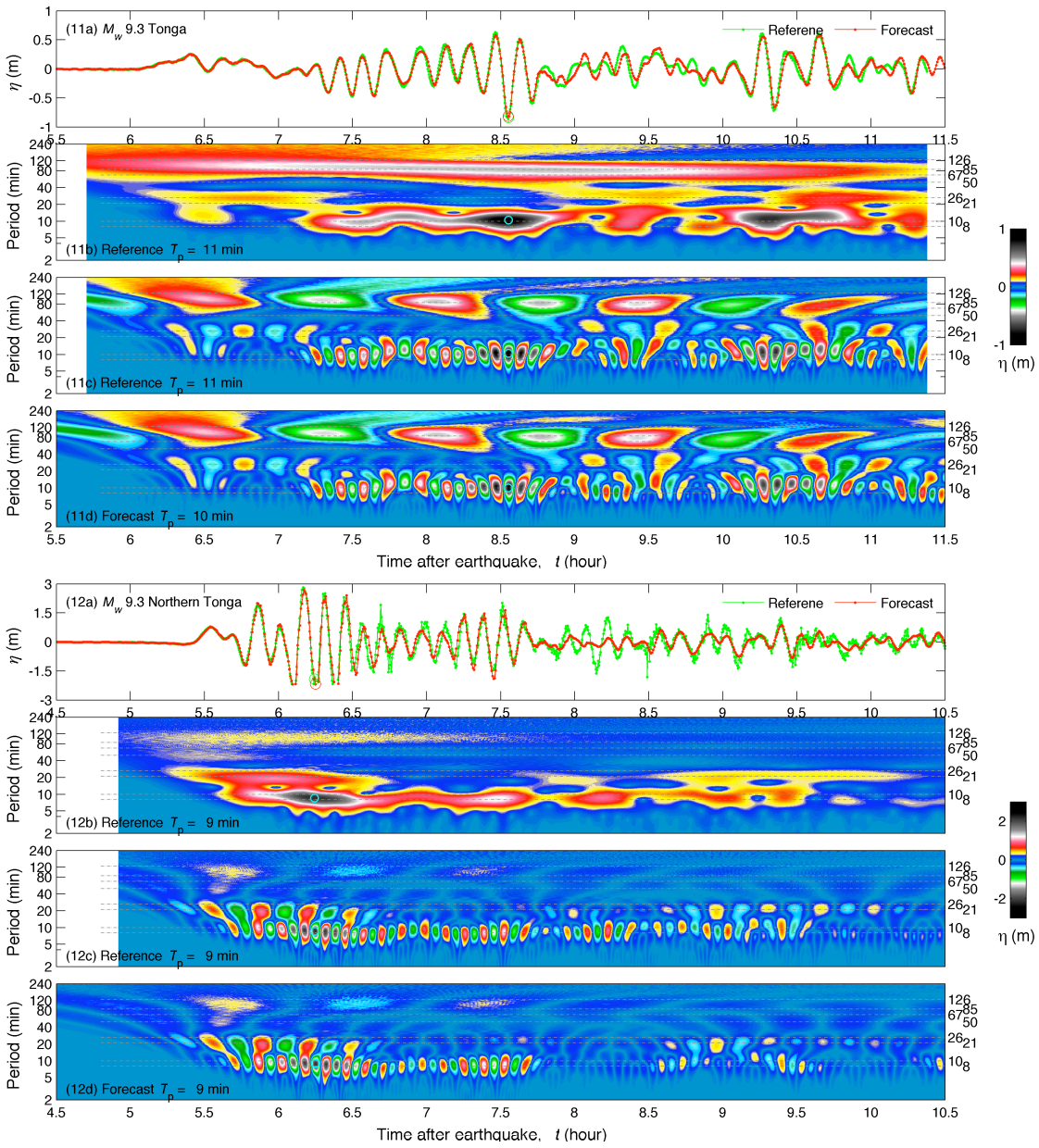
(11a) M_w 9.3 Tonga
Referene
Forecast
η (m)
Period (min)
(11b) Reference T_p = 11 min
(11c) Reference T_p = 11 min
(11d) Forecast T_p = 10 min
η (m)
Time after earthquake, t (hour)
(12a) M_w 9.3 Northern Tonga
Referene
Forecast
η (m)
Period (min)
(12b) Reference T_p = 9 min
(12c) Reference T_p = 9 min
(12d) Forecast T_p = 9 min
η (m)
Time after earthquake, t (hour)

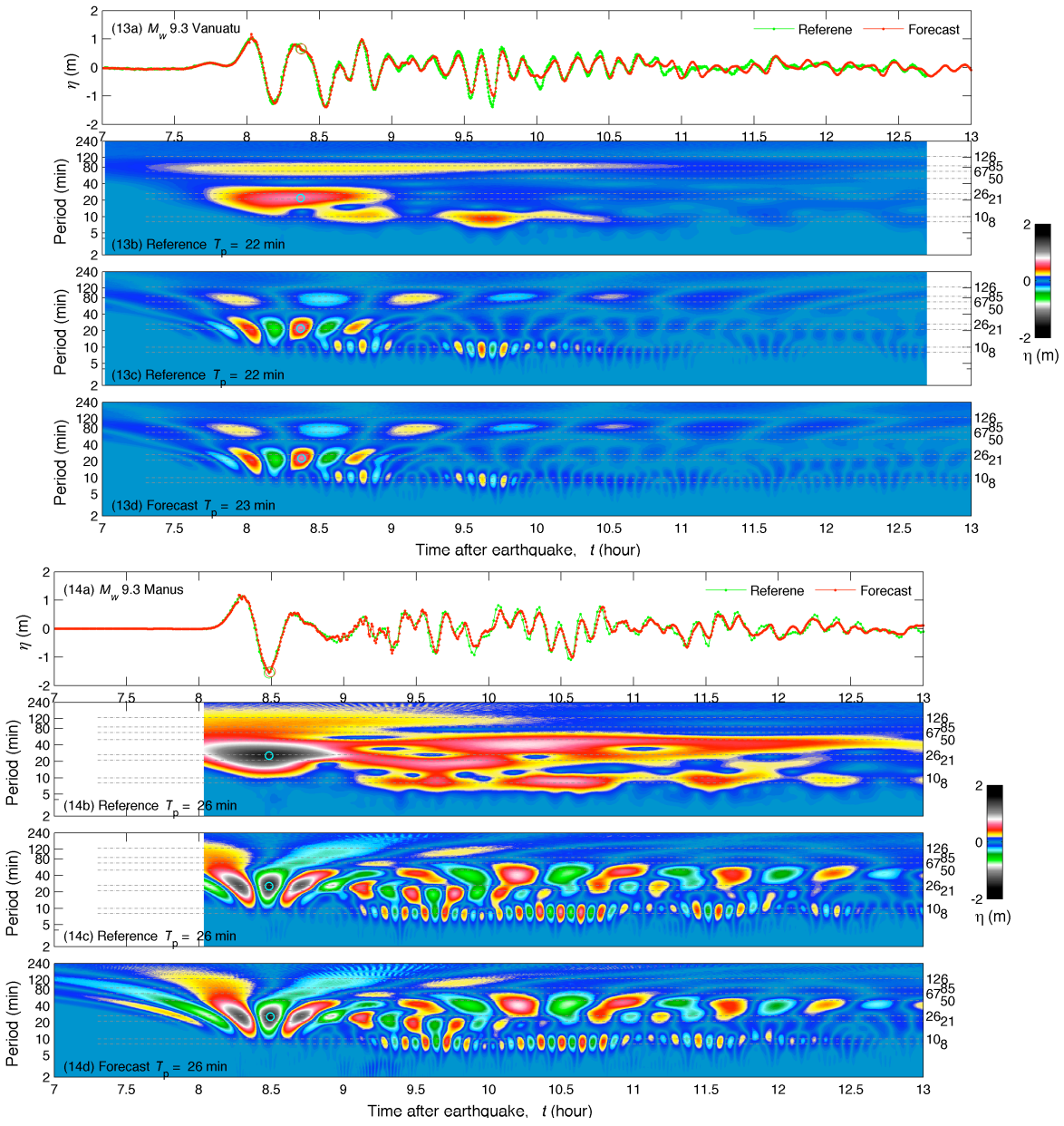
(13a) M_w 9.3 Vanuatu
Referene
Forecast
η (m)
Period (min)
(13b) Reference T_p = 22 min
(13c) Reference T_p = 22 min
(13d) Forecast T_p = 23 min
η (m)
Time after earthquake, t (hour)
(14a) M_w 9.3 Manus
Referene
Forecast
η (m)
Period (min)
(14b) Reference T_p = 26 min
(14c) Reference T_p = 26 min
(14d) Forecast T_p = 26 min
η (m)
Time after earthquake, t (hour)

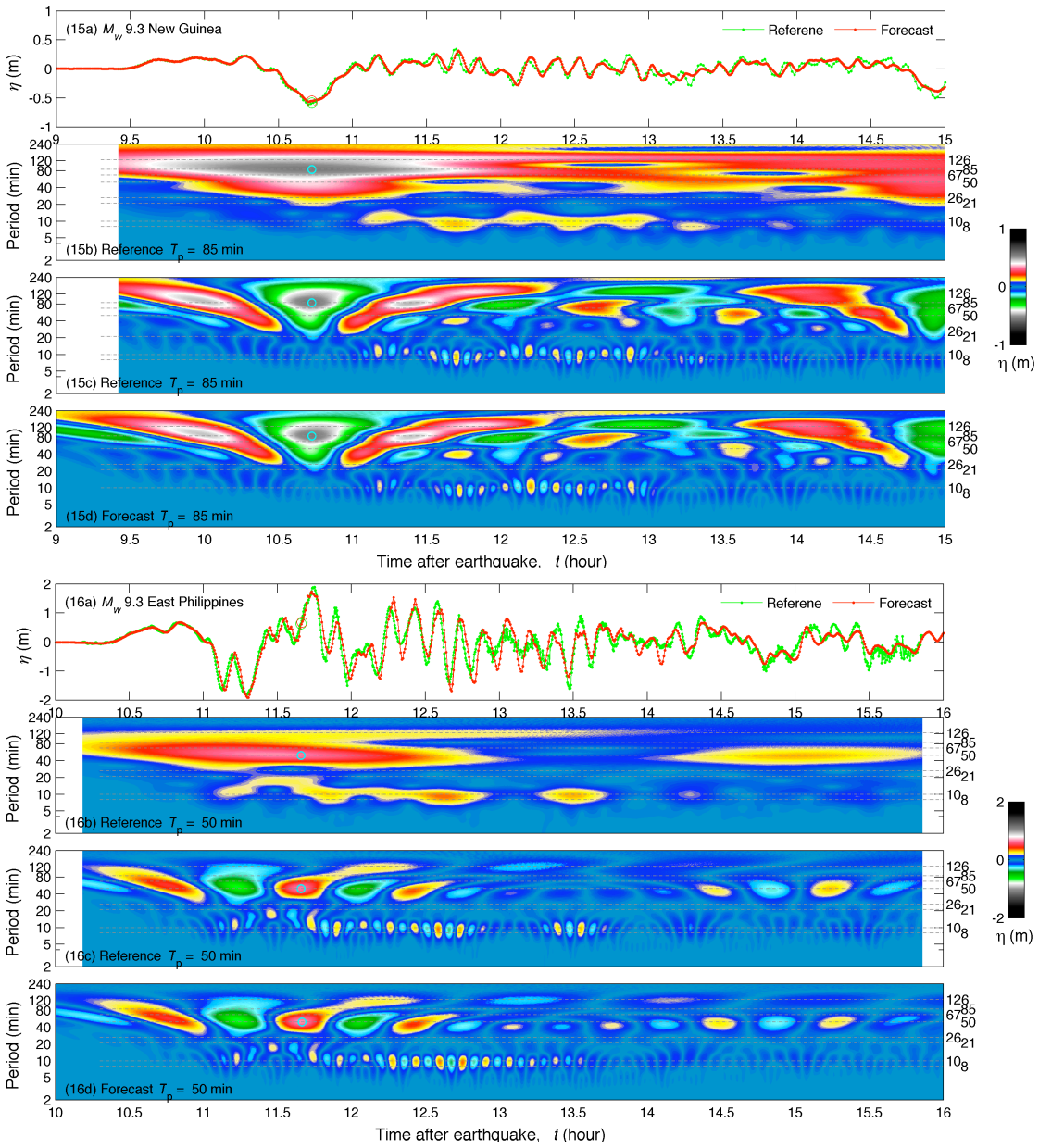
(15a) M_w 9.3 New Guinea
Referene
Forecast
η (m)
(15b) Reference T_p = 85 min
(15c) Reference T_p = 85 min
(15d) Forecast T_p = 85 min
Period (min)
Time after earthquake, t (hour)
(16a) M_w 9.3 East Philippines
(16b) Reference T_p = 50 min
(16c) Reference T_p = 50 min
(16d) Forecast T_p = 50 min

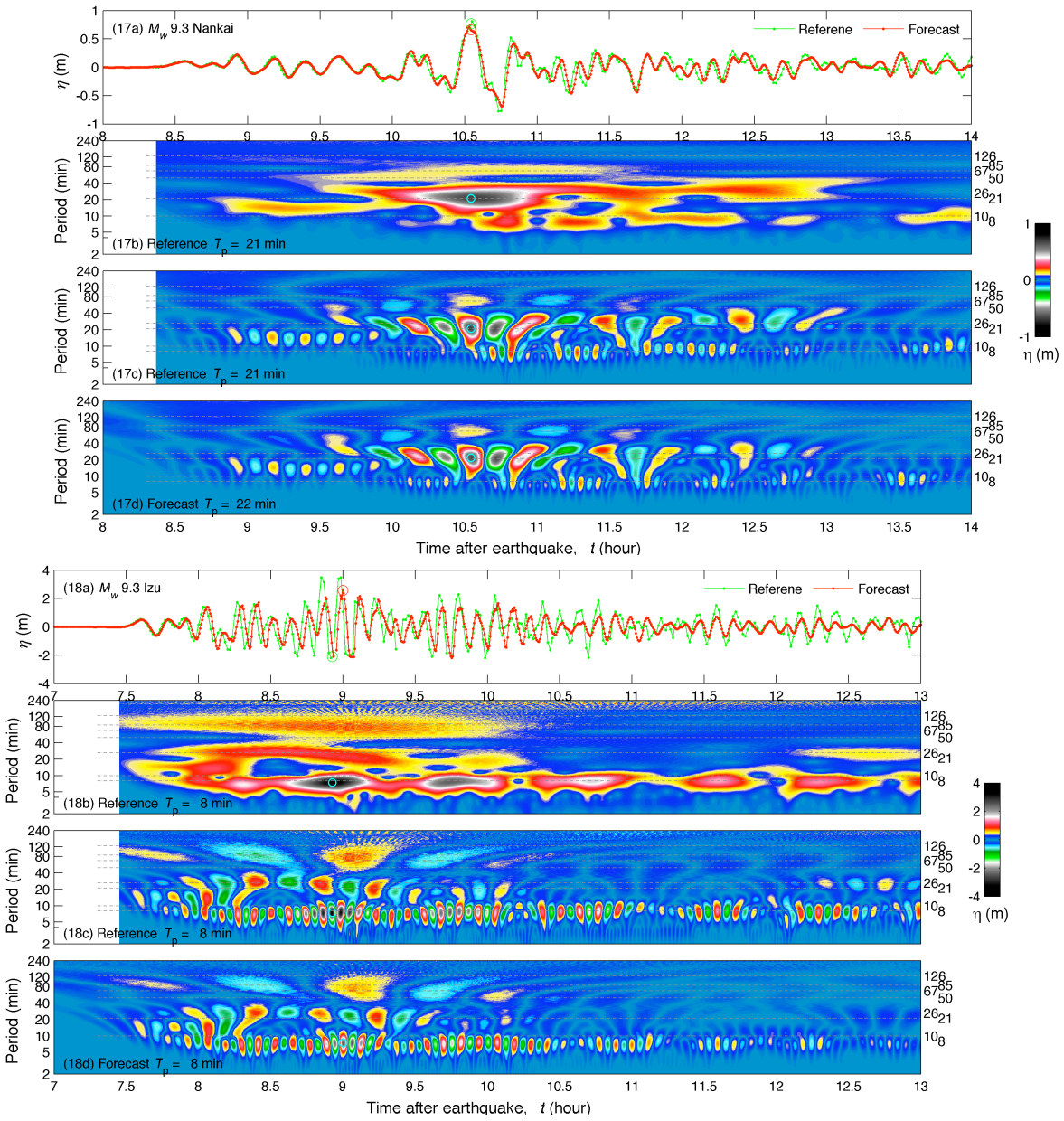

Figure 17 (1-18): (a) Modeled η time series at Kailua-Kona warning point for the 18 simulated M_w 9.3 tsunamis. (b) Wavelet-derived amplitude spectrogram for the reference model. (c and d) Real part of the spectrograms computed by the reference and forecast models.

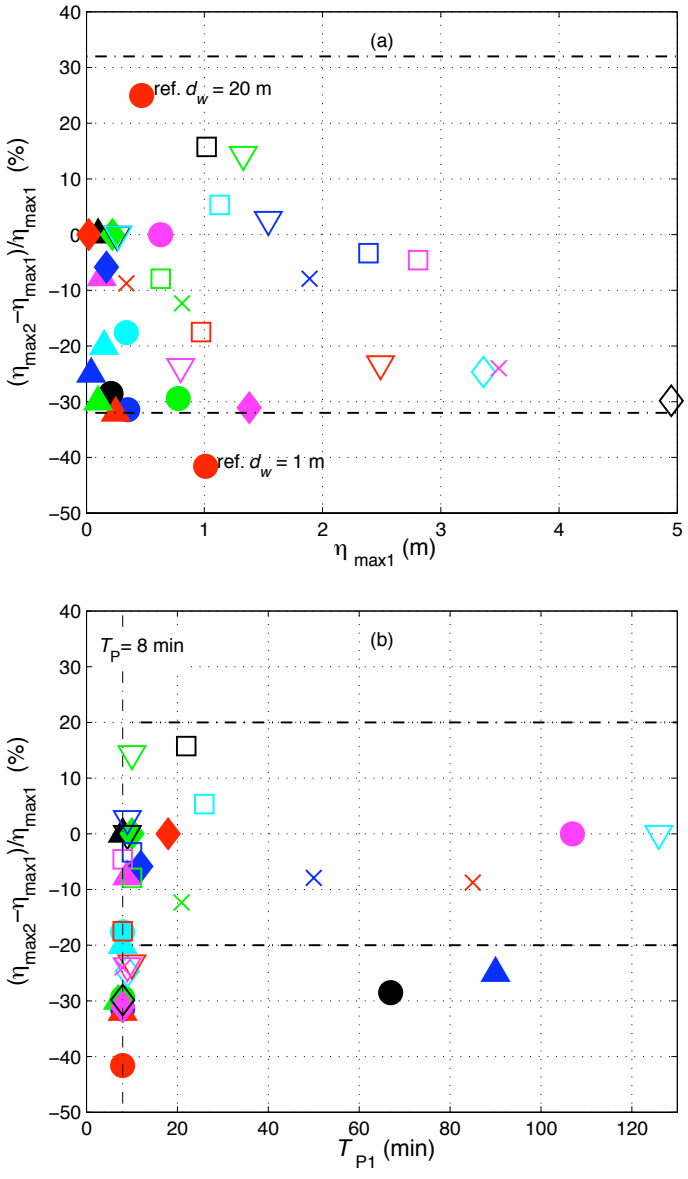

	η_{max1}	η_{max2}	$\Delta\eta$ (m)	(%)	T_{P1}	T_{P2}
19460401	1.01	0.59	−0.42	−42	8	8
19521104	0.35	0.24	−0.11	−31	8	8
19570309	0.78	0.55	−0.23	−29	8	8
19600522	0.63	0.63	0	0	107	107
19640328	0.21	0.15	−0.06	−29	67	67
19941004	0.34	0.28	−0.06	−18	8	8
19960610	0.25	0.17	−0.08	−32	8	8
20030925	0.04	0.03	−0.01	−25	90	90
20031117	0.1	0.07	−0.03	−30	7	8
20060503	0.13	0.12	−0.01	−8	9	9
20061115	0.1	0.1	0	0	8	8
20070113	0.15	0.12	−0.03	−20	8	8
20070815	0.02	0.02	0	0	18	18
20090929	0.17	0.16	−0.01	−6	12	12
20100227	0.22	0.22	0	0	10	10
20110311	1.38	0.95	−0.43	−31	8	8
Japan	4.95	3.47	−1.48	−30	8	8
Kamchatka	3.36	2.53	−0.83	−25	9	10
Central Aleutian	2.49	1.91	−0.58	−23	10	10
Unimak	1.54	1.58	0.04	3	9	9
Canada	1.33	1.52	0.19	14	10	9
Cascadia	0.8	0.61	−0.19	−24	9	8
Central American	0.26	0.26	0	0	9	38
Columbia–Ecuador	0.27	0.27	0	0	126	126
Chile	0.97	0.8	−0.17	−18	8	26
Southern Chile	2.39	2.31	−0.08	−3	10	10
Tonga	0.63	0.58	−0.05	−8	10	10
Northern Tonga	2.81	2.68	−0.13	−5	8	9
Vanuatu	1.02	1.18	0.16	16	22	22
Manus	1.13	1.19	0.06	5	26	26
New Guinea	0.34	0.31	−0.03	−9	85	85
East Philippines	1.89	1.74	−0.15	−8	50	50
Nankai	0.81	0.71	−0.1	−12	21	22
Izu	3.49	2.65	−0.84	−24	8	8

Figure 18: (a) Uncertainty in the η_{max} at Kailua-Kona warning point computed by the reference and forecast models for the 34 scenarios. (b) Large uncertainty is associated with short peak wave period near 8 min. Filled markers, 16 past tsunamis; open markers, 18 simulated M_w = 9.3 tsunamis.

Appendix B. Propagation Database: Pacific Ocean Unit Sources

These propagation source details reflect the database as of May 2013, and there may have been updates in the earthquake source parameters after this date.

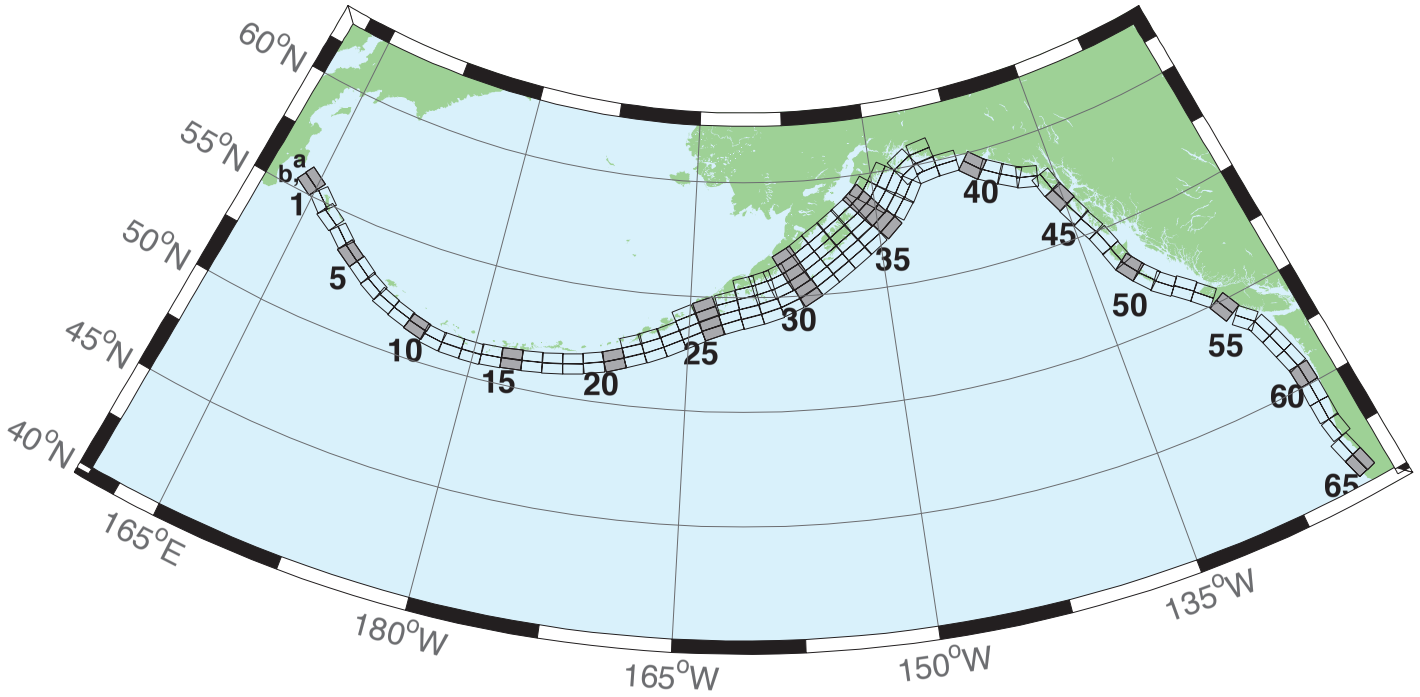

Figure B.1: Aleutian–Alaska–Cascadia Subduction Zone unit sources.

Table B.1: Earthquake parameters for Aleutian–Alaska–Cascadia Subduction Zone unit sources.

Segment	Description	Longitude(°E)	Latitude(°N)	Strike(°)	Dip(°)	Depth (km)
acsz–1a	Aleutian–Alaska–Cascadia	164.7994	55.9606	299	17	19.61
acsz–1b	Aleutian–Alaska–Cascadia	164.4310	55.5849	299	17	5
acsz–2a	Aleutian–Alaska–Cascadia	166.3418	55.4016	310.2	17	19.61
acsz–2b	Aleutian–Alaska–Cascadia	165.8578	55.0734	310.2	17	5
acsz–3a	Aleutian–Alaska–Cascadia	167.2939	54.8919	300.2	23.36	24.82
acsz–3b	Aleutian–Alaska–Cascadia	166.9362	54.5356	300.2	23.36	5
acsz–4a	Aleutian–Alaska–Cascadia	168.7131	54.2852	310.2	38.51	25.33
acsz–4b	Aleutian–Alaska–Cascadia	168.3269	54.0168	310.2	24	5
acsz–5a	Aleutian–Alaska–Cascadia	169.7447	53.7808	302.8	37.02	23.54
acsz–5b	Aleutian–Alaska–Cascadia	169.4185	53.4793	302.8	21.77	5
acsz–6a	Aleutian–Alaska–Cascadia	171.0144	53.3054	303.2	35.31	22.92
acsz–6b	Aleutian–Alaska–Cascadia	170.6813	52.9986	303.2	21	5
acsz–7a	Aleutian–Alaska–Cascadia	172.1500	52.8528	298.2	35.56	20.16
acsz–7b	Aleutian–Alaska–Cascadia	171.8665	52.5307	298.2	17.65	5
acsz–8a	Aleutian–Alaska–Cascadia	173.2726	52.4579	290.8	37.92	20.35
acsz–8b	Aleutian–Alaska–Cascadia	173.0681	52.1266	290.8	17.88	5
acsz–9a	Aleutian–Alaska–Cascadia	174.5866	52.1434	289	39.09	21.05
acsz–9b	Aleutian–Alaska–Cascadia	174.4027	51.8138	289	18.73	5
acsz–10a	Aleutian–Alaska–Cascadia	175.8784	51.8526	286.1	40.51	20.87
acsz–10b	Aleutian–Alaska–Cascadia	175.7265	51.5245	286.1	18.51	5
acsz–11a	Aleutian–Alaska–Cascadia	177.1140	51.6488	280	15	17.94
acsz–11b	Aleutian–Alaska–Cascadia	176.9937	51.2215	280	15	5
acsz–12a	Aleutian–Alaska–Cascadia	178.4500	51.5690	273	15	17.94
acsz–12b	Aleutian–Alaska–Cascadia	178.4130	51.1200	273	15	5
acsz–13a	Aleutian–Alaska–Cascadia	179.8550	51.5340	271	15	17.94
acsz–13b	Aleutian–Alaska–Cascadia	179.8420	51.0850	271	15	5
acsz–14a	Aleutian–Alaska–Cascadia	181.2340	51.5780	267	15	17.94
acsz–14b	Aleutian–Alaska–Cascadia	181.2720	51.1290	267	15	5
acsz–15a	Aleutian–Alaska–Cascadia	182.6380	51.6470	265	15	17.94
acsz–15b	Aleutian–Alaska–Cascadia	182.7000	51.2000	265	15	5
acsz–16a	Aleutian–Alaska–Cascadia	184.0550	51.7250	264	15	17.94
acsz–16b	Aleutian–Alaska–Cascadia	184.1280	51.2780	264	15	5
acsz–17a	Aleutian–Alaska–Cascadia	185.4560	51.8170	262	15	17.94
acsz–17b	Aleutian–Alaska–Cascadia	185.5560	51.3720	262	15	5
acsz–18a	Aleutian–Alaska–Cascadia	186.8680	51.9410	261	15	17.94
acsz–18b	Aleutian–Alaska–Cascadia	186.9810	51.4970	261	15	5
acsz–19a	Aleutian–Alaska–Cascadia	188.2430	52.1280	257	15	17.94
acsz–19b	Aleutian–Alaska–Cascadia	188.4060	51.6900	257	15	5
acsz–20a	Aleutian–Alaska–Cascadia	189.5810	52.3550	251	15	17.94
acsz–20b	Aleutian–Alaska–Cascadia	189.8180	51.9300	251	15	5
acsz–21a	Aleutian–Alaska–Cascadia	190.9570	52.6470	251	15	17.94
acsz–21b	Aleutian–Alaska–Cascadia	191.1960	52.2220	251	15	5
acsz–21z	Aleutian–Alaska–Cascadia	190.7399	53.0443	250.8	15	30.88
acsz–22a	Aleutian–Alaska–Cascadia	192.2940	52.9430	247	15	17.94
acsz–22b	Aleutian–Alaska–Cascadia	192.5820	52.5300	247	15	5
acsz–22z	Aleutian–Alaska–Cascadia	192.0074	53.3347	247.8	15	30.88
acsz–23a	Aleutian–Alaska–Cascadia	193.6270	53.3070	245	15	17.94
acsz–23b	Aleutian–Alaska–Cascadia	193.9410	52.9000	245	15	5
acsz–23z	Aleutian–Alaska–Cascadia	193.2991	53.6768	244.6	15	30.88
acsz–24a	Aleutian–Alaska–Cascadia	194.9740	53.6870	245	15	17.94
acsz–24b	Aleutian–Alaska–Cascadia	195.2910	53.2800	245	15	5
acsz–24y	Aleutian–Alaska–Cascadia	194.3645	54.4604	244.4	15	43.82
acsz–24z	Aleutian–Alaska–Cascadia	194.6793	54.0674	244.6	15	30.88

Continued on next page

Table B.1 – continued

Segment	Description	Longitude(°E)	Latitude(°N)	Strike(°)	Dip(°)	Depth (km)
acsz–25a	Aleutian–Alaska–Cascadia	196.4340	54.0760	250	15	17.94
acsz–25b	Aleutian–Alaska–Cascadia	196.6930	53.6543	250	15	5
acsz–25y	Aleutian–Alaska–Cascadia	195.9009	54.8572	247.9	15	43.82
acsz–25z	Aleutian–Alaska–Cascadia	196.1761	54.4536	248.1	15	30.88
acsz–26a	Aleutian–Alaska–Cascadia	197.8970	54.3600	253	15	17.94
acsz–26b	Aleutian–Alaska–Cascadia	198.1200	53.9300	253	15	5
acsz–26y	Aleutian–Alaska–Cascadia	197.5498	55.1934	253.1	15	43.82
acsz–26z	Aleutian–Alaska–Cascadia	197.7620	54.7770	253.3	15	30.88
acsz–27a	Aleutian–Alaska–Cascadia	199.4340	54.5960	256	15	17.94
acsz–27b	Aleutian–Alaska–Cascadia	199.6200	54.1600	256	15	5
acsz–27x	Aleutian–Alaska–Cascadia	198.9736	55.8631	256.5	15	56.24
acsz–27y	Aleutian–Alaska–Cascadia	199.1454	55.4401	256.6	15	43.82
acsz–27z	Aleutian–Alaska–Cascadia	199.3135	55.0170	256.8	15	30.88
acsz–28a	Aleutian–Alaska–Cascadia	200.8820	54.8300	253	15	17.94
acsz–28b	Aleutian–Alaska–Cascadia	201.1080	54.4000	253	15	5
acsz–28x	Aleutian–Alaska–Cascadia	200.1929	56.0559	252.5	15	56.24
acsz–28y	Aleutian–Alaska–Cascadia	200.4167	55.6406	252.7	15	43.82
acsz–28z	Aleutian–Alaska–Cascadia	200.6360	55.2249	252.9	15	30.88
acsz–29a	Aleutian–Alaska–Cascadia	202.2610	55.1330	247	15	17.94
acsz–29b	Aleutian–Alaska–Cascadia	202.5650	54.7200	247	15	5
acsz–29x	Aleutian–Alaska–Cascadia	201.2606	56.2861	245.7	15	56.24
acsz–29y	Aleutian–Alaska–Cascadia	201.5733	55.8888	246	15	43.82
acsz–29z	Aleutian–Alaska–Cascadia	201.8797	55.4908	246.2	15	30.88
acsz–30a	Aleutian–Alaska–Cascadia	203.6040	55.5090	240	15	17.94
acsz–30b	Aleutian–Alaska–Cascadia	203.9970	55.1200	240	15	5
acsz–30w	Aleutian–Alaska–Cascadia	201.9901	56.9855	239.5	15	69.12
acsz–30x	Aleutian–Alaska–Cascadia	202.3851	56.6094	239.8	15	56.24
acsz–30y	Aleutian–Alaska–Cascadia	202.7724	56.2320	240.2	15	43.82
acsz–30z	Aleutian–Alaska–Cascadia	203.1521	55.8534	240.5	15	30.88
acsz–31a	Aleutian–Alaska–Cascadia	204.8950	55.9700	236	15	17.94
acsz–31b	Aleutian–Alaska–Cascadia	205.3400	55.5980	236	15	5
acsz–31w	Aleutian–Alaska–Cascadia	203.0825	57.3740	234.5	15	69.12
acsz–31x	Aleutian–Alaska–Cascadia	203.5408	57.0182	234.9	15	56.24
acsz–31y	Aleutian–Alaska–Cascadia	203.9904	56.6607	235.3	15	43.82
acsz–31z	Aleutian–Alaska–Cascadia	204.4315	56.3016	235.7	15	30.88
acsz–32a	Aleutian–Alaska–Cascadia	206.2080	56.4730	236	15	17.94
acsz–32b	Aleutian–Alaska–Cascadia	206.6580	56.1000	236	15	5
acsz–32w	Aleutian–Alaska–Cascadia	204.4129	57.8908	234.3	15	69.12
acsz–32x	Aleutian–Alaska–Cascadia	204.8802	57.5358	234.7	15	56.24
acsz–32y	Aleutian–Alaska–Cascadia	205.3385	57.1792	235.1	15	43.82
acsz–32z	Aleutian–Alaska–Cascadia	205.7880	56.8210	235.5	15	30.88
acsz–33a	Aleutian–Alaska–Cascadia	207.5370	56.9750	236	15	17.94
acsz–33b	Aleutian–Alaska–Cascadia	207.9930	56.6030	236	15	5
acsz–33w	Aleutian–Alaska–Cascadia	205.7126	58.3917	234.2	15	69.12
acsz–33x	Aleutian–Alaska–Cascadia	206.1873	58.0371	234.6	15	56.24
acsz–33y	Aleutian–Alaska–Cascadia	206.6527	57.6808	235	15	43.82
acsz–33z	Aleutian–Alaska–Cascadia	207.1091	57.3227	235.4	15	30.88
acsz–34a	Aleutian–Alaska–Cascadia	208.9371	57.5124	236	15	17.94
acsz–34b	Aleutian–Alaska–Cascadia	209.4000	57.1400	236	15	5
acsz–34w	Aleutian–Alaska–Cascadia	206.9772	58.8804	233.5	15	69.12
acsz–34x	Aleutian–Alaska–Cascadia	207.4677	58.5291	233.9	15	56.24
acsz–34y	Aleutian–Alaska–Cascadia	207.9485	58.1760	234.3	15	43.82
acsz–34z	Aleutian–Alaska–Cascadia	208.4198	57.8213	234.7	15	30.88
acsz–35a	Aleutian–Alaska–Cascadia	210.2597	58.0441	230	15	17.94
acsz–35b	Aleutian–Alaska–Cascadia	210.8000	57.7000	230	15	5

Continued on next page

Table B.1 – continued

Segment	Description	Longitude(°E)	Latitude(°N)	Strike(°)	Dip(°)	Depth (km)
acsz–35w	Aleutian–Alaska–Cascadia	208.0204	59.3199	228.8	15	69.12
acsz–35x	Aleutian–Alaska–Cascadia	208.5715	58.9906	229.3	15	56.24
acsz–35y	Aleutian–Alaska–Cascadia	209.1122	58.6590	229.7	15	43.82
acsz–35z	Aleutian–Alaska–Cascadia	209.6425	58.3252	230.2	15	30.88
acsz–36a	Aleutian–Alaska–Cascadia	211.3249	58.6565	218	15	17.94
acsz–36b	Aleutian–Alaska–Cascadia	212.0000	58.3800	218	15	5
acsz–36w	Aleutian–Alaska–Cascadia	208.5003	59.5894	215.6	15	69.12
acsz–36x	Aleutian–Alaska–Cascadia	209.1909	59.3342	216.2	15	56.24
acsz–36y	Aleutian–Alaska–Cascadia	209.8711	59.0753	216.8	15	43.82
acsz–36z	Aleutian–Alaska–Cascadia	210.5412	58.8129	217.3	15	30.88
acsz–37a	Aleutian–Alaska–Cascadia	212.2505	59.2720	213.7	15	17.94
acsz–37b	Aleutian–Alaska–Cascadia	212.9519	59.0312	213.7	15	5
acsz–37x	Aleutian–Alaska–Cascadia	210.1726	60.0644	213	15	56.24
acsz–37y	Aleutian–Alaska–Cascadia	210.8955	59.8251	213.7	15	43.82
acsz–37z	Aleutian–Alaska–Cascadia	211.6079	59.5820	214.3	15	30.88
acsz–38a	Aleutian–Alaska–Cascadia	214.6555	60.1351	260.1	0	15
acsz–38b	Aleutian–Alaska–Cascadia	214.8088	59.6927	260.1	0	15
acsz–38y	Aleutian–Alaska–Cascadia	214.3737	60.9838	259	0	15
acsz–38z	Aleutian–Alaska–Cascadia	214.5362	60.5429	259	0	15
acsz–39a	Aleutian–Alaska–Cascadia	216.5607	60.2480	267	0	15
acsz–39b	Aleutian–Alaska–Cascadia	216.6068	59.7994	267	0	15
acsz–40a	Aleutian–Alaska–Cascadia	219.3069	59.7574	310.9	0	15
acsz–40b	Aleutian–Alaska–Cascadia	218.7288	59.4180	310.9	0	15
acsz–41a	Aleutian–Alaska–Cascadia	220.4832	59.3390	300.7	0	15
acsz–41b	Aleutian–Alaska–Cascadia	220.0382	58.9529	300.7	0	15
acsz–42a	Aleutian–Alaska–Cascadia	221.8835	58.9310	298.9	0	15
acsz–42b	Aleutian–Alaska–Cascadia	221.4671	58.5379	298.9	0	15
acsz–43a	Aleutian–Alaska–Cascadia	222.9711	58.6934	282.3	0	15
acsz–43b	Aleutian–Alaska–Cascadia	222.7887	58.2546	282.3	0	15
acsz–44a	Aleutian–Alaska–Cascadia	224.9379	57.9054	340.9	12	11.09
acsz–44b	Aleutian–Alaska–Cascadia	224.1596	57.7617	340.9	7	5
acsz–45a	Aleutian–Alaska–Cascadia	225.4994	57.1634	334.1	12	11.09
acsz–45b	Aleutian–Alaska–Cascadia	224.7740	56.9718	334.1	7	5
acsz–46a	Aleutian–Alaska–Cascadia	226.1459	56.3552	334.1	12	11.09
acsz–46b	Aleutian–Alaska–Cascadia	225.4358	56.1636	334.1	7	5
acsz–47a	Aleutian–Alaska–Cascadia	226.7731	55.5830	332.3	12	11.09
acsz–47b	Aleutian–Alaska–Cascadia	226.0887	55.3785	332.3	7	5
acsz–48a	Aleutian–Alaska–Cascadia	227.4799	54.6763	339.4	12	11.09
acsz–48b	Aleutian–Alaska–Cascadia	226.7713	54.5217	339.4	7	5
acsz–49a	Aleutian–Alaska–Cascadia	227.9482	53.8155	341.2	12	11.09
acsz–49b	Aleutian–Alaska–Cascadia	227.2462	53.6737	341.2	7	5
acsz–50a	Aleutian–Alaska–Cascadia	228.3970	53.2509	324.5	12	11.09
acsz–50b	Aleutian–Alaska–Cascadia	227.8027	52.9958	324.5	7	5
acsz–51a	Aleutian–Alaska–Cascadia	229.1844	52.6297	318.4	12	11.09
acsz–51b	Aleutian–Alaska–Cascadia	228.6470	52.3378	318.4	7	5
acsz–52a	Aleutian–Alaska–Cascadia	230.0306	52.0768	310.9	12	11.09
acsz–52b	Aleutian–Alaska–Cascadia	229.5665	51.7445	310.9	7	5
acsz–53a	Aleutian–Alaska–Cascadia	231.1735	51.5258	310.9	12	11.09
acsz–53b	Aleutian–Alaska–Cascadia	230.7150	51.1935	310.9	7	5
acsz–54a	Aleutian–Alaska–Cascadia	232.2453	50.8809	314.1	12	11.09
acsz–54b	Aleutian–Alaska–Cascadia	231.7639	50.5655	314.1	7	5
acsz–55a	Aleutian–Alaska–Cascadia	233.3066	49.9032	333.7	12	11.09
acsz–55b	Aleutian–Alaska–Cascadia	232.6975	49.7086	333.7	7	5
acsz–56a	Aleutian–Alaska–Cascadia	234.0588	49.1702	315	11	12.82
acsz–56b	Aleutian–Alaska–Cascadia	233.5849	48.8584	315	9	5

Continued on next page

Table B.1 – continued

Segment	Description	Longitude(°E)	Latitude(°N)	Strike(°)	Dip(°)	Depth (km)
acsz–57a	Aleutian–Alaska–Cascadia	234.9041	48.2596	341	11	12.82
acsz–57b	Aleutian–Alaska–Cascadia	234.2797	48.1161	341	9	5
acsz–58a	Aleutian–Alaska–Cascadia	235.3021	47.3812	344	11	12.82
acsz–58b	Aleutian–Alaska–Cascadia	234.6776	47.2597	344	9	5
acsz–59a	Aleutian–Alaska–Cascadia	235.6432	46.5082	345	11	12.82
acsz–59b	Aleutian–Alaska–Cascadia	235.0257	46.3941	345	9	5
acsz–60a	Aleutian–Alaska–Cascadia	235.8640	45.5429	356	11	12.82
acsz–60b	Aleutian–Alaska–Cascadia	235.2363	45.5121	356	9	5
acsz–61a	Aleutian–Alaska–Cascadia	235.9106	44.6227	359	11	12.82
acsz–61b	Aleutian–Alaska–Cascadia	235.2913	44.6150	359	9	5
acsz–62a	Aleutian–Alaska–Cascadia	235.9229	43.7245	359	11	12.82
acsz–62b	Aleutian–Alaska–Cascadia	235.3130	43.7168	359	9	5
acsz–63a	Aleutian–Alaska–Cascadia	236.0220	42.9020	350	11	12.82
acsz–63b	Aleutian–Alaska–Cascadia	235.4300	42.8254	350	9	5
acsz–64a	Aleutian–Alaska–Cascadia	235.9638	41.9818	345	11	12.82
acsz–64b	Aleutian–Alaska–Cascadia	235.3919	41.8677	345	9	5
acsz–65a	Aleutian–Alaska–Cascadia	236.2643	41.1141	345	11	12.82
acsz–65b	Aleutian–Alaska–Cascadia	235.7000	41.0000	345	9	5
acsz–238a	Aleutian–Alaska–Cascadia	213.2878	59.8406	236.8	15	17.94
acsz–238y	Aleutian–Alaska–Cascadia	212.3424	60.5664	236.8	15	43.82
acsz–238z	Aleutian–Alaska–Cascadia	212.8119	60.2035	236.8	15	30.88

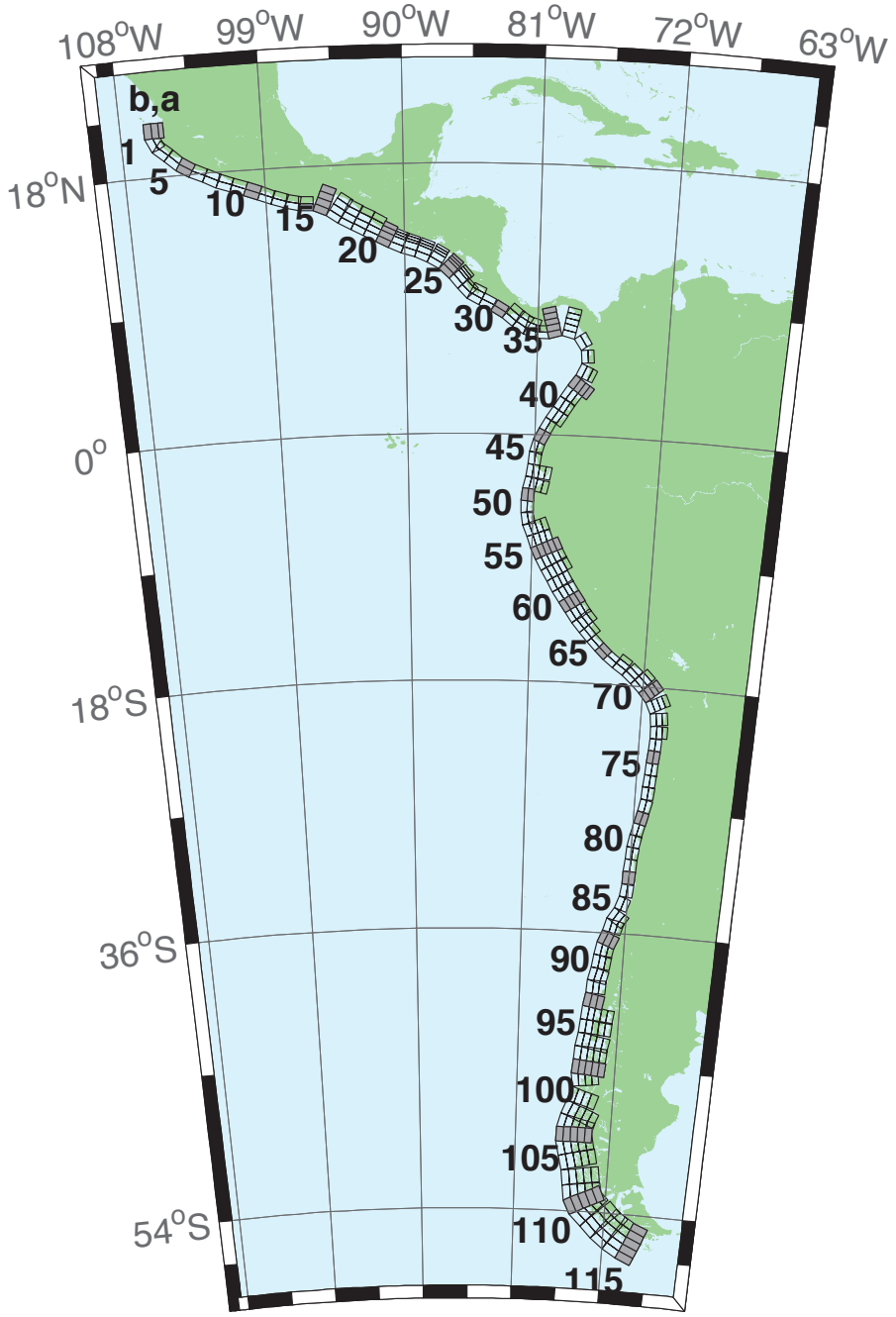

Figure B.2: Central and South America Subduction Zone unit sources.

Table B.2: Earthquake parameters for Central and South America Subduction Zone unit sources.

Segment	Description	Longitude(°E)	Latitude(°N)	Strike(°)	Dip(°)	Depth (km)
cssz–1a	Central and South America	254.4573	20.8170	359	19	15.4
cssz–1b	Central and South America	254.0035	20.8094	359	12	5
cssz–1z	Central and South America	254.7664	20.8222	359	50	31.67
cssz–2a	Central and South America	254.5765	20.2806	336.8	19	15.4
cssz–2b	Central and South America	254.1607	20.1130	336.8	12	5
cssz–3a	Central and South America	254.8789	19.8923	310.6	18.31	15.27
cssz–3b	Central and South America	254.5841	19.5685	310.6	11.85	5
cssz–4a	Central and South America	255.6167	19.2649	313.4	17.62	15.12
cssz–4b	Central and South America	255.3056	18.9537	313.4	11.68	5
cssz–5a	Central and South America	256.2240	18.8148	302.7	16.92	15
cssz–5b	Central and South America	255.9790	18.4532	302.7	11.54	5
cssz–6a	Central and South America	256.9425	18.4383	295.1	16.23	14.87
cssz–6b	Central and South America	256.7495	18.0479	295.1	11.38	5
cssz–7a	Central and South America	257.8137	18.0339	296.9	15.54	14.74
cssz–7b	Central and South America	257.6079	17.6480	296.9	11.23	5
cssz–8a	Central and South America	258.5779	17.7151	290.4	14.85	14.61
cssz–8b	Central and South America	258.4191	17.3082	290.4	11.08	5
cssz–9a	Central and South America	259.4578	17.4024	290.5	14.15	14.47
cssz–9b	Central and South America	259.2983	16.9944	290.5	10.92	5
cssz–10a	Central and South America	260.3385	17.0861	290.8	13.46	14.34
cssz–10b	Central and South America	260.1768	16.6776	290.8	10.77	5
cssz–11a	Central and South America	261.2255	16.7554	291.8	12.77	14.21
cssz–11b	Central and South America	261.0556	16.3487	291.8	10.62	5
cssz–12a	Central and South America	262.0561	16.4603	288.9	12.08	14.08
cssz–12b	Central and South America	261.9082	16.0447	288.9	10.46	5
cssz–13a	Central and South America	262.8638	16.2381	283.2	11.38	13.95
cssz–13b	Central and South America	262.7593	15.8094	283.2	10.31	5
cssz–14a	Central and South America	263.6066	16.1435	272.1	10.69	13.81
cssz–14b	Central and South America	263.5901	15.7024	272.1	10.15	5
cssz–15a	Central and South America	264.8259	15.8829	293	10	13.68
cssz–15b	Central and South America	264.6462	15.4758	293	10	5
cssz–15y	Central and South America	265.1865	16.6971	293	10	31.05
cssz–15z	Central and South America	265.0060	16.2900	293	10	22.36
cssz–16a	Central and South America	265.7928	15.3507	304.9	15	15.82
cssz–16b	Central and South America	265.5353	14.9951	304.9	12.5	5
cssz–16y	Central and South America	266.3092	16.0619	304.9	15	41.7
cssz–16z	Central and South America	266.0508	15.7063	304.9	15	28.76
cssz–17a	Central and South America	266.4947	14.9019	299.5	20	17.94
cssz–17b	Central and South America	266.2797	14.5346	299.5	15	5
cssz–17y	Central and South America	266.9259	15.6365	299.5	20	52.14
cssz–17z	Central and South America	266.7101	15.2692	299.5	20	35.04
cssz–18a	Central and South America	267.2827	14.4768	298	21.5	17.94
cssz–18b	Central and South America	267.0802	14.1078	298	15	5
cssz–18y	Central and South America	267.6888	15.2148	298	21.5	54.59
cssz–18z	Central and South America	267.4856	14.8458	298	21.5	36.27
cssz–19a	Central and South America	268.0919	14.0560	297.6	23	17.94
cssz–19b	Central and South America	267.8943	13.6897	297.6	15	5
cssz–19y	Central and South America	268.4880	14.7886	297.6	23	57.01
cssz–19z	Central and South America	268.2898	14.4223	297.6	23	37.48
cssz–20a	Central and South America	268.8929	13.6558	296.2	24	17.94
cssz–20b	Central and South America	268.7064	13.2877	296.2	15	5
cssz–20y	Central and South America	269.1796	14.2206	296.2	45.5	73.94
cssz–20z	Central and South America	269.0362	13.9382	296.2	45.5	38.28

Continued on next page

Table B.2 – continued

Segment	Description	Longitude(°E)	Latitude(°N)	Strike(°)	Dip(°)	Depth (km)
cssz–21a	Central and South America	269.6797	13.3031	292.6	25	17.94
cssz–21b	Central and South America	269.5187	12.9274	292.6	15	5
cssz–21x	Central and South America	269.8797	13.7690	292.6	68	131.8
cssz–21y	Central and South America	269.8130	13.6137	292.6	68	85.43
cssz–21z	Central and South America	269.7463	13.4584	292.6	68	39.07
cssz–22a	Central and South America	270.4823	13.0079	288.6	25	17.94
cssz–22b	Central and South America	270.3492	12.6221	288.6	15	5
cssz–22x	Central and South America	270.6476	13.4864	288.6	68	131.8
cssz–22y	Central and South America	270.5925	13.3269	288.6	68	85.43
cssz–22z	Central and South America	270.5374	13.1674	288.6	68	39.07
cssz–23a	Central and South America	271.3961	12.6734	292.4	25	17.94
cssz–23b	Central and South America	271.2369	12.2972	292.4	15	5
cssz–23x	Central and South America	271.5938	13.1399	292.4	68	131.8
cssz–23y	Central and South America	271.5279	12.9844	292.4	68	85.43
cssz–23z	Central and South America	271.4620	12.8289	292.4	68	39.07
cssz–24a	Central and South America	272.3203	12.2251	300.2	25	17.94
cssz–24b	Central and South America	272.1107	11.8734	300.2	15	5
cssz–24x	Central and South America	272.5917	12.6799	300.2	67	131.1
cssz–24y	Central and South America	272.5012	12.5283	300.2	67	85.1
cssz–24z	Central and South America	272.4107	12.3767	300.2	67	39.07
cssz–25a	Central and South America	273.2075	11.5684	313.8	25	17.94
cssz–25b	Central and South America	272.9200	11.2746	313.8	15	5
cssz–25x	Central and South America	273.5950	11.9641	313.8	66	130.4
cssz–25y	Central and South America	273.4658	11.8322	313.8	66	84.75
cssz–25z	Central and South America	273.3366	11.7003	313.8	66	39.07
cssz–26a	Central and South America	273.8943	10.8402	320.4	25	17.94
cssz–26b	Central and South America	273.5750	10.5808	320.4	15	5
cssz–26x	Central and South America	274.3246	11.1894	320.4	66	130.4
cssz–26y	Central and South America	274.1811	11.0730	320.4	66	84.75
cssz–26z	Central and South America	274.0377	10.9566	320.4	66	39.07
cssz–27a	Central and South America	274.4569	10.2177	316.1	25	17.94
cssz–27b	Central and South America	274.1590	9.9354	316.1	15	5
cssz–27z	Central and South America	274.5907	10.3444	316.1	66	39.07
cssz–28a	Central and South America	274.9586	9.8695	297.1	22	14.54
cssz–28b	Central and South America	274.7661	9.4988	297.1	11	5
cssz–28z	Central and South America	275.1118	10.1643	297.1	42.5	33.27
cssz–29a	Central and South America	275.7686	9.4789	296.6	19	11.09
cssz–29b	Central and South America	275.5759	9.0992	296.6	7	5
cssz–30a	Central and South America	276.6346	8.9973	302.2	19	9.36
cssz–30b	Central and South America	276.4053	8.6381	302.2	5	5
cssz–31a	Central and South America	277.4554	8.4152	309.1	19	7.62
cssz–31b	Central and South America	277.1851	8.0854	309.1	3	5
cssz–31z	Central and South America	277.7260	8.7450	309.1	19	23.9
cssz–32a	Central and South America	278.1112	7.9425	303	18.67	8.49
cssz–32b	Central and South America	277.8775	7.5855	303	4	5
cssz–32z	Central and South America	278.3407	8.2927	303	21.67	24.49
cssz–33a	Central and South America	278.7082	7.6620	287.6	18.33	10.23
cssz–33b	Central and South America	278.5785	7.2555	287.6	6	5
cssz–33z	Central and South America	278.8328	8.0522	287.6	24.33	25.95
cssz–34a	Central and South America	279.3184	7.5592	269.5	18	17.94
cssz–34b	Central and South America	279.3223	7.1320	269.5	15	5
cssz–35a	Central and South America	280.0039	7.6543	255.9	17.67	14.54
cssz–35b	Central and South America	280.1090	7.2392	255.9	11	5
cssz–35x	Central and South America	279.7156	8.7898	255.9	29.67	79.22
cssz–35y	Central and South America	279.8118	8.4113	255.9	29.67	54.47

Continued on next page

Table B.2 – continued

Segment	Description	Longitude(°E)	Latitude(°N)	Strike(°)	Dip(°)	Depth (km)
cssz–35z	Central and South America	279.9079	8.0328	255.9	29.67	29.72
cssz–36a	Central and South America	281.2882	7.6778	282.5	17.33	11.09
cssz–36b	Central and South America	281.1948	7.2592	282.5	7	5
cssz–36x	Central and South America	281.5368	8.7896	282.5	32.33	79.47
cssz–36y	Central and South America	281.4539	8.4190	282.5	32.33	52.73
cssz–36z	Central and South America	281.3710	8.0484	282.5	32.33	25.99
cssz–37a	Central and South America	282.5252	6.8289	326.9	17	10.23
cssz–37b	Central and South America	282.1629	6.5944	326.9	6	5
cssz–38a	Central and South America	282.9469	5.5973	355.4	17	10.23
cssz–38b	Central and South America	282.5167	5.5626	355.4	6	5
cssz–39a	Central and South America	282.7236	4.3108	24.13	17	10.23
cssz–39b	Central and South America	282.3305	4.4864	24.13	6	5
cssz–39z	Central and South America	283.0603	4.1604	24.13	35	24.85
cssz–40a	Central and South America	282.1940	3.3863	35.28	17	10.23
cssz–40b	Central and South America	281.8427	3.6344	35.28	6	5
cssz–40y	Central and South America	282.7956	2.9613	35.28	35	53.52
cssz–40z	Central and South America	282.4948	3.1738	35.28	35	24.85
cssz–41a	Central and South America	281.6890	2.6611	34.27	17	10.23
cssz–41b	Central and South America	281.3336	2.9030	34.27	6	5
cssz–41z	Central and South America	281.9933	2.4539	34.27	35	24.85
cssz–42a	Central and South America	281.2266	1.9444	31.29	17	10.23
cssz–42b	Central and South America	280.8593	2.1675	31.29	6	5
cssz–42z	Central and South America	281.5411	1.7533	31.29	35	24.85
cssz–43a	Central and South America	280.7297	1.1593	33.3	17	10.23
cssz–43b	Central and South America	280.3706	1.3951	33.3	6	5
cssz–43z	Central and South America	281.0373	0.9573	33.3	35	24.85
cssz–44a	Central and South America	280.3018	0.4491	28.8	17	10.23
cssz–44b	Central and South America	279.9254	0.6560	28.8	6	5
cssz–45a	Central and South America	279.9083	-0.3259	26.91	10	8.49
cssz–45b	Central and South America	279.5139	-0.1257	26.91	4	5
cssz–46a	Central and South America	279.6461	-0.9975	15.76	10	8.49
cssz–46b	Central and South America	279.2203	-0.8774	15.76	4	5
cssz–47a	Central and South America	279.4972	-1.7407	6.9	10	8.49
cssz–47b	Central and South America	279.0579	-1.6876	6.9	4	5
cssz–48a	Central and South America	279.3695	-2.6622	8.96	10	8.49
cssz–48b	Central and South America	278.9321	-2.5933	8.96	4	5
cssz–48y	Central and South America	280.2444	-2.8000	8.96	10	25.85
cssz–48z	Central and South America	279.8070	-2.7311	8.96	10	17.17
cssz–49a	Central and South America	279.1852	-3.6070	13.15	10	8.49
cssz–49b	Central and South America	278.7536	-3.5064	13.15	4	5
cssz–49y	Central and South America	280.0486	-3.8082	13.15	10	25.85
cssz–49z	Central and South America	279.6169	-3.7076	13.15	10	17.17
cssz–50a	Central and South America	279.0652	-4.3635	4.78	10.33	9.64
cssz–50b	Central and South America	278.6235	-4.3267	4.78	5.33	5
cssz–51a	Central and South America	279.0349	-5.1773	359.4	10.67	10.81
cssz–51b	Central and South America	278.5915	-5.1817	359.4	6.67	5
cssz–52a	Central and South America	279.1047	-5.9196	349.8	11	11.96
cssz–52b	Central and South America	278.6685	-5.9981	349.8	8	5
cssz–53a	Central and South America	279.3044	-6.6242	339.2	10.25	11.74
cssz–53b	Central and South America	278.8884	-6.7811	339.2	7.75	5
cssz–53y	Central and South America	280.1024	-6.3232	339.2	19.25	37.12
cssz–53z	Central and South America	279.7035	-6.4737	339.2	19.25	20.64
cssz–54a	Central and South America	279.6256	-7.4907	340.8	9.5	11.53
cssz–54b	Central and South America	279.2036	-7.6365	340.8	7.5	5
cssz–54y	Central and South America	280.4267	-7.2137	340.8	20.5	37.29

Continued on next page

Table B.2 – continued

Segment	Description	Longitude(°E)	Latitude(°N)	Strike(°)	Dip(°)	Depth (km)
cssz–54z	Central and South America	280.0262	-7.3522	340.8	20.5	19.78
cssz–55a	Central and South America	279.9348	-8.2452	335.4	8.75	11.74
cssz–55b	Central and South America	279.5269	-8.4301	335.4	7.75	5
cssz–55x	Central and South America	281.0837	-7.7238	335.4	21.75	56.4
cssz–55y	Central and South America	280.7009	-7.8976	335.4	21.75	37.88
cssz–55z	Central and South America	280.3180	-8.0714	335.4	21.75	19.35
cssz–56a	Central and South America	280.3172	-8.9958	331.6	8	11.09
cssz–56b	Central and South America	279.9209	-9.2072	331.6	7	5
cssz–56x	Central and South America	281.4212	-8.4063	331.6	23	57.13
cssz–56y	Central and South America	281.0534	-8.6028	331.6	23	37.59
cssz–56z	Central and South America	280.6854	-8.7993	331.6	23	18.05
cssz–57a	Central and South America	280.7492	-9.7356	328.7	8.6	10.75
cssz–57b	Central and South America	280.3640	-9.9663	328.7	6.6	5
cssz–57x	Central and South America	281.8205	-9.0933	328.7	23.4	57.94
cssz–57y	Central and South America	281.4636	-9.3074	328.7	23.4	38.08
cssz–57z	Central and South America	281.1065	-9.5215	328.7	23.4	18.22
cssz–58a	Central and South America	281.2275	-10.5350	330.5	9.2	10.4
cssz–58b	Central and South America	280.8348	-10.7532	330.5	6.2	5
cssz–58y	Central and South America	281.9548	-10.1306	330.5	23.8	38.57
cssz–58z	Central and South America	281.5913	-10.3328	330.5	23.8	18.39
cssz–59a	Central and South America	281.6735	-11.2430	326.2	9.8	10.05
cssz–59b	Central and South America	281.2982	-11.4890	326.2	5.8	5
cssz–59y	Central and South America	282.3675	-10.7876	326.2	24.2	39.06
cssz–59z	Central and South America	282.0206	-11.0153	326.2	24.2	18.56
cssz–60a	Central and South America	282.1864	-11.9946	326.5	10.4	9.71
cssz–60b	Central and South America	281.8096	-12.2384	326.5	5.4	5
cssz–60y	Central and South America	282.8821	-11.5438	326.5	24.6	39.55
cssz–60z	Central and South America	282.5344	-11.7692	326.5	24.6	18.73
cssz–61a	Central and South America	282.6944	-12.7263	325.5	11	9.36
cssz–61b	Central and South America	282.3218	-12.9762	325.5	5	5
cssz–61y	Central and South America	283.3814	-12.2649	325.5	25	40.03
cssz–61z	Central and South America	283.0381	-12.4956	325.5	25	18.9
cssz–62a	Central and South America	283.1980	-13.3556	319	11	9.79
cssz–62b	Central and South America	282.8560	-13.6451	319	5.5	5
cssz–62y	Central and South America	283.8178	-12.8300	319	27	42.03
cssz–62z	Central and South America	283.5081	-13.0928	319	27	19.33
cssz–63a	Central and South America	283.8032	-14.0147	317.9	11	10.23
cssz–63b	Central and South America	283.4661	-14.3106	317.9	6	5
cssz–63z	Central and South America	284.1032	-13.7511	317.9	29	19.77
cssz–64a	Central and South America	284.4144	-14.6482	315.7	13	11.96
cssz–64b	Central and South America	284.0905	-14.9540	315.7	8	5
cssz–65a	Central and South America	285.0493	-15.2554	313.2	15	13.68
cssz–65b	Central and South America	284.7411	-15.5715	313.2	10	5
cssz–66a	Central and South America	285.6954	-15.7816	307.7	14.5	13.68
cssz–66b	Central and South America	285.4190	-16.1258	307.7	10	5
cssz–67a	Central and South America	286.4127	-16.2781	304.3	14	13.68
cssz–67b	Central and South America	286.1566	-16.6381	304.3	10	5
cssz–67z	Central and South America	286.6552	-15.9365	304.3	23	25.78
cssz–68a	Central and South America	287.2481	-16.9016	311.8	14	13.68
cssz–68b	Central and South America	286.9442	-17.2264	311.8	10	5
cssz–68z	Central and South America	287.5291	-16.6007	311.8	26	25.78
cssz–69a	Central and South America	287.9724	-17.5502	314.9	14	13.68
cssz–69b	Central and South America	287.6496	-17.8590	314.9	10	5
cssz–69y	Central and South America	288.5530	-16.9934	314.9	29	50.02
cssz–69z	Central and South America	288.2629	-17.2718	314.9	29	25.78

Continued on next page

Table B.2 – continued

Segment	Description	Longitude(°E)	Latitude(°N)	Strike(°)	Dip(°)	Depth (km)
cssz–70a	Central and South America	288.6731	-18.2747	320.4	14	13.25
cssz–70b	Central and South America	288.3193	-18.5527	320.4	9.5	5
cssz–70y	Central and South America	289.3032	-17.7785	320.4	30	50.35
cssz–70z	Central and South America	288.9884	-18.0266	320.4	30	25.35
cssz–71a	Central and South America	289.3089	-19.1854	333.2	14	12.82
cssz–71b	Central and South America	288.8968	-19.3820	333.2	9	5
cssz–71y	Central and South America	290.0357	-18.8382	333.2	31	50.67
cssz–71z	Central and South America	289.6725	-19.0118	333.2	31	24.92
cssz–72a	Central and South America	289.6857	-20.3117	352.4	14	12.54
cssz–72b	Central and South America	289.2250	-20.3694	352.4	8.67	5
cssz–72z	Central and South America	290.0882	-20.2613	352.4	32	24.63
cssz–73a	Central and South America	289.7731	-21.3061	358.9	14	12.24
cssz–73b	Central and South America	289.3053	-21.3142	358.9	8.33	5
cssz–73z	Central and South America	290.1768	-21.2991	358.9	33	24.34
cssz–74a	Central and South America	289.7610	-22.2671	3.06	14	11.96
cssz–74b	Central and South America	289.2909	-22.2438	3.06	8	5
cssz–75a	Central and South America	289.6982	-23.1903	4.83	14.09	11.96
cssz–75b	Central and South America	289.2261	-23.1536	4.83	8	5
cssz–76a	Central and South America	289.6237	-24.0831	4.67	14.18	11.96
cssz–76b	Central and South America	289.1484	-24.0476	4.67	8	5
cssz–77a	Central and South America	289.5538	-24.9729	4.3	14.27	11.96
cssz–77b	Central and South America	289.0750	-24.9403	4.3	8	5
cssz–78a	Central and South America	289.4904	-25.8621	3.86	14.36	11.96
cssz–78b	Central and South America	289.0081	-25.8328	3.86	8	5
cssz–79a	Central and South America	289.3491	-26.8644	11.34	14.45	11.96
cssz–79b	Central and South America	288.8712	-26.7789	11.34	8	5
cssz–80a	Central and South America	289.1231	-27.7826	14.16	14.54	11.96
cssz–80b	Central and South America	288.6469	-27.6762	14.16	8	5
cssz–81a	Central and South America	288.8943	-28.6409	13.19	14.63	11.96
cssz–81b	Central and South America	288.4124	-28.5417	13.19	8	5
cssz–82a	Central and South America	288.7113	-29.4680	9.68	14.72	11.96
cssz–82b	Central and South America	288.2196	-29.3950	9.68	8	5
cssz–83a	Central and South America	288.5944	-30.2923	5.36	14.81	11.96
cssz–83b	Central and South America	288.0938	-30.2517	5.36	8	5
cssz–84a	Central and South America	288.5223	-31.1639	3.8	14.9	11.96
cssz–84b	Central and South America	288.0163	-31.1351	3.8	8	5
cssz–85a	Central and South America	288.4748	-32.0416	2.55	15	11.96
cssz–85b	Central and South America	287.9635	-32.0223	2.55	8	5
cssz–86a	Central and South America	288.3901	-33.0041	7.01	15	11.96
cssz–86b	Central and South America	287.8768	-32.9512	7.01	8	5
cssz–87a	Central and South America	288.1050	-34.0583	19.4	15	11.96
cssz–87b	Central and South America	287.6115	-33.9142	19.4	8	5
cssz–88a	Central and South America	287.5309	-35.0437	32.81	15	11.96
cssz–88b	Central and South America	287.0862	-34.8086	32.81	8	5
cssz–88z	Central and South America	287.9308	-35.2545	32.81	30	24.9
cssz–89a	Central and South America	287.2380	-35.5993	14.52	16.67	11.96
cssz–89b	Central and South America	286.7261	-35.4914	14.52	8	5
cssz–89z	Central and South America	287.7014	-35.6968	14.52	30	26.3
cssz–90a	Central and South America	286.8442	-36.5645	22.64	18.33	11.96
cssz–90b	Central and South America	286.3548	-36.4004	22.64	8	5
cssz–90z	Central and South America	287.2916	-36.7142	22.64	30	27.68
cssz–91a	Central and South America	286.5925	-37.2488	10.9	20	11.96
cssz–91b	Central and South America	286.0721	-37.1690	10.9	8	5
cssz–91z	Central and South America	287.0726	-37.3224	10.9	30	29.06
cssz–92a	Central and South America	286.4254	-38.0945	8.23	20	11.96

Continued on next page

Table B.2 – continued

Segment	Description	Longitude(°E)	Latitude(°N)	Strike(°)	Dip(°)	Depth (km)
cssz–92b	Central and South America	285.8948	-38.0341	8.23	8	5
cssz–92z	Central and South America	286.9303	-38.1520	8.23	26.67	29.06
cssz–93a	Central and South America	286.2047	-39.0535	13.46	20	11.96
cssz–93b	Central and South America	285.6765	-38.9553	13.46	8	5
cssz–93z	Central and South America	286.7216	-39.1495	13.46	23.33	29.06
cssz–94a	Central and South America	286.0772	-39.7883	3.4	20	11.96
cssz–94b	Central and South America	285.5290	-39.7633	3.4	8	5
cssz–94z	Central and South America	286.6255	-39.8133	3.4	20	29.06
cssz–95a	Central and South America	285.9426	-40.7760	9.84	20	11.96
cssz–95b	Central and South America	285.3937	-40.7039	9.84	8	5
cssz–95z	Central and South America	286.4921	-40.8481	9.84	20	29.06
cssz–96a	Central and South America	285.7839	-41.6303	7.6	20	11.96
cssz–96b	Central and South America	285.2245	-41.5745	7.6	8	5
cssz–96x	Central and South America	287.4652	-41.7977	7.6	20	63.26
cssz–96y	Central and South America	286.9043	-41.7419	7.6	20	46.16
cssz–96z	Central and South America	286.3439	-41.6861	7.6	20	29.06
cssz–97a	Central and South America	285.6695	-42.4882	5.3	20	11.96
cssz–97b	Central and South America	285.0998	-42.4492	5.3	8	5
cssz–97x	Central and South America	287.3809	-42.6052	5.3	20	63.26
cssz–97y	Central and South America	286.8101	-42.5662	5.3	20	46.16
cssz–97z	Central and South America	286.2396	-42.5272	5.3	20	29.06
cssz–98a	Central and South America	285.5035	-43.4553	10.53	20	11.96
cssz–98b	Central and South America	284.9322	-43.3782	10.53	8	5
cssz–98x	Central and South America	287.2218	-43.6866	10.53	20	63.26
cssz–98y	Central and South America	286.6483	-43.6095	10.53	20	46.16
cssz–98z	Central and South America	286.0755	-43.5324	10.53	20	29.06
cssz–99a	Central and South America	285.3700	-44.2595	4.86	20	11.96
cssz–99b	Central and South America	284.7830	-44.2237	4.86	8	5
cssz–99x	Central and South America	287.1332	-44.3669	4.86	20	63.26
cssz–99y	Central and South America	286.5451	-44.3311	4.86	20	46.16
cssz–99z	Central and South America	285.9574	-44.2953	4.86	20	29.06
cssz–100a	Central and South America	285.2713	-45.1664	5.68	20	11.96
cssz–100b	Central and South America	284.6758	-45.1246	5.68	8	5
cssz–100x	Central and South America	287.0603	-45.2918	5.68	20	63.26
cssz–100y	Central and South America	286.4635	-45.2500	5.68	20	46.16
cssz–100z	Central and South America	285.8672	-45.2082	5.68	20	29.06
cssz–101a	Central and South America	285.3080	-45.8607	352.6	20	9.36
cssz–101b	Central and South America	284.7067	-45.9152	352.6	5	5
cssz–101y	Central and South America	286.5089	-45.7517	352.6	20	43.56
cssz–101z	Central and South America	285.9088	-45.8062	352.6	20	26.46
cssz–102a	Central and South America	285.2028	-47.1185	17.72	5	9.36
cssz–102b	Central and South America	284.5772	-46.9823	17.72	5	5
cssz–102y	Central and South America	286.4588	-47.3909	17.72	5	18.07
cssz–102z	Central and South America	285.8300	-47.2547	17.72	5	13.72
cssz–103a	Central and South America	284.7075	-48.0396	23.37	7.5	11.53
cssz–103b	Central and South America	284.0972	-47.8630	23.37	7.5	5
cssz–103x	Central and South America	286.5511	-48.5694	23.37	7.5	31.11
cssz–103y	Central and South America	285.9344	-48.3928	23.37	7.5	24.58
cssz–103z	Central and South America	285.3199	-48.2162	23.37	7.5	18.05
cssz–104a	Central and South America	284.3440	-48.7597	14.87	10	13.68
cssz–104b	Central and South America	283.6962	-48.6462	14.87	10	5
cssz–104x	Central and South America	286.2962	-49.1002	14.87	10	39.73
cssz–104y	Central and South America	285.6440	-48.9867	14.87	10	31.05
cssz–104z	Central and South America	284.9933	-48.8732	14.87	10	22.36
cssz–105a	Central and South America	284.2312	-49.4198	0.25	9.67	13.4

Continued on next page

Table B.2 – continued

Segment	Description	Longitude(°E)	Latitude(°N)	Strike(°)	Dip(°)	Depth (km)
cssz–105b	Central and South America	283.5518	-49.4179	0.25	9.67	5
cssz–105x	Central and South America	286.2718	-49.4255	0.25	9.67	38.59
cssz–105y	Central and South America	285.5908	-49.4236	0.25	9.67	30.2
cssz–105z	Central and South America	284.9114	-49.4217	0.25	9.67	21.8
cssz–106a	Central and South America	284.3730	-50.1117	347.5	9.25	13.04
cssz–106b	Central and South America	283.6974	-50.2077	347.5	9.25	5
cssz–106x	Central and South America	286.3916	-49.8238	347.5	9.25	37.15
cssz–106y	Central and South America	285.7201	-49.9198	347.5	9.25	29.11
cssz–106z	Central and South America	285.0472	-50.0157	347.5	9.25	21.07
cssz–107a	Central and South America	284.7130	-50.9714	346.5	9	12.82
cssz–107b	Central and South America	284.0273	-51.0751	346.5	9	5
cssz–107x	Central and South America	286.7611	-50.6603	346.5	9	36.29
cssz–107y	Central and South America	286.0799	-50.7640	346.5	9	28.47
cssz–107z	Central and South America	285.3972	-50.8677	346.5	9	20.64
cssz–108a	Central and South America	285.0378	-51.9370	352	8.67	12.54
cssz–108b	Central and South America	284.3241	-51.9987	352	8.67	5
cssz–108x	Central and South America	287.1729	-51.7519	352	8.67	35.15
cssz–108y	Central and South America	286.4622	-51.8136	352	8.67	27.61
cssz–108z	Central and South America	285.7505	-51.8753	352	8.67	20.07
cssz–109a	Central and South America	285.2635	-52.8439	353.1	8.33	12.24
cssz–109b	Central and South America	284.5326	-52.8974	353.1	8.33	5
cssz–109x	Central and South America	287.4508	-52.6834	353.1	8.33	33.97
cssz–109y	Central and South America	286.7226	-52.7369	353.1	8.33	26.73
cssz–109z	Central and South America	285.9935	-52.7904	353.1	8.33	19.49
cssz–110a	Central and South America	285.5705	-53.4139	334.2	8	11.96
cssz–110b	Central and South America	284.8972	-53.6076	334.2	8	5
cssz–110x	Central and South America	287.5724	-52.8328	334.2	8	32.83
cssz–110y	Central and South America	286.9081	-53.0265	334.2	8	25.88
cssz–110z	Central and South America	286.2408	-53.2202	334.2	8	18.92
cssz–111a	Central and South America	286.1627	-53.8749	313.8	8	11.96
cssz–111b	Central and South America	285.6382	-54.1958	313.8	8	5
cssz–111x	Central and South America	287.7124	-52.9122	313.8	8	32.83
cssz–111y	Central and South America	287.1997	-53.2331	313.8	8	25.88
cssz–111z	Central and South America	286.6832	-53.5540	313.8	8	18.92
cssz–112a	Central and South America	287.3287	-54.5394	316.4	8	11.96
cssz–112b	Central and South America	286.7715	-54.8462	316.4	8	5
cssz–112x	Central and South America	288.9756	-53.6190	316.4	8	32.83
cssz–112y	Central and South America	288.4307	-53.9258	316.4	8	25.88
cssz–112z	Central and South America	287.8817	-54.2326	316.4	8	18.92
cssz–113a	Central and South America	288.3409	-55.0480	307.6	8	11.96
cssz–113b	Central and South America	287.8647	-55.4002	307.6	8	5
cssz–113x	Central and South America	289.7450	-53.9914	307.6	8	32.83
cssz–113y	Central and South America	289.2810	-54.3436	307.6	8	25.88
cssz–113z	Central and South America	288.8130	-54.6958	307.6	8	18.92
cssz–114a	Central and South America	289.5342	-55.5026	301.5	8	11.96
cssz–114b	Central and South America	289.1221	-55.8819	301.5	8	5
cssz–114x	Central and South America	290.7472	-54.3647	301.5	8	32.83
cssz–114y	Central and South America	290.3467	-54.7440	301.5	8	25.88
cssz–114z	Central and South America	289.9424	-55.1233	301.5	8	18.92
cssz–115a	Central and South America	290.7682	-55.8485	292.7	8	11.96
cssz–115b	Central and South America	290.4608	-56.2588	292.7	8	5
cssz–115x	Central and South America	291.6714	-54.6176	292.7	8	32.83
cssz–115y	Central and South America	291.3734	-55.0279	292.7	8	25.88
cssz–115z	Central and South America	291.0724	-55.4382	292.7	8	18.92

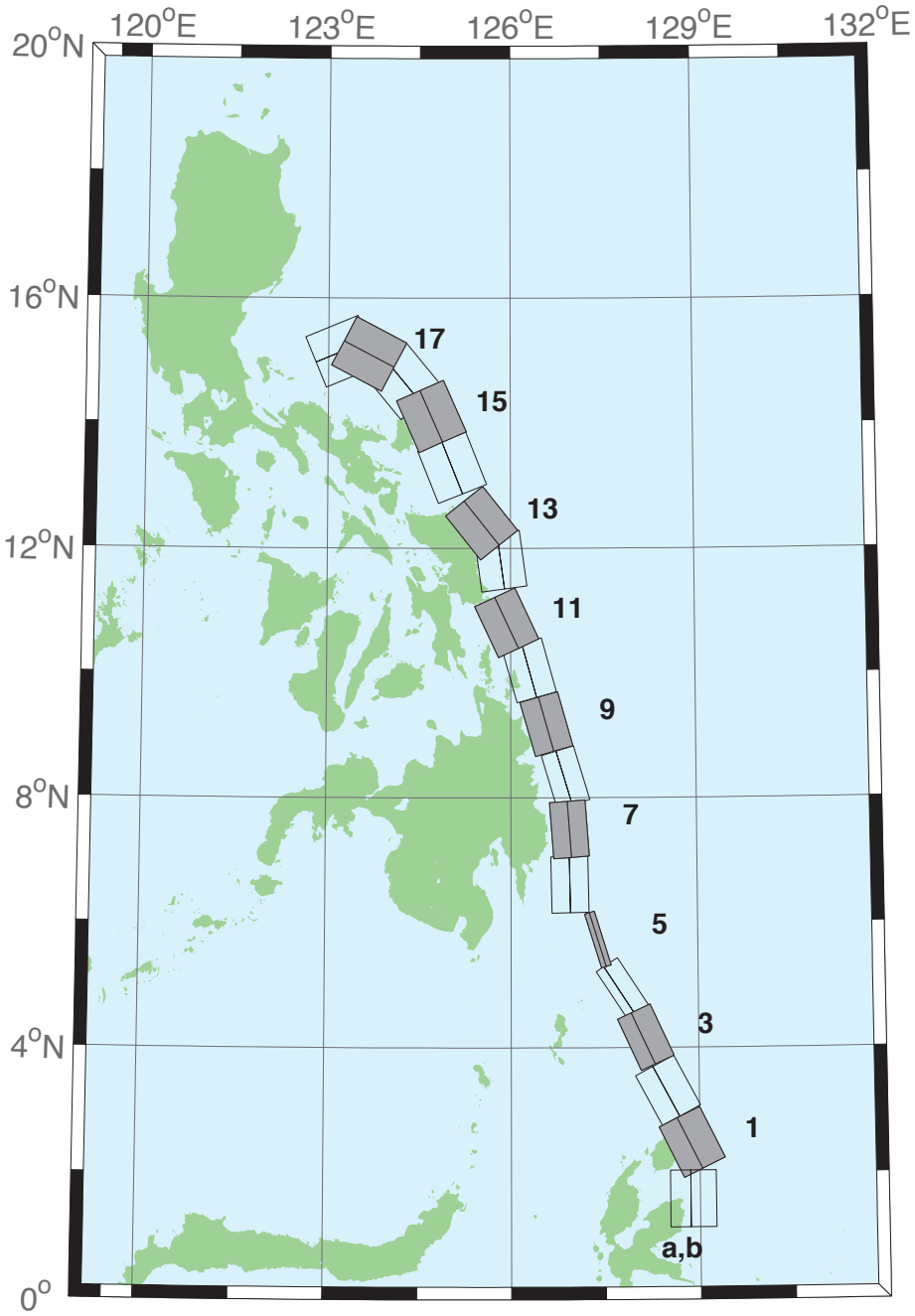

Figure B.3: Eastern Philippines Subduction Zone unit sources.

Table B.3: Earthquake parameters for Eastern Philippines Subduction Zone unit sources.

Segment	Description	Longitude(°E)	Latitude(°N)	Strike(°)	Dip(°)	Depth (km)
epsz–1a	Eastern Philippines	128.5521	2.3289	153.6	44.2	27.62
epsz–1b	Eastern Philippines	128.8408	2.4720	153.6	26.9	5
epsz–2a	Eastern Philippines	128.1943	3.1508	151.9	45.9	32.44
epsz–2b	Eastern Philippines	128.4706	3.2979	151.9	32.8	5.35
epsz–3a	Eastern Philippines	127.8899	4.0428	155.2	57.3	40.22
epsz–3b	Eastern Philippines	128.1108	4.1445	155.2	42.7	6.31
epsz–4a	Eastern Philippines	127.6120	4.8371	146.8	71.4	48.25
epsz–4b	Eastern Philippines	127.7324	4.9155	146.8	54.8	7.39
epsz–5a	Eastern Philippines	127.3173	5.7040	162.9	79.9	57.4
epsz–5b	Eastern Philippines	127.3930	5.7272	162.9	79.4	8.25
epsz–6a	Eastern Philippines	126.6488	6.6027	178.9	48.6	45.09
epsz–6b	Eastern Philippines	126.9478	6.6085	178.9	48.6	7.58
epsz–7a	Eastern Philippines	126.6578	7.4711	175.8	50.7	45.52
epsz–7b	Eastern Philippines	126.9439	7.4921	175.8	50.7	6.83
epsz–8a	Eastern Philippines	126.6227	8.2456	163.3	56.7	45.6
epsz–8b	Eastern Philippines	126.8614	8.3164	163.3	48.9	7.92
epsz–9a	Eastern Philippines	126.2751	9.0961	164.1	47	43.59
epsz–9b	Eastern Philippines	126.5735	9.1801	164.1	44.9	8.3
epsz–10a	Eastern Philippines	125.9798	9.9559	164.5	43.1	42.25
epsz–10b	Eastern Philippines	126.3007	10.0438	164.5	43.1	8.09
epsz–11a	Eastern Philippines	125.6079	10.6557	155	37.8	38.29
epsz–11b	Eastern Philippines	125.9353	10.8059	155	37.8	7.64
epsz–12a	Eastern Philippines	125.4697	11.7452	172.1	36	37.01
epsz–12b	Eastern Philippines	125.8374	11.7949	172.1	36	7.62
epsz–13a	Eastern Philippines	125.2238	12.1670	141.5	32.4	33.87
epsz–13b	Eastern Philippines	125.5278	12.4029	141.5	32.4	7.08
epsz–14a	Eastern Philippines	124.6476	13.1365	158.2	23	25.92
epsz–14b	Eastern Philippines	125.0421	13.2898	158.2	23	6.38
epsz–15a	Eastern Philippines	124.3107	13.9453	156.1	24.1	26.51
epsz–15b	Eastern Philippines	124.6973	14.1113	156.1	24.1	6.09
epsz–16a	Eastern Philippines	123.8998	14.4025	140.3	19.5	21.69
epsz–16b	Eastern Philippines	124.2366	14.6728	140.3	19.5	5
epsz–17a	Eastern Philippines	123.4604	14.7222	117.6	15.3	18.19
epsz–17b	Eastern Philippines	123.6682	15.1062	117.6	15.3	5
epsz–18a	Eastern Philippines	123.3946	14.7462	67.4	15	17.94
epsz–18b	Eastern Philippines	123.2219	15.1467	67.4	15	5
epsz–19a	Eastern Philippines	121.3638	15.7400	189.6	15	17.94
epsz–19b	Eastern Philippines	121.8082	15.6674	189.6	15	5
epsz–20a	Eastern Philippines	121.6833	16.7930	203.3	15	17.94
epsz–20b	Eastern Philippines	122.0994	16.6216	203.3	15	5
epsz–21a	Eastern Philippines	121.8279	17.3742	184.2	15	17.94
epsz–21b	Eastern Philippines	122.2814	17.3425	184.2	15	5

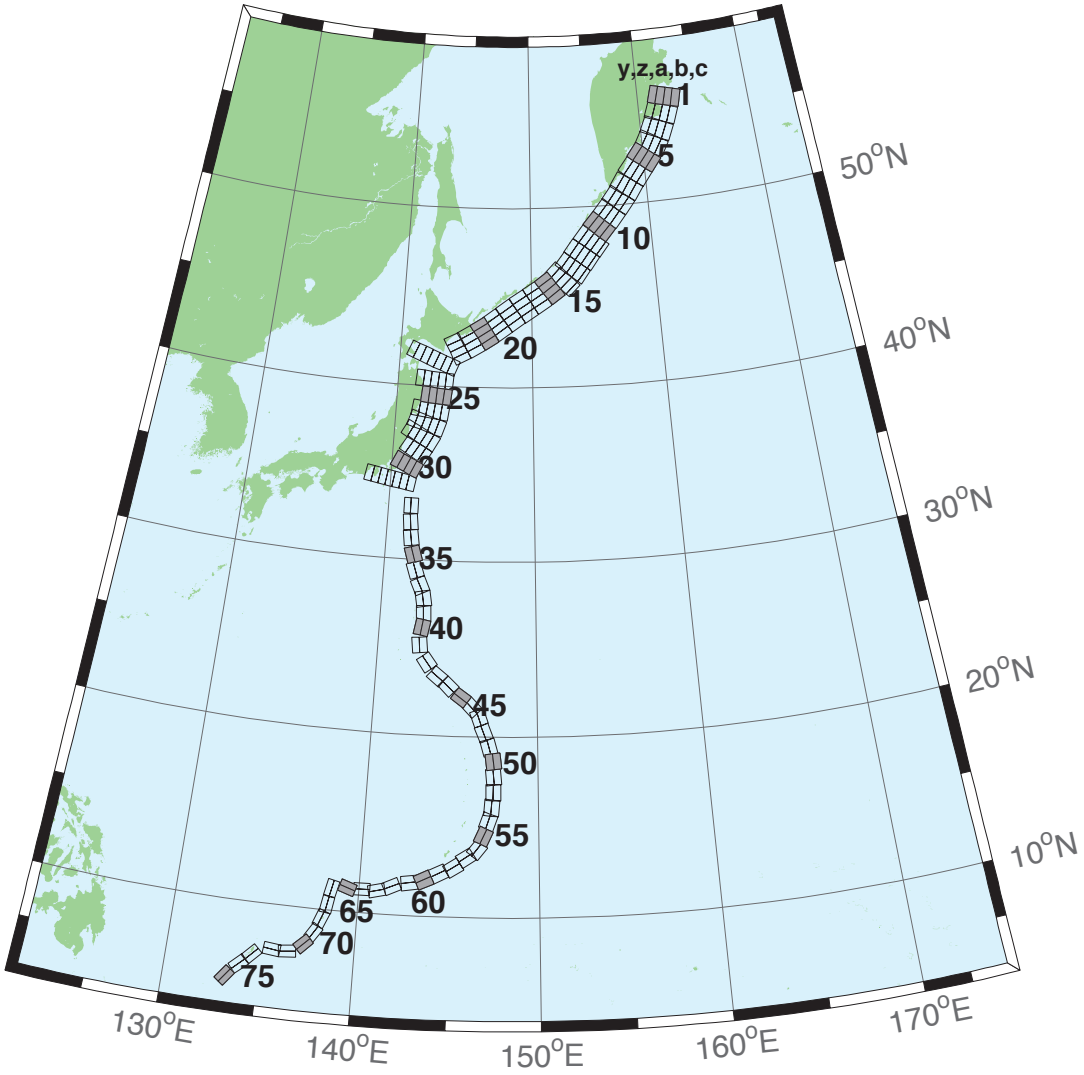

Figure B.4: Kamchatka-Kuril-Japan-Izu-Mariana-Yap Subduction Zone unit sources.

Table B.4: Earthquake parameters for Kamchatka-Kuril-Japan-Izu-Mariana-Yap Subduction Zone unit sources.

Segment	Description	Longitude(°E)	Latitude(°N)	Strike(°)	Dip(°)	Depth (km)
kisz–1a	Kamchatka-Kuril-Japan-Izu-Mariana-Yap	162.4318	55.5017	195	29	26.13
kisz–1b	Kamchatka-Kuril-Japan-Izu-Mariana-Yap	163.1000	55.4000	195	25	5
kisz–1y	Kamchatka-Kuril-Japan-Izu-Mariana-Yap	161.0884	55.7050	195	29	74.61
kisz–1z	Kamchatka-Kuril-Japan-Izu-Mariana-Yap	161.7610	55.6033	195	29	50.37
kisz–2a	Kamchatka-Kuril-Japan-Izu-Mariana-Yap	161.9883	54.6784	200	29	26.13
kisz–2b	Kamchatka-Kuril-Japan-Izu-Mariana-Yap	162.6247	54.5440	200	25	5
kisz–2y	Kamchatka-Kuril-Japan-Izu-Mariana-Yap	160.7072	54.9471	200	29	74.61
kisz–2z	Kamchatka-Kuril-Japan-Izu-Mariana-Yap	161.3488	54.8127	200	29	50.37
kisz–3a	Kamchatka-Kuril-Japan-Izu-Mariana-Yap	161.4385	53.8714	204	29	26.13
kisz–3b	Kamchatka-Kuril-Japan-Izu-Mariana-Yap	162.0449	53.7116	204	25	5
kisz–3y	Kamchatka-Kuril-Japan-Izu-Mariana-Yap	160.2164	54.1910	204	29	74.61
kisz–3z	Kamchatka-Kuril-Japan-Izu-Mariana-Yap	160.8286	54.0312	204	29	50.37
kisz–4a	Kamchatka-Kuril-Japan-Izu-Mariana-Yap	160.7926	53.1087	210	29	26.13
kisz–4b	Kamchatka-Kuril-Japan-Izu-Mariana-Yap	161.3568	52.9123	210	25	5
kisz–4y	Kamchatka-Kuril-Japan-Izu-Mariana-Yap	159.6539	53.5015	210	29	74.61
kisz–4z	Kamchatka-Kuril-Japan-Izu-Mariana-Yap	160.2246	53.3051	210	29	50.37
kisz–5a	Kamchatka-Kuril-Japan-Izu-Mariana-Yap	160.0211	52.4113	218	29	26.13
kisz–5b	Kamchatka-Kuril-Japan-Izu-Mariana-Yap	160.5258	52.1694	218	25	5
kisz–5y	Kamchatka-Kuril-Japan-Izu-Mariana-Yap	159.0005	52.8950	218	29	74.61
kisz–5z	Kamchatka-Kuril-Japan-Izu-Mariana-Yap	159.5122	52.6531	218	29	50.37
kisz–6a	Kamchatka-Kuril-Japan-Izu-Mariana-Yap	159.1272	51.7034	218	29	26.13
kisz–6b	Kamchatka-Kuril-Japan-Izu-Mariana-Yap	159.6241	51.4615	218	25	5
kisz–6y	Kamchatka-Kuril-Japan-Izu-Mariana-Yap	158.1228	52.1871	218	29	74.61
kisz–6z	Kamchatka-Kuril-Japan-Izu-Mariana-Yap	158.6263	51.9452	218	29	50.37
kisz–7a	Kamchatka-Kuril-Japan-Izu-Mariana-Yap	158.2625	50.9549	214	29	26.13
kisz–7b	Kamchatka-Kuril-Japan-Izu-Mariana-Yap	158.7771	50.7352	214	25	5
kisz–7y	Kamchatka-Kuril-Japan-Izu-Mariana-Yap	157.2236	51.3942	214	29	74.61
kisz–7z	Kamchatka-Kuril-Japan-Izu-Mariana-Yap	157.7443	51.1745	214	29	50.37
kisz–8a	Kamchatka-Kuril-Japan-Izu-Mariana-Yap	157.4712	50.2459	218	31	27.7
kisz–8b	Kamchatka-Kuril-Japan-Izu-Mariana-Yap	157.9433	50.0089	218	27	5
kisz–8y	Kamchatka-Kuril-Japan-Izu-Mariana-Yap	156.5176	50.7199	218	31	79.2
kisz–8z	Kamchatka-Kuril-Japan-Izu-Mariana-Yap	156.9956	50.4829	218	31	53.45
kisz–9a	Kamchatka-Kuril-Japan-Izu-Mariana-Yap	156.6114	49.5583	220	31	27.7
kisz–9b	Kamchatka-Kuril-Japan-Izu-Mariana-Yap	157.0638	49.3109	220	27	5
kisz–9y	Kamchatka-Kuril-Japan-Izu-Mariana-Yap	155.6974	50.0533	220	31	79.2
kisz–9z	Kamchatka-Kuril-Japan-Izu-Mariana-Yap	156.1556	49.8058	220	31	53.45
kisz–10a	Kamchatka-Kuril-Japan-Izu-Mariana-Yap	155.7294	48.8804	221	31	27.7
kisz–10b	Kamchatka-Kuril-Japan-Izu-Mariana-Yap	156.1690	48.6278	221	27	5
kisz–10y	Kamchatka-Kuril-Japan-Izu-Mariana-Yap	154.8413	49.3856	221	31	79.2
kisz–10z	Kamchatka-Kuril-Japan-Izu-Mariana-Yap	155.2865	49.1330	221	31	53.45
kisz–11a	Kamchatka-Kuril-Japan-Izu-Mariana-Yap	154.8489	48.1821	219	31	27.7
kisz–11b	Kamchatka-Kuril-Japan-Izu-Mariana-Yap	155.2955	47.9398	219	27	5
kisz–11y	Kamchatka-Kuril-Japan-Izu-Mariana-Yap	153.9472	48.6667	219	31	79.2
kisz–11z	Kamchatka-Kuril-Japan-Izu-Mariana-Yap	154.3991	48.4244	219	31	53.45
kisz–11c	Kamchatka-Kuril-Japan-Izu-Mariana-Yap	156.0358	47.5374	39	57.89	4.602
kisz–12a	Kamchatka-Kuril-Japan-Izu-Mariana-Yap	153.9994	47.4729	217	31	27.7
kisz–12b	Kamchatka-Kuril-Japan-Izu-Mariana-Yap	154.4701	47.2320	217	27	5
kisz–12y	Kamchatka-Kuril-Japan-Izu-Mariana-Yap	153.0856	47.9363	217	31	79.2
kisz–12z	Kamchatka-Kuril-Japan-Izu-Mariana-Yap	153.5435	47.7046	217	31	53.45
kisz–12c	Kamchatka-Kuril-Japan-Izu-Mariana-Yap	155.2208	46.8473	37	57.89	4.602
kisz–13a	Kamchatka-Kuril-Japan-Izu-Mariana-Yap	153.2239	46.7564	218	31	27.7
kisz–13b	Kamchatka-Kuril-Japan-Izu-Mariana-Yap	153.6648	46.5194	218	27	5

Continued on next page

Table B.4 – continued

Segment	Description	Longitude(°E)	Latitude(°N)	Strike(°)	Dip(°)	Depth (km)
kisz–13y	Kamchatka-Kuril-Japan-Izu-Mariana-Yap	152.3343	47.2304	218	31	79.2
kisz–13z	Kamchatka-Kuril-Japan-Izu-Mariana-Yap	152.7801	46.9934	218	31	53.45
kisz–13c	Kamchatka-Kuril-Japan-Izu-Mariana-Yap	154.3957	46.1257	38	57.89	4.602
kisz–14a	Kamchatka-Kuril-Japan-Izu-Mariana-Yap	152.3657	46.1514	225	23	24.54
kisz–14b	Kamchatka-Kuril-Japan-Izu-Mariana-Yap	152.7855	45.8591	225	23	5
kisz–14y	Kamchatka-Kuril-Japan-Izu-Mariana-Yap	151.5172	46.7362	225	23	63.62
kisz–14z	Kamchatka-Kuril-Japan-Izu-Mariana-Yap	151.9426	46.4438	225	23	44.08
kisz–14c	Kamchatka-Kuril-Japan-Izu-Mariana-Yap	153.4468	45.3976	45	57.89	4.602
kisz–15a	Kamchatka-Kuril-Japan-Izu-Mariana-Yap	151.4663	45.5963	233	25	23.73
kisz–15b	Kamchatka-Kuril-Japan-Izu-Mariana-Yap	151.8144	45.2712	233	22	5
kisz–15y	Kamchatka-Kuril-Japan-Izu-Mariana-Yap	150.7619	46.2465	233	25	65.99
kisz–15z	Kamchatka-Kuril-Japan-Izu-Mariana-Yap	151.1151	45.9214	233	25	44.86
kisz–16a	Kamchatka-Kuril-Japan-Izu-Mariana-Yap	150.4572	45.0977	237	25	23.73
kisz–16b	Kamchatka-Kuril-Japan-Izu-Mariana-Yap	150.7694	44.7563	237	22	5
kisz–16y	Kamchatka-Kuril-Japan-Izu-Mariana-Yap	149.8253	45.7804	237	25	65.99
kisz–16z	Kamchatka-Kuril-Japan-Izu-Mariana-Yap	150.1422	45.4390	237	25	44.86
kisz–17a	Kamchatka-Kuril-Japan-Izu-Mariana-Yap	149.3989	44.6084	237	25	23.73
kisz–17b	Kamchatka-Kuril-Japan-Izu-Mariana-Yap	149.7085	44.2670	237	22	5
kisz–17y	Kamchatka-Kuril-Japan-Izu-Mariana-Yap	148.7723	45.2912	237	25	65.99
kisz–17z	Kamchatka-Kuril-Japan-Izu-Mariana-Yap	149.0865	44.9498	237	25	44.86
kisz–18a	Kamchatka-Kuril-Japan-Izu-Mariana-Yap	148.3454	44.0982	235	25	23.73
kisz–18b	Kamchatka-Kuril-Japan-Izu-Mariana-Yap	148.6687	43.7647	235	22	5
kisz–18y	Kamchatka-Kuril-Japan-Izu-Mariana-Yap	147.6915	44.7651	235	25	65.99
kisz–18z	Kamchatka-Kuril-Japan-Izu-Mariana-Yap	148.0194	44.4316	235	25	44.86
kisz–19a	Kamchatka-Kuril-Japan-Izu-Mariana-Yap	147.3262	43.5619	233	25	23.73
kisz–19b	Kamchatka-Kuril-Japan-Izu-Mariana-Yap	147.6625	43.2368	233	22	5
kisz–19y	Kamchatka-Kuril-Japan-Izu-Mariana-Yap	146.6463	44.2121	233	25	65.99
kisz–19z	Kamchatka-Kuril-Japan-Izu-Mariana-Yap	146.9872	43.8870	233	25	44.86
kisz–20a	Kamchatka-Kuril-Japan-Izu-Mariana-Yap	146.3513	43.0633	237	25	23.73
kisz–20b	Kamchatka-Kuril-Japan-Izu-Mariana-Yap	146.6531	42.7219	237	22	5
kisz–20y	Kamchatka-Kuril-Japan-Izu-Mariana-Yap	145.7410	43.7461	237	25	65.99
kisz–20z	Kamchatka-Kuril-Japan-Izu-Mariana-Yap	146.0470	43.4047	237	25	44.86
kisz–21a	Kamchatka-Kuril-Japan-Izu-Mariana-Yap	145.3331	42.5948	239	25	23.73
kisz–21b	Kamchatka-Kuril-Japan-Izu-Mariana-Yap	145.6163	42.2459	239	22	5
kisz–21y	Kamchatka-Kuril-Japan-Izu-Mariana-Yap	144.7603	43.2927	239	25	65.99
kisz–21z	Kamchatka-Kuril-Japan-Izu-Mariana-Yap	145.0475	42.9438	239	25	44.86
kisz–22a	Kamchatka-Kuril-Japan-Izu-Mariana-Yap	144.3041	42.1631	242	25	23.73
kisz–22b	Kamchatka-Kuril-Japan-Izu-Mariana-Yap	144.5605	41.8037	242	22	5
kisz–22y	Kamchatka-Kuril-Japan-Izu-Mariana-Yap	143.7854	42.8819	242	25	65.99
kisz–22z	Kamchatka-Kuril-Japan-Izu-Mariana-Yap	144.0455	42.5225	242	25	44.86
kisz–23a	Kamchatka-Kuril-Japan-Izu-Mariana-Yap	143.2863	41.3335	202	21	21.28
kisz–23b	Kamchatka-Kuril-Japan-Izu-Mariana-Yap	143.8028	41.1764	202	19	5
kisz–23v	Kamchatka-Kuril-Japan-Izu-Mariana-Yap	140.6816	42.1189	202	21	110.9
kisz–23w	Kamchatka-Kuril-Japan-Izu-Mariana-Yap	141.2050	41.9618	202	21	92.95
kisz–23x	Kamchatka-Kuril-Japan-Izu-Mariana-Yap	141.7273	41.8047	202	21	75.04
kisz–23y	Kamchatka-Kuril-Japan-Izu-Mariana-Yap	142.2482	41.6476	202	21	57.12
kisz–23z	Kamchatka-Kuril-Japan-Izu-Mariana-Yap	142.7679	41.4905	202	21	39.2
kisz–24a	Kamchatka-Kuril-Japan-Izu-Mariana-Yap	142.9795	40.3490	185	21	21.28
kisz–24b	Kamchatka-Kuril-Japan-Izu-Mariana-Yap	143.5273	40.3125	185	19	5
kisz–24x	Kamchatka-Kuril-Japan-Izu-Mariana-Yap	141.3339	40.4587	185	21	75.04
kisz–24y	Kamchatka-Kuril-Japan-Izu-Mariana-Yap	141.8827	40.4221	185	21	57.12
kisz–24z	Kamchatka-Kuril-Japan-Izu-Mariana-Yap	142.4312	40.3856	185	21	39.2
kisz–25a	Kamchatka-Kuril-Japan-Izu-Mariana-Yap	142.8839	39.4541	185	21	21.28
kisz–25b	Kamchatka-Kuril-Japan-Izu-Mariana-Yap	143.4246	39.4176	185	19	5
kisz–25y	Kamchatka-Kuril-Japan-Izu-Mariana-Yap	141.8012	39.5272	185	21	57.12

Continued on next page

Table B.4 – continued

Segment	Description	Longitude(°E)	Latitude(°N)	Strike(°)	Dip(°)	Depth (km)
kisz–25z	Kamchatka-Kuril-Japan-Izu-Mariana-Yap	142.3426	39.4907	185	21	39.2
kisz–26a	Kamchatka-Kuril-Japan-Izu-Mariana-Yap	142.7622	38.5837	188	21	21.28
kisz–26b	Kamchatka-Kuril-Japan-Izu-Mariana-Yap	143.2930	38.5254	188	19	5
kisz–26x	Kamchatka-Kuril-Japan-Izu-Mariana-Yap	141.1667	38.7588	188	21	75.04
kisz–26y	Kamchatka-Kuril-Japan-Izu-Mariana-Yap	141.6990	38.7004	188	21	57.12
kisz–26z	Kamchatka-Kuril-Japan-Izu-Mariana-Yap	142.2308	38.6421	188	21	39.2
kisz–27a	Kamchatka-Kuril-Japan-Izu-Mariana-Yap	142.5320	37.7830	198	21	21.28
kisz–27b	Kamchatka-Kuril-Japan-Izu-Mariana-Yap	143.0357	37.6534	198	19	5
kisz–27x	Kamchatka-Kuril-Japan-Izu-Mariana-Yap	141.0142	38.1717	198	21	75.04
kisz–27y	Kamchatka-Kuril-Japan-Izu-Mariana-Yap	141.5210	38.0421	198	21	57.12
kisz–27z	Kamchatka-Kuril-Japan-Izu-Mariana-Yap	142.0269	37.9126	198	21	39.2
kisz–28a	Kamchatka-Kuril-Japan-Izu-Mariana-Yap	142.1315	37.0265	208	21	21.28
kisz–28b	Kamchatka-Kuril-Japan-Izu-Mariana-Yap	142.5941	36.8297	208	19	5
kisz–28x	Kamchatka-Kuril-Japan-Izu-Mariana-Yap	140.7348	37.6171	208	21	75.04
kisz–28y	Kamchatka-Kuril-Japan-Izu-Mariana-Yap	141.2016	37.4202	208	21	57.12
kisz–28z	Kamchatka-Kuril-Japan-Izu-Mariana-Yap	141.6671	37.2234	208	21	39.2
kisz–29a	Kamchatka-Kuril-Japan-Izu-Mariana-Yap	141.5970	36.2640	211	21	21.28
kisz–29b	Kamchatka-Kuril-Japan-Izu-Mariana-Yap	142.0416	36.0481	211	19	5
kisz–29y	Kamchatka-Kuril-Japan-Izu-Mariana-Yap	140.7029	36.6960	211	21	57.12
kisz–29z	Kamchatka-Kuril-Japan-Izu-Mariana-Yap	141.1506	36.4800	211	21	39.2
kisz–30a	Kamchatka-Kuril-Japan-Izu-Mariana-Yap	141.0553	35.4332	205	21	21.28
kisz–30b	Kamchatka-Kuril-Japan-Izu-Mariana-Yap	141.5207	35.2560	205	19	5
kisz–30y	Kamchatka-Kuril-Japan-Izu-Mariana-Yap	140.1204	35.7876	205	21	57.12
kisz–30z	Kamchatka-Kuril-Japan-Izu-Mariana-Yap	140.5883	35.6104	205	21	39.2
kisz–31a	Kamchatka-Kuril-Japan-Izu-Mariana-Yap	140.6956	34.4789	190	22	22.1
kisz–31b	Kamchatka-Kuril-Japan-Izu-Mariana-Yap	141.1927	34.4066	190	20	5
kisz–31v	Kamchatka-Kuril-Japan-Izu-Mariana-Yap	138.2025	34.8405	190	22	115.8
kisz–31w	Kamchatka-Kuril-Japan-Izu-Mariana-Yap	138.7021	34.7682	190	22	97.02
kisz–31x	Kamchatka-Kuril-Japan-Izu-Mariana-Yap	139.2012	34.6958	190	22	78.29
kisz–31y	Kamchatka-Kuril-Japan-Izu-Mariana-Yap	139.6997	34.6235	190	22	59.56
kisz–31z	Kamchatka-Kuril-Japan-Izu-Mariana-Yap	140.1979	34.5512	190	22	40.83
kisz–32a	Kamchatka-Kuril-Japan-Izu-Mariana-Yap	141.0551	33.0921	180	32	23.48
kisz–32b	Kamchatka-Kuril-Japan-Izu-Mariana-Yap	141.5098	33.0921	180	21.69	5
kisz–33a	Kamchatka-Kuril-Japan-Izu-Mariana-Yap	141.0924	32.1047	173.8	27.65	20.67
kisz–33b	Kamchatka-Kuril-Japan-Izu-Mariana-Yap	141.5596	32.1473	173.8	18.27	5
kisz–34a	Kamchatka-Kuril-Japan-Izu-Mariana-Yap	141.1869	31.1851	172.1	25	18.26
kisz–34b	Kamchatka-Kuril-Japan-Izu-Mariana-Yap	141.6585	31.2408	172.1	15.38	5
kisz–35a	Kamchatka-Kuril-Japan-Izu-Mariana-Yap	141.4154	30.1707	163	25	17.12
kisz–35b	Kamchatka-Kuril-Japan-Izu-Mariana-Yap	141.8662	30.2899	163	14.03	5
kisz–36a	Kamchatka-Kuril-Japan-Izu-Mariana-Yap	141.6261	29.2740	161.7	25.73	18.71
kisz–36b	Kamchatka-Kuril-Japan-Izu-Mariana-Yap	142.0670	29.4012	161.7	15.91	5
kisz–37a	Kamchatka-Kuril-Japan-Izu-Mariana-Yap	142.0120	28.3322	154.7	20	14.54
kisz–37b	Kamchatka-Kuril-Japan-Izu-Mariana-Yap	142.4463	28.5124	154.7	11	5
kisz–38a	Kamchatka-Kuril-Japan-Izu-Mariana-Yap	142.2254	27.6946	170.3	20	14.54
kisz–38b	Kamchatka-Kuril-Japan-Izu-Mariana-Yap	142.6955	27.7659	170.3	11	5
kisz–39a	Kamchatka-Kuril-Japan-Izu-Mariana-Yap	142.3085	26.9127	177.2	24.23	17.42
kisz–39b	Kamchatka-Kuril-Japan-Izu-Mariana-Yap	142.7674	26.9325	177.2	14.38	5
kisz–40a	Kamchatka-Kuril-Japan-Izu-Mariana-Yap	142.2673	26.1923	189.4	26.49	22.26
kisz–40b	Kamchatka-Kuril-Japan-Izu-Mariana-Yap	142.7090	26.1264	189.4	20.2	5
kisz–41a	Kamchatka-Kuril-Japan-Izu-Mariana-Yap	142.1595	25.0729	173.7	22.07	19.08
kisz–41b	Kamchatka-Kuril-Japan-Izu-Mariana-Yap	142.6165	25.1184	173.7	16.36	5
kisz–42a	Kamchatka-Kuril-Japan-Izu-Mariana-Yap	142.7641	23.8947	143.5	21.54	18.4
kisz–42b	Kamchatka-Kuril-Japan-Izu-Mariana-Yap	143.1321	24.1432	143.5	15.54	5
kisz–43a	Kamchatka-Kuril-Japan-Izu-Mariana-Yap	143.5281	23.0423	129.2	23.02	18.77
kisz–43b	Kamchatka-Kuril-Japan-Izu-Mariana-Yap	143.8128	23.3626	129.2	15.99	5

Continued on next page

Table B.4 – continued

Segment	Description	Longitude(°E)	Latitude(°N)	Strike(°)	Dip(°)	Depth (km)
kisz–44a	Kamchatka-Kuril-Japan-Izu-Mariana-Yap	144.2230	22.5240	134.6	28.24	18.56
kisz–44b	Kamchatka-Kuril-Japan-Izu-Mariana-Yap	144.5246	22.8056	134.6	15.74	5
kisz–45a	Kamchatka-Kuril-Japan-Izu-Mariana-Yap	145.0895	21.8866	125.8	36.73	22.79
kisz–45b	Kamchatka-Kuril-Japan-Izu-Mariana-Yap	145.3171	22.1785	125.8	20.84	5
kisz–46a	Kamchatka-Kuril-Japan-Izu-Mariana-Yap	145.6972	21.3783	135.9	30.75	20.63
kisz–46b	Kamchatka-Kuril-Japan-Izu-Mariana-Yap	145.9954	21.6469	135.9	18.22	5
kisz–47a	Kamchatka-Kuril-Japan-Izu-Mariana-Yap	146.0406	20.9341	160.1	29.87	19.62
kisz–47b	Kamchatka-Kuril-Japan-Izu-Mariana-Yap	146.4330	21.0669	160.1	17	5
kisz–48a	Kamchatka-Kuril-Japan-Izu-Mariana-Yap	146.3836	20.0690	158	32.75	19.68
kisz–48b	Kamchatka-Kuril-Japan-Izu-Mariana-Yap	146.7567	20.2108	158	17.07	5
kisz–49a	Kamchatka-Kuril-Japan-Izu-Mariana-Yap	146.6689	19.3123	164.5	25.07	21.41
kisz–49b	Kamchatka-Kuril-Japan-Izu-Mariana-Yap	147.0846	19.4212	164.5	19.16	5
kisz–50a	Kamchatka-Kuril-Japan-Izu-Mariana-Yap	146.9297	18.5663	172.1	22	22.1
kisz–50b	Kamchatka-Kuril-Japan-Izu-Mariana-Yap	147.3650	18.6238	172.1	20	5
kisz–51a	Kamchatka-Kuril-Japan-Izu-Mariana-Yap	146.9495	17.7148	175.1	22.06	22.04
kisz–51b	Kamchatka-Kuril-Japan-Izu-Mariana-Yap	147.3850	17.7503	175.1	19.93	5
kisz–52a	Kamchatka-Kuril-Japan-Izu-Mariana-Yap	146.9447	16.8869	180	25.51	18.61
kisz–52b	Kamchatka-Kuril-Japan-Izu-Mariana-Yap	147.3683	16.8869	180	15.79	5
kisz–53a	Kamchatka-Kuril-Japan-Izu-Mariana-Yap	146.8626	16.0669	185.2	27.39	18.41
kisz–53b	Kamchatka-Kuril-Japan-Izu-Mariana-Yap	147.2758	16.0309	185.2	15.56	5
kisz–54a	Kamchatka-Kuril-Japan-Izu-Mariana-Yap	146.7068	15.3883	199.1	28.12	20.91
kisz–54b	Kamchatka-Kuril-Japan-Izu-Mariana-Yap	147.0949	15.2590	199.1	18.56	5
kisz–55a	Kamchatka-Kuril-Japan-Izu-Mariana-Yap	146.4717	14.6025	204.3	29.6	26.27
kisz–55b	Kamchatka-Kuril-Japan-Izu-Mariana-Yap	146.8391	14.4415	204.3	25.18	5
kisz–56a	Kamchatka-Kuril-Japan-Izu-Mariana-Yap	146.1678	13.9485	217.4	32.04	26.79
kisz–56b	Kamchatka-Kuril-Japan-Izu-Mariana-Yap	146.4789	13.7170	217.4	25.84	5
kisz–57a	Kamchatka-Kuril-Japan-Izu-Mariana-Yap	145.6515	13.5576	235.8	37	24.54
kisz–57b	Kamchatka-Kuril-Japan-Izu-Mariana-Yap	145.8586	13.2609	235.8	23	5
kisz–58a	Kamchatka-Kuril-Japan-Izu-Mariana-Yap	144.9648	12.9990	237.8	37.72	24.54
kisz–58b	Kamchatka-Kuril-Japan-Izu-Mariana-Yap	145.1589	12.6984	237.8	23	5
kisz–59a	Kamchatka-Kuril-Japan-Izu-Mariana-Yap	144.1799	12.6914	242.9	34.33	22.31
kisz–59b	Kamchatka-Kuril-Japan-Izu-Mariana-Yap	144.3531	12.3613	242.9	20.25	5
kisz–60a	Kamchatka-Kuril-Japan-Izu-Mariana-Yap	143.3687	12.3280	244.9	30.9	20.62
kisz–60b	Kamchatka-Kuril-Japan-Izu-Mariana-Yap	143.5355	11.9788	244.9	18.2	5
kisz–61a	Kamchatka-Kuril-Japan-Izu-Mariana-Yap	142.7051	12.1507	261.8	35.41	25.51
kisz–61b	Kamchatka-Kuril-Japan-Izu-Mariana-Yap	142.7582	11.7883	261.8	24.22	5
kisz–62a	Kamchatka-Kuril-Japan-Izu-Mariana-Yap	141.6301	11.8447	245.7	39.86	34.35
kisz–62b	Kamchatka-Kuril-Japan-Izu-Mariana-Yap	141.7750	11.5305	245.7	35.94	5
kisz–63a	Kamchatka-Kuril-Japan-Izu-Mariana-Yap	140.8923	11.5740	256.2	42	38.46
kisz–63b	Kamchatka-Kuril-Japan-Izu-Mariana-Yap	140.9735	11.2498	256.2	42	5
kisz–64a	Kamchatka-Kuril-Japan-Izu-Mariana-Yap	140.1387	11.6028	269.6	42.48	38.77
kisz–64b	Kamchatka-Kuril-Japan-Izu-Mariana-Yap	140.1410	11.2716	269.6	42.48	5
kisz–65a	Kamchatka-Kuril-Japan-Izu-Mariana-Yap	139.4595	11.5883	288.7	44.16	39.83
kisz–65b	Kamchatka-Kuril-Japan-Izu-Mariana-Yap	139.3541	11.2831	288.7	44.16	5
kisz–66a	Kamchatka-Kuril-Japan-Izu-Mariana-Yap	138.1823	11.2648	193.1	45	40.36
kisz–66b	Kamchatka-Kuril-Japan-Izu-Mariana-Yap	138.4977	11.1929	193.1	45	5
kisz–67a	Kamchatka-Kuril-Japan-Izu-Mariana-Yap	137.9923	10.3398	189.8	45	40.36
kisz–67b	Kamchatka-Kuril-Japan-Izu-Mariana-Yap	138.3104	10.2856	189.8	45	5
kisz–68a	Kamchatka-Kuril-Japan-Izu-Mariana-Yap	137.7607	9.6136	201.7	45	40.36
kisz–68b	Kamchatka-Kuril-Japan-Izu-Mariana-Yap	138.0599	9.4963	201.7	45	5
kisz–69a	Kamchatka-Kuril-Japan-Izu-Mariana-Yap	137.4537	8.8996	213.5	45	40.36
kisz–69b	Kamchatka-Kuril-Japan-Izu-Mariana-Yap	137.7215	8.7241	213.5	45	5
kisz–70a	Kamchatka-Kuril-Japan-Izu-Mariana-Yap	137.0191	8.2872	226.5	45	40.36
kisz–70b	Kamchatka-Kuril-Japan-Izu-Mariana-Yap	137.2400	8.0569	226.5	45	5
kisz–71a	Kamchatka-Kuril-Japan-Izu-Mariana-Yap	136.3863	7.9078	263.9	45	40.36

Continued on next page

Table B.4 – continued

Segment	Description	Longitude(°E)	Latitude(°N)	Strike(°)	Dip(°)	Depth (km)
kisz–71b	Kamchatka-Kuril-Japan-Izu-Mariana-Yap	136.4202	7.5920	263.9	45	5
kisz–72a	Kamchatka-Kuril-Japan-Izu-Mariana-Yap	135.6310	7.9130	276.9	45	40.36
kisz–72b	Kamchatka-Kuril-Japan-Izu-Mariana-Yap	135.5926	7.5977	276.9	45	5
kisz–73a	Kamchatka-Kuril-Japan-Izu-Mariana-Yap	134.3296	7.4541	224	45	40.36
kisz–73b	Kamchatka-Kuril-Japan-Izu-Mariana-Yap	134.5600	7.2335	224	45	5
kisz–74a	Kamchatka-Kuril-Japan-Izu-Mariana-Yap	133.7125	6.8621	228.1	45	40.36
kisz–74b	Kamchatka-Kuril-Japan-Izu-Mariana-Yap	133.9263	6.6258	228.1	45	5
kisz–75a	Kamchatka-Kuril-Japan-Izu-Mariana-Yap	133.0224	6.1221	217.7	45	40.36
kisz–75b	Kamchatka-Kuril-Japan-Izu-Mariana-Yap	133.2751	5.9280	217.7	45	5

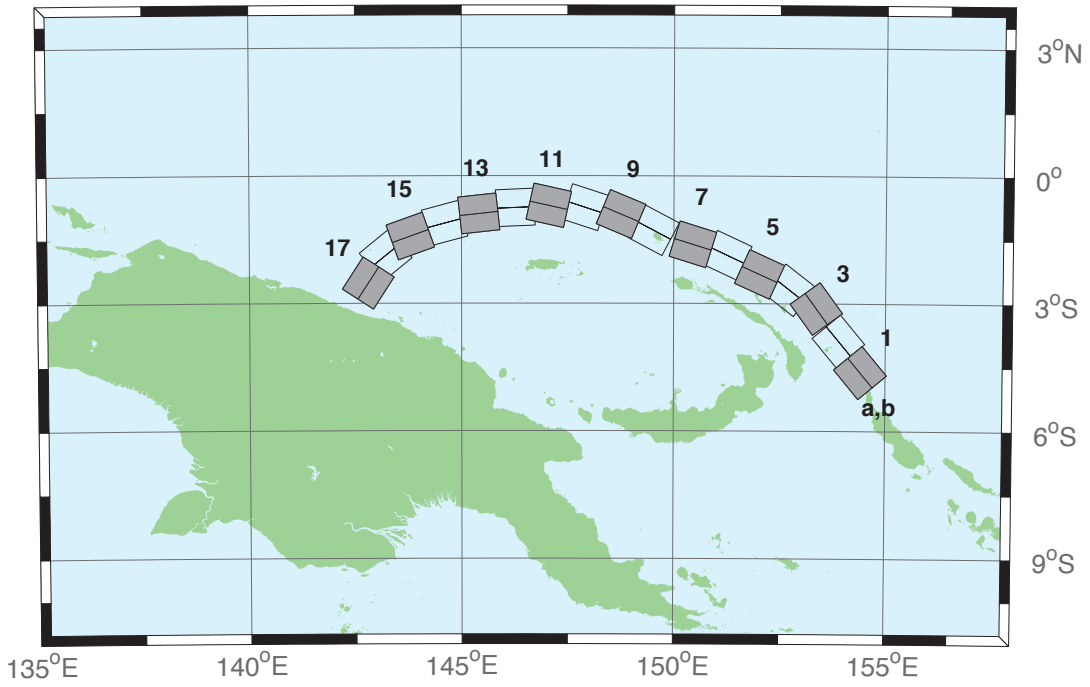

Figure B.5: Manus–Oceanic Convergent Boundary Subduction Zone unit sources.

Table B.5: Earthquake parameters for Manus–Oceanic Convergent Boundary Subduction Zone unit sources.

Segment	Description	Longitude(°E)	Latitude(°N)	Strike(°)	Dip(°)	Depth (km)
mosz–1a	Manus	154.0737	-4.8960	140.2	15	15.88
mosz–1b	Manus	154.4082	-4.6185	140.2	15	2.94
mosz–2a	Manus	153.5589	-4.1575	140.2	15	15.91
mosz–2b	Manus	153.8931	-3.8800	140.2	15	2.97
mosz–3a	Manus	153.0151	-3.3716	143.9	15	16.64
mosz–3b	Manus	153.3662	-3.1160	143.9	15	3.7
mosz–4a	Manus	152.4667	-3.0241	127.7	15	17.32
mosz–4b	Manus	152.7321	-2.6806	127.7	15	4.38
mosz–5a	Manus	151.8447	-2.7066	114.3	15	17.57
mosz–5b	Manus	152.0235	-2.3112	114.3	15	4.63
mosz–6a	Manus	151.0679	-2.2550	115	15	17.66
mosz–6b	Manus	151.2513	-1.8618	115	15	4.72
mosz–7a	Manus	150.3210	-2.0236	107.2	15	17.73
mosz–7b	Manus	150.4493	-1.6092	107.2	15	4.79
mosz–8a	Manus	149.3226	-1.6666	117.8	15	17.83
mosz–8b	Manus	149.5251	-1.2829	117.8	15	4.89
mosz–9a	Manus	148.5865	-1.3017	112.7	15	17.84
mosz–9b	Manus	148.7540	-0.9015	112.7	15	4.9
mosz–10a	Manus	147.7760	-1.1560	108	15	17.78
mosz–10b	Manus	147.9102	-0.7434	108	15	4.84
mosz–11a	Manus	146.9596	-1.1226	102.5	15	17.54
mosz–11b	Manus	147.0531	-0.6990	102.5	15	4.6
mosz–12a	Manus	146.2858	-1.1820	87.48	15	17.29
mosz–12b	Manus	146.2667	-0.7486	87.48	15	4.35
mosz–13a	Manus	145.4540	-1.3214	83.75	15	17.34
mosz–13b	Manus	145.4068	-0.8901	83.75	15	4.4
mosz–14a	Manus	144.7151	-1.5346	75.09	15	17.21
mosz–14b	Manus	144.6035	-1.1154	75.09	15	4.27
mosz–15a	Manus	143.9394	-1.8278	70.43	15	16.52
mosz–15b	Manus	143.7940	-1.4190	70.43	15	3.58
mosz–16a	Manus	143.4850	-2.2118	50.79	15	15.86
mosz–16b	Manus	143.2106	-1.8756	50.79	15	2.92
mosz–17a	Manus	143.1655	-2.7580	33	15	16.64
mosz–17b	Manus	142.8013	-2.5217	33	15	3.7

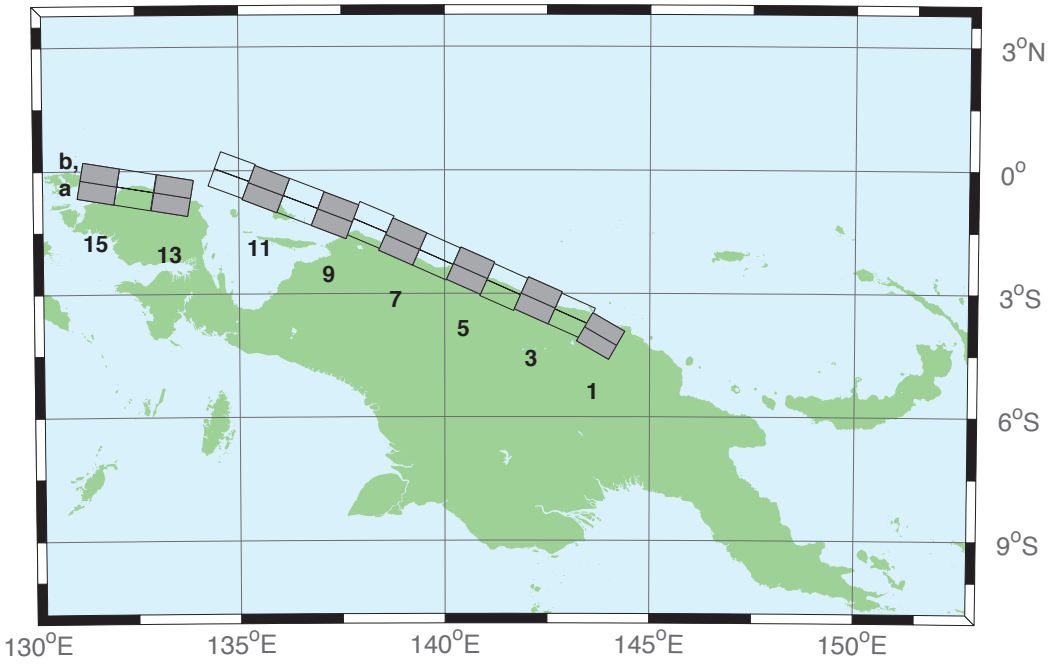

Figure B.6: New Guinea Subduction Zone unit sources.

Table B.6: Earthquake parameters for New Guinea Subduction Zone unit sources.

Segment	Description	Longitude(°E)	Latitude(°N)	Strike(°)	Dip(°)	Depth (km)
ngsz–1a	New Guinea	143.6063	-4.3804	120	29	25.64
ngsz–1b	New Guinea	143.8032	-4.0402	120	29	1.4
ngsz–2a	New Guinea	142.9310	-3.9263	114	27.63	20.1
ngsz–2b	New Guinea	143.0932	-3.5628	114	21.72	1.6
ngsz–3a	New Guinea	142.1076	-3.5632	114	20.06	18.73
ngsz–3b	New Guinea	142.2795	-3.1778	114	15.94	5
ngsz–4a	New Guinea	141.2681	-3.2376	114	21	17.76
ngsz–4b	New Guinea	141.4389	-2.8545	114	14.79	5
ngsz–5a	New Guinea	140.4592	-2.8429	114	21.26	16.14
ngsz–5b	New Guinea	140.6296	-2.4605	114	12.87	5
ngsz–6a	New Guinea	139.6288	-2.4960	114	22.72	15.4
ngsz–6b	New Guinea	139.7974	-2.1175	114	12	5
ngsz–7a	New Guinea	138.8074	-2.1312	114	21.39	15.4
ngsz–7b	New Guinea	138.9776	-1.7491	114	12	5
ngsz–8a	New Guinea	138.0185	-1.7353	113.1	18.79	15.14
ngsz–8b	New Guinea	138.1853	-1.3441	113.1	11.7	5
ngsz–9a	New Guinea	137.1805	-1.5037	111	15.24	13.23
ngsz–9b	New Guinea	137.3358	-1.0991	111	9.47	5
ngsz–10a	New Guinea	136.3418	-1.1774	111	13.51	11.09
ngsz–10b	New Guinea	136.4983	-0.7697	111	7	5
ngsz–11a	New Guinea	135.4984	-0.8641	111	11.38	12.49
ngsz–11b	New Guinea	135.6562	-0.4530	111	8.62	5
ngsz–12a	New Guinea	134.6759	-0.5216	110.5	10	13.68
ngsz–12b	New Guinea	134.8307	-0.1072	110.5	10	5
ngsz–13a	New Guinea	133.3065	-1.0298	99.5	10	13.68
ngsz–13b	New Guinea	133.3795	-0.5935	99.5	10	5
ngsz–14a	New Guinea	132.4048	-0.8816	99.5	10	13.68
ngsz–14b	New Guinea	132.4778	-0.4453	99.5	10	5
ngsz–15a	New Guinea	131.5141	-0.7353	99.5	10	13.68
ngsz–15b	New Guinea	131.5871	-0.2990	99.5	10	5

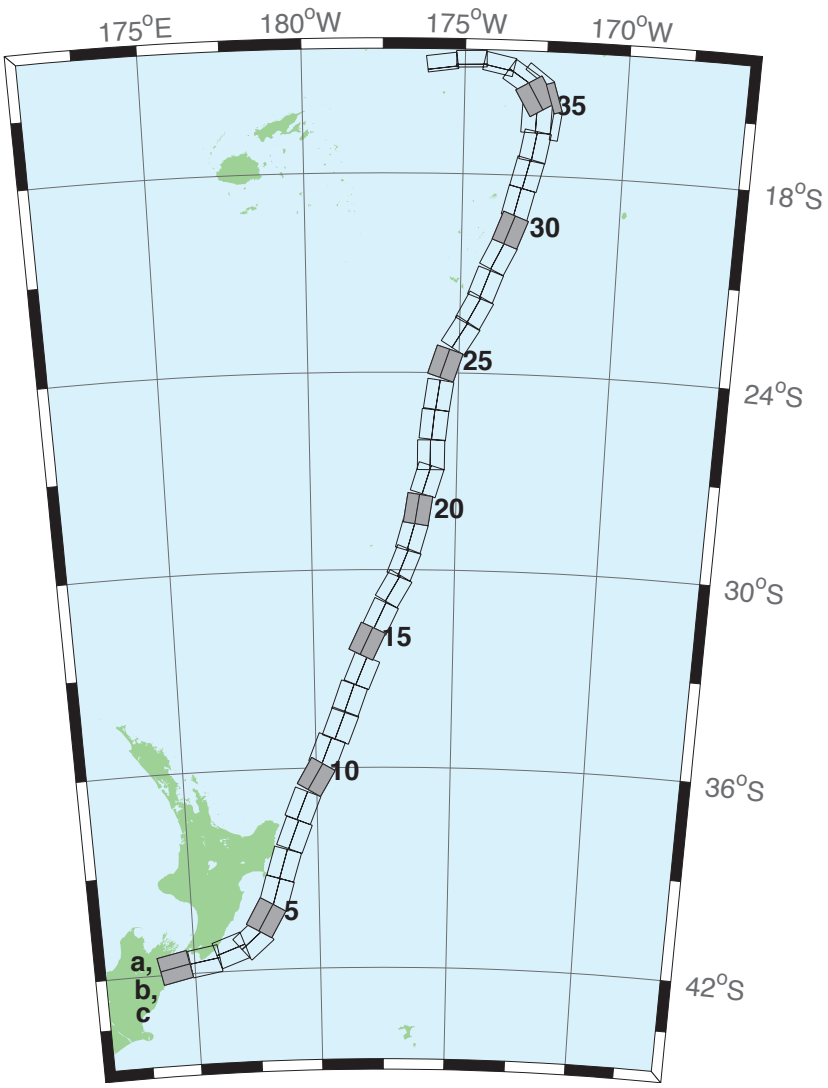

Figure B.7: New Zealand–Kermadec–Tonga Subduction Zone unit sources.

Table B.7: Earthquake parameters for New Zealand–Kermadec–Tonga Subduction Zone unit sources.

Segment	Description	Longitude(°E)	Latitude(°N)	Strike(°)	Dip(°)	Depth (km)
ntsz–1a	New Zealand–Tonga	174.0985	-41.3951	258.6	24	25.34
ntsz–1b	New Zealand–Tonga	174.2076	-41.7973	258.6	24	5
ntsz–2a	New Zealand–Tonga	175.3289	-41.2592	260.6	29.38	23.17
ntsz–2b	New Zealand–Tonga	175.4142	-41.6454	260.6	21.31	5
ntsz–3a	New Zealand–Tonga	176.2855	-40.9950	250.7	29.54	21.74
ntsz–3b	New Zealand–Tonga	176.4580	-41.3637	250.7	19.56	5
ntsz–4a	New Zealand–Tonga	177.0023	-40.7679	229.4	24.43	18.87
ntsz–4b	New Zealand–Tonga	177.3552	-41.0785	229.4	16.1	5
ntsz–5a	New Zealand–Tonga	177.4114	-40.2396	210	18.8	19.29
ntsz–5b	New Zealand–Tonga	177.8951	-40.4525	210	16.61	5
ntsz–6a	New Zealand–Tonga	177.8036	-39.6085	196.7	18.17	15.8
ntsz–6b	New Zealand–Tonga	178.3352	-39.7310	196.7	12.48	5
ntsz–7a	New Zealand–Tonga	178.1676	-38.7480	197	28.1	17.85
ntsz–7b	New Zealand–Tonga	178.6541	-38.8640	197	14.89	5
ntsz–8a	New Zealand–Tonga	178.6263	-37.8501	201.4	31.47	18.78
ntsz–8b	New Zealand–Tonga	179.0788	-37.9899	201.4	16	5
ntsz–9a	New Zealand–Tonga	178.9833	-36.9770	202.2	29.58	20.02
ntsz–9b	New Zealand–Tonga	179.4369	-37.1245	202.2	17.48	5
ntsz–10a	New Zealand–Tonga	179.5534	-36.0655	210.6	32.1	20.72
ntsz–10b	New Zealand–Tonga	179.9595	-36.2593	210.6	18.32	5
ntsz–11a	New Zealand–Tonga	179.9267	-35.3538	201.7	25	16.09
ntsz–11b	New Zealand–Tonga	180.3915	-35.5040	201.7	12.81	5
ntsz–12a	New Zealand–Tonga	180.4433	-34.5759	201.2	25	15.46
ntsz–12b	New Zealand–Tonga	180.9051	-34.7230	201.2	12.08	5
ntsz–13a	New Zealand–Tonga	180.7990	-33.7707	199.8	25.87	19.06
ntsz–13b	New Zealand–Tonga	181.2573	-33.9073	199.8	16.33	5
ntsz–14a	New Zealand–Tonga	181.2828	-32.9288	202.4	31.28	22.73
ntsz–14b	New Zealand–Tonga	181.7063	-33.0751	202.4	20.77	5
ntsz–15a	New Zealand–Tonga	181.4918	-32.0035	205.4	32.33	22.64
ntsz–15b	New Zealand–Tonga	181.8967	-32.1665	205.4	20.66	5
ntsz–16a	New Zealand–Tonga	181.9781	-31.2535	205.5	34.29	23.59
ntsz–16b	New Zealand–Tonga	182.3706	-31.4131	205.5	21.83	5
ntsz–17a	New Zealand–Tonga	182.4819	-30.3859	210.3	37.6	25.58
ntsz–17b	New Zealand–Tonga	182.8387	-30.5655	210.3	24.3	5
ntsz–18a	New Zealand–Tonga	182.8176	-29.6545	201.6	37.65	26.13
ntsz–18b	New Zealand–Tonga	183.1985	-29.7856	201.6	25	5
ntsz–19a	New Zealand–Tonga	183.0622	-28.8739	195.7	34.41	26.13
ntsz–19b	New Zealand–Tonga	183.4700	-28.9742	195.7	25	5
ntsz–20a	New Zealand–Tonga	183.2724	-28.0967	188.8	38	26.13
ntsz–20b	New Zealand–Tonga	183.6691	-28.1508	188.8	25	5
ntsz–21a	New Zealand–Tonga	183.5747	-27.1402	197.1	32.29	24.83
ntsz–21b	New Zealand–Tonga	183.9829	-27.2518	197.1	23.37	5
ntsz–22a	New Zealand–Tonga	183.6608	-26.4975	180	29.56	18.63
ntsz–22b	New Zealand–Tonga	184.0974	-26.4975	180	15.82	5
ntsz–23a	New Zealand–Tonga	183.7599	-25.5371	185.8	32.42	20.56
ntsz–23b	New Zealand–Tonga	184.1781	-25.5752	185.8	18.13	5
ntsz–24a	New Zealand–Tonga	183.9139	-24.6201	188.2	33.31	23.73
ntsz–24b	New Zealand–Tonga	184.3228	-24.6734	188.2	22	5
ntsz–25a	New Zealand–Tonga	184.1266	-23.5922	198.5	29.34	19.64
ntsz–25b	New Zealand–Tonga	184.5322	-23.7163	198.5	17.03	5
ntsz–26a	New Zealand–Tonga	184.6613	-22.6460	211.7	30.26	19.43
ntsz–26b	New Zealand–Tonga	185.0196	-22.8497	211.7	16.78	5
ntsz–27a	New Zealand–Tonga	185.0879	-21.9139	207.9	31.73	20.67

Continued on next page

Table B.7 – continued

Segment	Description	Longitude(°E)	Latitude(°N)	Strike(°)	Dip(°)	Depth (km)
ntsz–27b	New Zealand–Tonga	185.4522	-22.0928	207.9	18.27	5
ntsz–28a	New Zealand–Tonga	185.4037	-21.1758	200.5	32.44	21.76
ntsz–28b	New Zealand–Tonga	185.7849	-21.3084	200.5	19.58	5
ntsz–29a	New Zealand–Tonga	185.8087	-20.2629	206.4	32.47	20.4
ntsz–29b	New Zealand–Tonga	186.1710	-20.4312	206.4	17.94	5
ntsz–30a	New Zealand–Tonga	186.1499	-19.5087	200.9	32.98	22.46
ntsz–30b	New Zealand–Tonga	186.5236	-19.6432	200.9	20.44	5
ntsz–31a	New Zealand–Tonga	186.3538	-18.7332	193.9	34.41	21.19
ntsz–31b	New Zealand–Tonga	186.7339	-18.8221	193.9	18.89	5
ntsz–32a	New Zealand–Tonga	186.5949	-17.8587	194.1	30	19.12
ntsz–32b	New Zealand–Tonga	186.9914	-17.9536	194.1	16.4	5
ntsz–33a	New Zealand–Tonga	186.8172	-17.0581	190	33.15	23.34
ntsz–33b	New Zealand–Tonga	187.2047	-17.1237	190	21.52	5
ntsz–34a	New Zealand–Tonga	186.7814	-16.2598	182.1	15	13.41
ntsz–34b	New Zealand–Tonga	187.2330	-16.2759	182.1	9.68	5
ntsz–34c	New Zealand–Tonga	187.9697	-16.4956	7.62	57.06	6.571
ntsz–35a	New Zealand–Tonga	186.8000	-15.8563	149.8	15	12.17
ntsz–35b	New Zealand–Tonga	187.1896	-15.6384	149.8	8.24	5
ntsz–35c	New Zealand–Tonga	187.8776	-15.6325	342.4	57.06	6.571
ntsz–36a	New Zealand–Tonga	186.5406	-15.3862	123.9	40.44	36.72
ntsz–36b	New Zealand–Tonga	186.7381	-15.1025	123.9	39.38	5
ntsz–36c	New Zealand–Tonga	187.3791	-14.9234	307	57.06	6.571
ntsz–37a	New Zealand–Tonga	185.9883	-14.9861	102	68.94	30.99
ntsz–37b	New Zealand–Tonga	186.0229	-14.8282	102	31.32	5
ntsz–38a	New Zealand–Tonga	185.2067	-14.8259	88.4	80	26.13
ntsz–38b	New Zealand–Tonga	185.2044	-14.7479	88.4	25	5
ntsz–39a	New Zealand–Tonga	184.3412	-14.9409	82.55	80	26.13
ntsz–39b	New Zealand–Tonga	184.3307	-14.8636	82.55	25	5

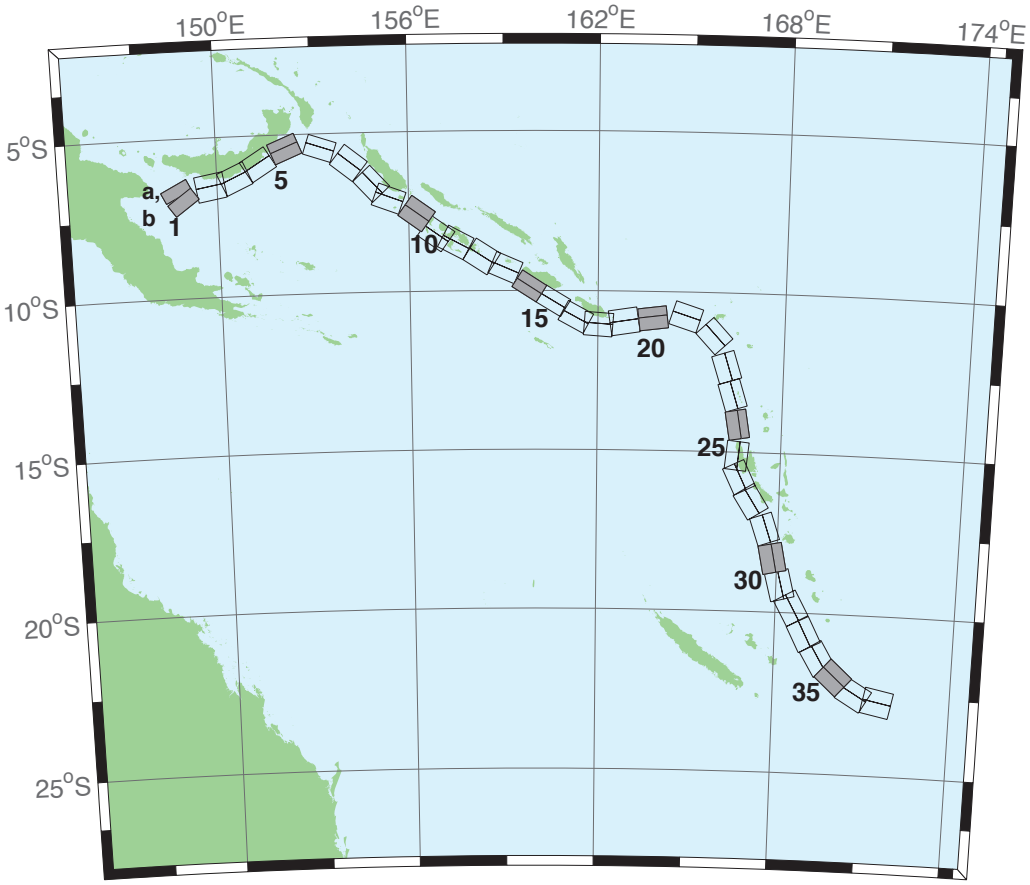

Figure B.8: New Britain–Solomons–Vanuatu Zone unit sources.

Table B.8: Earthquake parameters for New Britain–Solomons–Vanuatu Subduction Zone unit sources.

Segment	Description	Longitude(°E)	Latitude(°N)	Strike(°)	Dip(°)	Depth (km)
nvsz–1a	New Britain–Vanuatu	148.6217	-6.4616	243.2	32.34	15.69
nvsz–1b	New Britain–Vanuatu	148.7943	-6.8002	234.2	12.34	5
nvsz–2a	New Britain–Vanuatu	149.7218	-6.1459	260.1	35.1	16.36
nvsz–2b	New Britain–Vanuatu	149.7856	-6.5079	260.1	13.13	5
nvsz–3a	New Britain–Vanuatu	150.4075	-5.9659	245.7	42.35	18.59
nvsz–3b	New Britain–Vanuatu	150.5450	-6.2684	245.7	15.77	5
nvsz–4a	New Britain–Vanuatu	151.1095	-5.5820	238.2	42.41	23.63
nvsz–4b	New Britain–Vanuatu	151.2851	-5.8639	238.2	21.88	5
nvsz–5a	New Britain–Vanuatu	152.0205	-5.1305	247.7	49.22	32.39
nvsz–5b	New Britain–Vanuatu	152.1322	-5.4020	247.7	33.22	5
nvsz–6a	New Britain–Vanuatu	153.3450	-5.1558	288.6	53.53	33.59
nvsz–6b	New Britain–Vanuatu	153.2595	-5.4089	288.6	34.87	5
nvsz–7a	New Britain–Vanuatu	154.3814	-5.6308	308.3	39.72	19.18
nvsz–7b	New Britain–Vanuatu	154.1658	-5.9017	308.3	16.48	5
nvsz–8a	New Britain–Vanuatu	155.1097	-6.3511	317.2	45.33	22.92
nvsz–8b	New Britain–Vanuatu	154.8764	-6.5656	317.2	21	5
nvsz–9a	New Britain–Vanuatu	155.5027	-6.7430	290.5	48.75	22.92
nvsz–9b	New Britain–Vanuatu	155.3981	-7.0204	290.5	21	5
nvsz–10a	New Britain–Vanuatu	156.4742	-7.2515	305.9	36.88	27.62
nvsz–10b	New Britain–Vanuatu	156.2619	-7.5427	305.9	26.9	5
nvsz–11a	New Britain–Vanuatu	157.0830	-7.8830	305.4	32.97	29.72
nvsz–11b	New Britain–Vanuatu	156.8627	-8.1903	305.4	29.63	5
nvsz–12a	New Britain–Vanuatu	157.6537	-8.1483	297.9	37.53	28.57
nvsz–12b	New Britain–Vanuatu	157.4850	-8.4630	297.9	28.13	5
nvsz–13a	New Britain–Vanuatu	158.5089	-8.5953	302.7	33.62	23.02
nvsz–13b	New Britain–Vanuatu	158.3042	-8.9099	302.7	21.12	5
nvsz–14a	New Britain–Vanuatu	159.1872	-8.9516	293.3	38.44	34.06
nvsz–14b	New Britain–Vanuatu	159.0461	-9.2747	293.3	35.54	5
nvsz–15a	New Britain–Vanuatu	159.9736	-9.5993	302.8	46.69	41.38
nvsz–15b	New Britain–Vanuatu	159.8044	-9.8584	302.8	46.69	5
nvsz–16a	New Britain–Vanuatu	160.7343	-10.0574	301	46.05	41
nvsz–16b	New Britain–Vanuatu	160.5712	-10.3246	301	46.05	5
nvsz–17a	New Britain–Vanuatu	161.4562	-10.5241	298.4	40.12	37.22
nvsz–17b	New Britain–Vanuatu	161.2900	-10.8263	298.4	40.12	5
nvsz–18a	New Britain–Vanuatu	162.0467	-10.6823	274.1	40.33	29.03
nvsz–18b	New Britain–Vanuatu	162.0219	-11.0238	274.1	28.72	5
nvsz–19a	New Britain–Vanuatu	162.7818	-10.5645	261.3	34.25	24.14
nvsz–19b	New Britain–Vanuatu	162.8392	-10.9315	261.3	22.51	5
nvsz–20a	New Britain–Vanuatu	163.7222	-10.5014	262.9	50.35	26.3
nvsz–20b	New Britain–Vanuatu	163.7581	-10.7858	262.9	25.22	5
nvsz–21a	New Britain–Vanuatu	164.9445	-10.4183	287.9	40.31	23.3
nvsz–21b	New Britain–Vanuatu	164.8374	-10.7442	287.9	21.47	5
nvsz–22a	New Britain–Vanuatu	166.0261	-11.1069	317.1	42.39	20.78
nvsz–22b	New Britain–Vanuatu	165.7783	-11.3328	317.1	18.4	5
nvsz–23a	New Britain–Vanuatu	166.5179	-12.2260	342.4	47.95	22.43
nvsz–23b	New Britain–Vanuatu	166.2244	-12.3171	342.4	20.4	5
nvsz–24a	New Britain–Vanuatu	166.7236	-13.1065	342.6	47.13	28.52
nvsz–24b	New Britain–Vanuatu	166.4241	-13.1979	342.6	28.06	5
nvsz–25a	New Britain–Vanuatu	166.8914	-14.0785	350.3	54.1	31.16
nvsz–25b	New Britain–Vanuatu	166.6237	-14.1230	350.3	31.55	5
nvsz–26a	New Britain–Vanuatu	166.9200	-15.1450	365.6	50.46	29.05
nvsz–26b	New Britain–Vanuatu	166.6252	-15.1170	365.6	28.75	5
nvsz–27a	New Britain–Vanuatu	167.0053	-15.6308	334.2	44.74	25.46

Continued on next page

Table B.8 – continued

Segment	Description	Longitude(°E)	Latitude(°N)	Strike(°)	Dip(°)	Depth (km)
nvsz–27b	New Britain–Vanuatu	166.7068	-15.7695	334.2	24.15	5
nvsz–28a	New Britain–Vanuatu	167.4074	-16.3455	327.5	41.53	22.44
nvsz–28b	New Britain–Vanuatu	167.1117	-16.5264	327.5	20.42	5
nvsz–29a	New Britain–Vanuatu	167.9145	-17.2807	341.2	49.1	24.12
nvsz–29b	New Britain–Vanuatu	167.6229	-17.3757	341.2	22.48	5
nvsz–30a	New Britain–Vanuatu	168.2220	-18.2353	348.6	44.19	23.99
nvsz–30b	New Britain–Vanuatu	167.8895	-18.2991	348.6	22.32	5
nvsz–31a	New Britain–Vanuatu	168.5022	-19.0510	345.6	42.2	22.26
nvsz–31b	New Britain–Vanuatu	168.1611	-19.1338	345.6	20.2	5
nvsz–32a	New Britain–Vanuatu	168.8775	-19.6724	331.1	42.03	21.68
nvsz–32b	New Britain–Vanuatu	168.5671	-19.8338	331.1	19.49	5
nvsz–33a	New Britain–Vanuatu	169.3422	-20.4892	332.9	40.25	22.4
nvsz–33b	New Britain–Vanuatu	169.0161	-20.6453	332.9	20.37	5
nvsz–34a	New Britain–Vanuatu	169.8304	-21.2121	329.1	39	22.73
nvsz–34b	New Britain–Vanuatu	169.5086	-21.3911	329.1	20.77	5
nvsz–35a	New Britain–Vanuatu	170.3119	-21.6945	311.9	39	22.13
nvsz–35b	New Britain–Vanuatu	170.0606	-21.9543	311.9	20.03	5
nvsz–36a	New Britain–Vanuatu	170.9487	-22.1585	300.4	39.42	23.5
nvsz–36b	New Britain–Vanuatu	170.7585	-22.4577	300.4	21.71	5
nvsz–37a	New Britain–Vanuatu	171.6335	-22.3087	281.3	30	22.1
nvsz–37b	New Britain–Vanuatu	171.5512	-22.6902	281.3	20	5

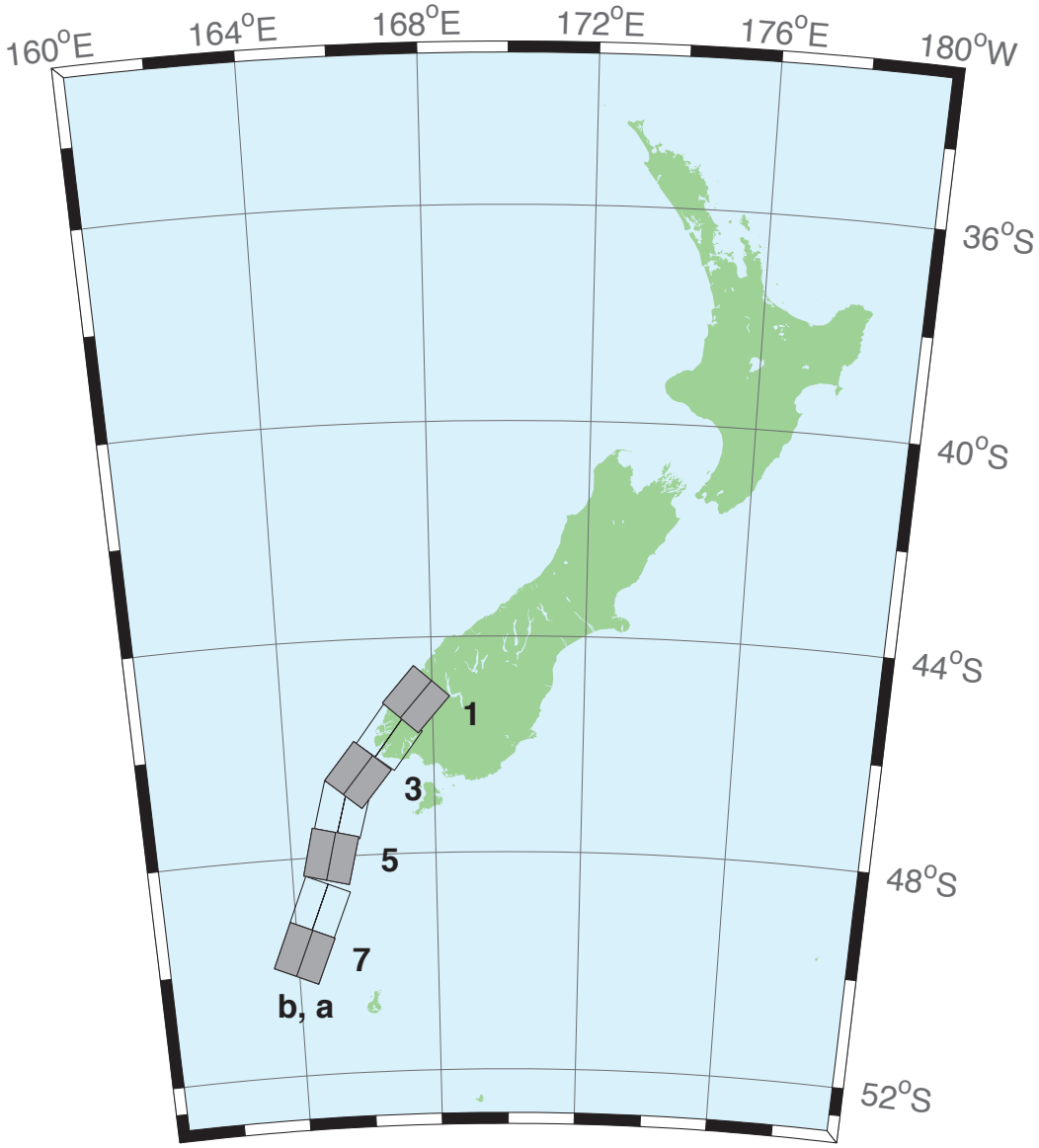

Figure B.9: New Zealand–Puysegur Zone unit sources.

Table B.9: Earthquake parameters for New Zealand–Puysegur Subduction Zone unit sources.

Segment	Description	Longitude(°E)	Latitude(°N)	Strike(°)	Dip(°)	Depth (km)
nzsz–1a	New Zealand–Puysegur	168.0294	-45.4368	41.5	15	17.94
nzsz–1b	New Zealand–Puysegur	167.5675	-45.1493	41.5	15	5
nzsz–2a	New Zealand–Puysegur	167.3256	-46.0984	37.14	15	17.94
nzsz–2b	New Zealand–Puysegur	166.8280	-45.8365	37.14	15	5
nzsz–3a	New Zealand–Puysegur	166.4351	-46.7897	39.53	15	17.94
nzsz–3b	New Zealand–Puysegur	165.9476	-46.5136	39.53	15	5
nzsz–4a	New Zealand–Puysegur	166.0968	-47.2583	15.38	15	17.94
nzsz–4b	New Zealand–Puysegur	165.4810	-47.1432	15.38	15	5
nzsz–5a	New Zealand–Puysegur	165.7270	-48.0951	13.94	15	17.94
nzsz–5b	New Zealand–Puysegur	165.0971	-47.9906	13.94	15	5
nzsz–6a	New Zealand–Puysegur	165.3168	-49.0829	22.71	15	17.94
nzsz–6b	New Zealand–Puysegur	164.7067	-48.9154	22.71	15	5
nzsz–7a	New Zealand–Puysegur	164.8017	-49.9193	23.25	15	17.94
nzsz–7b	New Zealand–Puysegur	164.1836	-49.7480	23.25	15	5

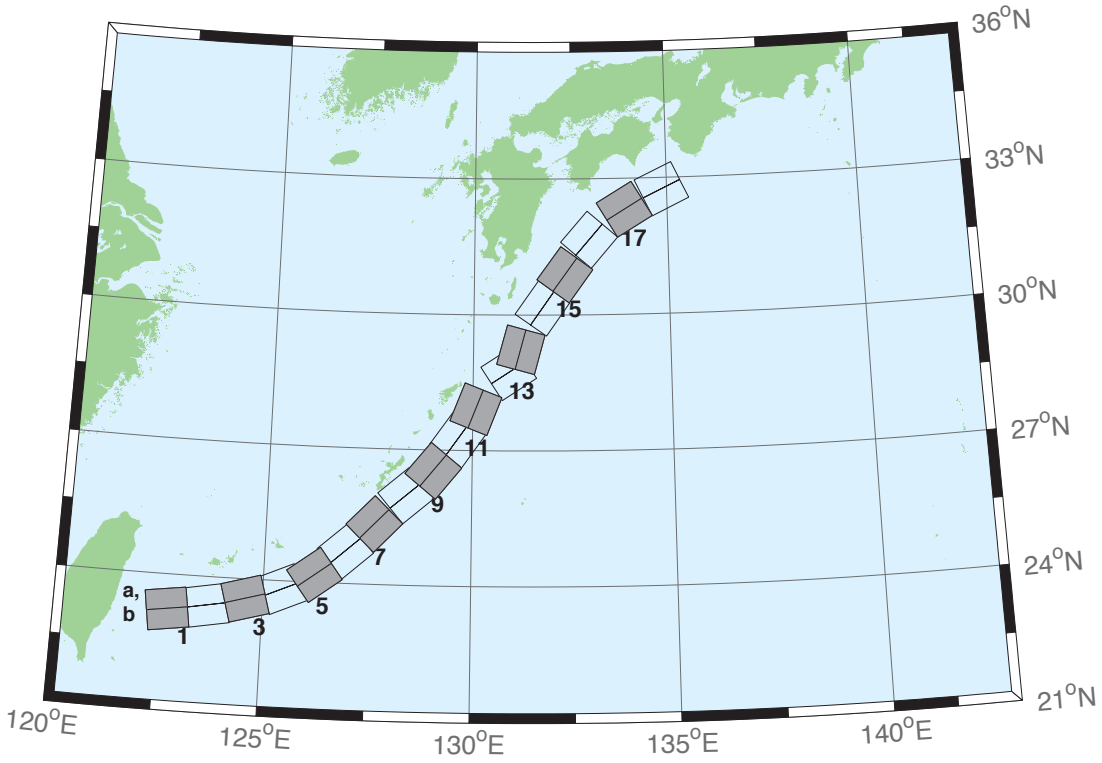

Figure B.10: Ryukyu–Kyushu–Nankai Zone unit sources.

Table B.10: Earthquake parameters for Ryukyu–Kyushu–Nankai Subduction Zone unit sources.

Segment	Description	Longitude(°E)	Latitude(°N)	Strike(°)	Dip(°)	Depth (km)
rnsz–1a	Ryukyu–Nankai	122.6672	23.6696	262	14	11.88
rnsz–1b	Ryukyu–Nankai	122.7332	23.2380	262	10	3.2
rnsz–2a	Ryukyu–Nankai	123.5939	23.7929	259.9	18.11	12.28
rnsz–2b	Ryukyu–Nankai	123.6751	23.3725	259.9	10	3.6
rnsz–3a	Ryukyu–Nankai	124.4604	23.9777	254.6	19.27	14.65
rnsz–3b	Ryukyu–Nankai	124.5830	23.5689	254.6	12.18	4.1
rnsz–4a	Ryukyu–Nankai	125.2720	24.2102	246.8	18	20.38
rnsz–4b	Ryukyu–Nankai	125.4563	23.8177	246.8	16	6.6
rnsz–5a	Ryukyu–Nankai	125.9465	24.5085	233.6	18	20.21
rnsz–5b	Ryukyu–Nankai	126.2241	24.1645	233.6	16	6.43
rnsz–6a	Ryukyu–Nankai	126.6349	25.0402	228.7	17.16	19.55
rnsz–6b	Ryukyu–Nankai	126.9465	24.7176	228.7	15.16	6.47
rnsz–7a	Ryukyu–Nankai	127.2867	25.6343	224	15.85	17.98
rnsz–7b	Ryukyu–Nankai	127.6303	25.3339	224	13.56	6.26
rnsz–8a	Ryukyu–Nankai	128.0725	26.3146	229.7	14.55	14.31
rnsz–8b	Ryukyu–Nankai	128.3854	25.9831	229.7	9.64	5.94
rnsz–9a	Ryukyu–Nankai	128.6642	26.8177	219.2	15.4	12.62
rnsz–9b	Ryukyu–Nankai	129.0391	26.5438	219.2	8	5.66
rnsz–10a	Ryukyu–Nankai	129.2286	27.4879	215.2	17	12.55
rnsz–10b	Ryukyu–Nankai	129.6233	27.2402	215.2	8.16	5.45
rnsz–11a	Ryukyu–Nankai	129.6169	28.0741	201.3	17	12.91
rnsz–11b	Ryukyu–Nankai	130.0698	27.9181	201.3	8.8	5.26
rnsz–12a	Ryukyu–Nankai	130.6175	29.0900	236.7	16.42	13.05
rnsz–12b	Ryukyu–Nankai	130.8873	28.7299	236.7	9.57	4.74
rnsz–13a	Ryukyu–Nankai	130.7223	29.3465	195.2	20.25	15.89
rnsz–13b	Ryukyu–Nankai	131.1884	29.2362	195.2	12.98	4.66
rnsz–14a	Ryukyu–Nankai	131.3467	30.3899	215.1	22.16	19.73
rnsz–14b	Ryukyu–Nankai	131.7402	30.1507	215.1	17.48	4.71
rnsz–15a	Ryukyu–Nankai	131.9149	31.1450	216	15.11	16.12
rnsz–15b	Ryukyu–Nankai	132.3235	30.8899	216	13.46	4.48
rnsz–16a	Ryukyu–Nankai	132.5628	31.9468	220.9	10.81	10.88
rnsz–16b	Ryukyu–Nankai	132.9546	31.6579	220.9	7.19	4.62
rnsz–17a	Ryukyu–Nankai	133.6125	32.6956	239	10.14	12.01
rnsz–17b	Ryukyu–Nankai	133.8823	32.3168	239	8.41	4.7
rnsz–18a	Ryukyu–Nankai	134.6416	33.1488	244.7	10.99	14.21
rnsz–18b	Ryukyu–Nankai	134.8656	32.7502	244.5	10.97	4.7
rnsz–19a	Ryukyu–Nankai	135.6450	33.5008	246.5	14.49	14.72
rnsz–19b	Ryukyu–Nankai	135.8523	33.1021	246.5	11.87	4.44
rnsz–20a	Ryukyu–Nankai	136.5962	33.8506	244.8	15	14.38
rnsz–20b	Ryukyu–Nankai	136.8179	33.4581	244.8	12	3.98
rnsz–21a	Ryukyu–Nankai	137.2252	34.3094	231.9	15	15.4
rnsz–21b	Ryukyu–Nankai	137.5480	33.9680	231.9	12	5
rnsz–22a	Ryukyu–Nankai	137.4161	34.5249	192.3	15	15.4
rnsz–22b	Ryukyu–Nankai	137.9301	34.4327	192.3	12	5

Appendix C. SIFT Testing Report

Kailua-Kona, Hawaii

Jean Newman

1.0 PURPOSE

Forecast models are tested with synthetic tsunami events covering a range of tsunami source locations. Testing is also done with selected historical tsunami events when available.

The purpose of forecast model testing is three-fold. The first objective is to assure that the results obtained with NOAA's tsunami forecast system, which has been released to the Tsunami Warning Centers for operational use, are identical or close to those obtained by the researcher during the development of the forecast model. The second objective is to test the forecast model for consistency, accuracy, time efficiency, and quality of results over a range of possible tsunami locations and magnitudes. The third objective is to identify bugs and issues in need of resolution by the researcher who developed the Forecast Model or by the forecast software development team before the next version release to NOAA's two Tsunami Warning Centers.

Local hardware and software applications, and tools familiar to the researcher(s), are used to run the Method of Splitting Tsunamis (MOST) model during the forecast model development. The test results presented in this report lend confidence that the model performs as developed and produces the same results when initiated within the forecast application in an operational setting as those produced by the researcher during the forecast model development. The test results assure those who rely on the Kailua-Kona tsunami forecast model that consistent results are produced irrespective of system.

2.0 TESTING PROCEDURE

The general procedure for forecast model testing is to run a set of synthetic tsunami scenarios and a selected set of historical tsunami events through the forecast system application and compare the results with those obtained by the researcher during the forecast model development and presented in the Tsunami Forecast Model Report. Specific steps taken to test the model include:

1. Identification of testing scenarios, including the standard set of synthetic events, appropriate historical events, and customized synthetic scenarios that may have been used by the researcher(s) in developing the forecast model.
2. Creation of new events to represent customized synthetic scenarios used by the researcher(s) in developing the forecast model, if any.
3. Submission of test model runs with the forecast system, and export of the results from A, B, and C grids, along with time series.
4. Recording applicable metadata, including the specific version of the forecast system used for testing.
5. Examination of forecast model results from the forecast system for instabilities in both time series and plot results.
6. Comparison of forecast model results obtained through the forecast system with those obtained during the forecast model development.
7. Summarization of results with specific mention of quality, consistency, and time efficiency.
8. Reporting of issues identified to modeler and forecast software development team.

9. Retesting the forecast models in the forecast system when reported issues have been addressed or explained.

Synthetic model runs were tested on a DELL PowerEdge R510 computer equipped with two Xeon E5670 processors at 2.93 Ghz, each with 12 MBytes of cache and 32GB memory. The processors are hex core and support hyperthreading, resulting in the computer performing as a 24 processor core machine. Additionally, the testing computer supports 10 Gigabit Ethernet for fast network connections. This computer configuration is similar or the same as the configurations of the computers installed at the Tsunami Warning Centers so the compute times should only vary slightly.

Results

The Kailua-Kona forecast models were tested with NOAA's tsunami forecast system. The propagation database used during development was dated in 2011.

The Kona1 and Kona2 forecast model were tested with four synthetic scenarios and one historical tsunami event. Test results from the forecast system and comparisons with the results obtained during the forecast model development are shown numerically in Table C1 for both models; and graphically in Figures C1 to C5 for Kona1. The results show that the forecast model is stable and robust, with consistent and high quality results across geographically distributed tsunami sources and mega-event tsunami magnitudes. For Kona1 model, the model run time (wall clock time) was around 20 minutes for 5 hours of simulation time, and under 16.5 minutes for 4 hours. This run time is above the 10 minute run time for 4 hours of simulation time that satisfies time efficiency requirements.

Four synthetic events were run on the Kona1 and Kona2 models. The modeled scenarios were stable for all cases tested, with no instabilities or ringing. Results show that the largest modeled height was 233.3/377.1 cm and originated in the Kamchatka-Yap-Mariana-Izu-Bonin (KISZ 22-31) source. Amplitudes greater than 100 cm were recorded for 2 out of 4 test sources. The smallest signal of 49/61 cm was recorded at the Aleutian-Alaska-Cascadia (ACSZ 56-65) source. Direct comparisons, of output from the forecast tool with results of both the historical event (Tohoku 2011) and available development synthetic events, demonstrated that the wave pattern were similar in shape, pattern and amplitude, though not the same (often very similar for the 1st hour or so). And, the resulting maximum wave amplitudes tended to be higher in the developmental results and should be investigated further to ascertain the cause.

Table C1. Table of maximum and minimum amplitudes (cm) at the Kailua-Kona, Hawaii warning point for synthetic and historical events tested using SIFT 3.2 and obtained during development.

Scenario Name	Source Zone	Tsunami Source	α [m]	SIFT Max (cm) kona1/kona2	Development Max (cm) Kona2	SIFT Min (cm) kona1/kona2	Development Min (cm) Kona2
Mega-tsunami Scenarios							
KISZ 22-31	Kamchatka-Yap-Mariana-Izu-Bonin	A22-A31, B22-B31	29	233.3/377.1	347	-309.8/-219.9	n/a
ASCZ 56-65	Aleutian-Alaska-Cascadia	A56-A65, B56-B65	29	49.0/60.6	61	-83.6/-97.4	n/a
CSSZ 86-95	Central and South America	A86-A95, B86-B95	29	78.3/80.4	80	-107.7/-104.4	n/a
NTSZ 30-39	New Zealand-Kermadec-Tonga	A30-A39, B30-B39	29	259.3/268.1	268	-217.5/-218.9	n/a
Historical Events							
Tohoku 2011	Kamchatka-Yap-Mariana-Izu-Bonin	4.66 b24 + 12.23 b25+26.31 a26+21.27 b26+22.75 a27 +4.98 b27		63.5/95.1	95	-95.1/-134.9	n/a

Kona1: with the regular Hawaiian A-grid.

Kona2: with an extra large A-grid extended further west and north.

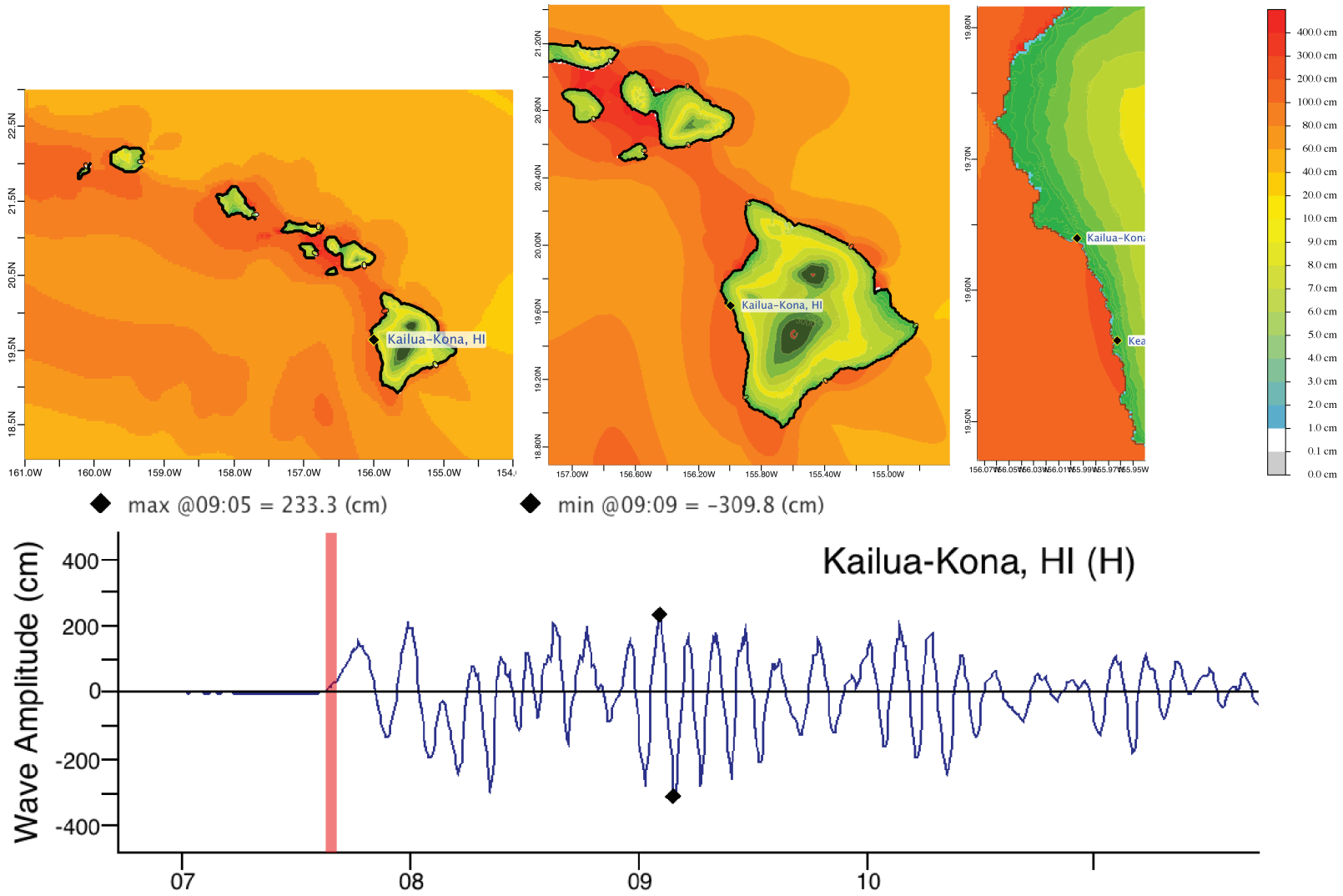

Figure 1: Response of the Kona1 forecast model to synthetic scenario KISZ 22-31 (alpha=29). Maximum sea surface elevation for (a) A-grid, b) B-grid, c) C-grid. Sea surface elevation time series at the C-grid warning point (d).

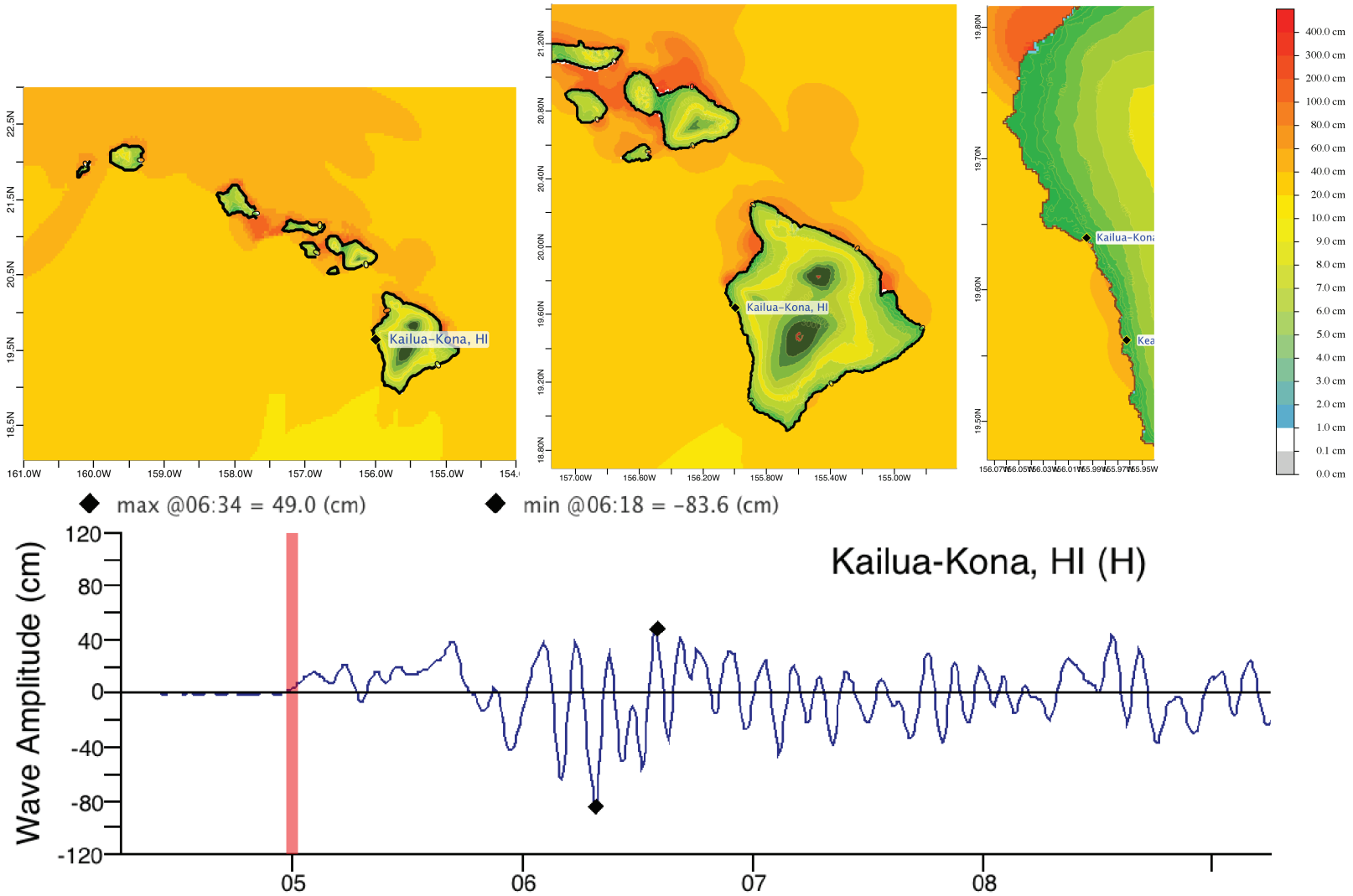

Figure 2: Response of the Kona1 forecast model to synthetic scenario ACSZ 56-65 (alpha=29). Maximum sea surface elevation for (a) A-grid, b) B-grid, c) C-grid. Sea surface elevation time series at the C-grid warning point (d).

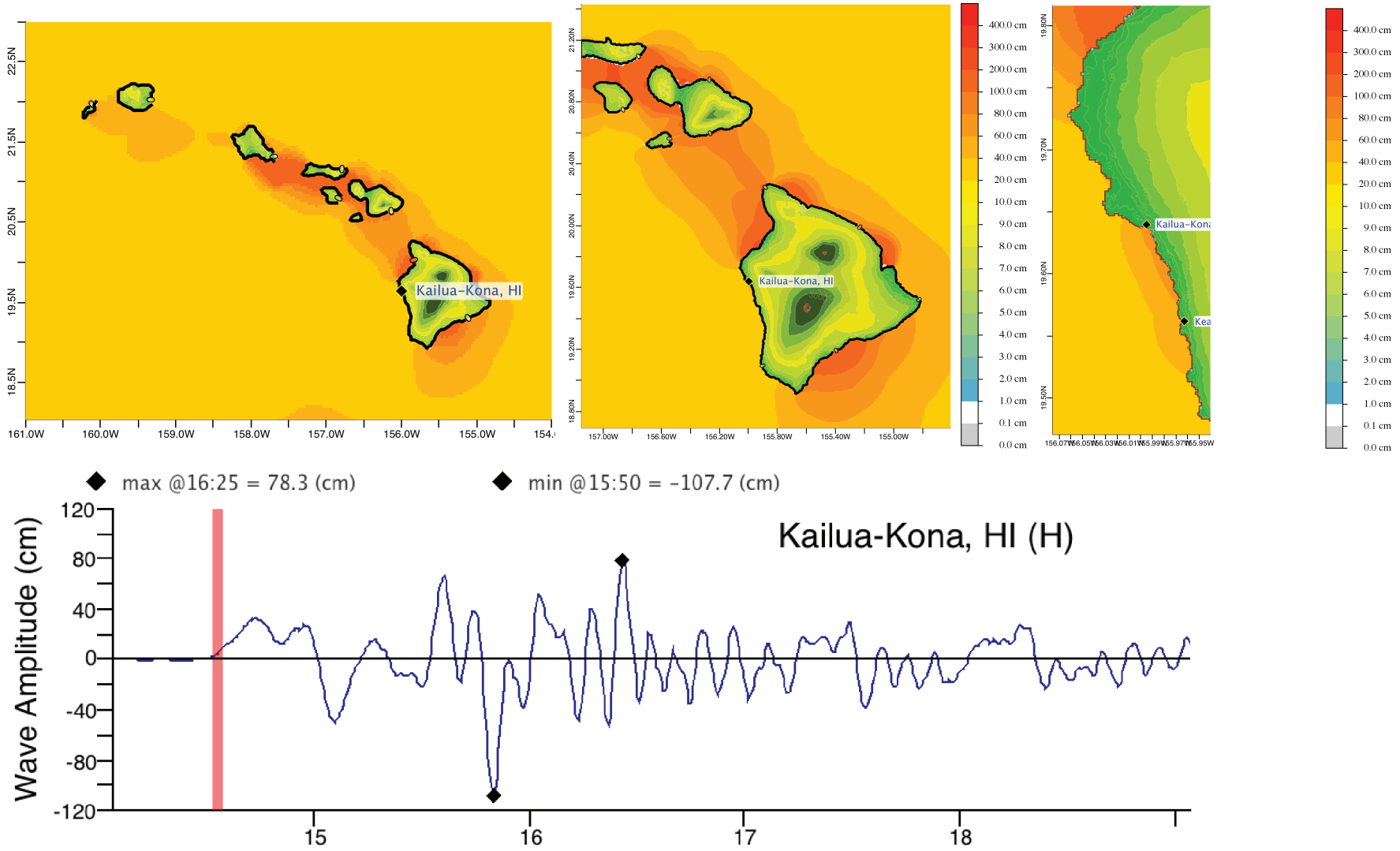

Figure 3: Response of the Kona1 forecast model to synthetic scenario CSSZ 86-95 (alpha=29). Maximum sea surface elevation for (a) A-grid, b) B-grid, c) C-grid. Sea surface elevation time series at the C-grid warning point (d).

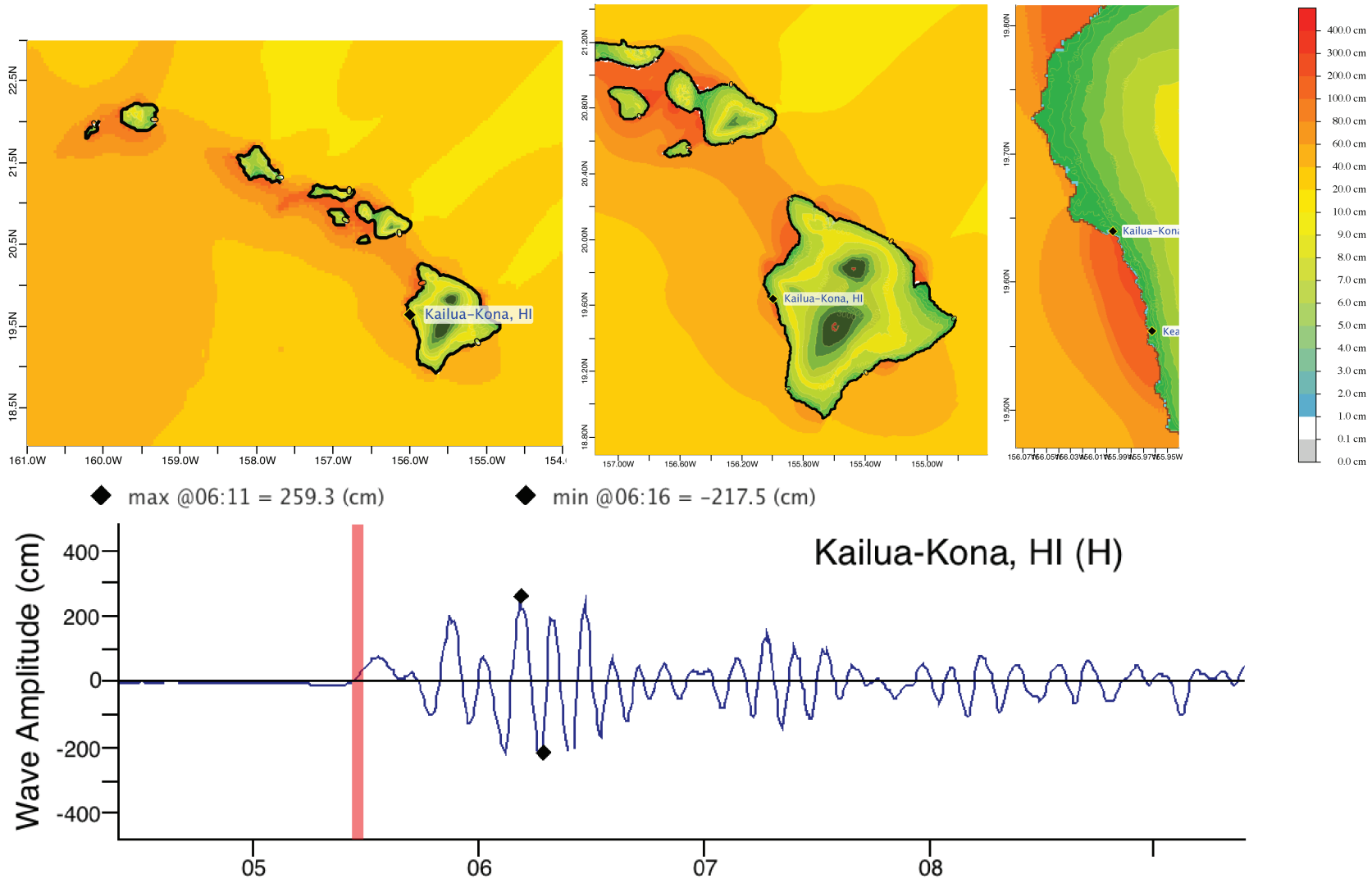

Figure 4: Response of the Kona1 forecast model to synthetic scenario NTSZ 30-39 (alpha=29). Maximum sea surface elevation for (a) A-grid, b) B-grid, c) C-grid. Sea surface elevation time series at the C-grid warning point (d).

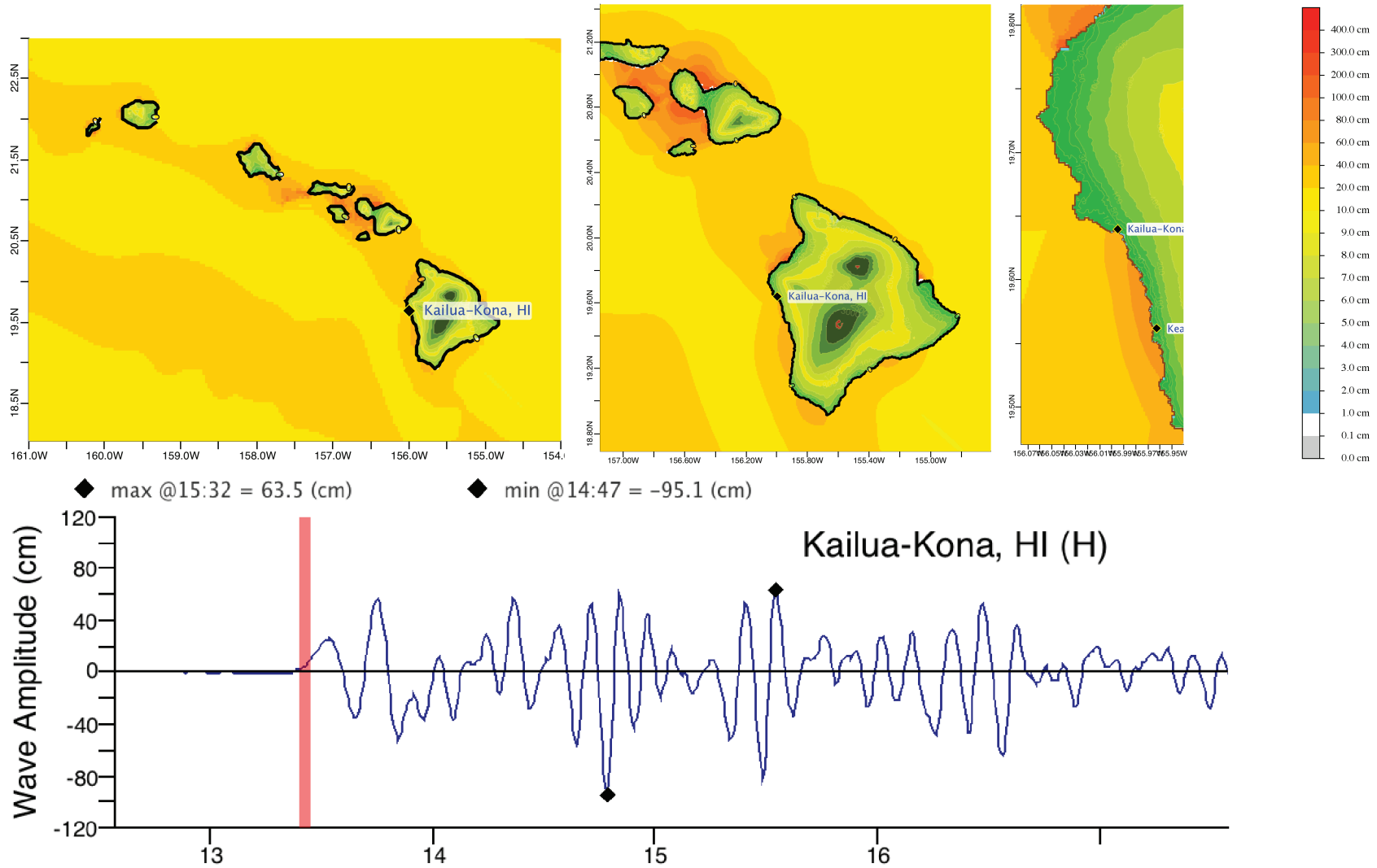

Figure 5: Response of the Kona1 forecast model to the 2011 Tohoku tsunami. Maximum sea surface elevation for (a) A-grid, b) B-grid, c) C-grid. Sea surface elevation time series at the C-grid warning point (d).